Heavy metal removal from water/wastewater using fly-ash derived zeolites

Archibald Frank Ankrah

(MSc Environmental Engineering)

Thesis Submitted for the degree of Doctor of Philosophy,
University of Nottingham

Department of Chemical and Environmental Engineering

November 2020

ABSTRACT

Heavy metal pollution in water has been a growing concern over the years and is under strict regulations from legislative bodies. Adsorption is an efficient and cost-effective way of metal removal from polluted water. Therefore, industries are seeking cheaper, environmentally friendly, easily accessible and efficient adsorbents for treating their effluents of heavy metals before disposal into surface waters. Activated carbon, the most popular commercial adsorbent, has become more expensive due to increasing demand, high cost of production and regeneration. Natural zeolites are not commercially available in most parts of the world while synthetic zeolites, produced from chemical precursors, are also expensive. Fly-ash derived zeolites provide a cheaper alternative as they can be synthesized from a waste product.

Initial research on fly-ash derived zeolite (Sodium P/ Gismondine) NaP1 has highlighted the potential for heavy metal removal from wastewater under different conditions without a clear understanding of the metal uptake mechanism and within industrial conditions (i.e. pelleting, multi-element adsorption with pellets and regeneration). Hence, there is limited information to adapt this material for industrial wastewater

treatment. This research aims to provide a thorough understanding of the characteristics of fly-ash derived NaP1 to harness its potential use in industrial wastewater treatment.

Results from this study indicate metal uptake capacities of NaP1 for zinc (34 mg/g) and lead (192 mg/g) were higher than other fly-ash derived NaP1, commercial activated carbon and clinoptilolite. In competitive adsorption, the metal selectivity for NaP1 followed the order $Pb^{2+}>Cu^{2+}>Zn^{2+}$, while multi-element removal efficiency was identified in the order NaP1 powder > NaP1 pellet > commercial 3A pellet.

Langmuir model and pseudo-second order kinetic model fitted best for all elements. The rate of metal uptake was fast and occurred in 15 min for all metals in contact with powder. The rate-determining step is controlled by diffusion of hydrated metals through microporous channels of NaP1. Copper regeneration from NaP1 was best achieved using Na and K salts at pH 5 and 22 ± 2 °C. NaCl and KCl solutions produced ~ 30% copper regeneration (representing 2.6 mg/g NaP1) while copper recovery with regeneration solutions was in the order $K^{+}>Na^{+}>H^{+}$.

After pelleting without binder, adsorption experiments showed a type II isotherm with an H3 hysteresis loop, indicating the presence of unrestricted monolayer – multilayer adsorption. The mean pore diameter for NaP1 pellet was 14.3 ± 0.275 nm compared to 10.95 ± 0.069 nm for powder NaP1. However, BET area of NaP1 pellets was 28% lower than the powder form.

This research has demonstrated the viability of NaP1 for heavy metal removal from wastewater. Fly-ash waste from coal power plants could be sourced in creating zeolite NaP1 instead of dumping them into landfills and enhancing secondary pollution. Secondly, NaP1 can be converted into pellets without a binder for industrial use since it displays quick kinetics of 15 mins for metal uptake. Furthermore, NaP1 works efficiently at pH 5 and can be regenerated easily with eluents such as NaCl and KCl.

ACKNOWLEDGEMENT

Father, thank you for your grace and goodness that has enabled me to come this far. I am grateful.

Romans 8: 28

I would like to thank God for how far he has brought us. I give God all the praise and honour my spiritual father, Prophet Jerome Fernando as my mentor, life coach and Prophet. I would like to say a big thank you to my wife, Dr. Deshani Gunasekera for all the love, support and wisdom. I couldn't have come this far without you.

A big thank you to the Ghana Education Trust Fund (GETFund) for the sponsorship, my parents; Mr. George Ankrah, Ms. Harriet Jamboe and Ms. Felicia Adade and family for all the encouragement and support. I say thank you to my supervisors; Prof. Colin Snape and Dr. Begum Tokay for their time, encouragement and faith in me, I couldn't have accomplished this without you.

Finally, I say thank you to everyone for their moral support, prayers and encouragement.

God richly bless you all and I dedicate this thesis to you.

ABBREVIATIONS

List of Chemicals

Zinc nitrate	$Zn(NO_3)_2$
Cadmium nitrate	$Cd(NO_3)_2.4H_2O$
Lead nitrate	$Pb(NO_3)_2$
Copper nitrate	$Cu(NO_3)_2.2.5H_2O$
Nitric acid	HNO_3
Sodium Hydroxide	NaOH
Hydrochloric acid	HCl
Sodium chloride	NaCl

List of Acronyms

CFA	Coal fly-ash
NaP1	Sodium P (Gismondine)
UKEA	United Kingdom Environmental Agency
USEPA	United States Environmental Protection Agency
Zn	Zinc
Cd	Cadmium
Pb	Lead
Cu	Copper
K	Potassium
Na	Sodium
H	Hydrogen

SEM	Scanning Electronic Microscope
XRD	X-Ray Diffraction
XRF	X-Ray Fluorescence
ICP - MS	Inductively Coupled Plasma Mass Spectrometry
AAS	Atomic Absorption Spectrometry/Spectroscopy
WHO	World Health Organisation
EU	European Union
EQS	Environmental Quality Standard
EC	European Commission
AWWA	American Water Works Association
SiO_4	Silicon oxide
AlO_4	Aluminium oxide
CEC	Cation Exchange Capacity
ISRIC	International Soil reference and Information Centre

List of Units

m^2/g	square meter per gram	surface area
cm^3/g	cubic centimetre per gram	Pore volume
nm	nanometre	Pore diameter
mg/g	milligram per gram	adsorptive capacity
g/cm^3	grams per cubic centimetre	Density
ppt	parts per trillion	concentration
ppb	Parts per billion	concentration
m/gl	Milligram per litre	Concentration

micro g/l	Microgram per litre	Concentration
µg/l	Microgram per litre	Concentration
MPa	Mega Pascal	Pressure
h	Hour	Time
ml	millilitre	volume
L	Litre	volume
°C	degree Celsius	Temperature
M	Molar	concentration
µm	micrometre	size/ diameter/length
rpm	rotations per minute	speed
min	minute	Time
µg/g	microgram per gram	weight/weight
mg	milligrams	weight
g/l	grams per litre	solid to liquid ratio

List of Symbols

q_e	adsorbate adsorbed per unit mass of adsorbent at equilibrium
q_t	adsorbate adsorbed per unit mass of adsorbent at time (t)
K_1	First order constant
K_2	Second order constant
β	Desorption coefficient
α	Initial adsorption rate
K_F	Freundlich constant

C_e Concentration of solute in solution

q_m Maximum adsorptive capacity

b Langmuir constant

Table of Contents

1 Introduction 18
1.1 Background 18
1.2 Aim and objectives 26
1.3 Novelty of research 27
1.4 Structure of thesis 27
2 Literature review 30
2.1 Introduction to heavy metals 30
2.2 Legislation 32
2.3 Heavy metals of interest in this study 35
2.3.1 Copper 35
2.3.2 Zinc 36
2.3.3 Lead 37
2.4 Heavy metal removal technologies 38
2.4.1 Chemical precipitation 39
2.4.2 Ion exchange 40
2.4.3 Electrochemical methods 41
2.4.4 Membrane separation 41
2.4.5 Adsorption 42
2.5 Adsorbents 43
2.5.1 Zeolites 45
2.5.2 Coal fly-ash as reactant during zeolite synthesis 49
2.6 Research on fly-ash zeolite NaP1 53
2.7 Pelleting 59
2.8 Regeneration of adsorbent 63
2.8.1 Chemical stability of adsorbent 66
2.9 Experimental conditions for metal removal via adsorption 68
2.9.1 Heavy metal concentration 68
2.9.2 Adsorbent mass 72
2.9.3 pH 73
2.9.4 Solubility of metal ions 75

2.9.5 Multi-element clean water matrix 79
2.10 Adsorption theory 88
2.10.1 Adsorption kinetics 89
2.10.2 Adsorption isotherm 94
2.10.3 BET and BJH Methods from Nitrogen adsorption 98
3 Materials and method 101
3.1 Introduction 101
3.2 Materials 101
3.3 Methods 102
3.3.1 Characterization of adsorbent 102
3.3.2 Pelleting 105
3.3.3 Determination of metals in liquid samples 109
3.3.4 Control experiments 110
3.3.5 Adsorption 113
3.3.6 Single element adsorption isotherm 115
3.3.7 Multi-element adsorption experiments 116
3.3.8 Metal removal with NaP1 and 3A pellets (kinetics) 116
3.3.9 Further leaching 117
3.4 Justification for experimental variables 118
3.5 Regeneration study 120
3.6 Cation exchange capacity (CEC) 121
4 Zeolite characterization 122
4.1 Introduction 122
4.2 SEM characterization 122
4.3 XRD characterization 124
4.4 XRF characterization 127
4.5 Chapter summary 128
5 Control experiments 129
5.1 Introduction 129
5.2 Leaching 129
5.3 Precipitation 133
5.4 Adsorption in syringe filters 135

5.5 Calibration and limits of detection for the ICP Instrument 136
5.6 Limit of detection and quantification 140
5.7 Chapter summary 142
6 Adsorption experiments 143
6.1 Introduction 143
6.2 Single element removal 143
6.2.1 Zinc removal 143
6.2.2 Lead removal 150
6.2.3 Copper removal 156
6.3 Single element adsorption kinetics 165
6.4 Adsorption isotherms for single heavy metals 167
6.5 Adsorption kinetic models 174
6.6 Ion selectivity 176
6.7 pH determination for multi-element adsorption 181
6.8 Chapter summary 190
7 Regeneration Study 192
7.1 Introduction 192
7.2 Regeneration tests 192
7.3 Validating regeneration with XRF scan 198
7.4 Validating regeneration with XRD scan 202
7.5 Determining optimum regeneration time 208
7.6 Chapter summary 218
8 Pelleting study 219
8.1 Introduction 219
8.2 Adsorption using NaP1 pellets 219
8.2.1 Amount of zeolite required 221
8.2.2 Loading pressure 222
8.2.3 Loading pressure time 223
8.3 Characterization of pellets 224
8.3.1 Nitrogen adsorption isotherms 225
8.3.2 Leaching from pellet vs powder 235
8.3.3 Cation exchange capacity (CEC) determination 241

8.4 Lead removal with NaP1 and 3A 246
8.4.1 Kinetics of lead removal by NaP1 versus 3A 249
8.4.2 Multi–element removal with NaP1 pellets compared to 3A pellets 263
8.4.3 Multi-element interaction 273
8.4.4 Chapter summary 281
9 Conclusions and future work 283
9.1 Advancement of results to this field 283
9.2 Limitations of this research 285
9.3 Future work 286
9.4 Conclusion 286
10 References 290

Table of Figures

Figure 2.1: Structure of zeolite NaP1 adopted from Structure Commission of International Zeolite Association (2017) 49
Figure 2.2: Theoretical solubility of copper hydroxide (Cushnie, 1985). 76
Figure 2.3: Theoretical solubility of zinc hydroxide (Cushnie, 1985). 77
Figure 2.4: Theoretical solubility of lead hydroxide (Cushnie, 1985). 78
Figure 3.1: Pelleting die assembly (image obtained from the manual). 106
Figure 3.2: A picture of the hydraulic press. 108
Figure 4.1: SEM image of coal fly-ash at 2 microns. 122
Figure 4.2: SEM image of NaP1 zeolite. 124
Figure 4.3: XRD pattern of coal fly-ash. 125
Figure 4.4: XRD pattern of zeolite NaP1 synthesized from coal fly-ash. 126
Figure 5.1: Cumulative concentrations of leached cations in water after 3 h. Conditions: 5 g of NaP1 dissolved in 1 l Milli-Q water at pH 3.5 and 20 ± 2 °C. Values presented are the mean of 3 repeat measurements and standard deviations. 130
Figure 5.2: Cumulative concentrations of leached target metal ions in water after 3 h. Conditions: 5 g of NaP1 dissolved in 1 l Milli-Q water at pH 3.5 and 20 ± 2 °C. Values presented are the mean of 3 repeat measurements and standard deviations. 131
Figure 5.3: Calibration curve of ICP-MS using external calibration standards (<0, 20, 40 and 100 µg/l) for a) zinc, b) lead and c) copper metals. 139
Figure 6.1: Decrease in zinc concentration in solution as a function of time when 5 g adsorbent is used in 1 l solution and compared to a control experiment at the same conditions without zeolite. Initial zinc amount is 250 mg/l, pH=3.5, t=3 h at 20 ± 2 °C. Values presented are mean with standard deviation from 3 repetitions. 145
Figure 6.2: Amount of zinc adsorbed per gram of zeolite as a function of equilibrium concentration of the zinc solution when 5 g adsorbent is stirred in 1 l solution at 300 rpm. Initial zinc amount varied from: (50, 250, 500, 1000 and 2500 mg/l), pH=3.5, t= 1 h at 20 ± 2 °C. The graphs presented are resulting from 2 repetitions. 146
Figure 6.3: Decrease in lead concentration as a function of time (90 min) when 5 g adsorbent is used in 1 l solution. Initial lead amount: (100 mg/l), pH= 3.5, t= 1.5 h at 20 ± 2 °C. Values presented are mean and standard deviation for the observation of 3 repetitions. 151
Figure 6.4: Amount of lead adsorbed per gram zeolite as a function of equilibrium concentration of the lead solution when 5 g adsorbent is stirred in 1 l solution at 300 rpm. Initial lead amount varied from (50, 250, 500, 1000, 2500 and 3500 mg/l), pH= 3.5, t= 1h T= 20 ± 2 °C. The graphs presented are resulting from two repetitions. 153
Figure 6.5: Decrease in copper concentration as a function of time when 5 g adsorbent is used in 1 l solution. Initial copper amount= (150 mg/l), pH= 3.5, T= 20 ± 2 °C. Values presented are mean and standard deviation for the observation of 3 repetitions. 157
Figure 6.6: Amount of copper adsorbed per gram zeolite as a function of equilibrium concentration of the copper solution when 5 g adsorbent is stirred in 1 l solution at 300 rpm. Initial copper amount varied in the range of 80, 120, 150, 500 and 1000 mg/l, pH= 3.5, t= 1 h, at 20 ± 2 °C. The data points presented are resulted from 3 repetitions. 158
Figure 6.7: Langmuir isotherm model for copper, zinc and lead (with concentrations of 50, 150, 250, 150, 500, 1000, 2000 and 3500 mg/l) on zeolite NaP1 (dosage 5 g/l) at 20 ± 2 °C and pH 3.5 at a constant stirring speed of 300 rpm. 168
Figure 6.8: Freundlich isotherm model for copper, zinc and lead (with concentrations of 50, 150, 250, 150, 500, 1000, 2000 and 3500 mg/l) on zeolite NaP1 (dosage 5 g/l) at 20 ± 2 °C and pH 3.5 at a constant stirring speed of 300 rpm. 170

Figure 6.9: Metal uptake as a function of pH, when 1 g zeolite is mixed in 1 litre solution for 1 h. Initial metal concentration= 12.5 mg/l for each heavy metals making a total of 37.5 mg/l at T= 20 ± 2 °C. 187
Figure 7.1: Amount of copper desorbed from 0.5 g NaP1 (loaded with ~3 mg copper) as a function of time. Conditions: 1 M HCl, pH 1 and 3.5, t= 7 h at 20 ± 2 °C.... 194
Figure 7.2: Amount of copper desorbed from 0.5 g NaP1 (loaded with ~3 mg copper) as a function of time. Conditions: 3 M NaCl, pH 3.5 and 5, t= 24 h at 20 ± 2 °C.195
Figure 7.3: Amount of copper desorbed from 0.5 g NaP1 (laden with ~3 mg copper) over time. Conditions: 3 M NaOH, pH 3.5, t= 6 h; 5 M NaCl pH 3.5, t= 24 h at 20 ± 2 °C. 196
Figure 7.4: Constituents of regenerated zeolite (0.5 g) determined by XRF scan. Conditions;("3 M_NaCl_PH3.5_24h"," 1 M_HCl_PH1_6h","5 M_NaCl_PH3.5_24h","3 M_NaOH_PH3.5_24h"," 1 M_HCl_PH3.5_6h","Original"). 201
Figure 7.5: XRD scan comparing the structural integrity of regenerated NaP1 to the original. Conditions: ("3 M NaCl_pH 3.5_24 h","1 M HCl_pH 1_6 h","5 M NaCl_pH 3.5_24 h","3 M NaOH_pH 3.5_24 h","1 M HCl_pH 3.5_6h","Original") at 20 ± 2 °C. 203
Figure 7.6: XRD scan comparing the structural integrity of NaP1 to the original after contact with distilled water at pH 3.5 for 24 h. 205
Figure 7.7: XRD scan comparing the structural integrity of NaP1 to the original after contact with distilled water at pH 5 for 24 h. 206
Figure 7.8: XRD scan comparing the structural integrity of NaP1 to the original after contact with distilled water at pH 10.5 for 24 h. 207
Figure 7.9: Results from copper removal experiment, mixing 100 ml copper solution of (50 mg/l) with 0.5 g NaP1 at pH 5, temperature 20 ± 2 °C. Samples were taken at time 15, 30 mins, 1 and 3 h. 210
Figure 8.1: Pellet pressed from 0.10 grams NaP1 powder using 5 tons loading for 5 min. 221
Figure 8.2: Nitrogen adsorption/desorption isotherms for NaP1 powder and pellets at 77 K. 226
Figure 8.3: Pore size distribution of NaP1 powder and pellet obtained from the nitrogen isotherm experiment. 229
Figure 8.4: Decrease in lead concentration in solution over time without an adsorbent (control), with NaP1 powder and pellet using the following conditions: 5 g of zeolite, 1 litre of 90, 89 and 85 mg/l concentration lead solution respectively, stirring at 300 rpm for 3 h at pH 5 and at 25 ± 2 °C. 247
Figure 8.5: A graph comparing lead concentration decrease in solution over time with NaP1 pellet and 3A pellet using the following conditions: 5 g zeolite, 1 litre of 98 and 85 mg/l concentration lead solution respectively, stirred at 300 rpm for 3 h at pH 5 and at 25 ± 2 °C. 248
Figure 8.6: A graph demonstrating pseudo-first order kinetic model of lead uptake by NaP1 powder at 25 ± 2 °C. 252
Figure 8.7: Pseudo-second order kinetic model of lead uptake by NaP1 powder at 25 ± 2 °C. 253
Figure 8.8: A graph demonstrating intraparticle diffusion kinetic model of lead uptake by NaP1 pellet at 25 ± 2 °C. 255
Figure 8.9: Elovich kinetic model of lead uptake by 3A pellet at 25 ± 2 °C. 256
Figure 8.10: Decrease of metal concentration in solution over time with NaP1 powder using the following conditions; 5 grams of each zeolite, 1 litre of 486 mg/l total metal concentration (98 mg/l lead, 240 mg/l zinc, 148 mg/l copper), stirred at 300 rpm for 3 h at pH 5 and 25 ± 2 °C. 264
Figure 8.11: Decrease of metal concentration in solution over time with NaP1 pellet. Conditions; 5 g of each zeolite, 1 l of 462 mg/l total metal concentration (92 mg/l lead, 230 mg/l zinc, 140 mg/l copper), stirred at 300 rpm for 3 h (180 min) at constant pH 5 and temperature 25 ± 2 °C. 265

Figure 8.12: Decrease of metal concentration in solution over time with 3A pellet. Conditions; 5 grams of each zeolite, 1 litre of 477 mg/ total metal concentration (92 mg/l lead, 245 mg/l zinc, 140 mg/l copper), stirred at 300 rpm for 3 h (180 min) at a constant pH 5 and temperature 25 ± 2 °C. 267

List of Tables

Table 2.1: Concentration of copper, zinc and lead in wastewater from various countries and industries. 70
Table 2.2: Precipitation pH of metals adopted from Dean et al. (1972). 74
Table 2.3: Single and multi-component adsorption of heavy metals from literature. 83
Table 5.1: Precipitation of heavy metals obtained as a function of pH (3.5, 6.5, 10.5) from control experiments when 1 litre water matrix is stirred without zeolite for 1 h. Initial metal concentration ~12.5 mg/l for each heavy metals making a total of at 37.5 mg/l, T= 20 ± 2 °C. 133
Table 5.2: Results obtained from testing 0.45 and 0.2 µm syringe filters with 40 mg/l copper concentration. 135
Table 5.3: Mean and standard deviation values of metals from ICP-MS calibration using four standard solutions of concentration <0, 20, 40 and 100 µg/l and repeated 3 times. 137
Table 5.4: Limit of detection and limit of quantification for Cu, Zn and Pb obtained from calibration curve parameters. 141
Table 6.1: Summary of adsorbent performance of works adopted from Koshy and Singh (2016) and other studies. 162
Table 6.2: A comparison of NaP1 adsorptive capacities for heavy metals between Langmuir and Freundlich models. 171
Table 6.3: Regression coefficients obtained from the kinetic models applied to the experimental adsorption data. 175
Table 6.4: Parameters from the Langmuir isotherm model for NaP1 and heavy metals under observation. 176
Table 6.5: Hydrated vs Un-hydrated radii of heavy metals. Adopted from Ouki and Kavanagh (1997) and Oter and Ackay (2007). 178
Table 6.6: Metal composition from leaching experiments with and without heavy metals at pH 3.5. Conditions: 1 g NaP1 mixed in 1 litre of distilled water (leaching) and water matrix (37.5 mg/l in total of Cu, Zn and Pb), time: 1 h and temperature: 20 ± 2 °C. 182
Table 6.7: Elements leached during multi-element adsorptions at various pH values (10.5, 6.5 and 3.5). Conditions: 1 g NaP1 mixed in 1 litre of water matrix (37.5 mg/l in total of Cu, Zn and Pb), time: 1 h and temperature: 20 ± 2 °C. 184
Table 7.1: Parameters/conditions investigated during the regeneration study of 0.5 g NaP1 loaded with 3 mg of copper. 193
Table 7.2: Initial cation quantity present in regeneration solutions. 197
Table 7.3: A summary of regeneration results showing copper amounts from 0.5 g zeolite before and after regeneration and comparing that to desorb copper amount with the expected amount. 200
Table 7.4: Results from repeated copper removal experiment for 3 h without sample extraction under the following conditions: 0.5 g of NaP1 used for copper removal of concentration 50 mg/l of 100 ml volume at 20 ± 2 °C and pH 5. 211
Table 7.5: Mean and standard deviation of triplicate results obtained from the regeneration experiments for 24 h, performed with 0.5 g spent NaP1 with ~ 4.5 mg copper and mixed with 100 ml of selected regeneration solutions (HCl, KCl, NaCl) at pH 5 at 20 ± 2 °C. 214
Table 8.1: Summary of pelleting parameter optimization tests. 220
Table 8.2: Manufacturer's typical loads to producing quality pellets. 222
Table 8.3: Surface area, pore volume, pore size obtained from the nitrogen adsorption of NaP1 powder and pellet at 77 K. 231
Table 8.4: Comparison of zeolite parameters from literature. 233

Table 8.5: Comparison of mean leaching results from NaP1 powder, NaP1 pellet and 3A pellet. Experimental conditions: 1-gram zeolite in 1 l distilled water, stirred at 300 rpm at pH 5 and room temperature 25 ± 2 °C. 237
Table 8.6: Cation exchange capacity (CEC) of NaP1 and 3A determined by stirring 100 ml of 1 M ammonium acetate solution with 0.25 g of zeolite NaP1/3A for 24 h at 25 ± 2 °C. 243
Table 8.7: A Cation exchange capacity (CEC) comparison between this study and in literature. 245
Table 8.8: Kinetic models tested with lead uptake experimental data by NaP1 powder, NaP1 pellet and 3A pellet..... 250
Table 8.9: Kinetic models of metal uptake mechanism of NaP1 compared to other adsorbents 260
Table 8.10: Multi-element concentration decrease in solution over time with NaP1 powder/pellet and 3A pellet using the following conditions; 1 gram of each zeolite, 1 litre of 1.7 mmol/l total metal concentration stirred at 300 rpm for 3 h (180 min) at a constant pH= 5 and temperature 25 ± 2 °C. 270
Table 8.11: Adsorptive capacity of powder and pellet NaP1 obtained from single/multi-element systems using pseudo-first*/second order kinetic models. . 274
Table 8.12: Multi-element results from literature using 2nd Order uptake capacity. 278

1 Introduction

1.1 Background

Heavy metals as water pollutants have received great attention for several decades owing to their carcinogenic and toxic properties. They are also known to accumulate in tissues along the food chain and be fatal in high concentrations. The United Nation's 2020 goal, target 6.3 for sustainable development has outlined the need for an environmentally sound means of managing chemicals while reducing their wastes released into the environment to minimize their adverse impact on nature (U.N. 2020). This cannot be achieved without international frameworks.

In this regard, their control and disposal in the environment, as a result of anthropogenic activities, is under control by various bodies such as the Urban Wastewater Treatment Directive (91/271/EEC), Water Framework Directive (2000/60/EC), Fish Directive (2006/44/EC) and Environmental Quality Standards (2008/EC). Over 30 heavy metals have been investigated and defined with maximum allowable limits in water with some classified as priority metals (Gardener et al., 2013). These metals are copper, lead and zinc (Wuana and Okieimen, 2011). These were identified through a UK programme for chemical

investigations (CIP) project reported by Gardener et al. (2013) as exceeding their allowable limit in industrial wastewater effluents (UK).

To work towards the United Nation's 2030 target of improving water quality by reducing pollution, minimizing the release of hazardous chemicals and halving the proportion of untreated water, industrial wastewater effluents as a major point source of heavy metal pollution in water bodies globally (Fergusson, 1990; Bradl, 2005) has come under scrutiny. Several industries such as electroplating, steel, mines, pharmaceuticals, paint, textile, etc. are known to use large volumes of water and produce effluents containing these heavy metals (Lokhande et al., 2011; Tchounwou et al., 2012). With industrialization on the rise worldwide, heavy metal pollution is bound to be on the ascendency in both developed and developing countries (Bazrafshan et al, 2015). Hence, there is the need to seek eco-friendly (Dixit et al., 2015), sustainable, cost effective and efficient means of eliminating pollution (Pap et al., 2016; Klučáková and Pavlíková, 2017) while building capacity within an economy through industrialization.

Adsorption is preferred to other metal removal technologies such as reverse osmosis, electrolysis, ultrafiltration, filtration, coagulation and sedimentation (Barakat, 2011; Lakherwal, 2014; Gunatilake, 2015). Adsorption is a more efficient and cost-effective way of metal removal from large volumes of wastewater with low concentrations (Perić et al., 2004) of metals and affordable by underdeveloped and developing countries (Tripathi and Ranjan, 2015). However in recent years, activated carbon, which is the most widely used commercial adsorbent for heavy metal removal (Bhatnagar, 2012; Zwain et al., 2014) has become more expensive (Panday et al., 1985; Nsami and Mbadcam, 2013) due to its increasing demand, high cost of production and regeneration (Erdem et al., 2004).

Hence, a lot of focus is given to the development of low cost, environmentally friendly and effective adsorbents for water and wastewater treatment industries (Babel and Kurniawan, 2003; Hegazi, 2013; Tripathi and Ranjan, 2015). Currently, adsorbents under development are from seashells, agricultural wastes, fishbone, char, zeolites, clay, chitosan, lignin and cellulose (Yu and Han, 2015; Tarachand et al., 2016).

Amongst these adsorbents, zeolites are well-known for their high adsorption and ion-exchange capabilities as one of the oldest adsorbents in history (Margeta et al., 2013). Existing as both natural and synthetic products, they have been used in petroleum refinery, water softening, heavy metal removal, and separation of gases, radioactive substance management, desiccants, insulated glass windows, dehumidifiers and many more applications (Sherman, 1999; Li et al., 2017). Large deposits of natural zeolites are not available in most countries to support commercial purposes (Geological Survey (US), 2015) requiring the synthesis of zeolites from chemical precursors such as alumina, silica and alkali earth metals (Otieno et al., 2019).

Since their development, synthetic zeolites have been preferred over natural zeolites for industrial purposes due to their higher ion-exchange capacity, tuneable and amenable properties, higher purity and thermal stability (Li et al., 2017). However, synthetic zeolites are also becoming more expensive due to the increasing demand, requiring cheaper precursors to promote sustainability (Gougazeh and Buhi, 2014). Fly-ash from coal combustion in power plants contains high amounts of quartz and mullite, composed of necessary precursors for the synthesis of zeolites (Yan et al., 2018). Thus, it is seen as a possible lower

cost alternative for preparing synthetic zeolites, recycling waste from coal fly-ash and recycling pollutants from water to reinforce sustainability.

Reports from Chunfeng et al. (2009) and Shumba et al. (2011) indicate an estimated 300 million tonnes increase in fly-ash worldwide every 3 years and predicts further increases in the coming years. The traditional use of fly-ash has mostly been in concrete and cement production (Thomas, 2007), representing about 48% of the total amount, while most of the fly-ash is disposed-off via landfill (Brännvall and Kumpiene, 2016). This practice is also under examination as environmental concerns for leachates have increased (Tiwari et al., 2015). Hence, some researchers proposed fly-ash as a cheap resource for developing commercial synthetic zeolites (Querol et al., 2002; Malik and Thapliyal, 2009), and a solution to fly-ash disposal with stringent conditions (Querol et al., 2002; Ahmaruzzaman, 2010). The recycling of fly-ash into zeolites is also in line with the United Nations' 2030 target of substantially increasing recycling and safe reuse globally. This is a likely source of revenue for countries generating fly-ash as a waste product.

Currently, there are several fly-ash derived zeolites such as X, A, chabazite, sodalite and NaP1, similar to synthetic zeolites. Zeolite X and A are mostly used in industry and in high demand

due to their uniform pore structure and larger pore size compared to NaP1 (Alvarez-Ayuso et al., 2003), sodalite and chabazite. However, fly-ash derived zeolites X and A are more expensive to synthesize compared to NaP1, through the conventional hydrothermal synthesis process as they require large quantities of raw materials (aluminate, silicon and NaOH) and a 2-step process (Hollman et al., 1999). Whereas fly-ash derived NaP1 can be produced with a high yield (45 – 75%) compared to fly-ash derived zeolites X and A (16 – 18%) in a one step process using less amount of raw materials (Moreno et al., 2001a; Moreno et al., 2000b; Querol et al., 2001; Querol et al., 2002). Thus, fly-ash derived NaP1 is preferable due to its high yield, cost and duration of production and ease of preparation.

NaP1 has been tested for removal of heavy metals (Pb, Cu, Zn, Ni, Cd and Mn) in acid mine water by Moreno et al. (2001), Querol et al. (2002) and Prasad & Mortimer (2011), electroplating wastewater by Steenbruggen and Hollman (1998), Juan et al. (2002) and Alvarez-Ayuso et al. (2003), and clean water matrix by Lee et al. (2000), Wang et al. (2006), Nascimento et al. (2009). These studies limit the scope of NaP1 applications in industry as removal conditions (i.e. pH, temperature and concentration of metals) considered were

either narrow to a localized wastewater (target specific) or not relevant to industrial conditions. In addition, current research on NaP1 does not present a clear distinction of the metal uptake mechanism (i.e. ion exchange / adsorption / precipitation) at relevant industrial conditions providing limited information to adopt NaP1 for industrial application. Steenbruggen and Hollman (1998) and Alvarez-Ayuso et al. (2003) suggested the possibility of metal recovery from NaP1 without demonstrating how this can be achieved. Thus, research on NaP1 has only remained at lab-scale without scale-up and no current information for industrial implementation.

All these works compared NaP1 to either natural clinoptilolite, other synthetic zeolites or commercial synthetic zeolites (A, X and NaP1) of the same kind with others testing NaP1 against clean water matrix, acid mine wastewater and electroplating wastewater. Furthermore, all except Steenbruggen and Hollman (1998) performed batch experiments, which exclude the use of pellets as in continuous treatment systems employed in industry. Although Moreno et al. (2001), Querol et al. (2002), Alvarez-Ayuso et al. (2003) and Prasad and Mortimer (2010) all studied the removal of metals from industrial effluents with multi-element systems, none of these works looked into the interactions and cause of removal between these elements

during an adsorption process. Also, none of these studies focused on regeneration of NaP1 after use, scale-up of the lab-scale experiments and costing involved in implementing this adsorbent on industrial scale.

Pelleting of well-known zeolites such as ZSM-5, Y, X and A have been studied by several researchers, with only one resource so far, available for NaP1 contributed by Rongsayamanont and Sopajaree (2007). Their study used bentonite as a binder and polyvinyl alcohol as a pore forming agent to create disc-shaped pellets of 70 mm diameter and 40 mm thickness through a hydraulic press.

Clearly, there is limited information in the literature to work towards the sustainable goals of reducing metal pollution into our environment through the recycling of fly-ash waste into a useful adsorbent NaP1. This research attempts to fill the gap within this area to inform on the complete study of NaP1 for heavy metal removal in industry.

1.2 Aim and objectives

Aim

The aim of the research is to provide a thorough understanding of the uptake mechanism and regeneration potential of zeolite NaP1 for removal of mixed heavy metals (e.g. lead, copper and zinc) from water. Achieving this aim will contribute towards developing a continuous adsorption/desorption process for water and wastewater using NaP1.

Objectives

- Determine the selectivity, kinetics and adsorptive capacity of NaP1 for copper, lead and zinc in a single and multi-element matrix with batch experiments.
- Identify a suitable pH working condition for effective metal removal.
- Determine the mechanism of heavy metal uptake for NaP1 from synthetic wastewater solutions using adsorption isotherm.
- Determine suitable regeneration conditions for metal recovery from NaP1. Characterize the regenerated sample to have a clear understanding of regeneration process.
- Characterize NaP1 powder and pellet
- Compare heavy metal removal performance of NaP1 pellets to commercial adsorbents.

1.3 Novelty of research

- Accounting for the effect of leaching and precipitation in adsorption experiments with fly-ash NaP1.
- Determine suitable regeneration conditions for metal recovery from NaP1 through a regeneration study.
- Assessing the evidence of NaP1 dealumination using XRD and XRF scans.
- Prepare NaP1 pellets from powder without a binder.
- Testing NaP1 pellet for multi-element adsorption.

1.4 Structure of thesis

Chapter 1 has provided a background to this study, the aim and objectives, novelty and structure of this thesis.

Chapter 2 is the literature review section which includes: an introduction to heavy metals, current legislation, heavy metals of interest, heavy metal removal technologies, adsorption as the selected technology, zeolites, conventional zeolite synthesis process, adsorption theory, adsorption kinetics and isotherm, which have been presented in this research. Further information on the initial research on fly-ash zeolite NaP1 including pelleting, regeneration and multi-element adsorption are covered in this section.

Chapter 3 describes the materials and chemicals used in the preparation of solution, characterization and pelleting and regeneration process. It further expands on the procedures used in characterizing the adsorbent material, pelleting, adsorption and regeneration processes, giving working parameters and conditions of experiments.

Chapter 4 focuses on zeolite characterization using Scanning Electron Microscope (SEM), X-Ray Diffraction (XRD) and X-Ray Fluorescence (XRF) analysis with the aim of demonstrating the presence of NaP1 after synthesis in comparison to fly-ash.

Chapter 5 demonstrates the robustness and reliability of experiments used in presenting findings from this study. Control experiments were used to test for leaching and precipitation at different experimental conditions, influence of syringe filter on experiments, calibration solutions used and limit of quantification/detection of ICP-MS (identify whether it was fit for purpose).

Chapter 6 focuses on adsorption experiments of copper, zinc and lead while assessing the kinetics, isotherms and ion selectivity of the respective metals with zeolite NaP1. Finally,

this section tests for the suitable pH of multi-element adsorption with NaP1.

Chapter 7 describes a preliminary baseline regeneration study to serve as a foundation for the final test. The purpose was to feed relevant information from this test into the final stage of metal regeneration. The parameters of interest in the preliminary regeneration test were the effect of time, pH and concentration of solution. These were latter used with selected reagents to obtain maximum regeneration.

Chapter 8 aims to convert NaP1 powder into pellets while testing it for lead and multi-element adsorption. NaP1 pellet was characterized by Nitrogen adsorption to identify surface area, pore volume and nature of pores. Comparisons were drawn with a commercial 3A pellet while a mole-based adsorption values were used to identify trends and competition in multi-element adsorption.

Chapter 9 summarizes the findings and future work relevant for the progression of this study.

2 Literature review

2.1 Introduction to heavy metals

Heavy metals including metalloids form a part of the earth's crust and an integral part of the natural environment (Yadav et al., 2019). They are found in mineral-rich ores within the lithosphere, in the oceans and water bodies including in the air, bound in different compounds of sulphides, oxides, and other metal salts (Verma and Kaur, 2016). However, their concentration varies from place to place within the earth's crust depending on the composition of the existing parent material (Furness, 2018).

Heavy metals are naturally released into the environment through volcanic activities and its resulting dust particles, weathering of rocks, erosion from soils, forest fires, biodegradation of plants and animals and dried water droplets from the oceans (Tchounwou et al., 2012). On the other hand, anthropogenic sources of emission into the environment are mainly through industrial activities (Velea et al., 2009). These industries include the alloy, chemical, leather tanning, paint, glass, pulp and paper mills, textile dying and printing, chemical fertilizer, petroleum refining, coal burning, metallurgy, mining

and ore processing and electroplating (Kabir et al., 2012; Jiao et al., 2015).

Some metals are useful to the existence of plant, animal, aquatic and human life while others are not (Izah et al., 2016). These useful metals play an important role in biochemical and physiological functions of life (Spears and Engle, 2016) within the ecosystem but are required in relatively small concentrations thus they are classified as trace/essential elements or micronutrients (Rattanachaiwong and Singer, 2019). The absence of these micronutrients is also bound to generate deficiencies and malfunctions in plant, animal, and human life. Examples of these heavy metals are cobalt (Co), copper (Cu), chromium (Cr), iron (Fe), magnesium (Mg), manganese (Mn), molybdenum (Mo), nickel (Ni), selenium (Se) and zinc (Zn) (Tchounwou et al., 2012).

Human exposure to these elements could be via inhalation of metal dust particles in the air, drinking contaminated water and beverages, oral ingestion of food (plant and animals) with high levels of these metals and physical contact with the skin (Hou et al., 2019; Rovira and Domingo, 2019). Heavy metals are soluble in water (Beochat et al., 2016) and can be absorbed into

living cells including aquatic organisms (Li and Tao, 2015). They are persistent in the environment and non-degradable in nature (Wingenfelder et al., 2005; Lakherwal, 2014). Thus, they tend to bio-accumulate (Sousa et al., 2010) in living tissues, becoming magnified in higher tropics of the food chain and consequently toxic to living organisms (Kragović et al., 2013; Tripathi and Ranjan, 2015). Thus, their release into the aquatic environment requires monitoring and control by regulations and legislations.

2.2 Legislation

Extensive and on-going research on existent and emerging pollutants (Awasthi et al., 2016; Huber et al., 2016; Cunha et al., 2018; Jeevanantham et al., 2019) have increased the awareness and further understanding of their hazards on the flora and fauna in the environment (Chibuike and Obiora, 2014; Uaf et al., 2017). Thus, placing a demand on the constant update and improvement of the current legislation governing the water treatment industries. As a result, growing legislations such as the EU Water framework directive, Groundwater Directive, and Urban wastewater directive have become stringent to ensure that industries help improve the quality of water bodies by regulating their effluents discharged into the

aquatic environment (Rule et al., 2006; Gardener et al., 2012; Gardener et al., 2013). This task performed by regulatory bodies has ensured a consistent review in the interest of establishing well-defined pollution control measures across the sub-region within their jurisdictions.

At present, more than 30 substances that previously had not been the focus of detailed monitoring and control have well-defined concentration limits used to assess water quality (EQS-EC, 2008). These substances/chemicals and heavy metals are responsible for endocrine disruption in fishes and fatal, carcinogenic and toxic even in the microgram concentration range, respectively. Therefore, current Water Framework Directive of water pollutants by Environmental Quality standards limits the presence of pollutants in effluents discharged to the environment between *ppt* (Buisson et al., 1984; W.H.O, 2003) and *sub-ppb* (1 nanogram - 0.1 micro G/l) (Environment Agency, 2011).

Previously, the solution to reducing pollutant concentration in final wastewater effluent has been through dilution with receiving waters, which has not proven effective in today's conditions with some elements (Gardener et al., 2012).

Following this, the UK Industry initiated a programme for chemical investigations (CIP) as part of the UK National Environment programme in 2012 under the supervision of UK Water Research Institute (UKWRI). The CIP was initiated to access the compliance of risk and to respond by formulating appropriate pollution control measures. The CIP was conducted in three phases by Gardener and co-workers (Gardener et al., 2012; Gardener et al., 2013) given below:

1. Investigations to assess risk from chemicals: Assessment of final effluents from 162 wastewater treatment works from England, Scotland and Wales to determine the concentration of chemicals discharged to receiving waters and their compliance with identified quality criteria.
2. Investigations to assess wastewater treatment works performance:

   Assessments of 28 wastewater treatment works to evaluate the treatment performance across primary, secondary and some tertiary treatment processes.
3. Source investigations: Assessments of nine urban catchment sources of the CIP specified chemicals discharged into sewers.

Gardener et al. (2013), reported chemical substances that have become a priority based on their concentration limit exceeding the required standard from over 50% of the wastewater treatment works. Amongst the heavy metals zinc, nickel, copper and lead were identified as exceeding their limits.

2.3 Heavy metals of interest in this study

Zinc, copper and lead are amongst the most widely researched heavy metals due to their toxicity and prevalence in the environment (Bhateria and Singh, 2019). Apart from zinc and copper, these metals are enlisted as priority substances under the environmental quality standards reference of toxic substances (EQS-EC, 2008; W.H.O, 2011). They exist as both dissolved and undissolved solids in water bodies with the former requiring advanced methods of treatment other than filtration. Knowledge of the toxicity and effects of these metals would help appreciate the need to control their concentration into surface waters.

2.3.1 Copper

Copper is noted as one of the essential heavy metals in the environment and primarily used as a metal or an alloy (Bhateria

and Singh, 2019). It is useful to plants, animals and most importantly humans (Appenroth, 2010; Mamtani et al., 2011). It is required in the human body to create red blood cells, helps in iron absorption, protects the cells and DNA from damage by free radicals and helps the body to maintain a healthy immune and nerve cell system (Mamtani et al., 2011).

However, it can be toxic in excessive doses within the human body with adverse effects. The allowable limit for copper in drinking water is 2 mg/l (W.H.O, 2004; Ongen et al., 2008) and higher doses have resulted in gastrointestinal distress, nausea, vomiting and abdominal pain as immediate responses (National Research Council (US), 2000). Furthermore, long exposure to excessive levels has been responsible for liver and kidney damage, fibrosis, anaemia, immune-toxicity, cancer and even death (Lewinsky, 2007). The maximum copper concentration permissible in industrial effluent discharge set by the USEPA is 0.25 mg/l (Tran et al., 2017).

2.3.2 Zinc

Zinc is one of the essential elements required by the body, plants, animals and micro-organisms in their daily metabolism (Jeejeebhoy, 2009; Fallah et al., 2018). The industries responsible for zinc emission into the environment are enlisted

as chemical, fertilizer, pesticide (Wu, 2017), mining, metal purifying, and steel manufacturing, coal burning and incineration sites (Zhang et al., 2011b).

The current maximum allowable zinc in drinking water and effluent discharge are set at 3 mg/l (W.H.O., 2008; Bhardwaj et al., 2019) and 0.80 mg/l, respectively (Tran et al., 2017). In aquatic organisms, a combination of high zinc concentration with pH and hardness of the water is noticed to increase fish mortality (Giardina et al., 2009; Hogstrand, 2011). In humans, taking large doses of zinc for a short time causes vomiting, cramps and nausea (Plum et al., 2010), whiles anaemia, pancreas damage and a decrease in the level of high-density lipoprotein (HDL) cholesterol are the results of a long-term exposure (Roney et al., 2006). High concentrations of zinc are stored in the bones, muscles, liver, kidney, endocrine glands and hair (Plum et al., 2010).

2.3.3 Lead

The industrial activities responsible for lead pollution are mining, smelting activities, gasoline, explosives and municipal sewage sludge (Sharma and Dubey, 2005). The allowable drinking water quality standard for lead is set at 10 µg/l by the World Health Organisation (2008) and 6.0 µg/L for effluent

discharge into surface waters (Tran et al., 2017). Excessive lead in plants strongly inhibits seed germination, root elongation, seedling development, plant growth, transpiration, chlorophyll production, and water and protein content (Pourrut et al., 2011). Exposure to fish causes death (Lee et al., 2019) while its accumulation in shellfish produces lethal and chronic effects even at 0.29 ppm (Anyanwu et al., 2018). Furthermore, exposure to humans has harmful effects on the central nervous system, reproductive system, kidney and is identified a carcinogen (Flora et al., 2012).

2.4 Heavy metal removal technologies

Chemical precipitation, ion exchange, membrane filtration, electrochemical method, adsorption, coagulation, and flotation are examples of technologies currently available for heavy metal removal from wastewater (Bisht et al., 2017). The choice of a treatment technology is based on factors such as cost and ease of operation, amount of energy required, hazards and waste management after treatment, the content of influent and final concentration of effluent required, environmental concerns and sustainability of treatment techniques (Crini and Lichtfouse, 2019).

2.4.1 Chemical precipitation

Chemical precipitation is one of the most widely used and effective ways for heavy metal removal (Dahman 2017; Ahuja, 2018). The process is easy to operate, safe and requires inexpensive equipment (Yadav et al., 2019). Lime and limestone treatment are the traditional precipitant often used in the industrial heavy metal removal (Rao et al., 2017) because of its abundant availability in many countries; it is efficient in solutions with less complex compounds and in instances where, economic recovery is not required (Zueva, 2018). The precipitates are then removed from the water by sedimentation and/or filtration for discharge or reuse (Fu and Wang, 2011). Major drawbacks with this process are the use of large quantities of chemicals, slow metal precipitation, poor settling, and excess sludge generation (Ojovan and Lee, 2014), which requires extra treatment and thus additional operational cost for disposal (Dutta and Sharma, 2019). There are also stringent regulations with sludge disposal since sludge contains heavy metals that could be leached into the environment again (Kurniawan et al., 2006, Aziz et al., 2008).

2.4.2 Ion exchange

Polymeric resins have been tested for heavy metal removal from water (Sapari et al., 1996; Rengaraj et al., 2003; Gode and Pehlivan, 2005). These resins are made-up of high molecular weight polyelectrolytes with mobile ions, which are exchangeable with ions of similar charges from the surrounding medium (Cheremisinoff, 2017). This technology is applied in the petroleum, chemical and water softening industries (Cheremisinoff, 2017). Regeneration and recovery of valuable heavy metals (Dabrowski et al., 2004) are possible. Low running cost and low energy requirement are the advantages of the method. However, high capital cost is needed for the process (Wang et al., 2009). The competition of the cations with the presence of multiple heavy metals makes the ion exchange difficult. In addition, resins can be fouled easily by components such as proteins, cellulose, living cells (bacteria), soil particles, Iron (III) ions and chlorine, when dealing with concentrated solutions. Therefore, the lifetime is reduced whilst resins generally have a long lifespan when maintained well (Kurniawan et al., 2006; Esmaeili and Foroutan, 2015).

2.4.3 Electrochemical methods

Electrochemical methods have been an improvement to already existing treatment methods such as coagulation, flocculation, flotation and the use of membranes. Electrical current is the dominant feature with the introduction of anodes and cathodes in these methods (Khattab et al., 2013). Electrochemical methods are more efficient compared to their conventional counterparts (coagulation, flocculation, and flotation) (Bazrafshan et al., 2015), reducing the volume of sludge created, the volume of chemicals used and enhancing the conventional methods by more than 10% with the ability to recover valuable metals easily. However, they require electrical energy, which could be very expensive and a huge start-up capital limiting its wide application in industry (Crini and Lichtfouse, 2018). Examples of these methods are electrocoagulation/electro-flocculation, electro-floatation, electro-oxidation and electrodialysis. Electrocoagulation is currently used in treating industrial wastewater from pulp and paper industries in North America, mining and metal-plating industries in South America and Europe (Joffe and Knieper, 2000).

2.4.4 Membrane separation

Membranes are semipermeable barriers, which control the rate of movement of molecules between two phases (Geankoplis,

2003). The types of membrane filtration employed in industry are ultrafiltration, nanofiltration and reverse osmosis depending on the particle size desired to be retained. These can be used in separating bacteria, viruses, microbes and macromolecules and further in removing dissolved salts and ions as in the case of nanofiltration and reverse osmosis (Gupta and Ali, 2013). Ultrafiltration membranes can separate heavy metals from wastewater and have gained attention due to their high efficiency, easy operation and space saving advantages (Fu and Wang, 2011). This technology is defined as a pressure or vacuum driven separation process in which particulate matter larger than 1 μm is rejected by a non-fibrous engineered barrier primarily through a size-exclusion mechanism (USEPA, 2003).

The major drawbacks with membrane technology are fouling, high operational cost resulting from fouling, biodegradation of some membrane materials and high-energy consumption in the case of reverse osmosis (Crini and Lichtfouse, 2018).

2.4.5 Adsorption

Adsorption has become a potential and viable alternative in wastewater treatment because it facilitates the removal or minimizing of heavy metal concentration even at very low

concentrations such as 0.2 mg/l (Margeta et al., 2013; Czikkely et al., 2018). It is a relatively cheaper process with the availability of raw materials (Rashed, 2013). The materials used are environmental-friendly with the possibility of effective regeneration and efficient treatment obtained (Zhang and Wang, 2011). Considering these properties, it accommodates the use of waste products, which are affordable across all economies, ranging from developed to underdeveloped countries (Abas et al., 2013). In addition, the raw materials used in the process could be tailored from the most abundant, easily accessible and obtainable products within that community and do not require the exportation of foreign materials, encouraging sustainability. Therefore, the adsorption treatment design and materials could be easily modelled to suit a location, making the process more convenient and applicable within different regions. Compared to other treatment methods, adsorption has become far more attractive and preferred to its counterparts (Margeta et al., 2013). Hence, it becomes the focus of this research.

2.5 Adsorbents

Over the years, adsorbents have emerged to meet the growing demand of cheaper and more effective techniques. Reviews in

this field have focused on properties defining the adsorbent materials such as chitin, cellulose (O'Connell et al., 2008), carbonaceous content, lignin, alumina, and silica, as a means of selecting and testing new adsorbents in the works of Pollard et al. (1992); Babel and Kurniawan, (2003); Hernandez-Ramirez and Holmes, (2008); Mohan and Pittman, (2007); Ngah and Hanafiah, (2008); Ali et al. (2012); Abas et al. (2013); Lim and Aris, (2014); Inyang et al. (2016); Malik et al. (2017); Dehariya and Lal, (2018).

Commercial adsorbents currently used in the wastewater treatment industry are activated carbon (De Gisi et al., 2016) and natural zeolites (Margeta et al., 2013). Activated carbon is the most widely used around the world due to its high porosity from micro to macroporous structures to trap low molecular weight chemicals (Hernandez-Ramirez and Holmes, 2007). Natural zeolite such as clinoptilolite is also being utilized commercially in areas of application other than water treatment as it is the most naturally abundant zeolite with large pore size and good ion-selectivity properties (Dyer et al., 2018).

2.5.1 Zeolites

Zeolites are porous inorganic crystalline structures formed by tetrahedral components of silicate (SiO_4) and aluminate (AlO_4) units connected through oxygen atoms. These alumino-silicate units present the possibility of forming a vast number of infinite lattice structures with different crystalline frameworks. The frameworks developed are composed of molecular pores with different geometries and dimensions, allowing the zeolite to be used as a molecular sieve depending on the molecule's shape and size (Hernandez-Ramirez and Holmes, 2007).

A lot of attention has been given to zeolites because of their useful properties: high thermal, mechanical and chemical resistance, high internal surface areas and molecular size pores, making them attractive for various applications such as gas and molecular separation, adsorption, ion exchange and catalysis (Perego and Millini, 2013). Naturally occurring zeolites were first discovered in the eighteenth century; nevertheless, it was the 1940s before synthetic species of zeolites were first created, some of them having no natural counterparts (Breck 1973; Cejka et al., 2007). Höller and Wirsching (1985), were amongst early researchers of zeolite synthesis from fly-ash and this was due to their observation of close compositional similarity of coal

fly-ash to volcanic material, a precursor of natural zeolite (Ahmaruzzaman, 2009).

Among all the studied natural zeolites, clinoptilolite was shown to have the highest selectivity for heavy metals of interest (Kesraoui-Ouki et al., 1994; Hernandez-Ramirez and Holmes, 2007). Clinoptilolite, chabazite, philipsite and mordenite have been used or tested in research for heavy metal removal. Campbell et al. (2018), tested natural zeolites such as analcime, stilbite, laumonites, clinoptilolite, chabazite, philipsite and mordenite, for mercury removal. They identified the following order of preference of zeolite for mercury cations ANA > CHA > STI > HEU > PHI > LAU >> MOR. Dal Bosco et al. (2005) showed the removal of Cr (III), Mn (II), Cd (II) and Ni (II) with scolecite and reported adsorptive capacity of 14.47 mg/g, 2.25 mg/g, 2.53 mg/g and 2.88 mg/g, respectively. Ibrahim et al. (2002) investigated the removal of Cu (II), Cr (III) and Fe (II) with a chabazite-phillipsite and obtained adsorptive capacity of 23.51 mg/g, 13.24 mg/g and 3.55 mg/g, respectively.

The advantages of zeolites over resins and activated carbon are their ion selective capacity, their low cost and abundant availability in nature (Margeta et al., 2013). Although activated carbon is a competitive and effective adsorbent for trace

quantity removal of heavy metals from wastewater, the high cost of production, laborious operational methods and regeneration of spent carbon (Crini et al., 2018) makes the use of zeolites a more attractive adsorbent (Margeta et al., 2013).

Synthetic zeolites

Synthetic zeolites have gained a lot of attention over the years due to their attractive properties as a possible replacement for current adsorbents in industry (Jha and Singh, 2016). They perform better than natural zeolites with high sorption capacity, amenable and tuneable properties, thermal stability and purity yield through conventional synthesis. Conventional zeolite synthesis has reproduced synthetic zeolites with similar properties, structure and framework like natural zeolites with more than 10 times sorption capacity (Alvarez-Ayuso et al., 2003), while some novel synthetic structures are yet to be identified in the current natural zeolite database (Sherman, 1999). Synthetic zeolites can be made from cheap raw materials containing precursors similar to natural zeolites and one major material is coal fly-ash; waste obtained from coal power generation plants.

Zeolite A, X, and P are examples of potential fly-ash derived zeolites from the conventional fly-ash synthesis process. Although zeolite A and X are commercially preferred due to their large pore size and high cation exchange capacity, their syntheses require a lot of raw materials whereas the resulting yield is low (between 16 and 18%). However, the yield of Zeolite P is 5 times higher than both zeolite A and X; obtained from a simple synthesis method requiring a few synthesis steps and less amounts of raw materials (Moreno et al., 2001a; Moreno et al., 2001b; Querol et al., 2001; Querol et al., 2002).

Despite these desirable properties, the potential of synthetic zeolites is yet to be fully explored in the water and wastewater treatment industry. Zeolite NaP1 amongst other synthetic zeolites is the most generated from the simple conventional synthesis method, yet its use has been limited to the detergent manufacturing industry (Cardoso et al., 2015; Sharma et al., 2016). None the less, fly-ash derived zeolite NaP1 may display different characteristics to its synthetic counterparts produced from chemical synthesis (Dubey, Goyal and Mishra, 2013).

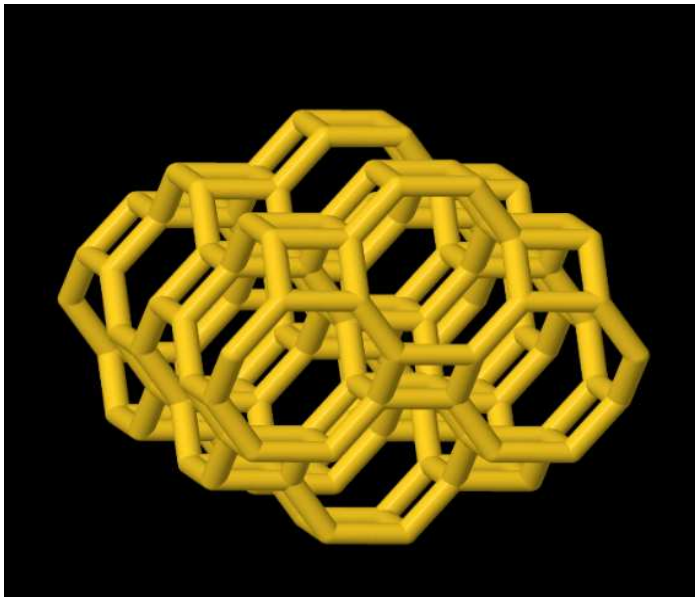


Figure 2.1: Structure of zeolite NaP1 adopted from Structure Commission of International Zeolite Association (2017)

Figure 2.1 shows the 3-dimensional structure of the NaP1 zeolite. NaP1 is the synthetic form of the gismondine-type zeolite. The crystal structure is made up of 2 dimensional pore system 8-member oxygen ringed channels (0.31 x 0.44 mm) and (0.26 x 0.49 mm) in the [100] and [010] direction respectively (Sharma et al., 2016) connected by a double crankshaft chain made up of four rings. The effective pore size of NaP1 is ~ 2.9 Å (Alvarez-Ayuso et al., 2003).

2.5.2 Coal fly-ash as reactant during zeolite synthesis

Coal fly-ash is a by-product obtained from the coal combustion plants as a result of burning finely ground coal in a boiler to produce electricity (Shumba et al., 2011). Over the past decade, the production of coal fly-ash from power plants has

increased by a great margin following the increasing demand for power from globalization, rapid industrialization and population increase. Reports from Chunfeng et al. (2009) and Shumba et al. (2011) mentioned an estimated 300 million tonnes with future predictions of an increase over the years. An update from Yao et al. (2015) has reported 750 million tonnes in 2015 with consequential increase to follow from global energy demands on coal (Gollakota et al., 2019). One of the major drawbacks of fly-ash is the enriched content of potentially toxic trace elements (Ahmaruzzaman, 2009). Therefore, coal fly-ash is considered as an environmental pollutant and requires care in its disposal and treatment. There is the need for fly-ash recycling and utilization in order to reduce the volumes of these potential hazards released into the environment.

The traditional use of fly-ash has mostly been in concrete and cement production with most of the fly-ash disposed as landfill, a practice which is of great environmental concern (Praharaj et al., 2002). However, new areas have been exploited since only about 25% of the total fly-ash is consumed globally (Hosseini et al., 2018). On that note, many researchers have suggested the possibility of utilizing fly-ash in various sectors and purposes including synthesis of zeolites (Querol et al., 2002).

Coal fly-ash zeolite synthesis

The conventional fly-ash zeolite synthesis process is done with coal fly-ash in place of synthetic sodium silicate and sodium aluminate and can be achieved through 3 phases. This is due to the rich content of these precursors in coal fly-ash. Hence, coal fly-ash is well mixed with hydroxide solution with the aid of a stirrer in a Teflon vessel. The hydroxide solution is often prepared by dissolving potassium or sodium hydroxide pellets in distilled water. The mixing phase is followed by an incubation phase, where, the mixture is kept at temperatures between 90 to 150 °C for a period of 8-24 h (Steenbruggen and Hollman, 1998; Shaobin and Peng, 2010). Based on the required target zeolite, reactions below 100 °C are heated with a thermostatic bath using a closed Teflon vessel while reactions above 100 °C are heated in an oven using steel bombs (Steenbruggen and Hollman, 1998).

This is followed by a cooling and filtration phase to obtain the solid particles from the mixture (Iqbal et al., 2019). These solid particles are later dried in the oven over a period. It is noteworthy that the experimental parameters during this synthesis process are varied to produce different types of

zeolites and is the main highlight of coal fly-ash research today. These include type of hydroxide solution, hydroxide concentration, solid/liquid ratio (S/L), temperature and incubation time (ISRIC, 1992; Cardoso et al., 2015).

The activation solution used in zeolite synthesis is either NaOH or KOH, but most studies have proven that NaOH produces better results with a higher conversion efficiency and yield over KOH (Querol et al., 2001). The concentration of activation solution adopted has been 2 – 3 M and a solid to liquid ratio of 1-20 ml activation solution for each gram of fly-ash (Hollman et al., 1999, Franus et al., 2014, Iqbal et al., 2019). The temperature of crystallization and duration of crystallization (activation time) both affect the kind of zeolites formed.

Temperature ranges between 105 and 150 °C are employed for NaP1 synthesis with a relatively short activation time, whereas low temperatures ranging between 60 and 90 °C with a longer activation time are used for X and A synthesis (Moreno et al., 2001a; Moreno et al., 2001b; Querol et al., 2001; Querol et al., 2002; Hui et al., 2005). Different zeolite phases such as Faujasite, Herschelite, Linde F, K-Chabazite, Phillipsite/KM-zeolite, Analcime, Morednite and many others can be obtained

by varying the parameters of the conventional treatment process (Querol et al., 2001; Querol et al., 2002). However, this is a field that is yet to be fully explored.

2.6 Research on fly-ash zeolite NaP1

Over the past 20 years, a limited number of studies have demonstrated the use of synthetic NaP1 for clean water and wastewater treatment on lab-scale and this section seeks to inform on current research in this area.

Steenbruggen and Hollman (1998) tested synthetic zeolite NaP1 with clean water matrix (multi-element solution) comprising Ba, Cd, Co, Cu, Ni, Zn and Pb with effluent from a wastewater treatment plant using both batch and column studies. Their study did not state the conditions of the experiments and did not quantify removal efficiency of the material. They also indicated that the results may be influenced by precipitation since the experiments were performed within pH range of 8 – 10 without adjustment. Steenbruggen and Hollman (1998), reported sorption selectivity of NaP1 in the order Ba>Cu>Cd≈Zn>Co>Ni while showing how zeolite synthesis had improved the cation exchange capacity from 0.02 to 2.4 meq/g.

Lee et al. (2000) demonstrated the superiority of synthetic NaP1 to synthetic counterparts' cancrinite, analcime, sodalite, natural faujasite and fly-ash in this study with batch experiments. Their experiments focused on metal removal (Pb^{2+}, Cu^{2+}, Zn^{2+} and Cd^{2+}) from clean water matrix of equal molar initial concentration (0.1 mM) with 0.1 g adsorbent at 25 °C. Although, there was no mention of initial pH and pH adjustment, results indicate 98, 89, 85 and 65% removal of Pb^{2+}, Cu^{2+}, Cd^{2+} and Zn^{2+}, respectively for NaP1. The adsorptive capacity of all the other adsorbents for Pb^{2+} were determined by Langmuir isotherm as a means of assessing superiority amongst the adsorbents in the of order; NaP1 > faujasite > sodalite > analcime > cancrinite > fly-ash with the following values 1.29, 1.23, 0.80, 0.75, 0.54, 0.19 mmol/g, respectively.

Moreno et al. (2001a) was amongst the first to investigate the decontamination of acid mine wastewater (multi-element solution) with synthetic NaP1 and compared its performance to a blend of commercial synthetic 4A and NaP1 through batch studies. The acid mine wastewater with initial pH of 2.5 was treated with 5-30 g/l zeolite dose for 1 hour without pH adjustment. Concentration of metals were reduced from Cu (3

mg/l), Zn (174 mg/l), Pb (1,516 µg/l) and Ni (443 µg/l) to Cu (< 0.1 mg/l), Zn (81 mg/l), Pb (< 0.1 µg/l) and Ni (315 µg/l) using 10 g/l solid/liquid ratio at pH 5.4. Their study further reported 96% removal efficiency for the same initial concentrations of Cu, Pb and Zn with commercial synthetic 4A except nickel, which produced 35% removal with 10 g/l solid/liquid ratio at pH 6.5. They later used a composite 80/20% blend of NaP1/4A to reduce leaching from NaP1, while obtaining metal reduction to Cu (0.5 mg/l), Zn (141 mg/l), Pb (< 0.1 µg/l) and Ni (373 µg/l) from the same metal concentrations with a solid/liquid ratio of 5 g/l at pH 5.1.

Moreno et al. (2001b) compared the performance of synthetic NaP1 with a blend of synthetic 4A-X zeolite for the treatment of an acid mine wastewater laden with several metals (multi-element solution) including Cu (3 mg/l), Zn (174 mg/l), Pb (1,516 µg/l) and Ni (443 µg/l) with batch experiments. Their study demonstrated an increase in pH from 2.5 to 7.1 as a result of the increase in zeolite mass (5 – 30 g/l). Zeolite 4A-X reduced initial metal concentrations to copper (0.3 mg/l), zinc (33 mg/l), lead (< 0.1 µg/l) and nickel (241 µg/l) when 10 g/l zeolite dose was used at pH 5. The zeolite 4A-X blend from Moreno at al. (2001b) performed better than NaP1 from Moreno at al.

(2001a) with zinc and nickel removal, while NaP1 performed better than zeolite 4A-X blend in copper removal. Both zeolites obtained 100% removal for lead. This could be due to the larger pore size of both 4A-X (4.1 Å – 7.3 Å) compared to NaP1 (2.9 Å). Juan et al. (2002) used NaP1 as a cation exchanger comparing it to a commercial exchanger (Amberlite IRC-50) for the removal of cations present in sewage through column studies. NaP1 displayed superiority in producing a higher retention of 0.7 meq/g, 1.16 meq/g, 1.45 meq/g and 1.57 meq/g for NH_4^+, Pb^{2+}, Zn^{2+} and Cr^{3+}, respectively, at pH 5. Pitcher et al. (2004) also demonstrated the use of another type of zeolite P (MAP), known as maximum aluminium P with Si/Al ratio ≤ 1, for metal removal from motorway stormwater. They achieved above 91% removal of Cd^{2+}, Pb^{2+}, Cu^{2+} and Zn^{2+} through batch studies with initial concentrations of 25, 50, 250 and 500 µg/l, respectively without pH adjustment.

Alvarez-Ayuso et al. (2003) later studied the sorption behaviour of synthetic NaP1 in comparison with natural clinoptilolite through batch experiments for the removal of Cr, Ni, Zn, Cu and Cd from metal electroplating wastewater. They employed metal concentration of 10 – 200 mg/l with a solid/liquid ratio of 2.5 - 10 g/l at varied pH 3 – 6 for 6 h with pH adjustment. They

reported the sorption capacity of NaP1 to be 10 times that of clinoptilolite. They further tested the treatment of nickel, chromium and acid zinc electroplating effluents at pH 6 for zinc and 4 for both chromium and nickel at solid/liquid ratio of 2.5 g/l. They obtained 66%, 86% and 91% removal for Zn, Ni and Cr, respectively, from initial concentrations of 138 mg/l, 50 mg/l and 108 mg/l in the same order.

Wang et al. (2006) demonstrated the best conditions for zeolite NaP1 synthesis with their research and further tested the zeolite for dye and metal removal (Cu and Ni) using single element clean water matrix. Wang et al. (2006) reported 90% and 70% removal for nickel and copper at 30 °C and pH 6.2, which dropped to 45% and 22%, respectively, when initial concentration was increased from 50 – 150 mg/l. They also reported 10% increase in copper removal when the temperature was increased from 30 °C to 40 °C; indicating the effect of temperature on copper adsorption. However, this was not the case with nickel. One parameter worth noting in their study was 240 hours contact time, which is the longest compared to other experiments, but this could be explained by the low solid to liquid ratio used (0.5 g/l).

Nascimento et al. (2009) also investigated the adsorption properties of fly-ash synthesized zeolite comprising zeolitic phases of zeolite A, cubic analcime, philipsite, hydroxycancrinite and zeolite P for the removal of Pb^{2+}, Cu^{2+}, Zn^{2+} and Mn^{2+} from synthetic single element solutions of concentration 100 – 3000 mg/l at 25 °C. The pH of the solutions was maintained between 4 and 5 to prevent cation precipitation. Their study showed 99% removal of Cu^{2+} and 85% of Mn^{2+} for 100 mg/l concentration of each element. Although, further details were not provided on the adsorption of Pb^{2+} and Zn^{2+}, their study concludes with a metal selectivity in the order: Pb > Cu > Mn $\geqslant$ Zn using the magnitude of adsorptive capacity obtained from Langmuir isotherm.

Finally, Prasad & Mortimer (2011) investigated NaP1, synthesised using various fly-ash samples in treating acid mine wastewater from two sources. Sorption efficiencies of both NaP1 and their fly-ash sources were evaluated for Pb, Zn, Cu and Ni removal with concentrations of 10 µg/l, 647 µg/l, 53 µg/l and 520 µg/l, respectively (multi-element solution). Batch experiments were conducted using max solid to liquid ratio of 40 g/l at pH=4.6 without adjustment. The removal efficiency

was reported as 100% Pb, 98.8% Zn, 85.6% Cu and 48.3% Ni within an hour for the NaP1.

It is noteworthy that fly-ash derived zeolites differ in properties based on their parent source material and the process of synthesis. With regards fly-ash source, the Si/Al ratio is known to contribute to the cation exchange capacity, thermal stability, hydrophobicity and catalytic activity of the zeolite (Sherman, 1999) and would play a vital role in metal uptake. Thus, a lower Si/Al ratio is known to increase metal uptake properties while a high Si/Al ratio is known to increase the thermal stability and hydrophobicity. This variation is likely to influence comparisons between different studies.

2.7 Pelleting

Unlike granules or pellets, powders are difficult to handle in the water treatment (Pizzi, 2010). They pose both operational and health risks. Using fine powder adsorbents in treating large volumes of water causes an extra challenge of ensuring the treated effluent is devoid of the spent adsorbent that will reduce the quality of treatment. In addition, regeneration and reuse of

spent powder will be unachievable since there is no guarantee of recovering such adsorbents after treatment (Bhatnagar, 2012).

Current commercial treatment methods tend to favour fixed bed process of water treatment rather than the batch process due to the advantages it presents (Patel, 2019). During this process, the adsorbents are packed in columns or towers, where, flow of the influent across the bed of adsorbent produces the desired treatment (Yang et al., 2015). Hence, using powder adsorbents will generate a high pressure drop (Yue et al., 2013) causing channelling of the influent, resulting in treatment failure (Akhtar et al., 2014; Moo-Young, 2019). Fine powder is a respiratory health hazard and can cause occupational asthma and skin irritation (Mapp et al., 2005). They can also act as a source of fuel in the case of a fire and cause ready explosions (Cloney and Snoeys, 2019). Therefore, there is the need to convert powders into desirable forms (Yue et al., 2013).

Pellets have been designed through 3 common processes such as extrusion to form cylindrical shapes, granulation to form spherical shapes and the combination of extrusion followed by rolling to form spheres (Ruthven, 1984 and Oliviera de

Magalhães, 2018). One common feature amongst these three processes is the addition of a clay binder such as bentonite, attapulgite, aluminas and kaolin, which helps bring the powdered particles together (Bingre et al., 2018).

Clay binders are generally known to improve the thermal stability, mechanical and structural properties of adsorbents (Whiting et al., 2016). However, these binders can also influence the adsorptive or catalytic properties of the adsorbent by changing the surface properties of the zeolite (Kleynhans et al., 2012). They can also contribute to clogging of the micropores (Akhtar et al., 2014; Hernando et al., 2019) of the zeolite while creating meso and macropores (Jasra et al., 2003). Thus, some researchers have resorted to developing binder-less pellets (Gleichmann et al., 2016) with binders that could be burnt-out or transformed into the final zeolite material through calcination (Pavlov et al., 2009; Schumann et al., 2012; Fawaz et al., 2018; Sun et al., 2018).

Commercially used zeolite pellets such as Y and X have been studied for the removal of methane, nitrogen, oxygen (Jasra et al., 2003), 3A for ethanol removal (Shukla et al., 2019), 13X and 4A for propylene and propane removal (Da Silva and

Rodrigues, 1999), 13X and 5A for carbon dioxide removal (Onyestyák et al., 1995). Thus, current research on the application of zeolite pellets have been directed towards either gas separation or the selective adsorption of molecules which were difficult to separate (eg. Olefin and paraffin). This is largely due to the selective adsorption nature of zeolites. While, there are limited resources available for zeolite NaP1 pellet, Rongsayamanont and Sopajaree (2007) identified to be early researchers in NaP1 pelleting. Rongsayamanont and Sopajaree (2007) used bentonite as a binder and polyvinyl alcohol as a pore forming agent to create disc shaped NaP1 pellets of 70 mm diameter and 40 mm thickness through a hydraulic press. Despite this, their study did not demonstrate the use of the designed pellet in any adsorption process.

In conclusion, there has been lots of work done in using commercial zeolite pellets A, NaX and NaY, ZSM-5 for selective adsorption/ separation of gases or molecules, which are difficult to separate. However, little attention has been paid to heavy metal removal with NaP1 pellets. This can be attested with the limited research produced in this direction.

2.8 Regeneration of adsorbent

Many studies showed suitable adsorbents for heavy metal removal but with little focus on the management of spent adsorbents (Bhatnagar and Minocha, 2006; Verbinnen et al., 2015; Lata et al., 2015). Disposal of spent adsorbents in the environment is considered as a secondary source of pollution, which consequently nullifies the aim of metal removal (Lata et al., 2015). Thus, effective regeneration/metal recovery and adsorbent reuse/recycle are considered essential qualities of a suitable commercial adsorbent. Ali et al. (2012), described these qualities as controlling factors for the cost of water treatment technology. Similarly, in a review conducted on the recovery of metals from adsorbents, Lata et al. (2015) identified various adsorbents such as activated carbon, activated alumina, silica gel, basic yttrium carbonate, metal loaded coral limestone, hematite, feldspar and hydrous zirconium oxide developed by researchers for heavy metal removal. These adsorbents were however deemed unsuitable for developing countries because of high cost, low removal efficiency and loss during regeneration.

In previous works, Mishra (2014) enlisted criteria presented by Muraleedharan et al. (1991) governing the choice of a suitable

economical adsorbent. Although they focused on bio-sorbents, these are applicable to adsorbents in general. These criteria include: (i) The adsorbent should be cheap and reusable, (ii) Metal uptake and recovery should be efficient and rapid and (iii) Regeneration of metals should preferably be metal-selective and economical feasible.

Arguably, there is a strong correlation between economical adsorbents with reusable properties and metal recovery. However, Mishra (2014) pointed out that a biosorbent can be termed economical when a suitable eluent is used for regeneration. In addition, Das (2010) mentioned that a successful regeneration process requires the proper selection of regeneration solution, which depends strongly on the adsorbent and mechanism of sorption. It can therefore be inferred that the economic viability of an adsorbent, of which regeneration plays a significant role, is not solely dependent on the adsorbent but also the recovery eluent. Thus, there is a need to identify an eluent, which does not destroy the adsorbent through the regeneration process but is efficient, cost effective, and eco-friendly (Das, 2010).

Katsou et al. (2011) studied the regeneration of clinoptilolite laden with lead and zinc from clean water matrix and wastewater. Their study obtained more than 99.5% desorption efficiency with 3 M KCl for lead (23 mg/g) and 98.5% desorption for zinc (13 mg/g) with 1 M KCl. These were achieved after over 9 and 4 successive regeneration cycles for lead and zinc respectively within 20 hours. Xu et al. (2012) later studied the regeneration of zinc-laden clinoptilolite with NaCl solutions of different properties (concentrations, pH and adsorbent–regenerant ratio). Their findings indicate zinc desorption of 0.44 g/kg of clinoptilolite when 20 g/l NaCl was used at pH 3 for 1 h with 10 g regenerant per sorbent ratio. Lata et al. (2015) has provided an extensive review on heavy metal regeneration with different low-cost adsorbents but failed to present any account of fly-ash derived zeolites.

There is evidently limited research concerning the regeneration of zeolite NaP1 in literature. Deng and Ge (2014), demonstrated 99% copper regeneration from NaP1 zeolite laden with 150 mg/l using 0.1 M NaOH solution. Prasad et al. (2013) used 0.1 M NaCl solution to recover 75% and 88% of $CaCO_3$ and calcium, respectively, from NaP1 laden with concentrations 404 mg/l and 111 mg/l, respectively in 1 hour. Both works used different

regeneration solutions (base and salt) to obtain results from NaP1 with an underlining difference in adsorbent material; indicating the need to identify a regeneration solution/eluent suitable for this NaP1. This study emulates the regeneration works of Katsou et al. (2011) in identifying the potential of NaP1 using regeneration solutions of different electrolytes (i.e. acid, base and salt) with different conditions. Hence, regeneration will be studied as a result of lack of knowledge in this area.

2.8.1 Chemical stability of adsorbent

Stability of any adsorbent is an important property to be investigated as it indicates the capability and limitations of the adsorbent under various industrial conditions (Majchrzak-Kucęba et al., 2019). Especially for synthetic adsorbents, there is a need to inform properties and working limits to determine suitable areas of application e.g., adsorption and catalysis. Parameters often tested are thermal stability and chemical stability (Shen et al., 2011; Moradi et al., 2019) in solution. Thermal stability tested by thermogravimetry (Madden and Curtin, 2016), differential thermal analysis and differential scanning calorimetry could provide useful information on dehydration, dehydroxylation and decarbonisation occurring in zeolites. It can also provide details of the quantity of organic

molecules within the pores and cavities of the adsorbent when organic substances are used in the synthesis of adsorbent material (Musyoka et al., 2015). Shevade and Ford (2004), tested the stability of zeolite NY6 for arsenate removal in solutions over a pH range of (2-13.2). Their XRD pattern showed zeolite NY6 to be unstable at pH 13.2 whilst working well within the range of 2-12.

In addition, Cruciani (2006) established a correlation between stability index and Si/Al ratio of natural zeolites with the conclusion that the latter had an influence on their stability. Their research, which compared the thermal stability of different types of zeolites with XRD studies, showed that zeolites with Si/Al ≤ 1.28 are unstable, Si/Al ≥ 3.80 are very stable and stability of zeolites with 3.80 ≤ Si/Al ≥ 1.28 cannot be determined from Si/Al ratio. Cruciani (2006) also determined that molecular sieve effects are enhanced in the dehydrated/calcined state and at relatively high temperatures. Thus, the understanding of the zeolite behaviour upon heating is of importance since there is a direct impact on sorptive and catalytic properties. Most zeolites may be dehydrated to some degree without major alteration of their crystal structure. They may subsequently be rehydrated from surrounding vapour while

others undergo irreversible structural changes and suffer total structural collapse when completely dehydrated (Breck, 1973).

2.9 Experimental conditions for metal removal via adsorption

2.9.1 Heavy metal concentration

Most research on adsorption have focused on using adsorbents to solve point-source pollution from industries within localised areas. Hence, concentration ranges selected for laboratory scale experiments are designed to suit specific places of interest. This limits the direct application of adsorbents on a broader scale to other industries without further laboratory tests. Although heavy metal concentrations from industries differ from place to place, in order to propose a product for commercial viability, there is a need to test the adsorbents across a range of existing industrial concentrations around the world.

Table 2.1, summarizes industrial wastewater concentrations from different parts of the world with varied heavy metal concentrations including copper: 5.19 – 1500 mg/l, zinc: 1.98 – 972 mg/l and lead: 0.005 – 709 mg/l. High end concentrations of metals from industrial effluents were obtained from metal electroplating industries in India and Turkey (Kadirvelu et al.,

2001; Kul and Oskay, 2015; Ghorpade and Ahammed, 2017), while low end concentrations were noted from Canada and Malaysia (Da'na and Sayari, 2012; Rahman et al., 2016). Concentrations of metals in this study were selected for both adsorption kinetic and isotherm experiment considering these industrial circumstances.

Again, concentrations were selected to account for possible fluctuations that may increase concentrations during industrial capacity expansion or change in industrial operations (considering a worst-case scenario). On the other hand, the high-end concentration for all metals; copper, zinc and lead with extreme values (1500, 972 and 709 mg/l, respectively) were discarded for kinetic experiments and considered as outliers since they negatively influenced the selection process. They were treated as extraordinary circumstances spiking the concentration range. Hence, the second highest concentration of metals; lead, copper and zinc (55, 98 mg/l and 168 mg/l respectively) were used for adsorption kinetic experiments while the high-end concentration values were still utilized in adsorption isotherm experiments.

Table 2.1: Concentration of copper, zinc and lead in wastewater from various countries and industries.

Location	Industry	pH	Copper (mg/l)	Zinc (mg/l)	Lead (mg/l)	References
India	Copper Electroplating	2.1	126	-	-	Kadirvelu et al., 2001
India	Radiator manufacturing	1.45	-	-	709	Kadirvelu et al., 2001
China	Electroplating	2.2	57.81	14.75	-	Wei et al., 2013
India	Electroplating	5.6	12.94			Husain et al., 2014
Tunisia	Electroplating wastewater	n/a	33	41		Adhoum et al., 2004
Iran	Battery making	5.6	n/a		55.5	Malakootian et al., 2011
Iran	Electroplating	6		41		Malakootian et al., 2011
Iran	Copper industries	5.8	57			Malakootian et al., 2011
Canada	Electroplating	n/a	25.9	17.5	0.6	Da'na and Sayari, 2012

Table 2.1: ……*continued.*

Location	Industry	pH	Copper (mg/l)	Zinc (mg/l)	Lead (mg/l)	References
Serbia and Montenegro	Electroplating	n/a	18.9	76.3		Sciban et al., 2007
China	Clean water matrix	5.5	30			Zhu et al., 2009
Turkey	Clean water matrix	4	25 - 250			Aksu and Isoglu, 2005
Leeds	Clean water matrix	5 - 6	50 - 200	n/a	50 - 200	Amarasinghe and Williams, 2007
China	Electroplating	5 -14		1.98 – 13.8		Xu et al., 2015
Nigeria	Electroplating	n/a	43.5	17.4	0.005	E. Bernard et al., 2013
India	Electroplating	0.66	1499	972	26.1	Ghorpade and Ahammed, 2018
Turkey	Electroplating	1.6	1527	689		Kul and Oskay, 2015
Malaysia	Electroplating	4	5.19	75.9	0.013	Rahman et al., 2016
Nigeria	Electroplating	0.83	97.57	167.6	4.94	Bankole et al., 2019

*Clean water matrix, also known as Laboratory prepared solution/ synthetic wastewater

2.9.2 Adsorbent mass

Adsorbent mass has been studied by many researchers as another influential parameter in the adsorption process of heavy metals. Rightly so, the concept of varying adsorbent mass can be described by the principle of collision, where, an increase in the number of adsorbent particles produces an effective increase in particle collision and increases the number of adsorptive surfaces for adsorbates. This increases the chances of adsorbent/adsorbate interaction and consequently increasing the adsorbate uptake. Reviewing several articles, the mass of different adsorbents has been varied based on the required uptake target of the adsorbent and how effective it has been within its optimal operating conditions such as pH, temperature and influent characteristics.

Sprynskyy et al. (2006) researched the removal of 20 mg/l each (lead, copper and nickel) with 0.5 g clinoptilolite in 200 ml aqueous solution. Zanin et al. (2017), also used the same mass (0.5 g) of clinoptilolite for the removal of 10 mg/l each (Iron, chromium and copper) in 100 ml solution. Tarek et al. (2010) studied the removal of 20 mg/l each (cadmium, copper, lead, zinc and nickel) with 0.8 g of zeolite A and X in 100 ml solution. Finally, Kocaoba et al. (2006) identified the optimum clinoptilolite amount for the removal of 100 mg/l each

(cadmium, copper and nickel) in 100 ml solution was 0.8 g. In all these studies, it was observed that > 80% metal removal was obtained (with 5-8 g adsorbent per litre of solution) and further increase in the adsorbent mass beyond this point did not cause a drastic change in the metal removal percentage. Varying the adsorbent mass together with other parameters is one way of effectively using the adsorbent material.

2.9.3 pH

pH is known from various studies as one of the determinants of adsorption and has a significant influence on adsorbent performance and solubility of the metals. Dean et al. (1972) published pH values of precipitation for heavy metals while studying heavy metal removal from wastewater, as shown in Table 2.2. They indicated the appropriate pH for dilute concentrations of metals and above this, precipitation of metal hydroxides was encouraged.

Table 2.2: Precipitation pH of metals adopted from Dean et al. (1972).

Metal ion	Precipitation pH	Metal ion	Precipitation pH
Fe^{3+}	>2.0	Na^{2+}	>6.7
Al^{3+}	>4.1	Cd^{2+}	>6.7
Cr^{3+}	>5.3	Zn^{2+}	>7.0
Cu^{2+}	>5.3	Hg^{2+}	>7.3
Fe^{2+}	>5.5	Mn^{2+}	>8.5
Pb^{2+}	>6.0	Co^{2+}	>6.9

On the other hand, several studies have used pH 5 or 6 (Moreno et al., 2001; Querol et al., 2002; Alvarez-Ayuso et al., 2003; Wang et al., 2005; Amarasinghe and Williams, 2007; Kocaoba et al., 2007; Wang et al., 2008; Zhu et al., 2009; Motsi et al., 2009; Krobba et al., 2012) for copper adsorption studies while others have used 3.5 – 4 (Aksu and Isoglu, 2005; Nascimento et al., 2009). Kumar et al. (2007) removed nickel from aqueous solution with Zeolite NaX at pH 5, while Qiu and Zheng (2009) employed pH 6 for the removal of lead, copper, nickel and zinc with a cancrinite type zeolite. Nibou et al. (2010) studied zinc removal on zeolite NaX and NaA at pH 6 while Rao et al. (2006) identified pH 6.5 to be optimal for zinc removal with zeolite 4A and 13X.

However, the choice of pH depends on the adsorbent, concentration of metal, solubility and type of metal to be tested. Consequently, identifying the best pH would be aimed at obtaining optimal metal removal without the effect of precipitation and leaching.

2.9.4 Solubility of metal ions

Factors affecting solubility of heavy metals at 20 ± 2 °C are pH and concentration of metal ions in water. Metal salts dissolved in water dissociate to form constituent cations and anions, following the hydration of the metal ions. These metal ions form metal complexes with ligands (e.g. water molecules) through coordinate bonds. The result is the formation of hexaaquo complex ions with an octahedral shape of water molecules bonded to it (Krężela and Maret, 2016).

However, hydroxides of these metal ions (which are insoluble in water) can form within certain pH and concentration range. Figure 2.2 is a theoretical solubility plot of dissolved copper concentration and pH indicating that copper concentration within 0.001 - 100 mg/l is soluble at a pH range between 2 and 5.5, whereas the higher-end of the same concentration range (10 - 100 mg/l) is likely to initiate copper hydroxide

precipitating above pH 5.5. Concentrations above 100 mg/l are needed to be assessed for possible precipitates through further tests.

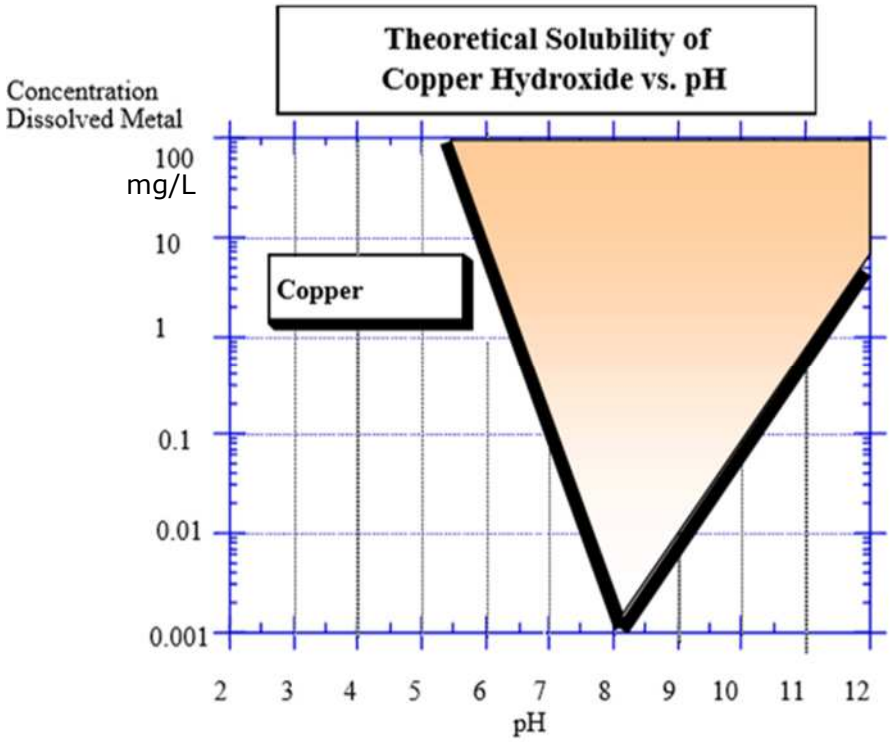


Figure 2.2: Theoretical solubility of copper hydroxide (Cushnie, 1985).

Unlike copper, zinc concentration ranging between 0.1 and 100 mg/l remain soluble in water within pH 2 and 7 after which zinc hydroxide precipitates are likely to be formed (Figure 2.3). Similarly, solubility of lower range zinc concentrations 0.001 - 0.1 mg/l is observed not to be affected by pH at 20 ± 2 °C. Thus, there is no possible zinc hydroxide precipitation from pH 2 to 12 with low concentrations of zinc (0.001 - 0.1 mg/l) at 20 ± 2 °C.

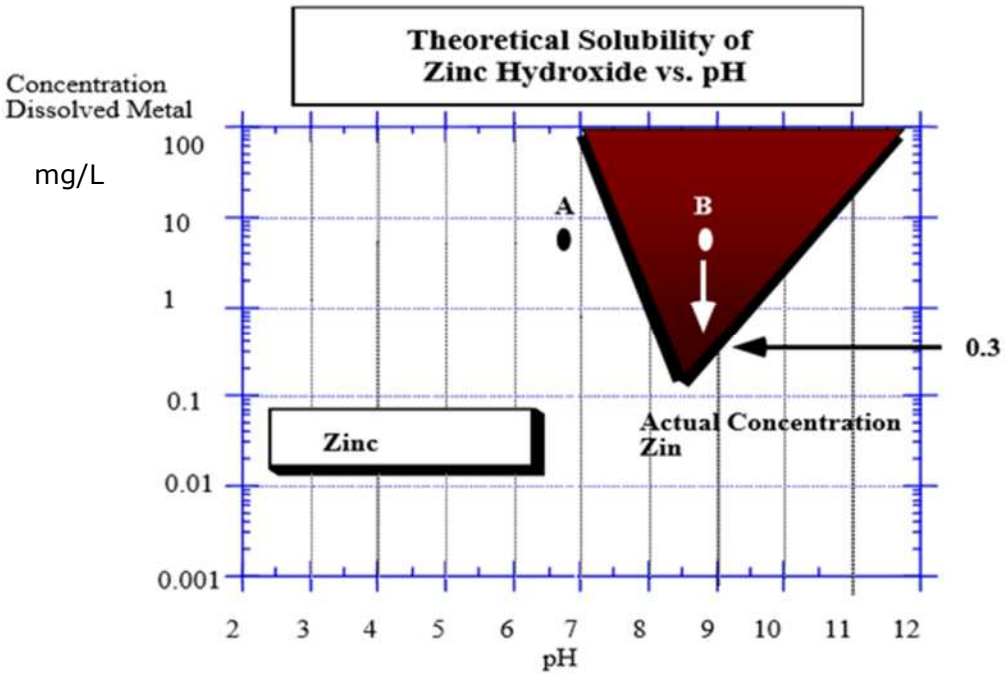


Figure 2.3: Theoretical solubility of zinc hydroxide (Cushnie, 1985).

Lead ions amongst the selected metals display the widest range of concentration and pH for its solubility in water at 20 ± 2 °C (Figure 2.4). The possibility of lead hydroxides forming is predicted over a narrow pH range between 8 and 10.5 for concentrations within 10 to 100 mg/l. In view of these observations, Lee et al. (2000) employed a metal concentration of 20 – 400 mg/l at 20 ± 2 °C for lead, zinc and copper solutions. Wang et al. (2006) used 50 – 150 mg/l concentration solutions of copper at pH 6.2. Moreno et al. (2002) also used 0.24, 0.316, 36 and 54 mg/l concentration solutions of lead,

nickel, copper and zinc, respectively in adsorption experiments at pH 5.5.

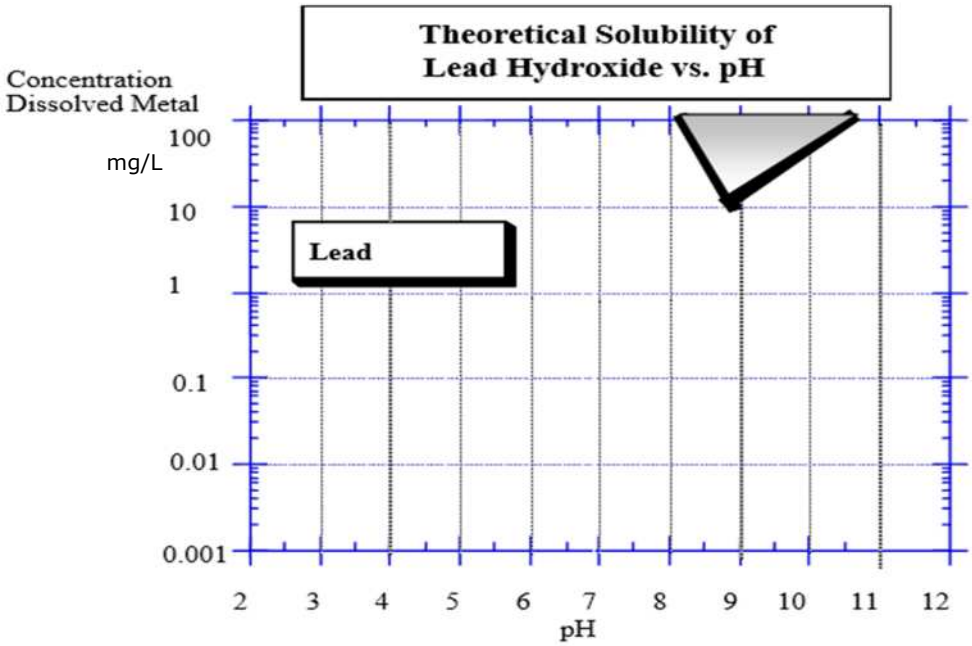


Figure 2.4: Theoretical solubility of lead hydroxide (Cushnie, 1985).

Although, the theoretical solubility graphs presented in this literature (Figures 2.2, 2.3 and 2.4) are informative, they are also limited to a concentration range 0.001 - 100 mg/l and would not inform the extent of metal hydroxide precipitation at higher concentrations (100 – 3000 mg/l). Hence, a control experiment would be used to investigate precipitation at high end concentrations employed in this research.

Nibou et al. (2010) treated 80 – 100 mg/l Zn from industrial wastewater from Algeria with zeolite NaA and NaX. Ismail (2010) tested zeolite X calcined from kaolin for the removal of 500 mg/l synthetic zinc solution. Rao et al. (2006) studied the removal of (25 -100 mg/l) aqueous cadmium and zinc synthetic solutions with zeolite 4A, 13X and bentonite. Apiratikul and Pavasant (2008) researched the removal of copper, cadmium and lead from 0 – 500 mg/l aqueous synthetic solution using zeolite X like Ismail (2014). These are similar concentration ranges employed in metal removal with these zeolites but possible varying solid/liquid ratio. However, they have one thing in common and this was the absence of precipitation check.

2.9.5 Multi-element clean water matrix

In the past, research on heavy metal adsorption from wastewater has mainly focused on single element adsorption systems (Rinaudo and Goycoolea, 2019). This was done with the aim of understanding the relationship between metal-adsorbent properties for various elements towards scale-up and industrial applications (Liu et al., 2008). However, real-world effluents contain a mixture of metals instead of single elements (Yaseen and Scholz, 2019). Therefore, there is a need to test

the interaction of these elements (Pb, Zn and Cu) with the adsorbent in a mixed system (Ouyang et al., 2019).

Batch equilibrium studies provide information as to the total capacity of a sorbent for a metal(s) in single element or multi-element systems (Patel, 2019). Additionally, isotherm constants, necessary in the mathematical modelling of sorption systems, may be obtained from representing equilibrium data as isotherm plots (Allen and Brown, 1995).

Multi-element adsorption studies should follow an accurate determination of equilibrium for single element adsorption systems, where, the elements are in their pure form. This helps to form a basis of comparison for multi-component systems. Multi-element equilibrium studies could be either through mass (weight) basis or mole (molar) basis (Ting and Teo, 1994; Bouhamed et al., 2015 and Jain et al., 2016). A mass-based equilibrium study gives a universal (real world) means of quantifying the metals, while a mole-based study presents a measure of the total number of ions adsorbed by the adsorbent. Mole-based quantification is an indication of the total number of sites available within the adsorbent. Hence, the mole-based measurement is preferred to the mass-based since it is more accurate in determining competition between multi-component metal mixtures (Allen and Brown, 1995). Multi-element

adsorption systems are complex to interpret because of the possible competition between existing metals/ions in the system and interaction between the solute and adsorbent surface (Neris et al., 2019). Other complexities arise from several factors that could potentially explain the behaviour of a multi-component adsorption system with the difficulty of pinpointing which factors are directly responsible (Gao et al., 2009).

These factors including electronegativity, ionic radius, solution pH, hydration capacity, adsorbent nature and capacity (Nguyen et al., 2015), would be taken into consideration during the multi-element study. As seen from Table 2.3, there has been less work done on the multi-component adsorption for NaP1 in comparison to other zeolites. Fly-ash zeolites 4A (Hui et al., 2005), Cancrinite (Qiu and Zheng, 2009), fly-ash zeolite (Visa et al., 2012) and Linde F (Cheng et al., 2018) have been tested for multi-component adsorption of heavy metals without a comparison to single-component adsorption, with the exception of Jha et al. (2008 and 2009) for fly-ash X.

Motsi et al. (2009), Hamdache et al. (2019) and Li et al. (2019) all focused on multi-component adsorption of metals on natural zeolites; bentonite, clinoptilolilte and NaCl-modified

clinoptilolite respectively in comparison to single-component adsorption. Lead, zinc and copper have been metals of focus from Table 2.3. Adsorption capacity values have been reported in mg/g for most studies except for Lee et al. (2000), Jha et al. (2008 and 2009) and Qiu and Zheng (2009) in mmol/g.

Table 2.3: Single and multi-component adsorption of heavy metals from literature.

Zeolite	Metal	Surface area (m^2/g)	Conc. (mg/l)	Conc. (mg/l)	Adsorptive capacity single (mg/g)	Adsorptive capacity Multi (mg/g)	2nd order (mg/g)	pH	Temp	S/l ratio (g/l)	Si/Al ratio	Time	Reference
NaP1	Cu Pb Zn Cd	-	0.1mM Or 20mg/l	0.1 – 2.0mM	267.2 1.29mmol	73.5 266.4 65.8 117.6	-	-	25	-	1.2	-	Lee et al., 2000
NaP1	Cu Zn Ni Cr Cd	27.7	10-200	100	50.5 32.6 20.1 43.6 50.8	-	-	4-6	-	2.5	1.7	6 h	Alvarez-Ayuso et al., 2003
NaP1	Cu Zn Pb Mn	-	100	100 - 3000	76.9 59.2 194.7 60.4	-	-	4-5	25	10	1.00	24 h	Nascimento et al., 2009
Fly-ash X	Ni Cd Cu Pb	67	500 500 500 1000	20-500 100-2000	1.20 1.44 1.72 2.65	0.721 mmol/g 0.131 2.598 3.165	1.12 1.08 1.67 1.23	6.8 - 7.5	25	2	2	24 h	Jha et al., 2008 Jha et al., 2009
Fly-ash Cancrinite	Pb Cu Ni Co Zn	278	-	0.5 – 4 mmol	-	2.130 mmol 2.081 1.532 1.242 1.154	-	6.0	25	0.5	1	2/72 h	Qiu and Zheng 2009

Table 2.3: ……*continued*.

Zeolite	Metal	Surface area (m^2/g)	Conc (mg/l)	Conc (mg/l)	Adsorptive capacity single (mg/g)	Adsorptive capacity Multi (mg/g)	2nd order (mg/g)	pH	Temp	S/l ratio (g/l)	Si/Al ratio	Time	Ref
Fly-ash zeolite	Pb Zn Cd	37.97	-	1350 350 700	-	2.009* 13.387 28.089	2500 18.87 30.21	6.6	20 - 25	5	2.4	1.5 h	Visa et al., 2012
Bentonite	Cu Zn Ni	-	2 mmol	10 - 1000	58.48 49.02 31.74	58.82 19.53 6.56	33.33 6.060 1.338	5	20	3	4.8	24 h	Hamdache et al., 2019
Clinoptilolite	Fe^{3+} Cu Mn Zn	15.88	400 120 20 20	40, 120	3.4 2.7 2.7 2.3	3.2 1.3 0.8 0.7	-	3.5	-	37	5.36	6 h	Motsi et al., 2009
Fly-ash 4A	Co Cr Cu Ni Zn	54.82	100	50 - 300	-	13.72 41.61 50.45 8.96 30.80	5.50 56.47 72.73 4.95 20.10	4	25	5	1.32	4 h	Hui et al., 2005
Fly-ash Linde F	Ni Cd Cu Pb	-	100	400	-	7.51 20.5 17.52 45.1	8.757 21.59 18.31 46.51	6	25	2	-	8 h	Cheng et al., 2018
NaCl-modified Clinoptilolite	Zn Cd Cu Pb	-	400	10 - 2500	28.12 37.30 29.20 45.30	3.60 23.10 13.60 44.40	28.98 38.80 29.96 177.6	5	25	10	5.36	4 h	Li et al., 2019

All the works from Table 2.3, reported similar working parameters with a few distinctions. The adsorption temperature was between 20 – 25 degrees Celsius while pH was maintained between 4 - 6 except Motsi et al. (2009) and Jha et al. (2008) and Jha et al. (2009) being the only two to use pH 3.5 and 7.5 respectively. Again, all fly-ash zeolites from Table 2.3 showed an Si/Al ratio between 1 – 2.4 while natural zeolites (bentonite and clinoptilolite) were in the range of 4.8 – 5.36.

However, the solid to liquid ratio of fly-ash derived zeolites employed in the adsorption experiments were low in the region of 0.5 – 10 g/L, while that of natural zeolites was between 3 – 37. Clinoptilolite by Motsi et al. (2009) used the most adsorbent per liquid ratio (37) while bentonite used the least adsorbent/liquid ratio (3) in Hamdache et al. (2019).

Fly-ash zeolite cancrinite used the lowest solid/liquid ratio 0.5 while clinoptilolite used 37 and this could be due to the large difference in surface area. Hence, fly-ash cancrinite with the largest surface area 278 m^2/g compared to clinoptilolite with the least surface area 15.6 m^2/g may be partly responsible for the difference in solid/liquid ratio requirement. However, the effect of using a low solid/ratio is noticed in the contact time, where, Qiu and Zheng (2009) used the longest contact period

recorded from literature compared to its counterparts (Table 2.3). Maximum contact periods for all other experiments were in the range of 1.5 to 24 h while concentration range varied for metals between 10 – 3000 mg/l across all experiments.

Li et al. (2019) investigated the sorption behaviour of synthetic clinoptilolite with multi-component aqueous solution containing 400 mg/l each of lead, zinc, copper and cadmium with 10 g/l solid to liquid ratio. Their study obtained an adsorption capacity of 31.47 mg/g (zinc), 181.8 mg/g (lead), 44.64 mg/g (cadmium), and 33.76 mg/g (copper) at pH 5 and 25 °C from Table 2.3.

In comparison to single element adsorption by clinoptilolite under the same conditions, Li et al. (2019) reported a lower adsorptive capacity for multi-component uptake than single component uptake for all elements except lead. Lead was the only element with the same adsorptive capacity both in the single and multi-component adsorption, thus not influenced by the competition posed by other ions in the multi-component solution (Table 2.3). Their work presented metal selectivity in the order Pb^{2+} > Cd^{2+} > Cu^{2+} > Zn^{2+}. Metal selectivity from multi-component systems with other natural zeolites (Bentonite

and Clinoptilolite) followed a similar pattern; $Cu^{2+} > Zn^{2+} > Ni^{2+}$ (Hamdache et al., 2019) and $Fe^{3+} > Cu^{2+} > Mn^{2+} > Zn^{2+}$ (Motsi et al., 2009) respectively.

Similar to natural zeolites, fly-ash derived zeolites NaP1 by Lee et al. (2000); $Pb^{2+} > Cd^{2+} > Cu^{2+} > Zn^{2+}$, Alvarez-Ayuso et al. (2003); $Cd^{2+} > Cu^{2+} > Cr^{3+} > Zn^{2+} > Ni^{2+}$ and Nascimento et al. (2009); $Pb^{2+} > Cu^{2+} > Mn^{2+} > Zn^{2+}$ demonstrated a similar order of metal selectivity to Li et al. (2019) for metals in single-component adsorption systems and multi-component adsorption by Hui et al. (2005) with fly-ash 4A; $Cu^{2+} > Cr^{3+} > Zn^{2+} > Co^{2+} > Ni^{2+}$ and Cheng et al. (2018) with fly-ash Linde F; $Pb^{2+} > Cd^{2+} > Cu^{2+} > Ni^{2+}$.

In contrast, Jha et al. (2008) and Jha et al. (2009) identified a different order of selectivity in both single: $Pb^{2+} > Cu^{2+} > Cd^{2+} > Ni^{2+}$ and multi-component system: $Pb^{2+} > Cu^{2+} > Ni^{2+} > Cd^{2+}$ with fly-ash zeolite X. Reports from Jha et al. (2009) indicate the order of metal selectivity in multi-component systems was similar to Qiu and Zheng (2009), with fly-ash cancrinite demonstrating that the order of selectivity was dependent on a number of factors including the metals in competition within the

multi-component system, pH, type of adsorbent surface and pore size of adsorbents.

2.10 Adsorption theory

Adsorption is the surface phenomenon, which can be expressed as the increase in concentration of a component at the surface of another material from two mediums. This is due to the unbalanced forces of attraction which atoms are subjected to, normal to the surface plane within a solid or liquid medium. Thus, the adsorption process occurs between two components; the adsorbent and the adsorbate. The adsorbent is described as the component with the surface producing the attractive forces and the adsorbate refers to the components whose atoms are being attracted to that surface (Noll, 1991).

Adsorption can be classified into two main types;

- Physical adsorption (referred to as Physisorption)
- Chemical adsorption (referred to as Chemisorption)

Table 2.4 presents a summary of the differences between these adsorption types comparing their properties. The occurrence of either sorption phenomenon is dependent on the chemical composition of the adsorbent surface and the interaction

between the adsorbate under different conditions of pH and temperature.

Table 2.4: Difference between Physisorption and Chemisorption (Noll, 1991; Venables, 2000; Bhushan, 2012).

Properties	Physisorption	Chemisorption
Bonds	Weak vans der Waals forces of attraction	Covalent bonds
Reactions	Reversible or desorption at same temperature	Irreversible or might require large amount of energy for desorption
Activation energy	Less activation energy	High activation energy
Temperature	Occurs at low temperatures	Occurs at high temperatures
Adsorbent material	Not site specific	Is site specific

This research will identify the type of adsorption which occurs between heavy metals and fly-ash derived zeolite.

2.10.1 Adsorption kinetics

The kinetic study of adsorption processes provides the efficiency of the adsorption and the feasibility of scale-up operations (Minceva et al., 2007). Both chemical and physical properties of

an adsorbent affect the adsorption kinetics and overall, on the adsorption mechanism. The adsorption or solute transfer mechanism is generalized for most adsorbents and described in four main steps (Montanher et al., 2007):

- Boundary film migration of solute particles from aqueous solution.
- Movement of solute particles to the adsorbent surface from the boundary film (external diffusion).
- Movement of solute particles from the adsorbent surface through the adsorbent pores to the intra-particle active sites (intra-particle diffusion).
- Attachment of solute particles on the active sites within the adsorbent.

The adsorption kinetic data can be determined by using several models namely: pseudo-first order reaction, pseudo-second order reaction, Elovich, intra-particle diffusion plot, etc. These will be used in this study.

Kinetic Models

The pseudo-first order kinetics based on Lagergren's equation is applicable only when the experimentally obtained equilibrium concentration (q_e) value is the same as that obtained from this

model. On the other hand, second order kinetics is used when the first order kinetics model is not applicable to systems. This is observed by the discrepancy in experimentally obtained and calculated q_e values (Ho and McKay, 1999). The Elovich equation describes second order kinetics for energetically heterogeneous solid surfaces. A linear plot of these models is produced using experimental data and constants obtained are used in describing the adsorption mechanism. Table 2.5 shows the equations adopted for the linear plot of each model stated including the constants required to describe the kinetics of the adsorption mechanism.

Regression coefficient (R^2) of each linear plot is used to identify the suitability of the model in describing the mass transfer mechanism of the metal uptake phenomenon. Thus, R^2 determined through method of least squares > 0.95 is appropriate as it represents a confidence interval > 95% of correlation to the experimental data.

Table 2.5: Adsorption Kinetic models.

Kinetic models	Equation	Linear plot	Rate Constant	References
Pseudo 1st order	$\frac{dq_t}{dt} = k_1 (q_e - q_t)$	Log (q_e - q_t) vs. t	K_1	Lagergren, 1898
Pseudo 2nd order	$\frac{dq_t}{dt} = k_2(q_e - q_t)^2$	t/q_t vs t	K_2	Blanchard et al., 1984; Ho and McKay., 1995; Kumar, 2007
Elovich	$q_t = \beta \ln(\alpha\beta) + \beta \ln t$	q_t vs. ln t	α, β	Chien and Clayton, 1980; Rudzinski and Panczyk, 2002; Ho, 2006

Variables used:

- q_e amount adsorbed per unit mass at equilibrium
- q_t amount adsorbed per unit mass at any time t
- K_1 is the first order constant of the reaction
- K_2 is the second order constant of the reaction
- β desorption coefficient
- α initial adsorption rate

Pseudo-second order reaction kinetics helps to identify the possible uptake mechanism and rate-limiting step of the metal uptake process (mass transfer process). Kumar (2007) compared pseudo-second order models proposed by Blanchard et al. (1984) and Ho and McKay (2000). He concluded that both models have similar ideas with different assumptions. Blanchard et al. (1984) suggested an ion exchange mechanism to be responsible for the uptake process while Ho and McKay proposed monolayer coverage and chemical adsorption to be responsible for the uptake process (Kumar, 2007).

Although, both models were developed based on heavy metal uptake, they used different adsorbents. Blanchard et al. (1984) was based on a natural zeolite (clinoptilolite) and Ho and McKay (2000) was based on peat. These adsorbents had different surface areas, functional groups and properties, displaying metal removal mechanisms based on their characteristics. Thus, the pseudo-second order reaction model could be either describing chemisorption or ion exchange depending on the adsorbent. However, in research today, many have had the pitfall of concluding chemisorption without considering the similarity of their material to that used in these models.

2.10.2 Adsorption isotherm

Adsorption isotherms are mathematical expressions used in linearizing complex functional models applied in describing an adsorption process with the aim of explaining the phenomenon. These linear expressions help in determining constants from the slope and intercept of the equation, which is used in describing the intensity of adsorption, adsorptive capacity, energy of adsorption and other characteristics of the adsorption process. The few widely used isotherms in describing characteristics of adsorbent-adsorbate relationship at equilibrium are Freundlich, Langmuir, Temkin, and Redlich-Peterson. Amongst these, Freundlich and Langmuir are the most commonly used.

Freundlich isotherm is applied in describing the adsorption phenomenon of heterogeneous adsorbents with multilayer formation of single adsorbates on the adsorbent surface.

This model expresses that at a constant temperature, the quantity of adsorbate uptake per mass of adsorbent (Q_e) is a logarithmic function of the residual concentration at phase equilibrium (C_e). Thus, at low adsorbate concentrations, the quantity of adsorbate uptake rises with an increase in solution concentrations but approaches a constant value at larger concentrations (Proctor and Toro-Vazquez, 1996).

In view of this, the gradient of curve obtained is greater at low concentrations of solute and reduces with an increase in concentration. Freundlich isotherm, however, has no saturation limit nor henry law limit and cannot be applied over an extensive adsorbate concentration range. The Freundlich equation is represented by equation in Table 2.6.

Table 2.6: Comparison of Langmuir and Freundlich adsorption theory (Chung et al., 2015).

Properties	**Freundlich**	**Langmuir**
Adsorbent surface	Heterogeneous	Homogenous (flat)
Adsorption	Multilayer	Monolayer
Limit	No saturation limit	Saturation limit
Concentration range	Low range	Wide range
Equation	$Q_e = K_F . C_e^{\frac{1}{n}}$	$\frac{C_e}{q_e} = \left(\frac{1}{bq_m}\right) + \frac{C_e}{q_m}$
Linear plot	Log Q_e vs. Log C_e	C_e/Q_e vs. C_e
Adsorptive capacity constants	K_f	Q_m
Isotherm constants	n showing favourable isotherm, heterogeneity and to distinguish between physisorption and chemisorption	b showing adsorbent affinity to metal

In the equation, K_F is the constant of Freundlich isotherm indicating the adsorption capacity of the adsorbent and 1/n is a representation of the adsorption intensity between the adsorbent and adsorbate molecules. A value of n between 1 and 10 is a suggestion of a favourable isotherm to the experiment Desta (2013). Desta (2013), identified the n value to also demonstrate the degree of nonlinearity between solution concentration and adsorption. Such that an n = 1 depicts a linear adsorption, n < 1 shows a chemisorption phenomenon while n > 1 signifies a physisorption process.

Langmuir (1918) modelled his adsorption isotherm on the kinetic principle stating that the adsorption rate is the same as the desorption rate of molecules from a flat surface (Ismadji et al., 2015). Langmuir's model helps in determining the affinity of adsorbates to adsorbent and adsorptive capacity of the adsorbent. It has a henry law limit, finite saturation limit and can be used over a wide range of concentration (Soni, 2014).
The Langmuir isotherm model is based on the assumptions of a fixed number of sites with no interaction between adsorbed molecules (Ruthven, 1984) and these assumptions are homogenous adsorbent surface, localized adsorption sites and single molecular sites (Do, 1998).

Langmuir isotherm, which assumes a monolayer adsorption on the adsorbent surface, is expressed in Table 2.6 (Crittenden et al., 2012; Chung et al., 2015).

Where, C_e in the equation is the adsorbate concentration in the solution at equilibrium, q_e is the amount of solute adsorbed per unit mass of adsorbent, b is the constant of Langmuir isotherm and q_m is the maximum adsorptive capacity of the adsorbent at equilibrium. The Langmuir constants (b) represents the affinity of the adsorbent for the adsorbate and related to the energy of sorption (enthalpy of hydration), while (q_m) represents maximum adsorptive capacity of the adsorbent. These constants are determined from the intercept and slope of the line respectively. The lower the value of b for an experiment, the higher the affinity of the adsorbate towards the adsorbent, while a higher value of adsorptive capacity implies high uptake of the adsorbate by the adsorbent (Davis et al., 2003).

2.10.3 BET and BJH Methods from Nitrogen adsorption

Determination of pore size distribution, surface area and pore volume of adsorbents was based on the equilibrium between gas molecules and solid particles through Van der Waals forces of attraction (Bardestani et al., 2019). Gases such as argon (87 K) and nitrogen (77 K) of different molecular sizes are commonly used to explore these properties of unknown adsorbents, catalysts, resins and different types of porous materials (Sotomayer et al., 2018). The Brunauer-Emmett-Teller (BET) method is used to determine the surface area of a material and is often described as an extension of the Langmuir monolayer adsorption model to multilayers (Chen et al., 2017).

The BET theory assumes that gas molecules interact with the adsorbent surface only in the vertical direction neglecting the lateral interactions between adsorbed molecules. The second assumption is that the adsorption energy is independent of the adsorption sites as in Langmuir model (Bardestani et al., 2019). The adsorption isotherm generated through the plot of volume of gas adsorbed vs. relative pressure is used to determine the surface area. The relative pressure (P/P_o) region from 0.05 – 0.35 provides a linear region depending on the adsorbate/adsorbent interaction (Ainscough et al., 1982),

indicating monolayer adsorption and is used to obtain the sum of the intercept and slope for surface area determination.

$$W_{\mathrm{ml}} = \frac{1}{\beta_0+\beta_1} \qquad \textbf{(1)}$$

$$\mathrm{SA} = \frac{W_{\mathrm{ml}} \times N \times A}{M \times m} \qquad \textbf{(2)}$$

Equations **1** and **2** (Bardestani et al., 2019) are used in the surface area determination. Where, Mass of Gas forming monolayer (W_{ml}), intercept of the linear region (β_o), slope of the linear region (β_1), Surface area (SA), Cross-sectional area of gas (A), Avogadro's number (N), Molar mass of gas (M), sample mass of adsorbent used (m). The BET theory is however not applicable to micropores below <2 nm width over the linear (P/P_o) region from 0.05 – 0.35, where, nitrogen fills micropores instead of multilayer adsorption (Rouquerol et al. 2007).

The Barrett, Joyner and Halenda method (BJH) helps in determining the pore size distribution from the gas adsorption isotherm based on two main assumptions (Bardestani et al., 2019). The pores modelled are cylindrical in shape and the adsorbed quantity of gas is the total of gases along the pore walls and capillary condensation in mesopores (Kuila and Prasad, 2013). Hence, BJH determines the change in thickness

of adsorbed films in pores through the desorption process (Roberts, 1967). A correlation between the pore volume and radius from the BJH theory is used to determine the pore size distribution in an iterative method by the computer with Equation **3** (Barrett et al., 1951). This is because, numerous numbers of pores (n) are expected to be present within a porous material and this would be arduous task to accomplish manually.

$$V_{Pn} = R_n\,\Delta V_n - R_n\,\Delta t_n \sum_{j=1}^{n-1}\left(\frac{\bar{r}_c}{\bar{r}_p}\right)_j A_{Pj} \qquad \textbf{(3)}$$

Where, V_p = pore volume, ΔV is the observed volume of the desorbed gas, R is the pore radius, Δt is the thickness of the physically adsorbed layer by amount, A_p is the pore area, $\overline{r}_c$ is the average capillary radius and $\overline{r}_p$ is the average pore radius and n and j are the number of pores present in the adsorbent.

3 Materials and method

3.1 Introduction

This chapter describes the materials and chemicals used in the preparation of solutions, characterization and pelleting and regeneration process. It further expounds on the procedures used in characterizing the adsorbent material, pelleting, adsorption and regeneration processes, giving working parameters and conditions of the experiments.

3.2 Materials

Zeolite NaP1 was obtained from Lublin University of Technology, Poland, synthesized from class F fly-ash obtained from a Polish power plant with the following conditions: 20 kg of fly-ash, 12 kg NaOH, 90 L of distilled water, seeding temperature of 80 °C for 36 h. Copper nitrate (98%), zinc nitrate (98%), lead nitrate (98%), sodium chloride (99.5%) and sodium hydroxide pellets, potassium chloride (99%), nitric acid (68%), hydrochloric acid (37%) and ammonium acetate were obtained from Fisher Scientific. Distilled water was obtained from Millipore Milli-Q plus Water Purification System.

3.3 Methods

3.3.1 Characterization of adsorbent

X-ray diffractometer (XRD)

A Bruker D8 Advance X-ray diffractometer (XRD) was used to characterize the crystal structure of the powder samples before and after regeneration. Wet zeolites after regeneration were oven dried for 6 h at 50 °C before use in the XRD. Approximately, 1 gram of powder was used on the sample stage with a plexi-glass dome. Samples were measured with a 0.6 slit for 2 h at temperature 25 ± 2 °C. Samples were scanned between 5° - 65° 2θ. Observations were made in increments of 0.05° in 2 s. Cu Kα radiation was used at 40 kV and 35 mA. EVA Software was used to identify the minerals present in the samples.

X-ray fluorescence analyser (XRF)

A Panalytical Epsilon 3XL model X-ray fluorescence analyser (XRF) was used in determining both the qualitative and quantitative elemental composition of the zeolite samples before adsorption, spent zeolite after adsorption and after regeneration. Powder samples were finely ground, placed in a plastic cup to about 4.9 cm in depth and covered with a plastic

film at the bottom (source of radiation). Approximately 5 g of zeolite powder was used during measurements. Omnion software was used for analysing oxides of elements present within the sample. The data is obtained with constituents of the sample presented in ppm (mg/g) of the sample.

Scanning electronic microscope (SEM)

A Philips XL30 tungsten filament was used in characterizing the shape and size of the NaP1 formed in comparison to original fly-ash. SEM was operated using an accelerating voltage of 15 kV with spot size of 3 nm and 20000x magnification. NaP1 sample was sprinkled on sample stubs with carbon adhesives using the spatula and pressed slightly to settle. The sample stubs were turned upside down with a gentle tap to remove loose NaP1. The settled NaP1 on the sample stubs were then carbon coated before being used in the SEM instrument. The Philips XL30 tungsten filament was vented with sample placed in position. X and Y axis are set to zero while the position of the sample is properly adjusted. The Z axis is finally set to 10 and the sample door is held in place while a vacuum is created in the chamber by clicking the pump button. The sample is identified on the monitor, brightness and contrast are set while zooming in on the sample until the sharpest focus is obtained. Final

adjustments were made before saving the preferred image of the sample.

Nitrogen adsorption/desorption isotherms

Surface area and pore size characterization of both NaP1 powder and pellet were performed using Micromeritics ASAP 2420 V2.09 with nitrogen adsorption at 77 K. Samples were degassed in the chamber to remove any form of adsorbed gases and water. Degassing begun by creating a vacuum over 30 mins at an evacuation rate of 5.0 mmHg/s followed by both NaP1 powder and pellet samples of 0.28 grams being heated to 250 °C in increment of 10 °C for 15 h and finally purged with liquid nitrogen at 77 K. Liquid nitrogen was released into the chamber at 77 K during the adsorption process at a relative pressure of 0.010 (P/Po) with a gradual increment till 0.987 (P/Po) followed by desorption phase over a 10 h period. Results from this experiment were analysed mainly by the Brunauer, Emmett and Teller (BET), Barrett, Joyner and Halenda (BJH) methods. Surface area determination and monolayer removal capacity for zeolite NaP1 were obtained by the BET method while pore size distribution, micropore surface area and pore volume were determined by the BJH method.

3.3.2 Pelleting

Pelletizing is an important part of commercializing adsorbents. While making them easy to handle in industry and safe for transportation, they present an added advantage of reducing pressure drop through a fixed bed column (Jasra et al., 2003). Powdered adsorbents are shaped into bodies such as granules, spheres, and extrudate prior to their use as adsorbents and catalysts and would need high mechanical strength to withstand repeated usage.

Prior to using the hydraulic press, the NaP1 powder was ground in a mortar to obtain a fine and smoothened powder. Samples to be used during the pelleting process were weighed with a weighing boat using a digital measuring scale. A Specac Atlas 15 Ton and 25 Ton hydraulic press was used in preparing disc shaped tablets with the aid of applied pressure to powdered NaP1 in a die assembly.

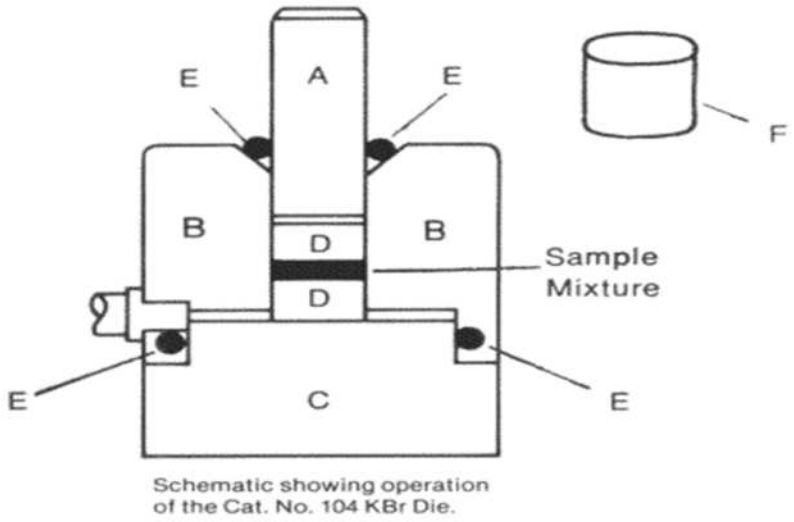


Figure 3.1: Pelleting die assembly (image obtained from the manual).

The pelleting die assembly is assembled initially with parts C, E, and B, as in Figure 3.1 to form a cylinder body. The two dies (D1: bottom and D2: top) are both wiped with industrial grade methanol to remove any sticky substance/ organic matter or fingerprints. The first die (D1) is placed with the polished side up and with the use of a spatula, the zeolite powder is filled through the bore of the cylinder. The sides of the cylinder were tapped gently to have the powder evenly distributed across the surface of the polished die (D1).

Following this, the second die (D2) is placed centrally down but gently through the bore of the cylinder body with the polished side down. This step was carefully done not to jam the pellet. Finally, the plunger (A) was inserted into the cylinder body with its non-chamfered edge end facing downwards. The die

assembly is then sealed with an O-ring seal (E) around the chamfered section of the plunger.

The final pelleting assembly is lifted gently and placed under the hydraulic press, where, pressure will be applied to compress the NaP1 powder. The hydraulic press is made up of a pressing side, pressure gauge, lever and leadscrew as shown in Figure 3.2. A 10 mm pelleting die assembly was used in this research. The die assembly was placed centrally into the pressing side, the leadscrew is screwed down in place to hold the plunger while the lever was used to apply pressure to the die assembly. All safety guards on the press were closed, while load to the plunger was applied for a period to produce the desired quality of pellet sample.



Figure 3.2: A picture of the hydraulic press.

The desired loading generated from the applied pressure is observed using the loading/pressure gauge. This loading is then allowed a suitable time before released by means of the loading gauge screw. In producing the best NaP1 pellets, the following parameters were varied and optimized:

- Amount of NaP1 powder required to produce desired pellets
- Amount of loading/pressure applied
- Loading pressure time

All pelleting experiments were repeated 5x times to ascertain results and conclusions drawn on the most suitable parameters. The parameters tested and optimized were the amount of NaP1 powder (0.2 – 0.05 g) required to produce desired pellets, amount of loading/pressure applied (3 – 5 tons) and loading pressure time (1 – 10 min). The pellets produced were later characterized for surface area, pore distribution and cation exchange capacity.

3.3.3 Determination of metals in liquid samples

Metal concentrations in the liquid samples were measured by iCAP QC Inductively Coupled Plasma (ICP) – Mass Spectrometry (MS) incorporating Dionex ICS3000 High Performance Liquid Chromatography (HPLC) and auto-sampler. Samples collected during experiments were centrifuged using Hettich Rotofix 32A benchtop centrifuge (at 4000 rpm for 6 mins), filtered with 0.2 and 0.45-micron Minisart syringe filters and stabilised with 2% nitric acid before analyses. Calibration of the instrument was performed prior to sample analysis with external calibration standards between 0 – 100 µg/l for trace elements and 0 – 30 mg/l for alkali and alkali-earth metals. Although calibration of ICP-MS is linear over 8 orders of magnitude, samples with metal concentration above 60 mg/l and alkali-earth metal

concentration (e.g., Na, Mg, K and Ca) above 200 mg/l required dilution before testing for more accurate results. The volume of solution required for testing was between 5 – 10 ml. Results from sample concentration are presented by a spreadsheet with standard deviation values of metal concentrations in µg/l (trace elements) and mg/l (alkali and alkali-earth metals). Detection limit for metals Cu (0.61 µg/l), Pb (0.98 µg/l) and Zn (2.1 µg/l) were determined with calibration standards (0, 20, 40 and 100 µg/l) during calibration. Four repetitions of calibration experiments were performed, and the average presented with standard deviations.

3.3.4 Control experiments

Leaching test

The test for leachate helps to determine whether the zeolite is fit for purpose. Through this test, data on metals leached into the treatment system can be quantified and compared against water treatment standards to decide whether the proposed zeolite NaP1 is useful for water treatment purposes.

Zeolite NaP1 was tested for leachates under the same adsorption conditions to assess the possible elements released into water during the experiments. Five grams of NaP1 was mixed in 1 litre Milli-Q water at pH 3.5 and temperature 22 ± 2

°C for 3 hours. Sample (10 ml) was collected at time interval 0, 15, 30, 60 and 180 min and filtered with a 0.2-micron syringe filter for ICP-MS analyses. The experiment was repeated 3 times and the average results were presented to identify possible discrepancies.

Precipitation

The effect of precipitation was quantified by means of control experiments and deducted from the resulting metal uptake experiment. Precipitation of heavy metals was tested at pH (3.5, 6.5 and 10.5) through control experiments when a clean water matrix was stirred without zeolite over the experiment contact time. These are displayed on adsorption graphs in the results chapter. However, the precipitation reported in the control experiment was for multi-element adsorption pH study. Initial metal concentration ~12.5 mg/l for each heavy metal making a total of 37.5 mg/l at T= 20 ± 2 °C was used in this experiment to determine the influence of pH on precipitation during multi-element adsorption.

Effect of syringe filters

Minisart syringe filters (0.45 and 0.2 μm) were tested as a quality control measure to determine whether the syringe filters contributed or removed metals from solution during the experimental procedure. This was done to eliminate sources of doubt and to ascertain that adsorption was only by means of the zeolite. Thus, 10 ml samples were collected from 40 mg/l copper solution with a syringe and filtered through 0.2 and 0.45 μm syringe filters. Three repetitions were made, and samples were tested with ICP-MS.

Calibration and limits of detection/quantification

Instrument calibration was performed with 4 repetitions prior to sample testing. External standards produced by PerkinElmer were used with concentrations 0, 20, 40 and 100 μg/l. Ultrapure Milli-Q water was used as a wash liquid before and after running calibration standards to prevent contamination. Standards were fed through an auto-sampling unit several times to obtain mean values. Calibration results were presented as an excel data and curve plotted. The limit of detection and limit of quantification of target metals for ICP-MS were obtained from the standard error of calibration curve (STEYX) and slope of calibration curve (S). Thus, limit of detection (LOD) was calculated by

3.3*(STEYX/S) and limit of quantification (LOQ) by 10*(STEYX/S).

3.3.5 Adsorption

The pH for this research was determined after careful consideration of the relationship between pH-metal solubility/precipitation. The objective of this study is to ensure that heavy metal removal was solely by adsorption/ion exchange and not precipitation from clean water matrix. Following this, X-ray fluorescence spectroscopy (XRF) was performed to determine the constituents of zeolite NaP1. The XRF results showed the presence of elements in different quantities and was used to aid in the decision-making process. Thus, pH 3.5 was selected as the starting point to prevent the formation of metal hydroxides and consequent precipitation of target metals (Cu, Pb and Zn) during adsorption from the clean water matrix.

All glassware was first washed with laboratory grade-detergent and rinsed with tap water. Afterwards, they were soaked in 20% (v/v) nitric acid between 4 to 24 hours and rinsed with Milli-Q water 3 times before use (EPA method 200.8). The Jenway 570

pH meter with temperature correction function was used for pH adjustment during experiments.

Based on concentrations selected from current literature for the target metals, the following concentration ranges were chosen to determine the adsorption isotherm of NaP1: copper; 50 – 1000 mg/l, zinc; 50 – 3500 mg/l and lead; 50 – 3500 mg/l. Lead, copper and zinc concentrations selected for adsorption kinetic experiment were set at 100, 150 and 250 mg/l respectively. The aim was to consider possible increases in both current and future concentrations of the wastewater effluents published by Gardener et al. (2013).

A fixed mass of 5 g of zeolite NaP1 was mixed with 1 litre of metal solution in a 2-litre beaker. The pH of the solutions was maintained at a range of 3-4 using 68% HNO_3 and 2% wt/v NaOH solutions to prevent precipitation of copper ions at pH 5-6 before adsorption. The solutions were mixed at 300 rpm up to 3 h, with a magnetic stirrer (IKA RH Basic 2) at 22 ± 2 °C. Twelve ml sample was taken from the solution into centrifuge tubes at time intervals of 0, 15, 30, 60- and 180-min. Samples taken were filtered using the Minisart 0.2 µm filters before ICP-MS analyses. Two repeat experiments were conducted to

observe errors associated in the experiment while a control experiment was performed without zeolite in the same conditions to account for the precipitation of metals. The total sampling volume did not exceed 5 – 10% of the total solution volume considering a confidence interval above 95 % for error margins.

3.3.6 Single element adsorption isotherm

Batch experiments were performed by mixing a fixed mass of zeolite (0.5 g), in 100 ml solutions of varied zinc, lead and copper nitrate concentrations (50, 150, 250 and 500, 1000, 2500 and 3500 mg/l) in a single-element adsorption test. All experiments were carried out at 22 ± 2 °C and pH between 3 and 4. The experiments were terminated at 180 min (zinc) and 60 min (lead), because zeolite NaP1 had demonstrated a higher affinity for lead than zinc. Samples were collected into 50 ml centrifuge tubes for centrifugation at 4000 rpm for 8 min and filtered using the Minisart 0.2 µm syringe filters. High concentration solutions were diluted with 1- and 10-ml graduated pipettes or Pipetman P100 micro-pipette for ICP-MS analyses. Experiments were repeated twice during the process. A control experiment was performed with the same conditions without zeolite to determine precipitation.

3.3.7 Multi-element adsorption experiments

Multi-element control experiments were performed 3 times by mixing 1 gram of zeolite NaP1 in 1 litre of multi-elements (12.5 mg/l each of Cu, Zn and Pb) at various pH (3.5, 6.5 and 10) and 22 ± 2 °C for 1 h. The control experiment was used to investigate the effect of precipitation.

The adsorption experiments were performed by mixing 5 grams of NaP1 powder, NaP1 pellet and commercial grade 3A zeolite pellets at 300 rpm with a litre of 500 mg/l concentration of multi-elements (Zn=250 mg/l, Cu=150 mg/l and Pb=100 mg/l) at pH=5 for 3 h, 22 ± 2 °C. Ten ml of samples were collected during the experiments at 0, 15, 30, 60, 180 min and analysed with the ICP-MS. The mean results from triplicate experiments with their standard deviations were presented.

3.3.8 Metal removal with NaP1 and 3A pellets (kinetics)

Five grams of NaP1 powder, NaP1 pellet and commercial grade 3A zeolite pellets were separately introduced into a litre of 90 mg/l concentration lead solution, stirred at 300 rpm for 3 h at a constant pH=5 and temperature=22 ± 2 °C. Samples collected from the experiments at 15, 30, 60 and 180 min were analysed by ICP-MS. The experiment was repeated 3x with the mean and

standard deviation calculated. A control experiment was also performed under the same conditions without any zeolite to determine precipitation.

3.3.9 Further leaching

Further leaching was also required under adsorption isotherm experimental conditions, since they varied from the adsorption kinetics conditions. Hence, 0.5 g NaP1 was mixed in 100 ml Milli-Q water at pH 3.5, temperature 22 ± 2 °C for 60 and 180 minutes, respectively. The samples were collected into 50 ml centrifuge tubes, centrifuged for 8 min at 4000 rpm and filtered with 0.2-micron syringe filters for ICP analyses.

Leaching tests were also repeated using NaP1 powder, NaP1 pellet and commercial grade 3A zeolite pellets for comparison. One gram (1 g) of each material was stirred in 1 litre of distilled water at 300 rpm, at 22 ± 2 °C and pH 5. Samples collected from the experiments at 15, 30, 60 and 180 min were analysed by ICP-MS. The experiment was repeated 3x with the mean and standard deviation calculated.

3.4 Justification for experimental variables

Mass of zeolite: This study had a limited amount of synthesized fly-ash NaP1 and had to be managed to obtain the required results. This is because, the purity of synthetized zeolite varies from batch to batch and could present inconsistencies in results obtained. Hence, this posed a limitation in the number of repeats and how much sample could be used to investigate different properties. The mass of zeolite used was decided after reviewing what had been used in literature for NaP1 adsorption in connection to the available zeolite quantity. Hence, 5 grams of zeolite was used for most experiments, while, a scale down to 1 g and 0.5 g, were used when experiments required more repeats. The number of repeats was mostly limited to 2 concordant results for experiments that required more zeolite (eg. Adsorption kinetics and isotherm) and in cases where, there were discrepancies, 3 repeats were required to affirm these results. Concordant results in the range of < 5% relative standard error were accepted in line with > 95 % confident limit for results.

Temperature: The temperature of each experiment was recorded as the room temperature when these experiments were conducted (20 – 25 °C). This is in line with the expectation of these zeolites will being used in natural conditions in industry.

However, most experiments were at 22 ± 2 °C and it is noteworthy that this range will have no significant impact on the adsorption results.

Concentration: The concentrations of metals used in the adsorption experiments were obtained from real-world industrial wastewater (electroplating, acid mine, to mention a few). The real-world metal concentrations were increased by 33 % to the nearest whole number, considering a possible influx in present concentrations for adsorption experiments. However, multi-element lab-synthesized water matrix and regeneration-based copper adsorption concentrations were set below 50 mg/l, because all elements were best adsorbed at low concentrations within that region from previous experiments and the literature.

Contact times: Initial contact time for NaP1 adsorption chosen after reviewing the literature was 3 hours. This was optimized to 1 hour after fly-ash NaP1 demonstrated a quick kinetic. Hence, this study used 1 hour for adsorption isotherm experiments for all metals. Multi-element adsorption was limited to 3 hours as the optimum contact time bearing in mind the presence of competitive adsorption being a possible inhibitor to maximum adsorption. Regeneration experiments were

conducted within 6 - 24 hours and later optimized to the optimum contact time (3 hours) after preliminary experiments.

3.5 Regeneration study

Prior to the regeneration study, the above adsorption experiment was performed, and the spent adsorbent was used for the regeneration study. A 1 l stock solution of 50 mg/l copper concentration was prepared in a volumetric flask using copper nitrate. Zeolite sample (0.5 g) was mixed with 100 ml of 50 mg/l copper solution in a 200 ml beaker for adsorption. The mixture was stirred at 300 rpm for 1 h (equilibrium time) while maintaining the pH at 3.5 with 68% HNO_3 and 1 M NaOH solutions. After 1 h, the mixture was centrifuged at 4000 rpm for 6 min to separate the liquid from the solid. The liquid was filtered with Minisart 0.2 µm syringe filters for ICP analyses while the solid sample was dried at 100 °C for 24 h, analysed by XRD/XRF and used for regeneration experiments.

The regeneration study was performed with acid (HCl), base (NaOH) and salts (NaCl and KCl) of varied concentrations (1 M, 3 M and 5 M), at pH=1, 3 and 5 for 1 – 48 h at 20 ± 2 °C in a batch system. Experiments were conducted under the same conditions, where, 0.5 g zeolite was mixed repeatedly in 100 ml

regeneration solution at 300 rpm, 20 ± 2 °C, pH (1, 3.5 and 5) and various times (e.g. 2 h, 6 h, 12 h etc.) till maximum (90-100%) regeneration was obtained. Solid/liquid separation was obtained through centrifugation at 4000 rpm for 6 minutes, followed by filtration of liquid through 0.2 µm syringe filter for ICP analysis.

3.6 Cation exchange capacity (CEC)

Zeolites have also been used in ion-exchange systems and it would be vital to know the ion-exchange capacity of fly-ash derived NaP1 in comparison to a commercial zeolite.

The cation exchange capacity of NaP1 powder, pellet and 3A pellet was determined by means of ammonium acetate. One molar ammonium acetate solution was prepared in a 1 litre volumetric flask. A 100 ml of this solution was poured into a 200 ml beaker and stirred with 0.25 g of zeolite NaP1/3A for 24 h. The solution was filtered with a 0.45-micron Minisart filter and analysed by the ICP-MS. A sample of the ammonium acetate solution was measured as a blank and compared to the results from NaP1 powder and pellet and 3A pellet. Three replications of the same experiment at 22 ± 2 °C with the mean and standard deviations were calculated and presented.

4 Zeolite characterization

4.1 Introduction

This chapter focuses on zeolite characterization using a Scanning Electron Microscope (SEM), X-Ray Diffraction (XRD) and X-Ray Fluorescence (XRF) analysis with the aim of demonstrating the presence of NaP1 after synthesis in comparison to fly-ash.

4.2 SEM characterization

The SEM images of coal fly-ash prior to synthesis and after synthesis are shown in Figure 4.1 and 4.2, respectively. As mentioned earlier, coal fly-ash was synthesised by collaborators from the Lublin University of Technology, Poland.

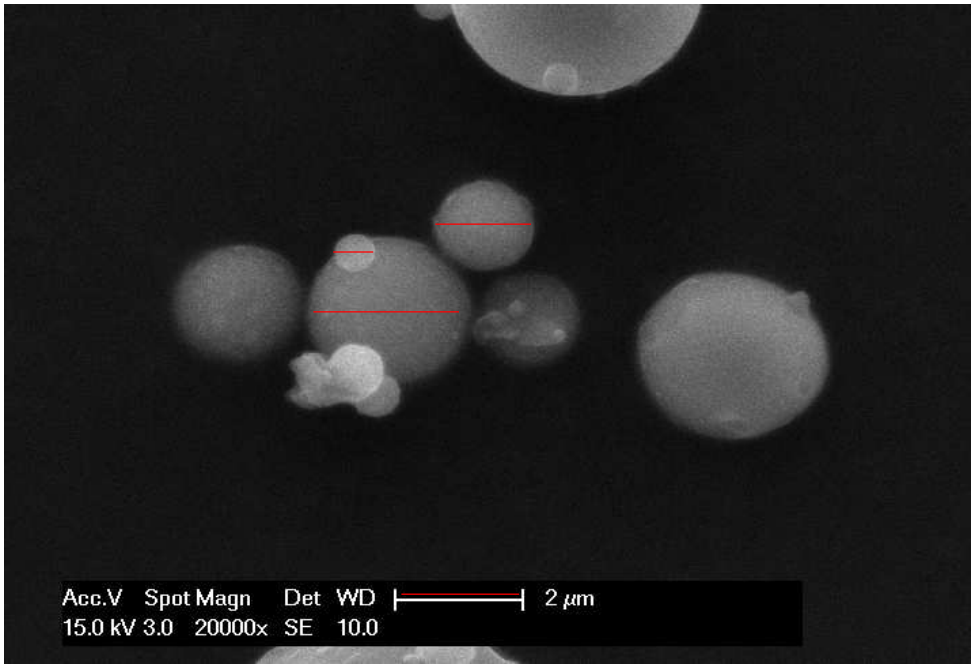


Figure 4.1: SEM image of coal fly-ash at 2 microns.

The SEM image of coal fly-ash (Figure 4.1) depicts smooth spherical particles with sizes from 0.6 to 4 μm before synthesis such as the reports of Querol et al. (2007) and Wdowin et al. (2014).

Figure 4.1, which agrees with works from Querol et al. (2007) and Wdowin et al. (2014), depicts a different morphology to that of the synthesized coal fly-ash observed in Figure 4.2. The SEM image from synthesized NaP1 shows the agglomeration of rectangular pieces (cubes) into a large structure (Figure 4.2). The cubes of minimum 0.2 μm aggregated into larger pieces greater than 2 μm (from 4.5 to 6 μm), forming a rough heterogeneous surface. Wdowin et al. (2014) describes this appearance as lamellar aggregates of plate-like shapes as a characteristic feature of NaP1.

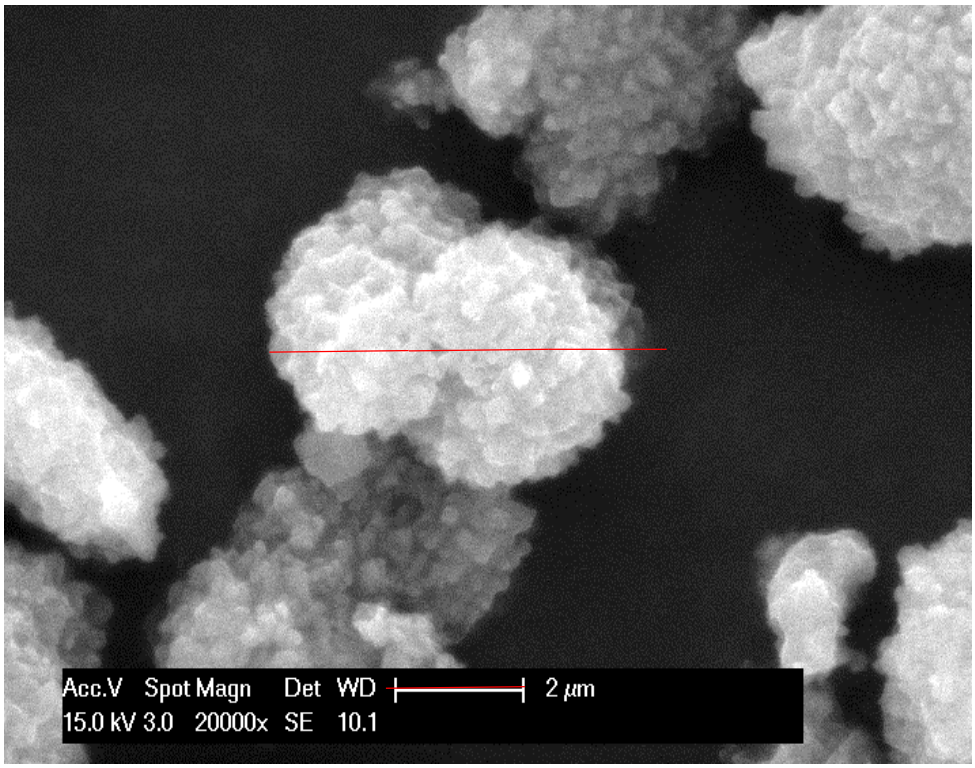


Figure 4.2: SEM image of NaP1 zeolite.

4.3 XRD characterization

Coal fly-ash is generally known to be composed of aluminosilicate glass, quartz, and mullite (Wdowin et al., 2014). Figure 4.3 shows the XRD pattern of coal fly-ash. The pattern indicates peaks for components within the substance reinforcing the dominance of quartz at 20.8°, 26.6°, 50.2° and mullite at 16.5°, 26°, 26.2°, 31°, 33.2°, 35.4°, 40.8°, 42.6° and 60.7° 2 Theta(°). Quartz is noticed to display the highest peak at 26.6° 2θ and closely followed by mullite at 26.2° 2θ angles.

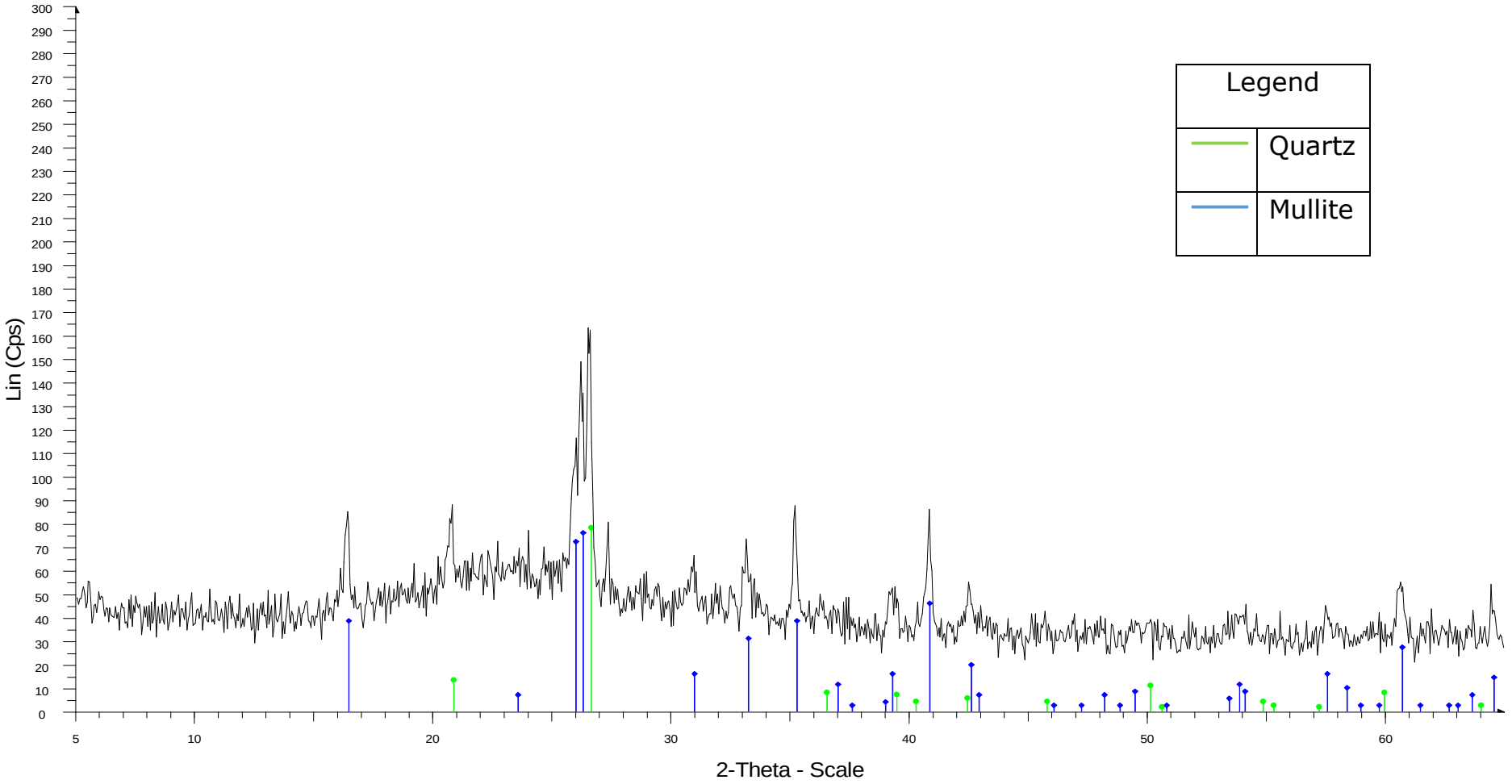


Figure 4.3: XRD pattern of coal fly-ash.

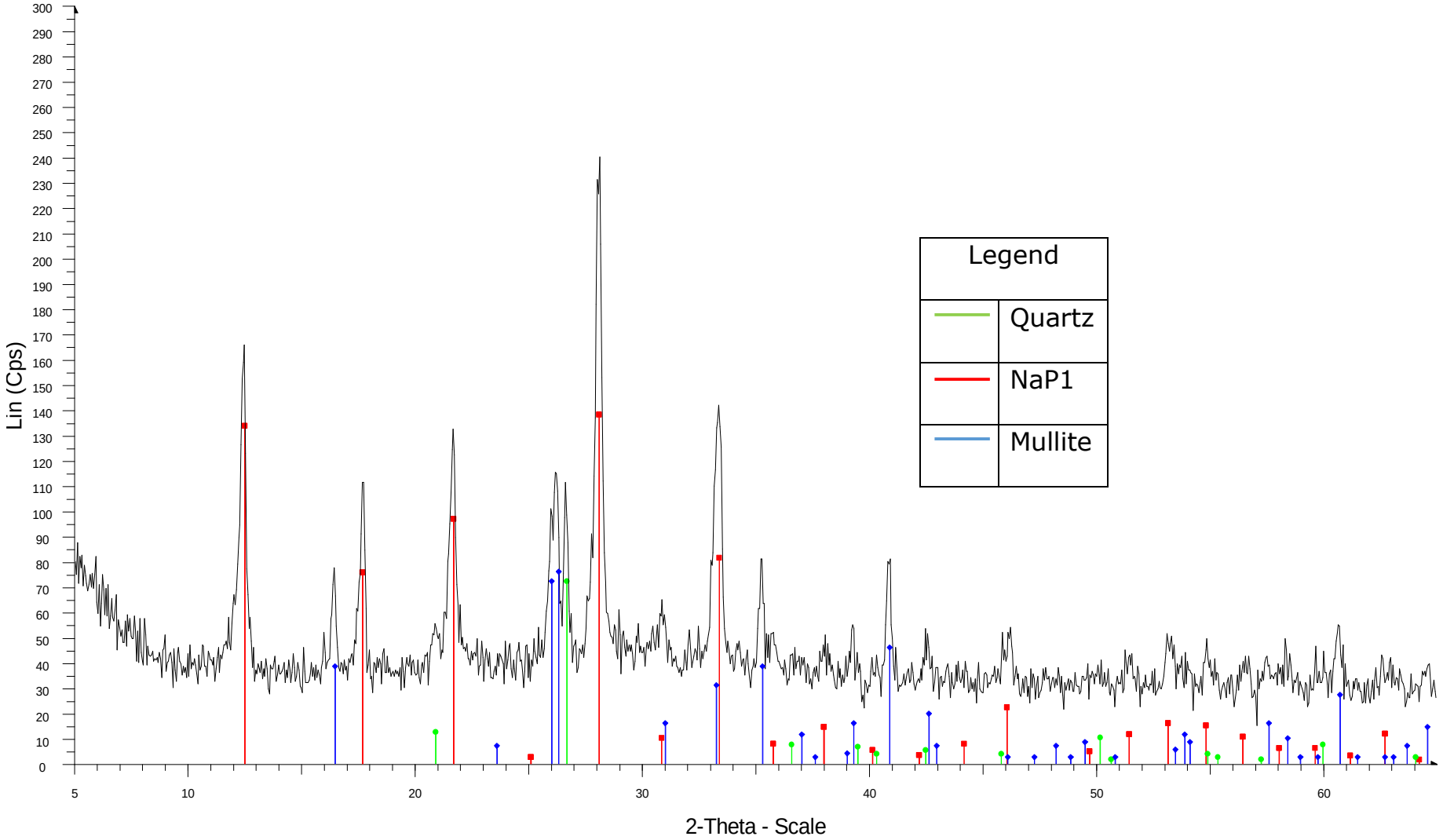


Figure 4.4: XRD pattern of zeolite NaP1 synthesized from coal fly-ash.

Comparatively, the XRD pattern of zeolite NaP1 shown in Figure 4.4, indicates the dominant presence of P formed at 12.5°, 17.8°, 21.6°, 28.2°, 33.4°, 31° and 46° 2θ. The XRD pattern of the synthesized zeolite shown in Figure 4.4 further indicates very high peaks of a crystalline substance with chemical composition equivalent to that of NaP1 with low peaks of mullite and quartz.

4.4 XRF characterization

The percentage composition of zeolite NaP1 synthesized from coal fly-ash is shown in Table 4.1. Quantitative analysis of zeolite NaP1 from X-ray fluorescence showed ~44, 29 and 17% of SiO_2, Al_2O_3 and Na_2O, respectively, while oxides of Mg, Ca and Fe accounted for ~7 - 8% of the remaining composition.

Table 4.1: Percentage composition of zeolite NaP1 obtained from XRF using 5 g sample.

Percentage Composition	
Compounds	**NaP1 (%)**
Na_2O	17.2
MgO	0.7
Al_2O_3	29.0
SiO_2	43.8
CaO	2.9
Fe_2O_3	3.9
Other metals	2.5

Silicon dioxide to aluminium oxide (SiO_2/Al_2O_3) ratio for NaP1 was calculated as 1.51. The SiO_2/Al_2O_3 ratio has been used as a means of predicting zeolites with good sorption properties (Ouki and Kavannagh, 1997). Generally, zeolites with low Si/Al ratios indicate the potential of higher sorption and ion exchange capability. This is due to the exchange of aluminium ions with silicon ions providing a negative framework for that zeolite.

4.5 Chapter summary

SEM scans illustrate smooth spheres of fly-ash transformed into cubes of 0.2 μm aggregated into larger pieces greater than 2 μm (from 4.5 to 6 μm) and forming a rough heterogeneous surface after synthesis. XRD scans demonstrate the presence of zeolite NaP1 crystals from mullite and quartz with peaks at 12.5°, 17.8°, 21.6°, 28.2°, 33.4°, 31° and 46° 2θ while XRF scans demonstrated the composition of zeolite NaP1 with a 1.51 (SiO_2/Al_2O_3) ratio. These showed evidence of the presence of NaP1 from fly-ash.

5 Control experiments

5.1 Introduction

The chapter demonstrates the reliability of experiments used to derive the findings in this study. Control experiments were used to test for leaching and precipitation under different experimental conditions, influence of syringe filter on experiments, calibration solutions used and limit of quantification/detection of ICP-MS (identify whether it was fit for purpose).

5.2 Leaching

The presence of leachates during batch adsorption experiments were tested via mixing 5 g zeolite in 1 litre Milli-Q water for 3 hours (maximum adsorption period) at pH 3.5 and at 20 ± 2 °C. Samples (10 ml) taken at various times (0, 15, 30, 60 and 180 min) were filtered and analysed by ICP-MS. Compared to other research with synthetic zeolites, limited investigation has been done in the area of leachates (Lee et al., 2000; Moreno et al., 2001; Querol et al., 2002; Alvarez-ayuso et al., 2003, Prasad and Mortimer, 2010). This study helps to resolve whether the synthetic material is fit for treatment purpose and to help inform other areas of suitable applications.

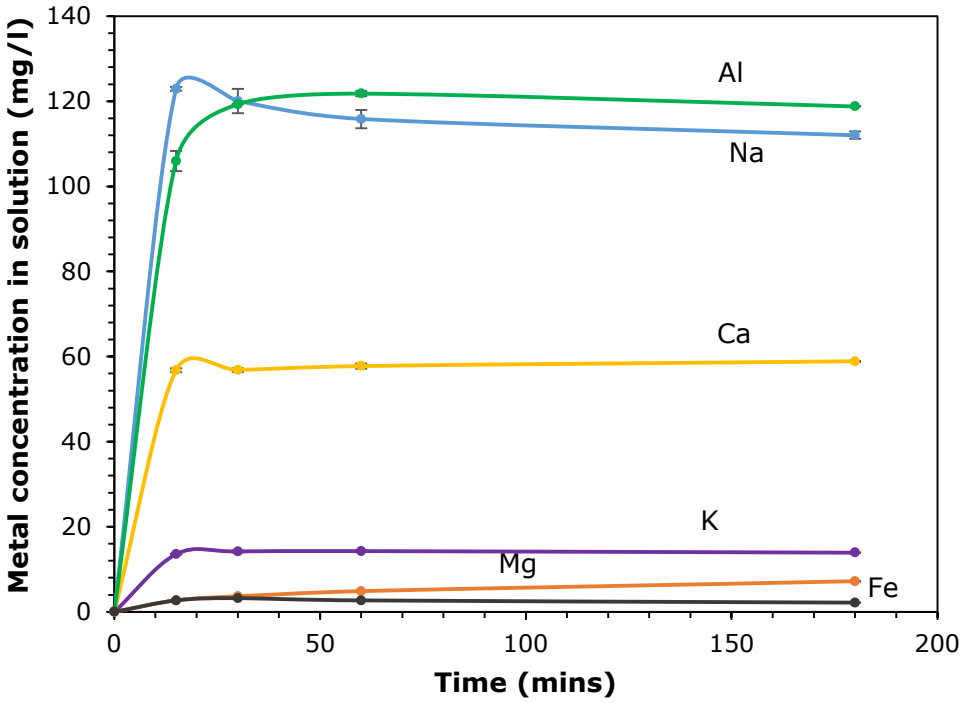


Figure 5.1: Cumulative concentrations of leached cations in water after 3 h. Conditions: 5 g of NaP1 dissolved in 1 l Milli-Q water at pH 3.5 and 20 ± 2 °C. Values presented are the mean of 3 repeat measurements and standard deviations.

From Figure 5.1, total leachate concentration of cations is identified to increase within the first 15 minutes from 0.5 ± 0.1 mg/l to 305 ± 3.41 mg/l. Further increase to 318 ± 3.54 mg/l was observed in 30 min with aluminium as the main contributor. This may be due to the presence of extra framework aluminium. The total concentration of leachates remained constant (318 ± 3.57 mg/l) from 30 to 60 min, although for individual elements such as Al^{3+}, Ca^{2+} and Mg^{2+} an increase was recorded. However, for Na^{+} and Fe^{2+}, a decrease in concentration was observed towards the end of the leaching process.

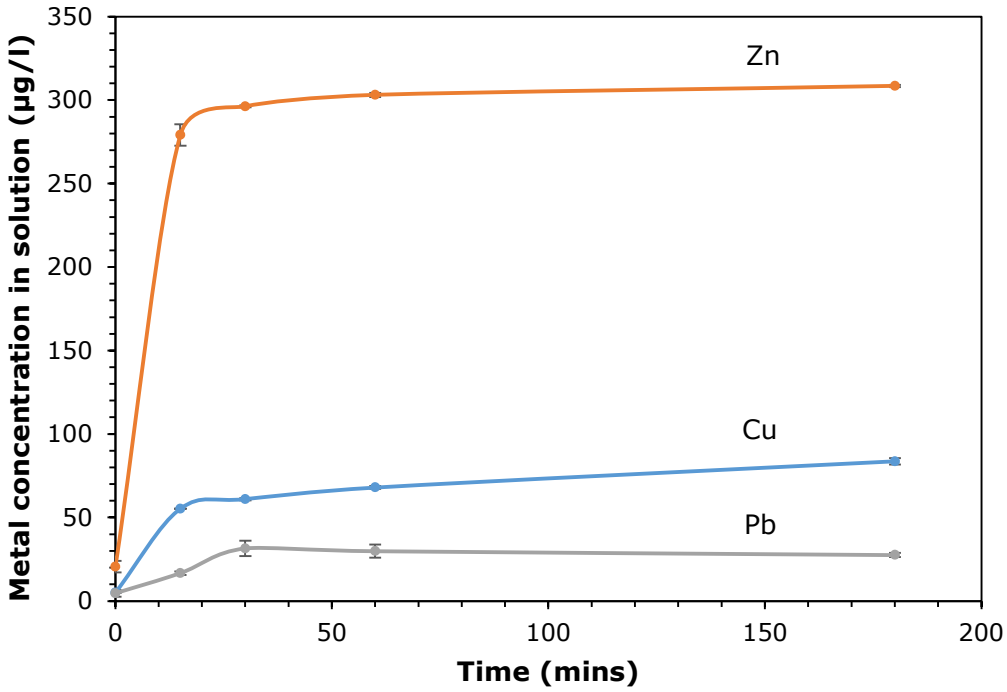


Figure 5.2: Cumulative concentrations of leached target metal ions in water after 3 h. Conditions: 5 g of NaP1 dissolved in 1 l Milli-Q water at pH 3.5 and 20 ± 2 °C. Values presented are the mean of 3 repeat measurements and standard deviations.

From Figure 5.2, concentration of target metal ions in µg/l (Cu, Pb, and Zn) remained constant through the timeframe (30 – 180 min). An equilibrium in total leachate concentration was reached from 30 to 60 min. At 180 min (see Figure 5.2), total leachate concentration is observed to decrease by 4 mg/l. This decrease is approximately 3% the total quantity of leachates obtained and could be attributed to experimental error. A similar leaching trend is observed for all metals over the experiment

duration. However, zinc was easily released from zeolite NaP1 followed by copper and least of all, lead. This depicts how strongly these metals are held to the surface of zeolite NaP1. Hence, the affinity of these metals to NaP1 follows the order Pb > Cu > Zn.

Elements such as Na, Al and Ca formed majority of these leachates with 37.55%, 37.15% and 18.37% respectively by mass percentage composition. Target metals (Cu, Zn and Pb) formed the remaining 0.13%. Although the concentration of target metals such as Cu and Zn were below their allowable effluent discharge limit (0.25 mg/l and 0.8 mg/l, respectively) into water, other elements i.e. Al, Fe and Pb were above their acceptable limits (200 µg/l for Al, 300 µg/l for Fe and 6.0 µg/l for Pb). Thus, fly-ash zeolite NaP1 can be pre-treated by preliminary washing before being used for water treatment. In addition, rinsing of fly-ash zeolite is known to reduce the alkalinity and improve its ion exchange property (Ferrarini, 2016).

Finally, the composition of zeolite NaP1 from previous XRF analysis was identified to contain 153 mg Al per gram zeolite and 93 mg Na per gram zeolite. Hence, the quantity of leachates for Al and Na represent 15% Al and 25% Na, percentage mass composition of 1 g zeolite NaP1. Aluminium obtained from

leaching may be extra framework material while Na could be from residual NaOH used.

5.3 Precipitation

The effect of precipitation was quantified by means of control experiments and deducted from the resulting metal uptake experiment. Table 5.1 presents the mean of two repetitions from the control experiment as evidence of precipitation in mass percentage. To the best of my knowledge, there is no current literature which has determined suitable pH for multi-element removal while demonstrating the effect of precipitation.

Table 5.1: Precipitation of heavy metals obtained as a function of pH (3.5, 6.5, 10.5) from control experiments when 1 litre water matrix is stirred without zeolite for 1 h. Initial metal concentration ~12.5 mg/l for each heavy metals making a total of at 37.5 mg/l, T= 20 ± 2 °C.

pH	Cu (mg/l)	Zn (mg/l)	Pb (mg/l)
pH 3.5 at t = 0	11.4	13.1	12.4
t = 1h	11.2	13.0	12.3
pH 6.5 at t = 0	11.4	13.1	12.4
t = 1h	8.79	11.9	9.51
pH 10.5 at t = 0	11.4	13.1	12.4
t = 1h	0.00448	0.0529	0.547

The highest percentage of precipitation for all the metals (above 95%) is noticed at pH 10.5 due to an increase in metal hydroxide formation. These metal hydroxides are not soluble in solution above the following pH values (Cu= 5.3, Zn= 7, Pb= 6) and begin to precipitate out of solution. Thus, the lowest heavy metal removal of 1 mg/l was noticed at pH 10.5 mainly due to precipitation of metals as the main phenomenon for metal concentration reduction. This can be further emphasized by the results from Table 5.1, indicating the quantity of metals at different pH values (3.5, 6.5 and 10.5).

Metal precipitation by mass at pH 3.5 was below 3% the initial quantity of metals for all target metals (Table 5.1). This can be attributed to experimental errors and implying the absence of precipitation at pH 3.5 as expected. Copper and lead amongst the metals were observed to precipitate by 2.61 and 2.89 mg/l respectively, representing approximately 23% of the starting concentration at pH 6.5. Zinc precipitation recorded 1.2 mg/l also representing 9.2% of the starting concentration at pH 6.5. Copper and lead hydroxide formation/ precipitation begin from pH > 5.3 and pH > 6 respectively while zinc hydroxide formation begin beyond pH > 6.5. This explains why zinc precipitation was least observed (< 10%) at pH 6.5.

5.4 Adsorption in syringe filters

Table 5.2 displays results obtained from testing the influence of syringe filters on adsorption experiments. Minisart syringe filters of pore size 0.45 and 0.22 μm were tested with 40 mg/l concentration of copper solution.

Table 5.2: Results obtained from testing 0.45 and 0.2 μm syringe filters with 40 mg/l copper concentration.

Sample	Cu concentration (mg/l)	Average Cu concentration (mg/l)
Initial sample	39.43	
Filter (0.45 *μm*)		
sample 1	38.91	
sample 2	38.90	38.9 ± 0.011
sample 3	38.89	
Filter (0.2 *μm*)		
sample 1	39.27	
sample 2	39.43	39.4 ± 0.57
sample 3	39.43	

Table 5.2 shows that 0.45 μm syringe filter produced an average concentration of 38.9 ± 0.011 mg/l from 39.43 ± 0.57 mg/l starting concentration. An average quantity of 0.53 ± 0.011 mg/l equivalent to 1.33% copper appeared to be lost from samples filtered with 0.45 μm syringe filter. This implies that 0.45 μm syringe filter made-up of cellulose-acetate had adsorbed ~ 1% of copper metals from the filtered solution.

Weltje et al. (2003) studied the adsorption of metals on membrane filters and identified free metal ions (K, Mn, Zn, Cu and La) to bind onto cellulose-acetate filters through an electrostatic bonding mechanism. However, samples filtered with 0.22 µm syringe filter produced on average 39.4 ± 0.09 mg/l for all triplicates with no identifiable losses in copper concentration although it is also made of cellulose-acetate. This may be the result of 0.45 µm syringe filter having a larger surface for attraction compare 0.22 µm syringe filter. Nonetheless, both 0.45 and 0.22 µm syringe filters display RSDs less than 5% the initial concentration and could be used. However, 0.22 µm syringe filter was used due to low volume filtrates produced from the experiments.

5.5 Calibration and limits of detection for the ICP Instrument

Table 5.3 presents the mean values and standard deviation for external calibration standards used for ICP-MS calibration. Instrument calibration was performed with four standard solutions of concentration; <0, 20, 40 and 100 µg/l. Repetitions were made 3 times prior to sample testing with fresh standards (ISO 11095:1996).

Table 5.3: Mean and standard deviation values of metals from ICP-MS calibration using four standard solutions of concentration <0, 20, 40 and 100 µg/l and repeated 3 times.

Calibration standards (µg/l)	**Cu (µg/l)**	**Zn (µg/l)**	**Pb (µg/l)**
0	0.0079	0.0894	0.0027
20	20.29 ± 0.55	21.09 ± 0.54	20.47 ± 1.52
40	40.16 ± 0.59	40.25 ± 0.64	40.26 ± 1.88
100	99.88 ± 0.29	99.68 ± 0.30	99.80 ± 1.05

The instrument produced an average relative standard deviation (RSD) of 2.8% for 20 µg/l calibration solution of Cu and Zn except for Pb, which was highest at 7.5%. The RSD decreased to 1% and 0.29% as the concentration of the calibration solutions increased from 20 to 40 and from 40 to 100 µg/l, respectively for Cu and Zn. A similar observation is made with Pb, which decreased from 4.7% at 40 µg/l to 1% at 100 µg/l. This is an indication of the difficulty observed in preparing calibration standards of very low concentration in the µg/l region as opposed to higher concentration and requires extra care (Zougagh et al., 2012). It's noteworthy that all RSD errors were within 5% error margin except Pb concentration (20 µg/l) where, the RSD was 7%.

Figure 5.3 gives a graphical representation of calibration standards in obtaining a calibration for the metals using results shown in Table 5.3. The coefficient of regression R^2 obtained from the calibration results was 1 for all metals, depicting a well-represented correlation between the prepared and measured calibration standard solutions with ICP-MS.

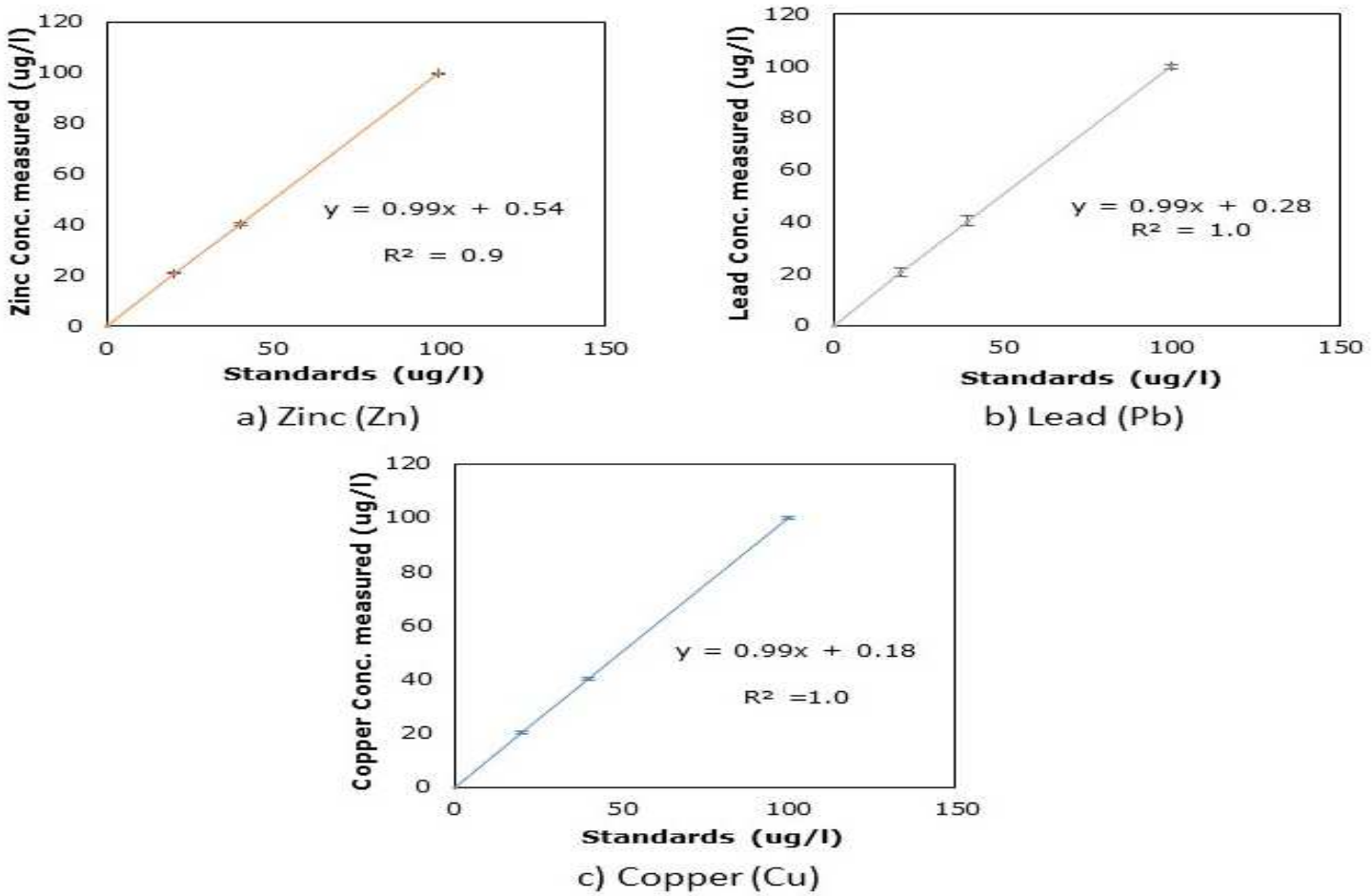


Figure 5.3: Calibration curve of ICP-MS using external calibration standards (<0, 20, 40 and 100 µg/l) for a) zinc, b) lead and c) copper metals.

As mentioned earlier, ICP-MS has a dynamic range of 8 orders of magnitude and a linear calibration across 10,000,000 units. Hence, a calibration within the µg/l range could be applied in measuring sample concentrations in the mg/l range. However, when sample concentrations are likely to exceed 60 mg/l for heavy metal/trace elements, dilutions are required to have more precise observations.

5.6 Limit of detection and quantification

Limit of detection (LoD) and limit of quantification (LoQ) were determined based on the calibration curves in Figure 5.3. Table 5.4 shows results obtained for LoD, LoQ and data set used in determining these parameters. LoD expresses the smallest concentration of an analyte that can be reliably measured by an analytic procedure (Rajakovic et al., 2012), while Armbruster and Pry (2008) defined LoQ as the lowest concentration at which the analyte can not only be reliably detected but at which some predefined goals for bias and imprecision are met. LoD and LoQ were calculated with equations (4) and (5) using calibration data from Figure 5.3.

$$\mathrm{LoD} = 3.3 * \mathrm{STEYX/S} \qquad (4)$$

$$\mathrm{LoQ} = 10 * \mathrm{STEYX/S} \qquad (5)$$

Where, STEYX known as standard error of the regression/estimate is also referred to as standard deviation of the calibration curve and S represents the slope of the calibration curve.

Table 5.4: Limit of detection and limit of quantification for Cu, Zn and Pb obtained from calibration curve parameters.

Parameters	**Cu (µg/l)**	**Zn (µg/l)**	**Pb (µg/l)**
Equation of line	y = 0.9976x + 0.18	y = 0.9927x + 0.55	y = 0.9962x + 0.28
Coefficient of regression	R^2 = 1.0	R^2 = 0.99	R^2 = 1.0
Slope (S)	0.998	0.993	0.996
STEYX = $\sqrt{\frac{\Sigma(y_i - \hat{y}_i)^2}{(n-2)}}$	0.184	0.627	0.295
LoD	0.61	2.08	0.98
LoQ	1.84	6.31	2.96

The LoD and LoQ for copper was observed as the lowest with zinc recording the highest in the order Zn > Pb > Cu. This parameter is very important in asserting the presence of any analyte in its lowest concentration detectable by the ICP-MS, below which it can be concluded as not present, immeasurable or undetected. This limit also informs on threshold for

adsorption experiments indicating whether the instrument would be suitable in obtaining expected metal reduction limits. Compared to the acceptable effluent discharge limits of Pb: 6.0 µg/l (Tran et al., 2017), Zn: 0.8 mg/l (Tran et al., 2017) respectively and Cu: 0.25 mg/l (Tran et al., 2017), both LoD and LoQ are above the required limits. Hence, this equipment (ICP-MS) can be confidently used is monitoring metal concentrations at levels lower than the acceptable effluent discharge limits and suitable for the experiments.

5.7 Chapter summary

Both 0.45 and 0.22 µm syringe filters display RSDs less than 5% the initial concentration and suitable to be used. Precipitation of metals was least at pH 3.5 and more after pH 6.5 – 10. This implies that metal removal in solution can only be due to adsorption within pH 3.5 – 6.5 for zeolite NaP1, after which the effect of precipitation can be considered. Leaching was prevalent at pH 3.5 while the ICP-MS could detect limits lower the acceptable effluent discharge limit and affirmed as fit for determining adsorption concentration.

6 Adsorption experiments

6.1 Introduction

This chapter focuses on adsorption experiments of copper, zinc and lead while assessing the kinetics, isotherms and ion selectivity of the respective metals with zeolite NaP1. Finally, this section tests for the suitable pH of multi-element adsorption with NaP1.

6.2 Single element removal

6.2.1 Zinc removal

Zinc removal with control experiments was performed using 5 grams of zeolite NaP1 mixed with 1 litre of synthetic zinc nitrate solutions of concentration 250 mg/l for ~ 3 hours at 20 ± 2 °C with constant pH at 3.5. Experiments were repeated 3 times and values presented in Figure 6.1 shows mean with standard deviation for the observations. Figure 6.1 shows a steep decline in concentration, which is observed within the first 15 min followed by a steady decrease from 30 min till 180 min, where, zinc concentration remained constant at 217 mg/l. This trend indicates the saturation of available sites within the first 15 min, followed by a slow diffusion of zinc ions through the pores of zeolite NaP1 until saturation is achieved (Inglezakis et al., 2003;

Sprynskyy et al., 2006; Amarasinghe and Williams, 2007; Motsi et al., 2009).

In comparison, a control experiment without NaP1 performed under the same conditions as the metal uptake experiment (Figure 6.1), showed no decrease in zinc concentration over the same period. A stable concentration of zinc (250.5 ± 3.6 mg/l) was recorded throughout the metal uptake period (3 h) from the control experiment. This demonstrated that the decrease in zinc concentration obtained during the adsorption experiment could only be due to the presence of zeolite NaP1 and not precipitation.

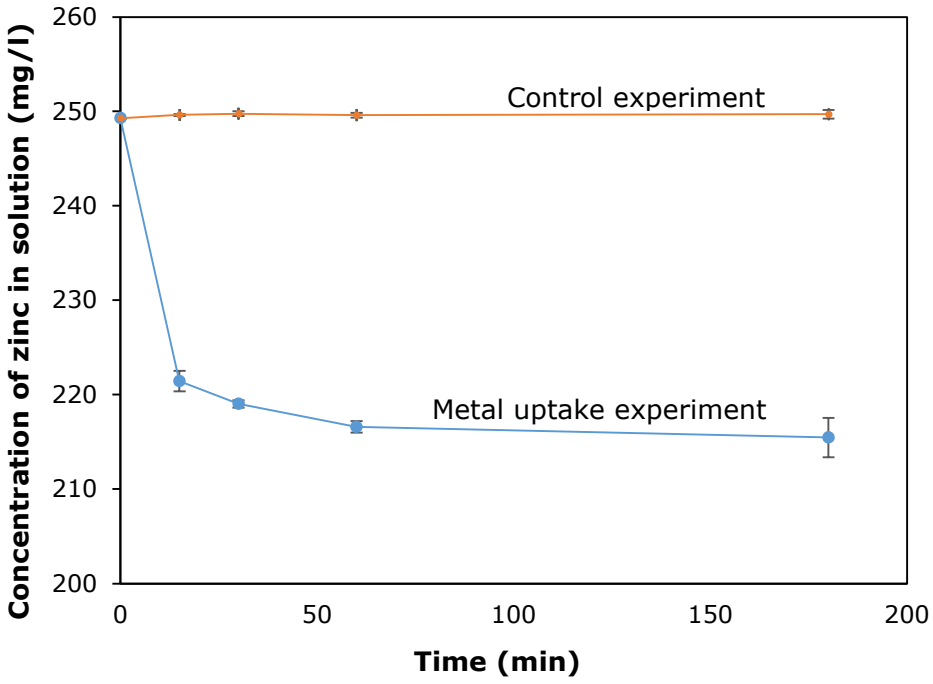


Figure 6.1: Decrease in zinc concentration in solution as a function of time when 5 g adsorbent is used in 1 l solution and compared to a control experiment at the same conditions without zeolite. Initial zinc amount is 250 mg/l, pH=3.5, t=3 h at 20 ± 2 °C. Values presented are mean with standard deviation from 3 repetitions.

Figure 6.1 also indicates active available sites were occupied in 3 hours, after which further zinc uptake was not possible. The difference in metal uptake at 60 min and 180 min was < 1 mg/l, equivalent to 0.5% of the concentration at 60 min. Thus, this difference can be attributed to experimental error and implying maximum capacity of metal uptake occurred at 60 min instead of 180 min. The total zinc uptake was 33.4 ± 2.1 mg/l,

approximately 14% of the overall starting concentration. The isotherm of zinc was obtained in Figure 6.2 by stirring 5 grams of zeolite NaP1 with a range of aqueous zinc nitrate concentrations (50 – 2500 mg/l) in 1 litre solution at a mixing speed of 350 rpm for 3 h at pH 3.5 and 20 ± 2 °C.

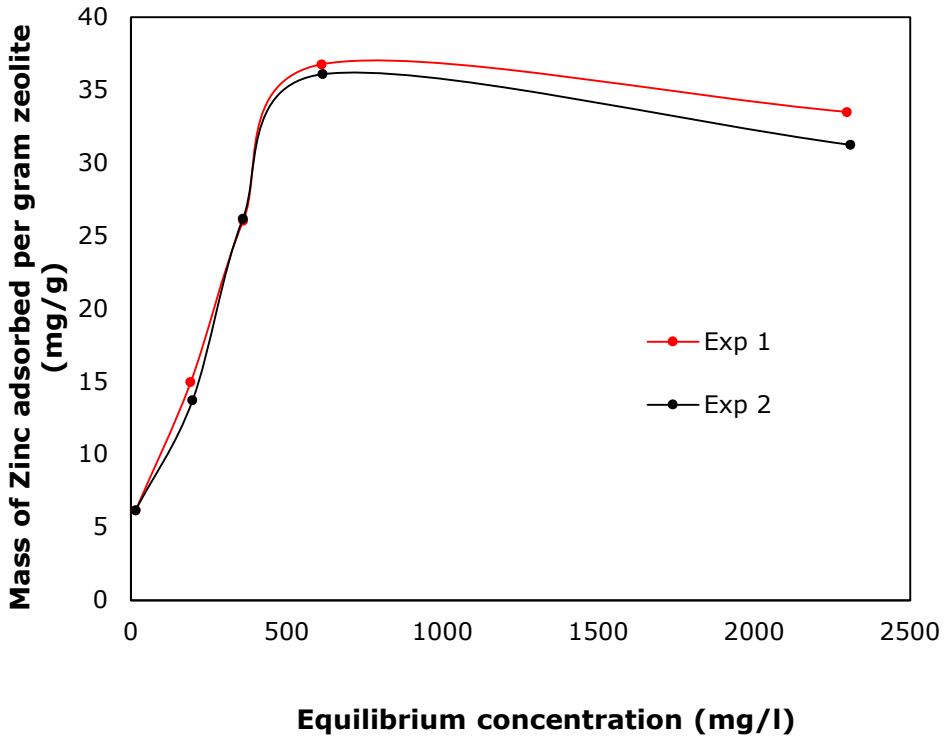


Figure 6.2: Amount of zinc adsorbed per gram of zeolite as a function of equilibrium concentration of the zinc solution when 5 g adsorbent is stirred in 1 l solution at 300 rpm. Initial zinc amount varied from: (50, 250, 500, 1000 and 2500 mg/l), pH=3.5, t= 1 h at 20 ± 2 °C. The graphs presented are resulting from 2 repetitions.

Figure 6.2 shows the amount of zinc adsorbed per gram of zeolite over the range of zinc concentrations for two repetitions. Maximum uptake capacity obtained from the graph is 34.2 mg zinc per gram zeolite from both experiments. Experiments 1 and 2 are observed to be similar in trend. An increase in initial concentration from 50 mg/l – 600 mg/l increased the concentration gradient of zinc ions towards available sites, thereby increasing the uptake untill the point of saturation, where, further concentration increase made no difference in metal uptake (Arshadi et al., 2014). The shape of the isotherm in Figure 6.2, based on Giles et al. (1974) isotherm classification, with slope and curvature is identical to Langmuir isotherm and Type 1 isotherm (Hinz, 2001). The adsorption curve is characterised by a constant maximum sorption and a convex shape. This indicates that the sorption affinity of the isotherms increases with decreasing concentration (Hinz, 2001).

Thus, at lower concentrations, more zinc ions can be removed from solution by NaP1. This property of NaP1 gives it an edge over other technologies as most current techniques are unable to reduce metal concentrations at very low concentrations in large volumes of water (Lakherwal, 2014). However, Figure 6.2 also shows a reduction in adsorption capacity at zinc

concentration of 2500 mg/l. This could be the result of possible competition between hydrogen ions and influx (higher concentration) of zinc ions present in solution at pH 3.5 (Reddy et al., 1995).

In comparison to other studies, Lee et al. (2000) explored synthetic NaP1 for zinc removal from water matrix of concentration (6.54 mg/l) using 0.1 g zeolite in a litre of solution at 25 °C. Although, there is no record of pH adjustment and contact time, Lee et al. (2000) obtained 65.8 mg/g adsorptive capacity (65 mg zinc /g zeolite) compared to 34.2 mg/g in this study (50 mg zinc /g zeolite). Their result could be attributed to the effect of undisclosed contact time, a combined effect of precipitation and adsorption at an undisclosed pH, possibly higher than the precipitation pH of zinc (precipitation starts at 7 for Zn, (Dean et al., 1972) in the absence of pH adjustment.

Zeolite NaP1 is known to increase OH^- ions of an aqueous solution. This is achieved by replacing H^+ ions with Na^+ ions, which increases the pH of the solution (Alvarez-Ayuso et al., 2003). Hence, zinc hydroxides are easily formed and may precipitate at a pH higher than 7; reducing the zinc concentration in solution. The resulting reduced metal

concentration could inaccurately be attributed to metal uptake of the adsorbent while neglecting the effect of precipitation.

In contrast, Querol et al. (2002), Moreno et al. (2001) and Prasad and Mortimer (2010) tested synthetic NaP1 on zinc removal from acid mine wastewater of concentration 0.65 mg/l, 54 mg/l and 174 mg/l, respectively. Contact time for all experiments was reported as 1 h with initial pH values > 4.6, 5.5 and 2.5 - 5.5, respectively, without further pH adjustment during the experiment. These experiments with mass of zinc to zeolite ratio 0.02 mg/g, 1.8 mg/g and 5.8 mg/g, respectively, all produced more than 94% removal efficiency for NaP1. As discussed earlier, the difference in removal efficiency > 94% compared to this study (18.6 ± 0.8%) can be attributed to an experiment without pH adjustment and the low zinc to zeolite ratio in these works. A low zinc to zeolite ratio will increase the available saturation sites of the adsorbent for a low quantity of adsorbates. This would lead to a higher adsorptive capacity while no pH adjustment is also known to increase metal reduction in solution by precipitation above pH 7.

Finally, Alvarez-Ayuso et al. (2003) treated zinc from an electroplating wastewater finishing effluent of concentration 125 mg/l at pH 6 in contact time (1 h) using 2.5 mg/l solid to liquid ratio. They obtained 32.6 mg/g adsorptive capacity for

synthetic NaP1 in a multi-element system compared to 34.2 mg/g in this study with the same zinc to zeolite ratio of 50 mg/g. Adsorptive capacity of adsorbents are generally higher in single element adsorption compared to multi-element due to metal competition within the system (Mohan and Singh, 2002) and one of the reasons for the higher adsorptive capacity observed in this experiment over Alvarez-Ayuso et al. (2003).

The adsorptive capacity of fly-ash derived NaP1 in this study is lower compared to works of Lee et al. (2000), Querol et al. (2002), Moreno et al. (2001) and Prasad and Mortimer (2010), as it produced an uptake capacity of 34.2 mg/g at pH 3.5, eventhough these are not directly comparable for reasons explained above. However, the adsorptive capacity of this study is higher than in Alvarez-Ayuso et al. (2003), the only comparable study so far with a different pH (3.5 in this study and 6 in Alvarez-Ayuso et al. (2003).

6.2.2 Lead removal

Figure 6.3 shows the result of metal removal experiment with initial lead concentration in solution of 100 mg/l over 90 min. Experiments were repeated 3 times and values presented in Figure 6.3 for the observations. Similar to zinc from Figure 6.1,

NaP1 displayed the highest uptake within 15 min for lead, indicating fast kinetics of the adsorbent.

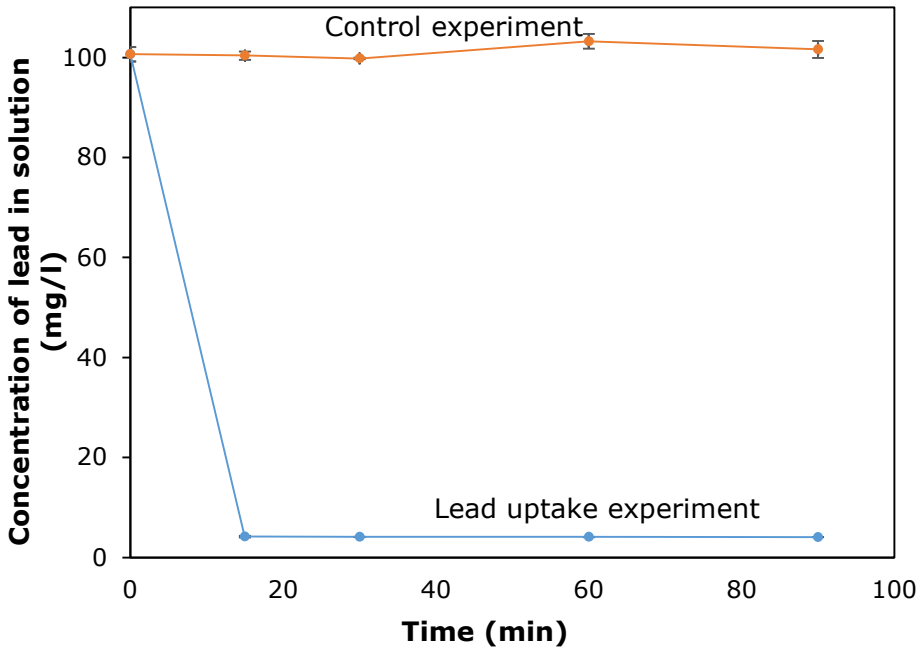


Figure 6.3: Decrease in lead concentration as a function of time (90 min) when 5 g adsorbent is used in 1 l solution. Initial lead amount: (100 mg/l), pH= 3.5, t= 1.5 h at 20 ± 2 °C. Values presented are mean and standard deviation for the observation of 3 repetitions.

In Figure 6.3, lead concentration from the metal uptake experiment decreased to 4.21 ± 0.16 mg/l from an initial concentration of 100 ± 1.45 mg/l in 15 min. The concentration remained constant at 4.11 ± 0.04 mg/l in 30 min until the end of the experiment (90 min). Optimum contact time, where, saturation of the adsorbent seemed to have occurred for lead, was after 15 min. The control experiment, which was 100 mg/l

lead concentration without NaP1 was also conducted for 1.5 h, at pH 3.5 and temperature of 20 ± 2 °C to validate the metal uptake process. Lead concentration from the control experiment remained constant throughout the experiment, compared to the adsorption experiment in Figure 6.3, demonstrating that there was no lead precipitation.

Similar to zinc experiments, lead ions in solution are also attracted towards the NaP1 surface with a possible adsorption mechanism, dictating uptake process over the entire period. Metal attraction to the surface of NaP1 due to weak van der Waals forces may be responsible for a fast metal uptake within the first 15 min followed by further slow passage of lead ions through the NaP1 micropores until available sites are occupied (Inglezakis et al., 2002; Myroslav et al., 2006; Amarasinghe and Williams, 2007; Motsi et al., 2009).

Equilibrium experiments conducted in Figure 6.4 were conducted to determine the maximum lead uptake for fly-ash derived zeolite NaP1. Lead solutions of concentration range (50 – 3500 mg/l) were mixed with 5 g of NaP1 in each solution volume of 1 L, mixing speed of 300 rpm, pH 3.5 and at 20 ± 2 °C.

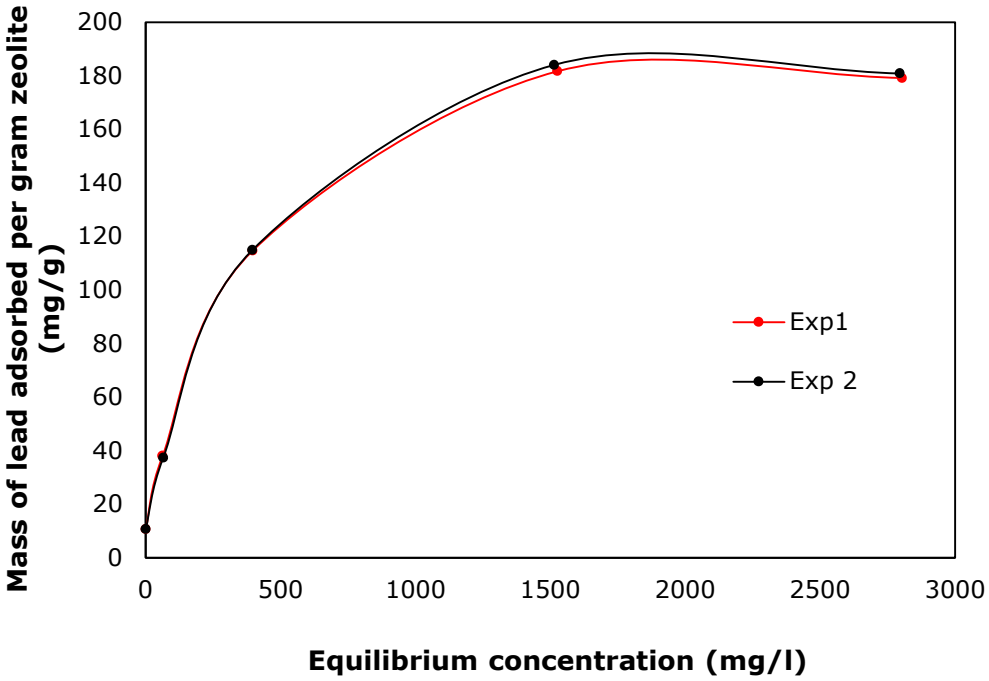


Figure 6.4: Amount of lead adsorbed per gram zeolite as a function of equilibrium concentration of the lead solution when 5 g adsorbent is stirred in 1 l solution at 300 rpm. Initial lead amount varied from (50, 250, 500, 1000, 2500 and 3500 mg/l), pH= 3.5, t= 1h T= 20 ± 2 °C. The graphs presented are resulting from two repetitions.

The experiments performed twice due to limited NaP1 are displayed in Figure 6.4. Equilibrium experiments 1 and 2 are observed to be similar in trend with minimal differences from Figure 6.4. Lead equilibrium with NaP1 produced maximum lead uptake of 192 mg/g from both experiments. This is a reflection of the maximum uptake capacity of NaP1 for lead, where, available sites in NaP1 are occupied by lead (Nalaparaju et al.,

2009) and further increase in concentration does not influence metal uptake anymore. The shape of the isotherm seen in Figure 6.4 is similar to the Langmuir and Type 1 isotherm, as observed for zinc. However, the lead isotherm is relatively steeper than zinc isotherm, showing a higher affinity of NaP1 to lead than zinc at lower concentrations as demonstrated in other works (Steenbruggen and Hollman, 1998; Lee et al., 2000; Querol et al., 2002). This implies that lead ions would be removed quicker from solution at lower concentrations compared to zinc (Hinz, 2001). The percentage removal of lead decreased by 2-5% as the initial lead concentration increased by 50 mg/l over the range of experiments (50 – 3500 mg/l).

Nascimento et al. (2009) tested NaP1 for lead removal from water matrix and reported an adsorptive capacity of 195 mg/g compared to 192 mg/g achieved in this research. Their experimental conditions were pH 4-5, at 25 °C, metal concentration of 100 – 3000 mg/l and solid to liquid (S/L) ratio of 10 g/l. The marginal increase in adsorptive capacity recorded in their study could be the result of pH difference as the higher pH value implies a reduced concentration of competitive H^+ ions against metal ions. Also, they used a solid to liquid ratio, 2 times more than what was used in this research indicating the use of 2 times more zeolite than what was used in this research. This

implies that NaP1 used in this research is 2 times more efficient than that used by Nascimento et al. (2009). As mentioned earlier, zeolites with a lower Si/Al ratio are known to possess better adsorption capacity than their counterparts with higher Si/Al values. In this study, NaP1 has a Si/Al ratio of 1.51, compared to 2.32 from Nascimento et al. (2009). This could also be another factor contributing to NaP1 from this study demonstrating superiority over that from Nascimento et al. (2009).

Lee et al. (2000) also studied the removal of lead from water matrix obtaining an adsorptive capacity of 267 mg/g with 0.1 g zeolite NaP1, concentration (20 – 400 mg/l), temperature 25 °C without pH adjustment. Their study did not disclose the starting pH nor the duration of the experiment and cannot be readily compared with this research. Zeolite NaP1 increased the pH of metal solution from 5 to 11 without pH adjustment (Moreno et al. 2001). Increase in pH reduces heavy metal concentration by precipitation, thus, pH adjustment is required to ensure that heavy metal uptake is either by ion exchange or adsorption and not precipitation.

Chaudhuri and Saminal (2011) and Rahman et al. (2016) tested the removal of lead with commercial activated carbon at pH 5,

concentration; 10 – 100 mg/l and 6 – 227 mg/l respectively, time; 2.5 h and 72 h respectively and S/L ratio; 4 and 2 g/l respectively. Their results generated 7.5 and 23.4 mg/g respectively, which were also low compared to 192 mg/g obtained from this result. Arguably, zeolite NaP1 from this study has proven to be superior compared to its counterparts from the literature for lead removal. Although, these studies did not provide BET areas to compare, available comparable attributes such as Si/Al ratio, solid/liquid ratio, pH and concentration range were used to reach this conclusion.

6.2.3 Copper removal

Copper uptake was also tested with NaP1.Two experiments (control and metal uptake) were performed in triplicates. Both experiments were conducted under the same experimental conditions such as 150 mg/l copper amount used in 1 l solution at pH 3.5 over 180 min at 20 ± 2 °C. The control experiment was performed without NaP1, while, during the metal uptake experiment, 5 g of NaP1 was used. The control experiment (Figure 6.5) maintained a steady concentration (150 mg/l) as the initial concentration without changing over the duration of the experiment (3 h). This suggests, there was no precipation of copper under these experimental conditions.

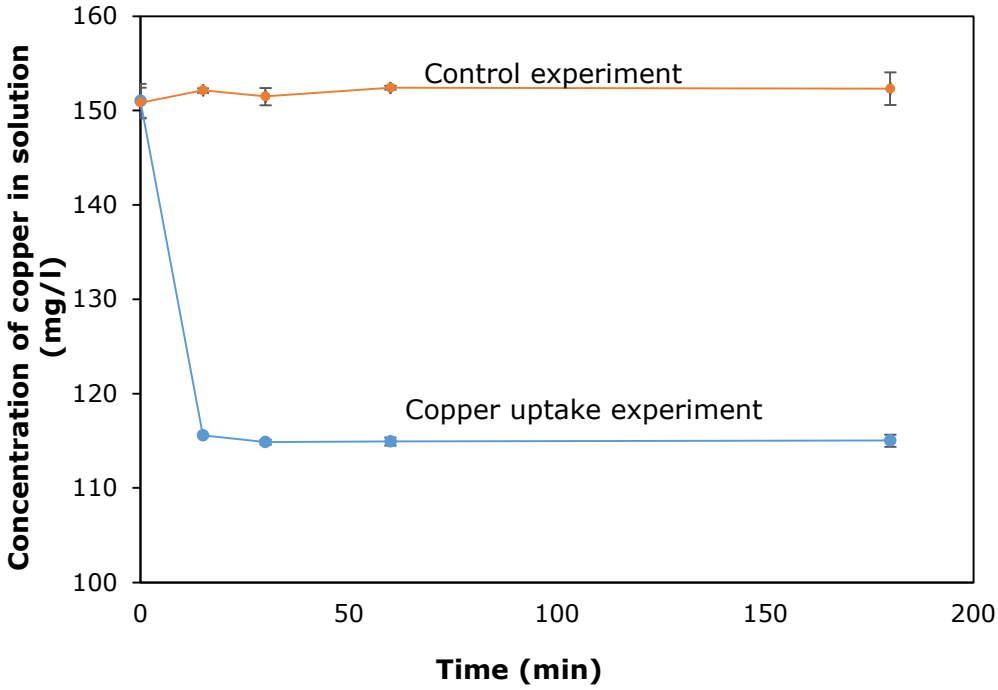


Figure 6.5: Decrease in copper concentration as a function of time when 5 g adsorbent is used in 1 l solution. Initial copper amount= (150 mg/l), pH= 3.5, T= 20 ± 2 °C. Values presented are mean and standard deviation for the observation of 3 repetitions.

In contrast to the control experiment, copper concentration in the metal uptake experiment dropped to 115 mg/l within the first 15 min and remained constant till the end of the experiment. This is 35 mg/l reduction in copper concentration. The observation from Figure 6.5 is indicative of copper uptake as a result of the presence of NaP1. The selected equilibrium time from the copper uptake experiment was 60 min to maintain a consistent time with zinc and lead experiments in leading to multi-element experiments and meaningful comparisons.

The selected equilibrium time was used as the duration for the equilibrium experiment observed in Figure 6.6. Equilibrium experiments were performed to determine the maximum copper uptake for NaP1. Copper solutions with a concentration range of 80 – 1000 mg/l were mixed with 5 g of NaP1 in 1 l with mixing speed of 300 rpm, at pH 3.5 and at 20 ± 2 °C.

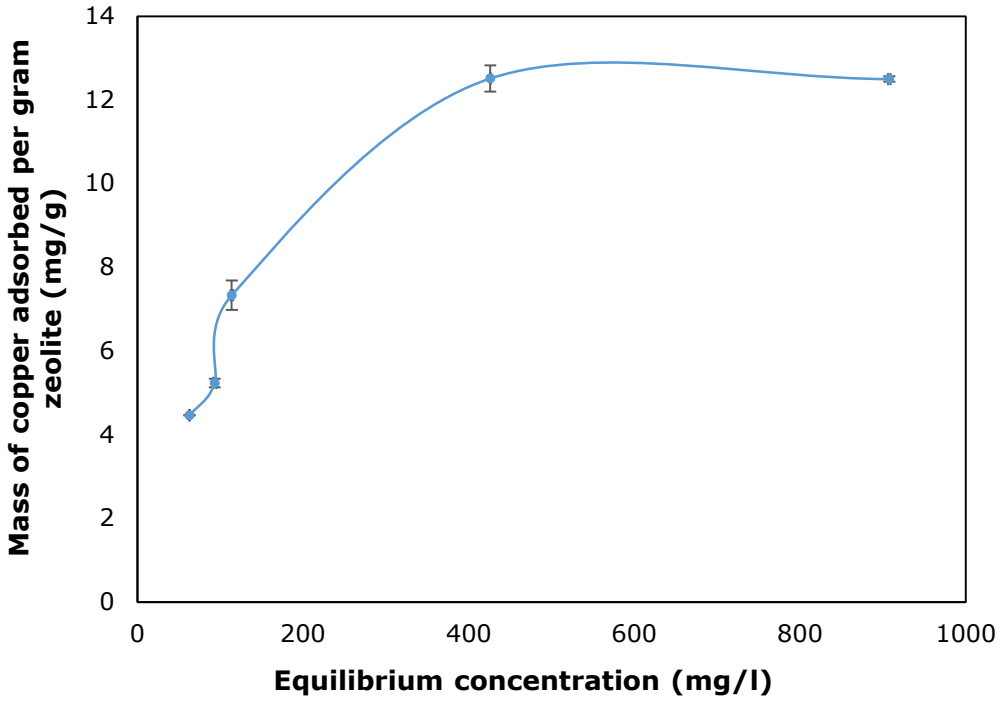


Figure 6.6: Amount of copper adsorbed per gram zeolite as a function of equilibrium concentration of the copper solution when 5 g adsorbent is stirred in 1 l solution at 300 rpm. Initial copper amount varied in the range of 80, 120, 150, 500 and 1000 mg/l, pH= 3.5, t= 1 h, at 20 ± 2 °C. The data points presented are resulted from 3 repetitions.

NaP1 produced maximum copper uptake of 12 mg/g. This is reflective of the maximum uptake capacity of NaP1 for copper. In comparison to zinc and lead from previous experiments, NaP1 produced the least up-take with copper. The shape of the isotherm observed from Figure 6.6 is as the Type 1 Langmuir isotherm, similar to the ones observed with zinc and lead equilibrium experiments. However, the gentle slope depicting the copper uptake interaction process, indicates a reduced affinity of NaP1 for copper compared to lead and zinc. This can be descriptive of a gradually controlled uptake mechanism linked with the pore size of NaP1 versus the size of hydrated copper ions in solution.

The maximum copper uptake capacity for NaP1 obtained from this study differs from NaP1 of Nascimento et al. (2009): 76.9 mg/g, Alvarez-Ayuso et al. (2003): 50.5 mg/g, and Lee et al. (2000): 73.5 mg/g. Copper uptake from this research produced the lowest results of 12 mg/g. Nascimento et al. (2009) and Alvarez-Ayuso et al. (2003) are the closest comparisons with this research since they indicated all relevant working parameters. Nascimento et al. (2009) tested NaP1 for copper removal from wastewater matrix with the following parameters: pH ranges 4 - 5, an experimental time of 2 h, a temperature of 25 °C, concentration range 100 - 3000 mg/l and solid to liquid

ratio of 10 g/l. Their research employed longer contact time, a higher pH and a higher solid to liquid ratio like Alvarez-Ayuso et al. (2003). These factors respectively increase metal uptake. The main difference between their research and this study is the solid to liquid ratio. As mentioned earlier, a high solid to liquid ratio implies increased material (available metal uptake sites) with respect to adsorbate in solution increasing the amount of metal uptake.

Secondly, high pH values imply a decrease in hydrogen ion concentration, which tend to compete for metal uptake sites while high pH above the solubility limit of target elements is also known to increase the effect of precipitation. The parameters are notably responsible for either increasing the metal uptake process or erroneously distorting the actual uptake quantity. Hence, it is no surprise to see NaP1 from this research produce such low results for the uptake of copper under these experimental conditions.

NaP1 has also demonstrated superior metal removal capabilities (adsorptive capacity), in comparison to other commercial adsorbents such as activated carbon and clinoptilolite. Table 6.1 shows a summary of adsorbents (commercial activated carbon and Clinoptilolite) tested by researchers under the same

conditions as NaP1, to produce metal removal capacity less than 10 mg/g for zinc and copper except lead in one case, 23 mg/g. This is a promising development to further display the potential of NaP1 as an alternative adsorbent in comparison to counterparts from literature summarized in Table 6.1.

Table 6.1: Summary of adsorbent performance of works adopted from Koshy and Singh (2016) and other studies.

Fly-ash origin	Ionic Species	Q_e (mg/g)	Lang. constant (l/mg)	pH	Time (h)	Temp. (°C)	Conc. (mg/l)	S/L ratio (g/l)	Reference
South Korea (NaP1)	Cu	73.5	21.91	N/A	N/A	25	20 - 400	0.1	Lee et al., 2000
	Pb	266.4	457.29						
	Zn	65.8	8.29						
Spain (NaP1)	Cu	50.5	0.68	5	6	22	10 - 200	2.5	Alvarez-Ayuso et al., 2003
	Zn	32.6	1.48						
	Ni	20.1	1.06						
Brazil (NaP1)	Cu	76.9	0.0021	4-5	2	25	100 – 3000	10	Nascimento et al., 2009
	Zn	59.2	0.0009						
	Pb	194.7	0.0014						

Table 6.1: ……*continued.*

Fly-ash origin	Ionic Species	Q_e (mg/g)	Lang. constant (l/mg)	pH	Time (h)	Temp. (°C)	Conc. (mg/l)	S/L ratio (g/l)	Reference
Malaysia (CAC)	Pb	7.55	0.17	5	2.5	N/A	10 – 100	4	Chaudhuri and Saminal, 2011
Germany (CAC)	Pb	23.42	0.02	5	72	N/A	6 - 227	2	Rahman et al., 2014
	Ni	3.18	0.131						
Turkey (Clinoptilolite)	Cu	8.96	1160	6 – 7	5.5	30	100 - 400	20	Erdem et al., 2004
	Zn	8.75	850						

Table 6.1: ……*continued.*

Fly-ash origin	Ionic Species	Q_e (mg/g)	Lang. constant (l/mg)	pH	Time (h)	Temp. (°C)	Conc. (mg/l)	S/L ratio (g/l)	Reference
Spain (Clinoptilolite)	Cu	5.91	0.15	5	6	22	10 - 200	2.5	Alvarez-Ayuso et al., 2003
	Zn	3.45	0.11						
	Ni	1.98	1.03						
UK (Clinoptilolite)	Cu	3.37	0.11	3.5	6	22	20 - 400	37	Motsi et al., 2009
	Zn	5.38	0.02						
Results (NaP1)	Cu	14.6	0.008	3.5	1	20	80 - 1000	5	This Research
	Zn	34.2	0.009		6		50 - 3500		
	Pb	191.9	0.006		1		50 – 3500		

6.3 Single element adsorption kinetics

The kinetic results for all the metals showed a fast metal uptake between the metals and NaP1. More than 80% of the overall uptake occurred within the first 15 min of the experimental duration (Sánchez-Hernández et al., 2018), while the remaining uptake was slow and gradual until no further uptake. Lead uptake was the highest as 96 mg/l representing 96% of the starting concentration was removed in 30 minutes, followed by copper with 35 mg/l in 15 min and finally zinc with 33 mg/l in 60 min. Zinc uptake took the longest time (1 h) and was chosen as the equilibrium time for further equilibrium experiments. The equilibrium time from time study (1 h) was the shortest compared to other studies on NaP1; Alvarez-Ayuso et al. (2003) – 6 h, Nascimento et al. (2009) – 2 h.

The fast metal uptake kinetic of NaP1 indicates a quick sorption time and would be a useful property in industry since time is an asset in process engineering. The shorter a process, the more value it obtains as it is preferred to its longer counterparts (time is money). Reducing the process time of any process, saves money on labour cost, energy cost and wear of machines used. This is one-way industries can save money while achieving their intended targets. This phenomenon is the likely demonstration

of competition between aqueous ions in solution and could be explored in industry for selective metal removal. In further analyses, the kinetic data was tested against the Lagergren's kinetic models (pseudo-first and second order models) to further describe the uptake mechanism.

The pseudo-second order best fitted the kinetic data with a strong correlation coefficient (R^2) of 1 for Pb/Zn/Cu using NaP1 and emphasizing that it was most suitable in describing the mass transfer phenomenon. The pseudo-second order model identifies with a heterogenous surface and could either suggest a chemisorption or an ion-exchange mechanism depending on the functional group of the adsorbent (Blanchard et al., 1998; Kumar, 2006). Physisorption is proposed by Blanchard et al. (1984) with the use of clinoptilolite (natural zeolite), whereas Ho and McKay's (2000) expression was derived assuming chemisorption and monolayer coverage with peat (Kumar, 2006).

Compared to clinoptilolite and peat, fly-ash derived NaP1 closely relates to clinoptilolite from the same functional group, thus indicating physisorption as the main metal uptake mechanism. Erdem et al. (2004) and Nascimento et al. (2009) also identified

physisorption as the mechanism governing metal uptake using the pseudo-second order kinetic model. The rate controlling step is particle diffusion through the porous channel of fly-ash derived NaP1 (Erdem et al., 2004; Hendricks, 2016). Metal cations are first attracted to the surface of the NaP1 through weak Van der Waal's forces (electrostatic attraction) and diffuse through the pores of NaP1. Diffusion is fast (15 min) but becomes slow (30 – 180 min) as metals move through the porous structure since the pore dimensions are close to the molecular size of the metals mentioned earlier (Erdem et al., 2004).

6.4 Adsorption isotherms for single heavy metals

Data from the adsorption experiments were evaluated using Langmuir and Freundlich Isotherm models to determine which model best fits the experimental data in order to describe and understand the uptake phenomenon. The Langmuir model, which assumes a monolayer adsorption on the adsorbent surface and expressed by a linear plot of C_e/Q_e versus C_e is displayed in Figure 6.7, where, C_e is the adsorbate concentration in the solution at equilibrium, q_e is the amount of solute adsorbed per unit mass of adsorbent, b is the constant of Langmuir isotherm representing the affinity of the adsorbent

to adsorbate and relates to sorption energy and q_m is the maximum sorption capacity of the adsorbent at equilibrium. The constants b and q_m are determined from the intercept and slope of the line, respectively.

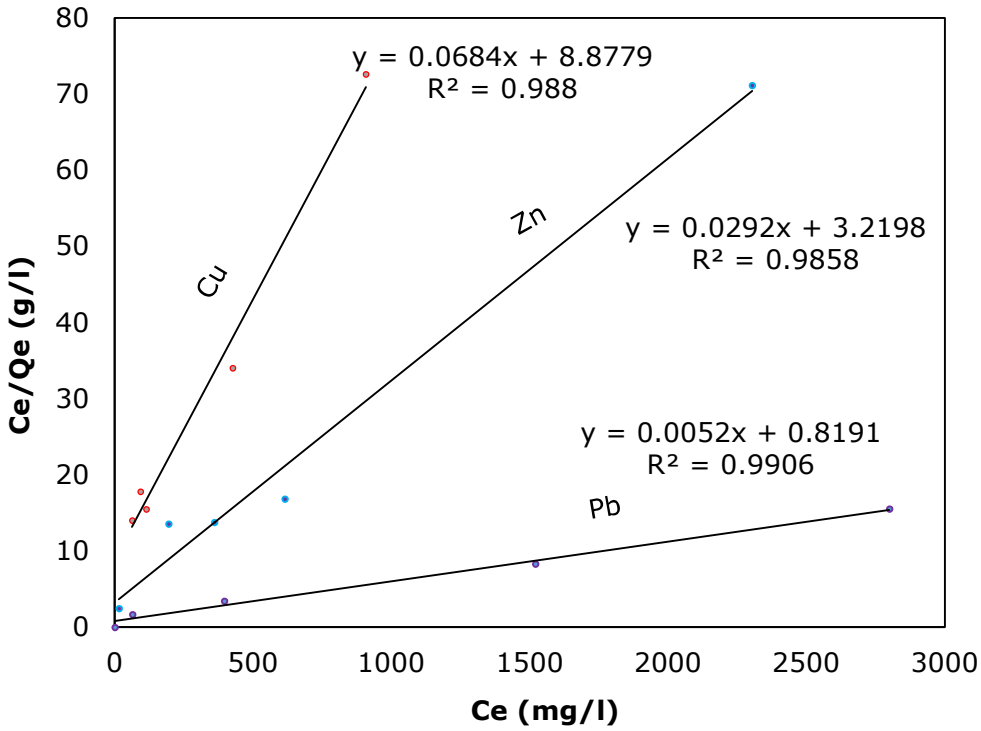


Figure 6.7: Langmuir isotherm model for copper, zinc and lead (with concentrations of 50, 150, 250, 150, 500, 1000, 2000 and 3500 mg/l) on zeolite NaP1 (dosage 5 g/l) at 20 ± 2 °C and pH 3.5 at a constant stirring speed of 300 rpm.

The Langmuir model fitted well when tested with the sorption data obtained for zinc, copper and lead experiments as R^2 values are ~ 0.99 in both cases, as shown in Figure 6.7. As seen earlier, equilibrium plots for zinc (Fig. 6.2), lead (Fig. 6.4) and

copper (Fig. 6.6) are like Type 1 isotherm for physical adsorption classified by Brunauer et al. (1940). This isotherm is used to describe microporous adsorbents with pore size ~ 0.29 nm (Sharma et al., 2016), not much greater than the molecular diameter of the sorbate molecule (Pb= 0.266, Zn= 0.166, Cu= 0.164 nm). This is because the adsorbents have a definite saturation limit corresponding to the complete filling of the micro-pores (Ruthven, 1984).

However, the Type 1 isotherm is also obtained through the Langmuir equation and often associated with physisorption than chemisorption, where, adsorbate molecules are assumed to occupy a fixed number of well-defined localized sites without mobility and no interaction with neighbouring sites. The Langmuir equation could also be applied to mobile physical adsorption at relatively low coverage, where, adsorbate molecules are localized due to saturation of the adsorbent (Ruthven, 1984). Hence, Langmuir isotherm is further emphasizing physisorption for fly-ash zeolite NaP1.

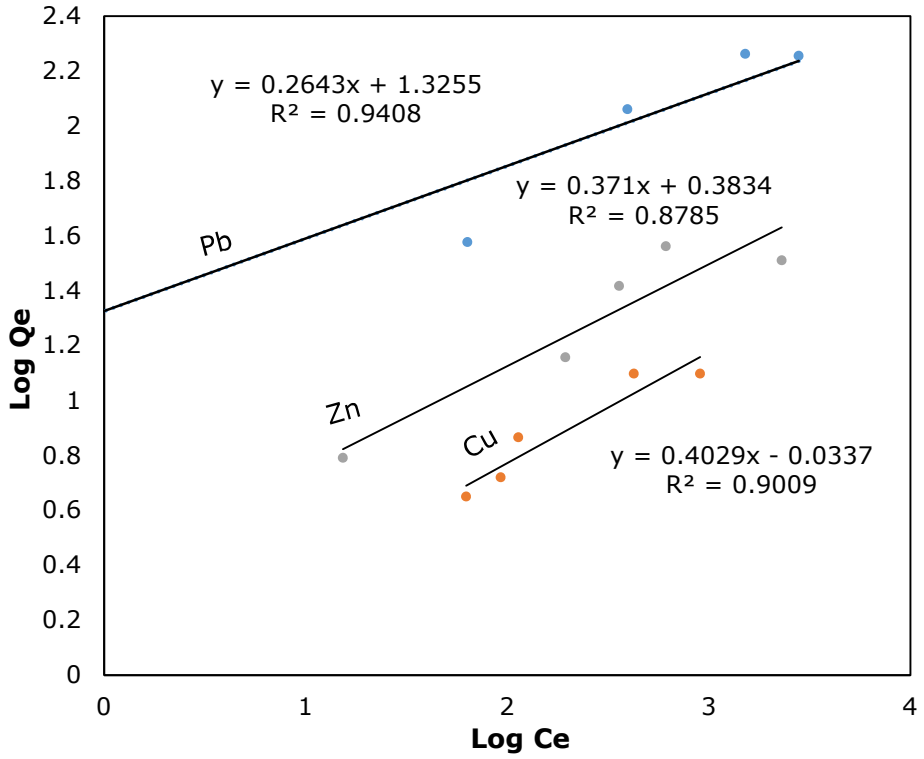


Figure 6.8: Freundlich isotherm model for copper, zinc and lead (with concentrations of 50, 150, 250, 150, 500, 1000, 2000 and 3500 mg/l) on zeolite NaP1 (dosage 5 g/l) at 20 ± 2 °C and pH 3.5 at a constant stirring speed of 300 rpm.

However, Freundlich isotherm was also applied in describing experimental results for Pb, Zn and Cu, which proved regression coefficients of 0.94 and 0.88 and 0.90, respectively (Figure 6.8). Freundlich isotherm indicates a multilayer adsorption for heterogeneous surface adsorbents and the existence of van der Waals attractive forces between the surfaces involved. The parameters determined from this isotherm; K^F (the adsorptive capacity) and n (degree of heterogeneity) are populated in Table 6.2.

Table 6.2: A comparison of NaP1 adsorptive capacities for heavy metals between Langmuir and Freundlich models.

	Langmuir			Freundlich		
Element	**Adsorptive capacity (mg/g)**	**Langmuir constant (b)**	**R^2**	**Adsorptive capacity (mg/g)**	**Degree of heterogeneity (n)**	**R^2**
Zinc	34.3	0.00906	0.986	2.41	2.70	0.878
Copper	14.6	0.00770	0.988	0.925	2.48	0.901
Lead	192	0.00636	0.991	21.1	3.72	0.941

The adsorptive capacity and regression coefficient (R^2) of Freundlich compared to Langmuir is low for all metals from Table 6.2. Hence, Langmuir model was preferred to Freundlich model, in describing the adsorption isotherm while results from Freundlich model complemented that of Langmuir model. First, the degree of heterogeneity (n) shows the intensity of metal uptake and how the surface of the adsorbent can be distinguished into different patches with different sorption energy levels (Dabrowski, 1998). The constant (n) also indicated chemisorption or physisorption according to Desta (2013). Thus, a larger ($n > 1$) value shows a more heterogeneous system (Do, 1998) and a physisorption mechanism (Desta, 2013). From the Table 6.2, it is observed that the n value for all metal adsorption with NaP1 are greater than 1. This supports the physisorption mechanism suggested from the pseudo-second order kinetic reaction. The cause of system heterogeneity is by complex porous structures made up of micropores of different dimensions (Dabrowski, 1998).

From Table 6.2, lead adsorption demonstrated an **n** value of 3.7 indicating accessibility to nearly four different heterogeneous surfaces due to the size of hydrated radius while zinc and copper had access to 2.5. On average, all the elements had access to ~3 layer/patch sides/heterogeneous surfaces within the zeolite

framework while ensuring a single layer Langmuir adsorption. In industrial application, heterogeneous adsorbents with different patches are made of different energy levels and these energy levels are filled starting from the patches with the least energy. Thus, patches last filled are the first to be desorbed during desorption (Dabrowski, 1998). Similarly, ease of metal uptake in a multi-element system would follow the order Pb > Zn > Cu.

The Langmuir isotherm is proven to be the best model in describing the adsorption phenomenon for all the elements as it presents a regression coefficient R^2 approximately 1 and higher than Freundlich (see Table 6.2). A regression coefficient value of $0.95>R^2>1$ represents a 95 – 100% confidence interval of the experimental data being described by the selected isotherm, and a compromise ($R^2 < 0.95$) results in an inaccurate description of the experimental data with the selected model (Nascimento et al., 2009). Thus, a lower regression coefficient ($R^2 < 0.95$) results in a less accurate determination of adsorptive capacity and sorption parameters. Nascimento et al. (2009) used both the Langmuir and Freundlich isotherms in describing the experimental data as the regression coefficient for both models was above 0.91 for all metals. Alvarez-Ayuso et al. (2003) described their experimental data with Langmuir

as that produced R^2 values > 0.99 with no reference to Freundlich. In contrast, works from Lee et al. (2000) fitted best to Freundlich isotherm than the Langmuir with R^2 values > 0.82. Al Lagtah et al. (2011) also used Langmuir model to identify physisorption as the mechanism of metal uptake for Cd, Cu, Cr and Zn for commercial activated carbon. Sugiarti et al., (2019) reported Langmuir isotherm and physisorption (using Gibbs free energy) of synthetic NaP1 from natural zeolite. This research concludes on Langmuir model being the best isotherm to describe the adsorption mechanism behind the metal uptake for fly-ash derived NaP1 re-enforcing physisorption as the mechanism.

6.5 Adsorption kinetic models

Adsorption data obtained from the experiments were evaluated using Lagergren's kinetic models in order to describe the kinetics governing the uptake of heavy metals with zeolite NaP1. From the models tested, pseudo-second order kinetics best describes the heavy metal uptake process for all heavy metals tested in this study and adsorbent-adsorbate relationship as the regression coefficient $R^2 = 1$ for all metals presented in Table 6.3.

Table 6.3: Regression coefficients obtained from the kinetic models applied to the experimental adsorption data.

Lagergren's Kinetic models	**Regression Coefficients R^2**		
	Pb	**Cu**	**Zn**
Pseudo-first order	0.039	0.039	0.13
Pseudo-second order	1.0	1.0	0.99

Compared to the pseudo-second order, the first-order model produced low regression coefficient values, as seen in Table 6.3, when fitted to the experimental data. This is an indication of a weak correlation between this model and the experimental data and would not be suitable in describing the heavy metal uptake process.

6.6 Ion selectivity

Cation selectivity of an adsorbent can be influenced by electrostatic attraction (influenced by hydrated radius), cation charge, and enthalpy of hydration, sieve action, complex and precipitate formation (Helfferich, 1962; Hendricks, 2016). Among these properties, hydrated radius, enthalpy of hydration and sieve action were selected to explain selectivity of fly-ash derived NaP1. Effects of cation charge, complex and precipitate formation were dismissed as all metals are divalent (same charge) and experiments were performed at pH 3.5 to prevent the influence of complex formation and precipitation. Maximum sorption capacity (q_m) calculated in Table 6.4 from the Langmuir model follows this order of cation selectivity $Pb^{2+} > Zn^{2+} > Cu^{2+}$.

Table 6.4: Parameters from the Langmuir isotherm model for NaP1 and heavy metals under observation.

Parameters **Element**	**Maximum sorption capacity, Q_m (mg/g)**	**Langmuir constant (b)**	**Regression Coefficient, R^2**
Zinc	34.3	0.00906	0.986
Copper	14.6	0.00770	0.988
Lead	192	0.00636	0.991

This order of metal selectivity is in line with Mohan and Gandhinathi (2009) for fly-ash; $Pb^{2+} > Cd^{2+} > Zn^{2+} > Cu^{2+} > Mn^{2+}$. However, it differs from the order of cation selectivity proposed by Zamzow et al. (1990) and Erdem et al. (2004) for natural clinoptilolite ($Co^{2+} > Cu^{2+} > Zn^{2+} > Mn^{2+}$), Hui et al. (2005) for coal fly-ash and zeolite 4A ($Cu^{2+} > Cr^{3+} > Zn^{2+} > Co^{2+} > Ni^{2+}$) according to the adsorption capacity. Again, this differs from reports published by Steenbruggen and Hollman (1998), Lee et al. (2000), Sprynskyy et al. (2006) and He et al. (2015) who reported selectivity as $Pb^{2+} > Cu^{2+} > Zn^{2+}$ for fly-ash derived NaP1.

The difference may arise from adsorbent properties such as Si/Al ratio and experimental conditions e.g. pH and solid/liquid ratio. The Langmuir constants (b) from Table 6.4 for these elements also followed the order ($Zn^{2+} > Cu^{2+} > Pb^{2+}$) in magnitude. As mentioned earlier, a lower magnitude of Langmuir constant (b) indicates a higher affinity of the adsorbent for the metal. Thus, results of the Langmuir constant (b) from this study will follow the order of $Pb^{2+} > Cu^{2+} > Zn^{2+}$, in line with Steenbruggen and Hollman (1998) and Lee et al. (2000). Table 6.5 shows hydrated radius of metals in the order of $Pb^{2+} > Cu^{2+} > Zn^{2+}$ in agreement with Langmuir constant (b),

where, a lower Langmuir constant (b) indicates a higher affinity to metals.

Table 6.5: Hydrated vs Un-hydrated radii of heavy metals. Adopted from Ouki and Kavanagh (1997) and Oter and Ackay (2007).

Metal	Hydrated Radius (nm)	Un-hydrated Radius (nm)	Enthalpy of hydration (kJ/mol)	Langmuir constant (b)
Zn	0.430	0.0830	-2050	0.00906
Cu	0.419	0.0820	-2100	0.00770
Pb	0.401	0.1320	-1480	0.00636

Thus, a smaller hydrated radius experiences a high electrostatic force of attraction to the surface of the NaP1, explaining the higher metal uptake and affinity of NaP1 for Pb^{2+} than the other metals. This also implies that less energy is required to attract Pb^{2+} than required to attract Cu^{2+} and Zn^{2+}. From Table 6.5, the hydrated radius of Cu^{2+} is lower than Zn^{2+} and should be preferred by NaP1 in the order (Cu^{2+} > Zn^{2+}) according to the size of the hydrated radius. However, the experimental results show otherwise (Zn^{2+} > Cu^{2+}) in order of metal uptake from Table 6.4. This can be explained by the enthalpy of hydration for these metals from Table 6.5.

During metal uptake from NaP1, hydrated ions may need to lose their water of hydration in order to diffuse through NaP1 pores since their hydrated radii is closer to the pore dimensions (0.31 nm x 0.45 nm) and (0.28 nm x 0.48 nm) of the adsorbent (Alvarez-Ayuso et al., 2003). Enthalpy of hydration (Table 6.5), represents the affinity of metals to be in solution rather than the solute phase. Hence, a low absolute value for enthalpy of hydration indicates ease with which such cations will lose water and return to the solute phase. This is evident in the order of heavy metal affinity (Pb^{2+} > Zn^{2+} > Cu^{2+}) observed in this study.

Therefore, Zn^{2+} is noticed to have a higher metal uptake than Cu^{2+} because, it can relatively return to the solute phase easier than Cu^{2+} with the ability to go through the NaP1 micropores. In addition, Table 6.5 shows Pb^{2+} with the smallest hydrated radius (0.401 nm) and enthalpy of hydration (-1480 KJ/mol) among the cations tested (Cu=0.419 nm, Zn= 0.430 nm). Compared to NaP1 with pore dimensions (0.31 nm x 0.45 nm) and (0.28 nm x 0.48 nm) and active pore channel ~ 0.29 nanometres (Sharma et al., 2016), it is most likely to be preferred to its counterparts.

Although, the un-hydrated radii of all the elements are below the accessible channels and could get through the zeolite pores, the metals do not exist as single elements in water but are bound to water molecules as hexa-aqua complexes, thus increasing their radii. Therefore, these metals would have to be stripped of the water in order to pass through the narrow pores of NaP1.In conclusion, aqueous metal cations exist in water as hydrated ions with radii larger than the pore size of NaP1.

The electrostatic forces of attraction between the surface of the zeolite and hydrated cations are influenced by the sizes of the heavy metals. Thus, smaller sized hydrated heavy metals are most attracted to the surface of the zeolite. Hence, heavy metals with a low enthalpy of hydration means they can easily be stripped of water molecules and consequently removed by NaP1. Therefore, in describing the ion selectivity process according to sorption capacity, $Pb^{2+} > Zn^{2+} > Cu^{2+}$ is in line with Hendricks (2016) and this is determined by the size of the hydrated cation and its enthalpy of hydration, while $Pb^{2+} > Cu^{2+} > Zn^{2+}$ is also in line with Zamzow et al. (1990), Erdem et al. (2004), Hui et al. (2005), Steenbruggen and Hollman (1998) and Lee et al. (2000) according to Langmuir constant (b) and regression coefficient (R^2) values obtained from the Langmuir isotherm.

6.7 pH determination for multi-element adsorption

Multi-element adsorption experiments were performed with 1 g NaP1, mixed in 1 litre of controlled laboratory solution containing Pb= 11.4 mg/l, Cu= 11.5 mg/l and Zn= 13.3 mg/l at pH 3.5 and 20 ± 2 °C for 1 hour. Leaching experiments were also performed for comparison by using 1 g NaP1 in 1 litre distilled water at pH 3.5 in the presence and absence of heavy metals. Sodium (Na), aluminium (Al) and calcium (Ca) were the major contributors of the leachates with 37.6%, 37.2% and 18.7% respectively, as shown in Table 6.6. Potassium and magnesium were also measured to contribute ~4.5% and 1.5%, respectively.

Table 6.6 shows that the quantity of cations released from the leaching experiment (317.41 ± 3.56 mg) was 3 times more than the one obtained from the multi-element experiment (101.95 ± 1.22 mg). This suggests more cations are released from fly-ash zeolite NaP1 when in distilled water than in a concentrated heavy metal solution. Thus, the presence of metals within the laboratory multi-element matrix is apparently inhibiting the release of cations by 1/3 of the original quantity.

Table 6.6: Metal composition from leaching experiments with and without heavy metals at pH 3.5. Conditions: 1 g NaP1 mixed in 1 litre of distilled water (leaching) and water matrix (37.5 mg/l in total of Cu, Zn and Pb), time: 1 h and temperature: 20 ± 2 °C.

Elements	Number of cations leaching without heavy metals pH=3.5 (mg/l)	Number of cations leaching in the presence of heavy metals (pH 3.5) (mg/l)
Na	116 ± 2.14	34.8 ± 0.502
Mg	4.90 ± 0.00387	2.12 ± 0.00816
K	14.3 ± 0.209	4.37 ± 0.00976
Ca	57.8 ± 0.595	18.6 ± 0.142
Al	122 ± 0.590	39.6 ± 0.468
Fe	2.73 ± 0.0290	2.41 ± 0.0910
Total	317 ± 3.56	102 ± 1.22

Although the quantity of cations in both experiments are different, the proportion of these cations is closely related by a factor of 3 (Table 6.6). This implies that the proportional composition of these cations released from fly-ash zeolite NaP1 is constant irrespective of the quantity.

A reduction in cation concentration for Na, Ca, Mg and K was observed in the presence of heavy metals. Iron amongst other cations is noticed to be constant from both experiments and can

be considered a leachate, as it is not influenced by the presence/absence of heavy metals (see Table 6.6). Thus, cations with concentrations influenced by the presence of heavy metal from this observation can be considered as exchangeable ions (i.e. Na, Ca, Mg and K) while those not influenced can be classified as leachates (such as Fe). Aluminium concentration can be considered as extra framework aluminium.

Table 6.7 summarizes the results obtained from multi-element pH tests, to determine a suitable pH for metal uptake without precipitation and leaching. The effect of precipitation was measured by performing a control experiment under the same conditions without a zeolite. Sodium amount in solutions increased by 5 times at pH 6.5 and 10.5 compared to pH 3.5. This may be partially due to the addition of NaOH during the pH adjustment.

Table 6.7: Elements leached during multi-element adsorptions at various pH values (10.5, 6.5 and 3.5). Conditions: 1 g NaP1 mixed in 1 litre of water matrix (37.5 mg/l in total of Cu, Zn and Pb), time: 1 h and temperature: 20 ± 2 °C.

	Leachates						**Concentration of heavy metals adsorbed**
pH	**Na (mg/l)**	**Mg (mg/l)**	**K (mg/l)**	**Ca (mg/l)**	**Al (mg/l)**	**Fe (mg/l)**	**Total removal (mg/l)**
10.5	176 ± 3.893	0.383 ± 0.0291	3.72 ± 0.205	5.20 ± 0.277	0.312 ± 13.2	0.0160 ± 1.43	0.983 ± 0.350
6.5	181 ± 6.95	1.24 ± 0.0773	4.15 ± 0.0136	18.2 ± 1.16	0.0957 ± 0.0228	0.0212 ± 0.00701	19.1 ± 3.34
3.5	34.8 ± 0.502	2.12 ± 0.00816	4.37 ± 0.00976	18.6 ± 0.142	39.6 ± 0.468	2.40 ± 0.910	16.3 ± 0.357

Aluminium and iron are observed to be prevalent at pH 3.5 compared to other pH because they remain soluble at this pH and begin to precipitate at higher pH (above 4). On the other hand, potassium and calcium decreased by 5% and 2%, respectively from pH 3.5 to 6.5 and further decreased by 15% and 82% at pH 10.5, respectively. Potassium and calcium begin to precipitate at high pH 14 and 12 (Neal and Stanger, 1984), respectively. Thus, their reduced quantity at pH 10.5 in solution is not resulting from precipitation but possibly due to the low concentration of heavy metals in solution. Out of all the leachates in solution, sodium, calcium, potassium and magnesium are the possible exchangeable ions from the zeolite with sodium being the dominant exchange ion. This section signifies that fly-ash derived NaP1 has both ion exchange and adsorption qualities and either of these properties can be harnessed under specific pH conditions.

Multi-element and control experiments were performed 3 times by mixing 1 gram of zeolite NaP1 in 1 litre of 37.5 mg/l multi-elements (12.5 mg/l for each heavy metals) at various pH values (3.5, 6.5 and 10) at 20 ± 2 °C for 1 h. The control experiment was conducted with the same conditions but without zeolite (Refer to Chapter 5.3).

Figure 6.9 shows metal uptake of zeolite NaP1 in a multi-element-controlled laboratory solution as a function of pH and in the absence of precipitation. At pH 3.5, where, the concentration of H^+ ions is highest, a low lead uptake is noticed as seen in Figure 6.9. However, at pH 10.5, where, the lowest concentration of H^+ ions are present compared to pH 3.5 and 6.5, the uptake of lead is also lower than at 3.5 and 6.5.

Lead uptake was identified as the lowest amongst the metals at pH 3.5 but the highest at both pH 6.5 and 10.5. Comparing conditions of the experiments at pH 3.5, 6.5 and 10.5, concentration of H^+ ions is the main separating factor. Although, there is the possibility of metal competition (Faur-Brasquet et al., 2002; Rao and Khatoon, 2017) at these pH values, the uptake of lead is seen to be influenced by the increased concentration of H^+ ions. Thus, lead ions are displaced by the presence of hydroxonium ions in solution (Bhatnagar, 2012; Surisetty et al., 2013).

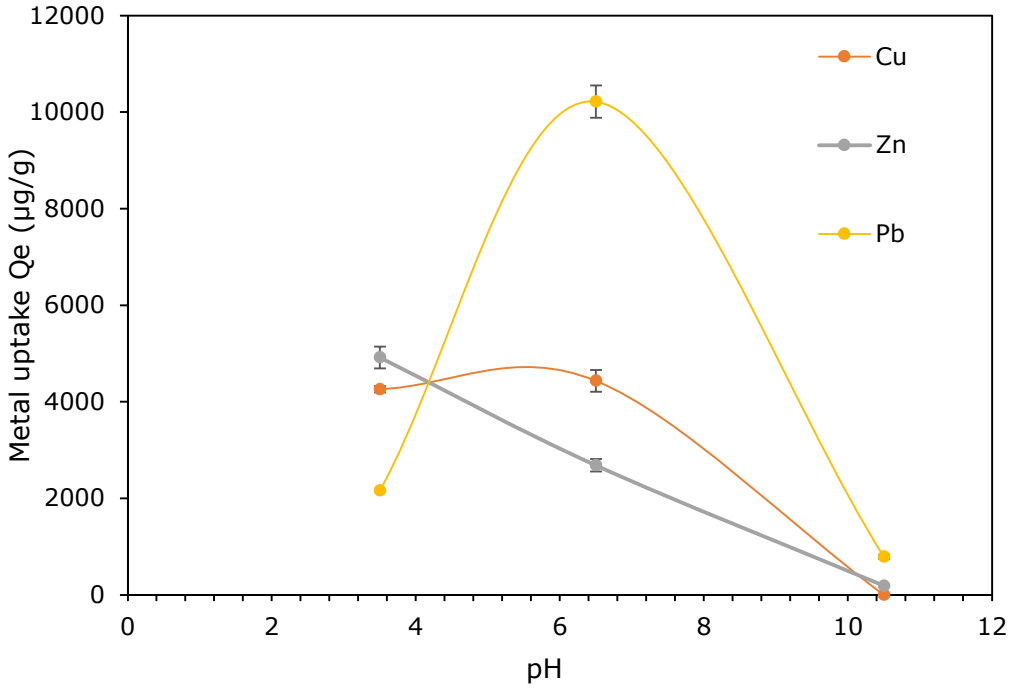


Figure 6.9: Metal uptake as a function of pH, when 1 g zeolite is mixed in 1 litre solution for 1 h. Initial metal concentration= 12.5 mg/l for each heavy metals making a total of 37.5 mg/l at T= 20 ± 2 °C.

As mentioned earlier, pH > 6 favours the formation of lead hydroxides and these hydroxides begin to precipitate with increasing pH since they are insoluble at higher pH. Thus, more than 95% lead is observed to have precipitated from the control experiment at pH 11. Copper is noted to exhibit a similar trend as lead but in a lower quantity at pH 6.5. Competition between multi-elements may be the major factor determining metal uptake at pH 6.5 in the presence of low H^+ ions. In this case, the metal uptake in terms of magnitude follows the order; Pb^{2+}

> Cu^{2+} > Zn^{2+}, which is in line with the hydrated radius of the metals (Steenbruggen and Hollman, 1998; Lee et al., 2000). This implies that, the size of the metal ions (Pb: 0.401 nm, Cu: 0.419 nm, Zn: 0.430 nm) is influencing the metal uptake process through NaP1 pore size (~ 0.29 nm) (Sharma et al., 2016). Thus, the smaller the size of the metal, the higher its affinity to NaP1 through the forces of attraction exerted by the adsorbent. As a result, zinc is observed with the least metal uptake since available sites are competitively occupied by lead followed by copper at pH 6.5.

However, from Figure 6.9, zinc is seen to obtain its highest metal uptake at pH 3.5 followed by a decrease in metal uptake at pH 6.5 and 10.5. Hence, suitable pH for zinc in a multi-element solution is 3.5 while that for lead and copper are 6.1 and 5.2, respectively. From Figure 6.9, pH 4.2 seemed to be a point of intersection for lead, copper and zinc, where, an equal amount of uptake is expected for all the metals and could be used to adequately assess metal selectivity or remove these metals in the presence of other substances (selective adsorption). These pH values would be useful in selective metal uptake of metals in an industrial effluent to achieve specific metal concentration limits depending on the composition of that solution.

As expected, precipitation was most observed at pH 10.5 with > 95% of Pb/Zn/Cu ions precipitating from the control experiments while all the elements showed the least precipitation at pH 3.5 (< 2.8%). However, at pH 6.5, both copper and lead showed 23% precipitation while zinc showed 8.9%. This was because both lead and copper begin to form hydroxides which are insoluble beyond pH 5.3 and 6 for copper and lead respectively, while zinc beyond pH 7 (Escudero Espinoza and Rao, 2017). On the other hand, leaching of metals in NaP1 was observed to be lowest at pH 3.5 and 10.5 but highest at pH 6.5.

Among the exchangeable elements, sodium (Na), aluminium (Al) and potassium (K) recorded the highest concentrations of 181, 39 and 4 mg/l respectively. It was also interesting to note that pH 6.5 recorded the highest multi-element uptake amongst all three with 19 mg/l removal from 37.5 mg/l while pH 3.5 recorded the second highest 16 mg/l. Hence, a good compromise between high multi-element uptake without the effect of precipitation and reduced leachable/ exchangeable elements was identified at pH 5. This is a significant finding going forward for multi-element adsorption.

6.8 Chapter summary

Metal adsorption with NaP1 was in the order of Pb (192 mg/g) > Zn (34 mg/g) > Cu (14 mg/g) through Langmuir isotherm while adsorption also showed lead removal by fly-ash derived NaP1 as the highest amongst all three metals tested in this research, recording a maximum 96 ± 0.2 mg/l within 15 min. Kinetics of metal removal with NaP1 was very fast for all metals in the first 15 min, followed by a slow uptake afterwards till the end of adsorption. Equilibrium contact time for NaP1 was 1 h. The pseudo-second order kinetic model and Langmuir isotherm were best fits for the adsorption mechanism of NaP1 with metals. The rate determining step of the uptake mechanism was the diffusion of metal ions through the pores of NaP1.

NaP1 is identified as a crystal structure with heterogenous surface for physical multilayer adsorption of metals while ion selectivity according to sorption capacity was in the order Pb^{2+} > Zn^{2+} > Cu^{2+}, in line with Hendricks (2016) and this is determined by the size of the hydrated cation and its enthalpy of hydration.

The suitable pH for zinc in a multi-element solution is 3.5 while that for lead and copper are 6.1 and 5.5, respectively. However, at pH 4.2, all metals are expected to be equally removed from

solution. These pH values would be useful in selective metal uptake of metals in an industrial effluent to achieve specific metal concentration limits depending on the composition of that solution. The available sites for multi-element heavy metals irrespective of pH is ~ 16 mg/g zeolite at 20 ± 2 °C in 1 h (maximum contact time) without the influence of precipitation.

7 Regeneration Study

7.1 Introduction

This section describes a preliminary baseline regeneration study to serve as a foundation for the final test. The purpose was to feed relevant information from this test into the final stage of metal regeneration. The parameters of interest in the preliminary regeneration tests were effect of time, pH and concentration of solution.

7.2 Regeneration tests

Copper was selected for the preliminary regeneration tests as its affinity towards NaP1 was between lead (highest affinity) and zinc (lowest affinity). Hence, these preliminary results would not be either over/under-estimating the potential of NaP1 for regeneration. Removed copper was recovered using HCl, NaOH and NaCl solutions from 0.5 g NaP1 loaded with 3 mg of copper, with different concentrations (1 M, 3 M and 5 M) at different pH=1, 3.5, 5 up to 24 h at 20 ± 2 °C in a batch system. The regeneration agents were selected due to the ease of accessibility on industrial scale and their history of being efficient agents from previous research (Katsou et al., 2011).

Table 7.1 outlines the conditions investigated for several experiments.

Table 7.1: Parameters/conditions investigated during the regeneration study of 0.5 g NaP1 loaded with 3 mg of copper.

Regen. Soln.	Conc.	pH	Time	pH adjustment solution
NaCl	3 M	5	24 h	1 M NaOH/ 37% HCl
	3 M	3.5	24 h	1 M NaOH/ 37% HCl
	5 M	3.5	24 h	1 M NaOH/ 37% HCl
HCl	1 M	3.5	6 h	5 M NaOH/ 37% HCl
	1 M	1	6 h	5 M NaOH/ 37% HCl
NaOH	3 M	3.5	6 h	1 M NaOH/ 37% HCl

Figure 7.1 displays the results from 1 M HCl regeneration of copper at pH (1 and 3.5) for 6 h while Figure 7.2 shows the results from 3 M NaCl regeneration at pH (3.5 and 5) for 24 h. From Figure 7.1, maximum copper (0.12 mg / 3 mg) is recovered in 1 h with 1 M HCl at both pH. pH change was noticed not to have a significant influence on copper regeneration by 1 M HCl at pH 1 or 3.5. Both experiments are observed to show the same trend over time.

3 M NaCl regeneration was also tested for copper recovery from Figure 7.2 at different pH (3.5 and 5). Results also demonstrate 0.3 mg copper recovered from spent zeolite NaP1 in 24 h. Unlike HCl, regeneration with NaCl is slow and took 24 hours to attain its maximum recovery potential of 0.31 mg copper. However, 50% of 0.31 mg copper recovery occurred within the first 2 hours with NaCl (both pH 3.5 and 5). Hence, both HCl and NaCl were unable to produce above 10% copper recovery from 0.5 g zeolite. The performance of 3 M NaCl remained the same when compared at pH 3.5 and 5 (see Figure 7.2) like results from HCl regeneration (Figure 7.1). Thus, pH had no significant effect on the amount of copper recovered.

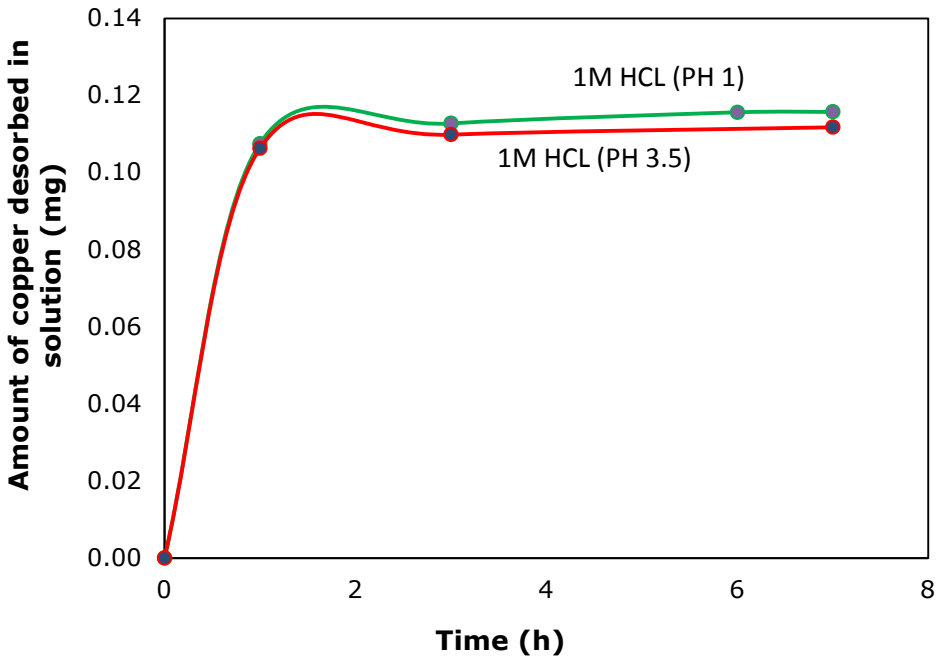


Figure 7.1: Amount of copper desorbed from 0.5 g NaP1 (loaded with ~3 mg copper) as a function of time. Conditions: 1 M HCl, pH 1 and 3.5, t= 7 h at 20 ± 2 °C.

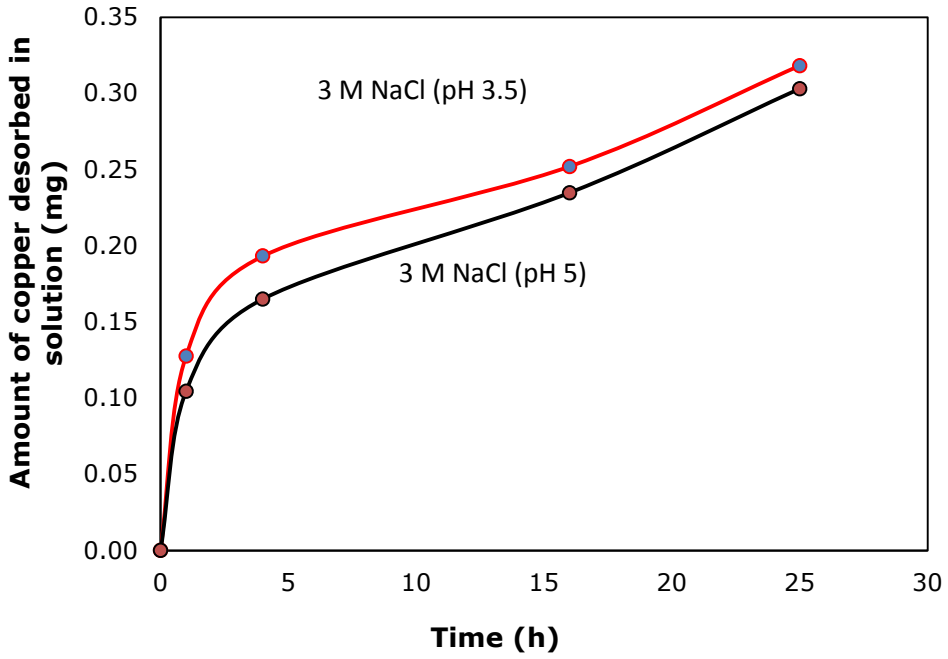


Figure 7.2: Amount of copper desorbed from 0.5 g NaP1 (loaded with ~3 mg copper) as a function of time. Conditions: 3 M NaCl, pH 3.5 and 5, t= 24 h at 20 ± 2 °C.

3 M NaCl produced 10% copper recovery (equivalent to 0.30 mg copper) within these conditions as seen from Figure 7.2. Figure 7.3 compares regeneration with 3 M NaOH and 5 M NaCl, at pH 3.5. All these experiments were performed at temperature 20 ± 2 °C and contact time of 24 hours except for NaOH at 6 h. However, an increase in NaCl concentration from 3 to 5 M caused three times desorption (~ 1.0 mg) obtained for copper within 24 h (Figure 7.3).

This may be due to an increased concentration gradient created in solution by the increase of initial Na^+ and compelling the exchange of copper from the zeolite structure. Thus, a strong ion exchange mechanism is witnessed as the main driving force for desorption from these experiments. Comparing regeneration between 3 M NaOH and 3 M NaCl both at pH 3.5, temperature 20 ± 2 °C and time 6 h, 24 h respectively from Figures 7.2 and 7.3; 3 M NaOH solution is observed to produce a maximum (1 mg copper equivalent to 30%) desorption from the spent zeolite at pH 3.5.

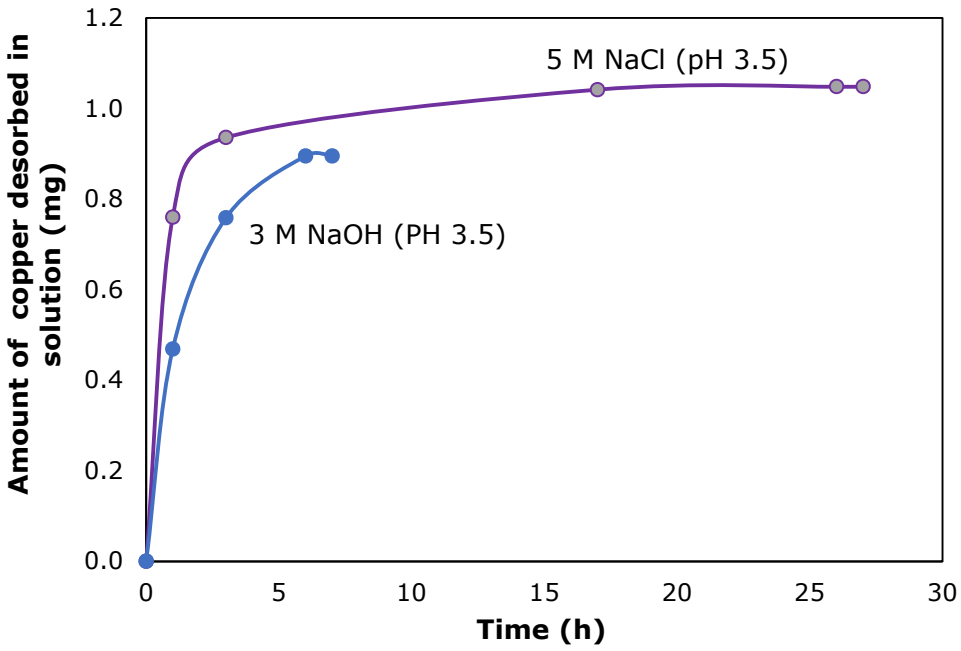


Figure 7.3: Amount of copper desorbed from 0.5 g NaP1 (laden with ~3 mg copper) over time. Conditions: 3 M NaOH, pH 3.5, t= 6 h; 5 M NaCl pH 3.5, t= 24 h at 20 ± 2 °C.

Table 7.2 proves that there is little or no difference between the two regeneration agents in molarity/quantity of Na^+ ions present in solution, although they differ in efficiency. This indicates that the presence of anions (such as Cl^- and OH^-) in solution possibly influences regeneration; more so, the type of anion attached to the exchanging cation from the regenerating agent.

Table 7.2: Initial cation quantity present in regeneration solutions.

Cation quantity in 100 ml solution	Cations	Regeneration agents
6.904 g	Na^+	3 M NaCl
11.506 g	Na^+	5 M NaCl
6.897 g	Na^+	3 M NaOH

Fly-ash derived NaP1 has demonstrated a similar preference for potassium to sodium ions such as other natural zeolites including Clinoptilolite, Philipsite, Chabazite and Mordenite as shown by Ouki et al. (1994). Katsou et al. (2011) investigated the potential of regeneration agents (HNO_3, KCl, NaCl and NH_4Cl) for lead and zinc removal from Clinoptilolite and their findings identified KCl to possess superior regeneration efficiency compared to its counterparts. Erwe et al. (2003) treated zinc-loaded synthetic zeolite P (57 mg/l) with 20 wt%

NaCl at pH 5 and obtained 95% desorption. Chunfeng et al. (2009) also used 5% NaCl to achieve 93% Cu^{2+} and 86% Zn^{2+} recovery from spent synthetic zeolite A (50 mg/l) at pH 3. Although, there is no present information concerning regeneration study of NaP1, the performance of potassium over sodium and hydrogen is in order with ion selectivity according to electrostatic forces of attraction ($Na^{+} > H^{+}$) (Hendricks, 2016).

Following results from the regeneration experiment, both XRF and XRD scans of the regenerated zeolite NaP1 were taken to evaluate the regeneration results. The XRF scan was conducted to verify the presence of unrecovered copper trapped in the zeolite matrix while the XRD scan was to confirm the possibility of structural changes (wet stability) to the zeolite after regeneration.

7.3 Validating regeneration with XRF scan

Parameters displayed in Table 7.3 were obtained through different means to validate the metal recovery process and are described in this section. Copper adsorbed was calculated as the difference between initial copper concentration and final copper concentration through the ICP-MS from adsorption experiments. Copper desorbed was also obtained through the

ICP-MS as the quantity of copper in solution after regeneration. Copper expected in zeolite was obtained from the difference between adsorbed and desorbed copper amounts. However, copper present in zeolite after regeneration was determined through X-ray fluorescence scan of the regenerated sample

All measurements were with 0.5 g zeolite and in 100 ml volume of regeneration solution. Values reported in Table 7.3 are precisely the mass of copper obtained in mg from one experiment. Results from the XRF scan in Table 7.3 show the amount of unrecovered copper in the zeolite is less than the expected amount after regeneration for all regeneration agents. Si/Al ratio values are noted to have reduced to 66% of the original zeolite sample. It had been established earlier by Chunfeng et al. (2009) that possible collapse of the zeolite structure in acidic mediums (pH 3.5 during adsorption and regeneration) could prevent the recovery of copper by trapping the metals completely.

Table 7.3: A summary of regeneration results showing copper amounts from 0.5 g zeolite before and after regeneration and comparing that to desorb copper amount with the expected amount.

Experimental conditions	Copper adsorbed (mg)	Copper desorbed (mg)	Copper expected in zeolite after regeneration (mg)	Cu present in zeolite after regeneration (mg)	Si/Al ratio
3 M_NaCl_pH3.5_24h	2.9	0.38	2.6	0.11	1.0
1 M_HCl_pH1_6h	2.9	0.22	2.7	0.012	0.91
5 M_NaCl_pH3.5_24h	3.2	1.1	2.2	0.12	1.0
3 M_NaOH_pH3.5_6h	3.1	0.90	2.2	0.070	0.80
1 M_HCl_pH3.5_6h	3.1	0.12	3.0	0.021	0.82
Original zeolite sample	n/a	n/a	n/a	n/a	1.51

XRF scans of the regenerated samples (0.5 g) further proved structural changes as the constituent elements of fly-ash derived NaP1 had changed compared to the original sample (Figure 7.4). Figure 7.4 shows a significant difference in material or elemental composition between the spent and original NaP1 zeolite. All the regeneration conditions showed an increase in aluminium quantity depicting a structural change in the crystallinity of the spent zeolite compared to the original. Hence, altering the Si/Al ratio between (24 ± 14%) across all samples against the original sample.

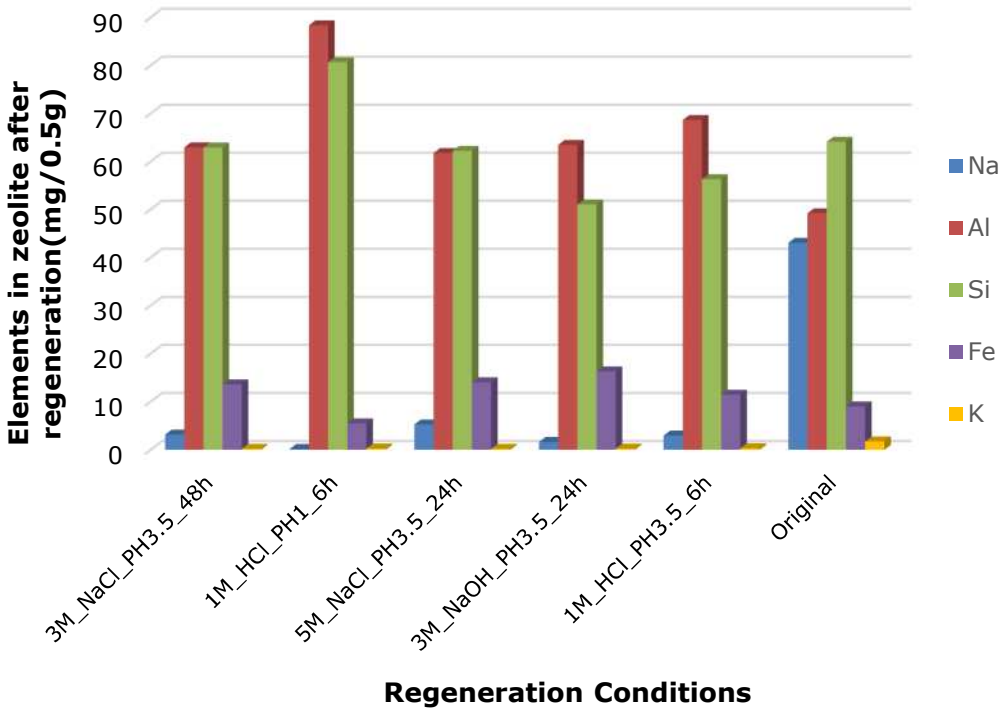


Figure 7.4: Constituents of regenerated zeolite (0.5 g) determined by XRF scan. Conditions;("3 M_NaCl_PH3.5_24h"," 1 M_HCl_PH1_6h","5 M_NaCl_PH3.5_24h","3 M_NaOH_PH3.5_24h"," 1 M_HCl_PH3.5_6h","Original").

A low Si/Al ratio has previously been established in this research as a sign of poor adsorption capabilities for an adsorbent. All other regeneration agents displayed a Si/Al ratio ≤ 1. Samples from NaCl regeneration with Si/Al ratio of 1, known as Maximum Aluminium P (MAP; a different kind of zeolite used for detergents) (Luqman, 2012) may have been created. The resulting NaP1 obtained after first regeneration at pH 1/3.5 was identified as different from the original unused NaP1 but could be further studied using XRD scans.

7.4 Validating regeneration with XRD scan

X-ray diffraction analyses were made of the regenerated samples to validate the results and completely understand what was happening during the regeneration process for different regeneration solutions. X-ray diffraction patterns shown in Figure 7.5, demonstrates crystal units of the regenerated samples. NaP1 peaks in fly-ash derived NaP1 identified prior to adsorption and regeneration (at 12.5, 18, 22, 28 ϴ) are noticed to have been lost, whereas, quartz and mullite peaks (at 16.5, 21, 26, 26.5, 31.2 and 41 ϴ) are observed to increase in intensity. Zeolite NaP1 may have degenerated/decomposed into its mineral forms after regeneration at pH 3.5. This might be the result of a structural collapse in acidic medium (Chunfeng et al. 2009).

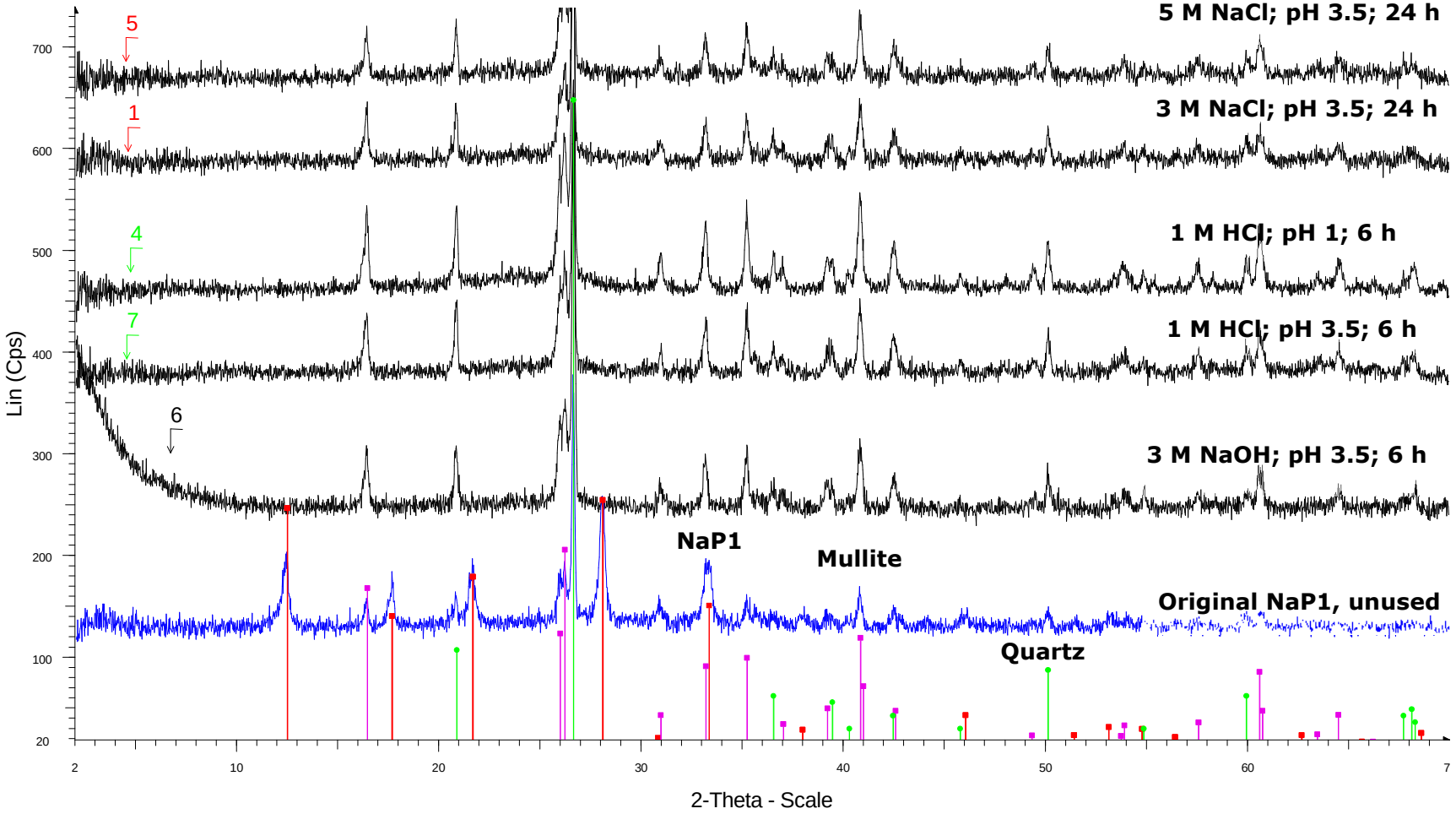


Figure 7.5: XRD scan comparing the structural integrity of regenerated NaP1 to the original. Conditions: ("3 M NaCl_pH 3.5_24 h","1 M HCl_pH 1_6 h","5 M NaCl_pH 3.5_24 h","3 M NaOH_pH 3.5_24 h","1 M HCl_pH 3.5_6h","Original") at 20 ± 2 °C.

Hence, the increase in the aluminium and silicon composition from the XRF experiment in Figure 7.4, compared to the original NaP1 is the decomposition of the crystal lattice from the zeolite structure back into the starting material (parent material; quartz and mullite). The structural collapse is the possible result of dealumination during regeneration at pH 3.5 for long hours.

The spent NaP1 from both XRF and XRD scans give evidence of structural and compositional alteration at pH 3.5 and 1. This demonstrates that low pH range (1 – 3.5) are not suitable working ranges for zeolite NaP1.

A final experiment was performed to identify which pH would be suitable for further adsorption and regeneration process. Hence, 0.5 g NaP1 was mixed in 100 ml distilled water of different pH (3.5, 5 and 10) at 20 ± 2 °C for 24 hours. The filtered NaP1 was air-dried and scanned with the XRD scan and the results produced shown in Figures 7.6, 7.7 and 7.8.

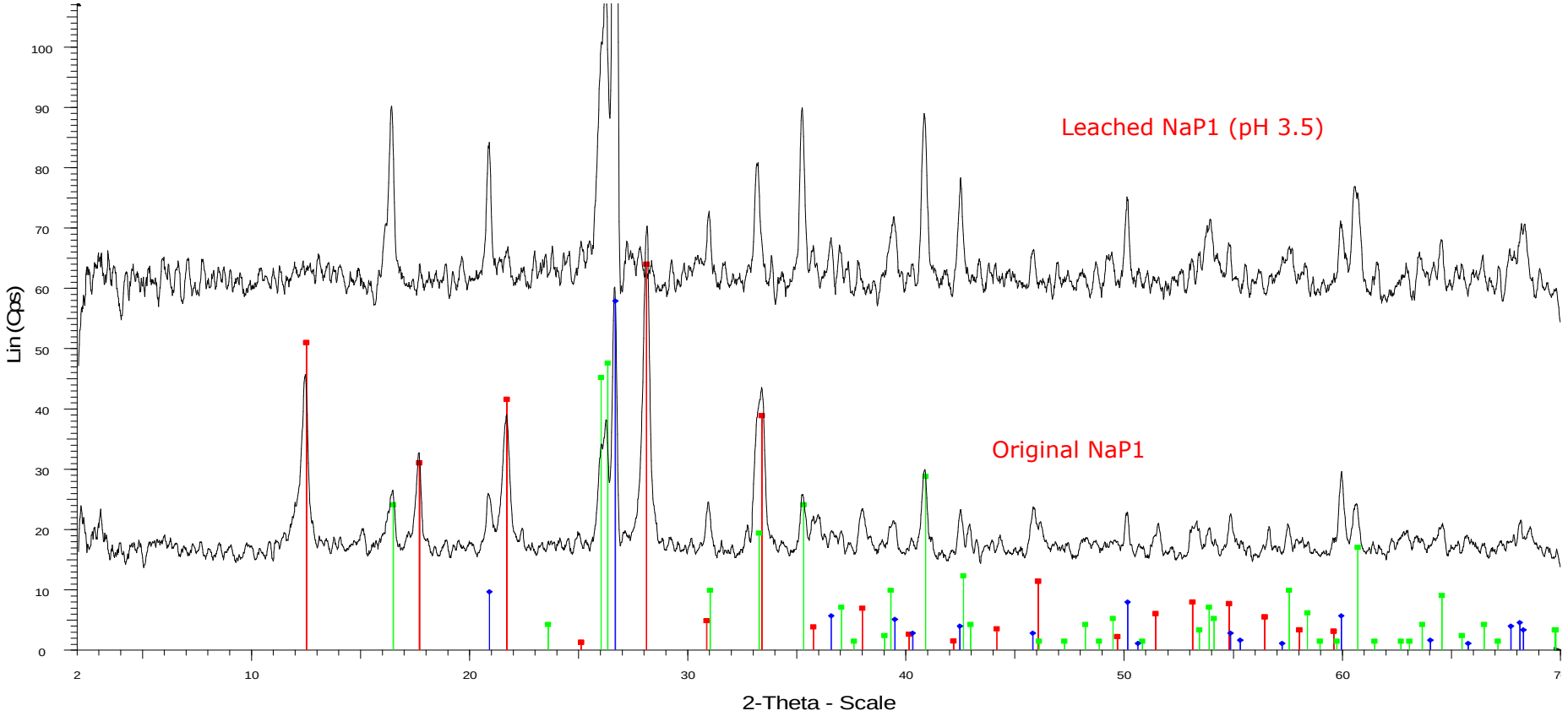


Figure 7.6: XRD scan comparing the structural integrity of NaP1 to the original after contact with distilled water at pH 3.5 for 24 h.

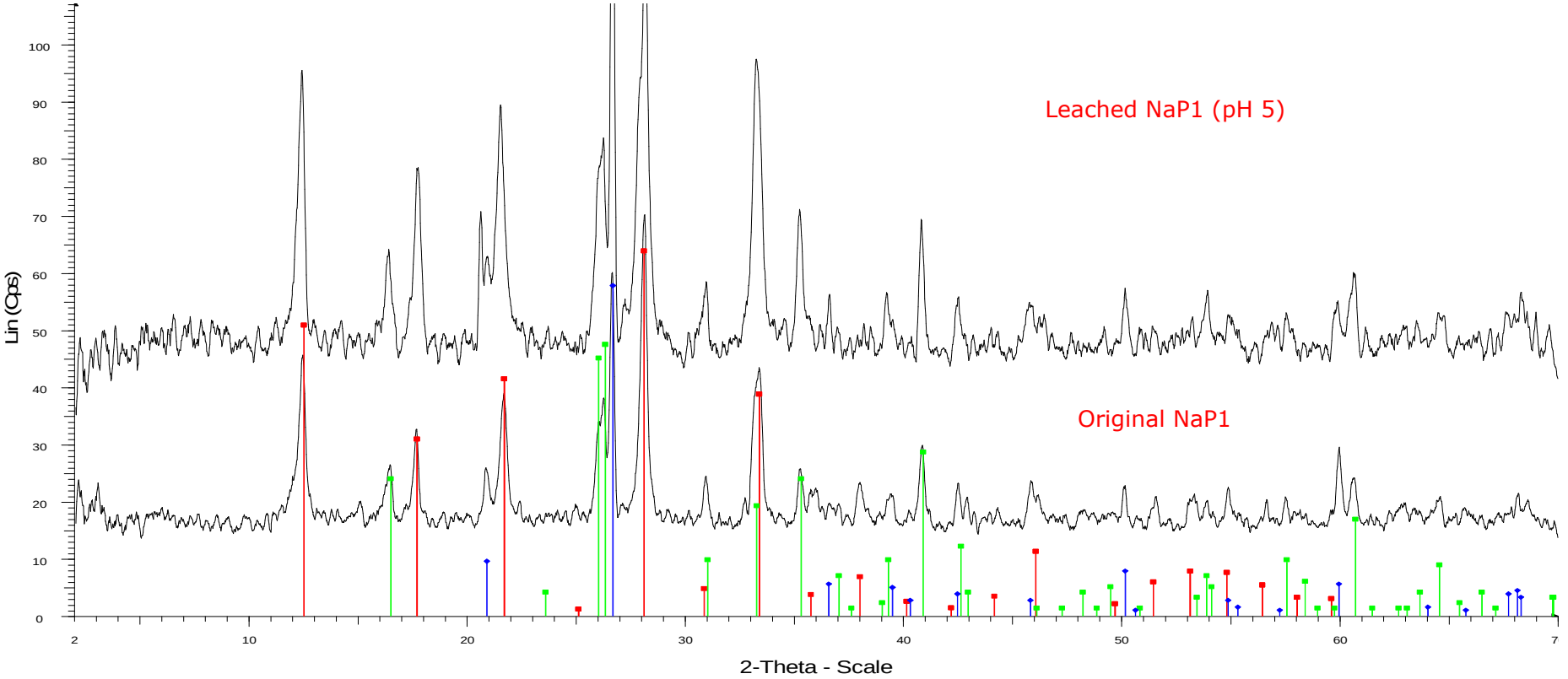


Figure 7.7: XRD scan comparing the structural integrity of NaP1 to the original after contact with distilled water at pH 5 for 24 h.

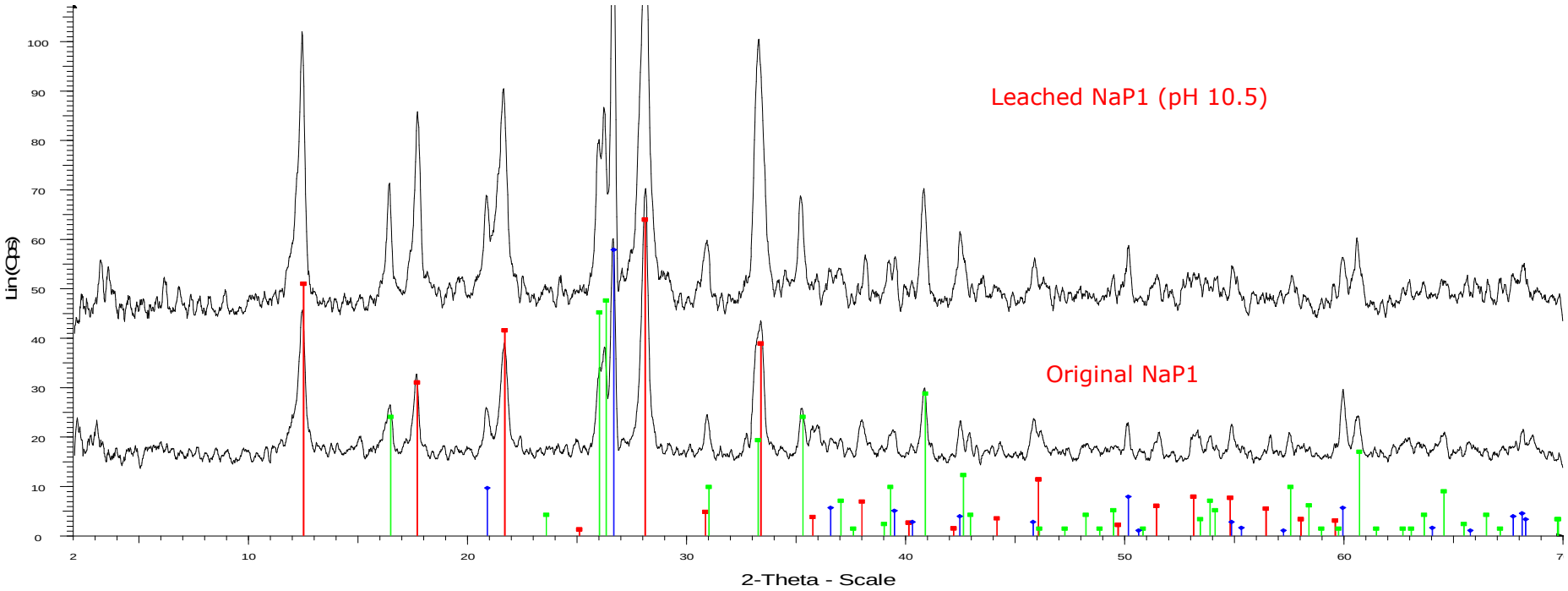


Figure 7.8: XRD scan comparing the structural integrity of NaP1 to the original after contact with distilled water at pH 10.5 for 24 h.

Figure 7.6 shows the XRD scan of NaP1 mixed with distilled water at pH 3.5 compared with the original sample. It can be observed that NaP1 peaks previously at 12.5, 17.8, 21.5 and 28 Θ, were lost after the experimental process whereas an increase in intensity of mullite and quartz peaks was noticed. This suggests the dissolution of NaP1 crystals into solution leaving the mullite and quartz impurities.

In contrast, the XRD scan of NaP1 from both experiments performed at both pH 5 (Figure 7.7) and 10.5 (Figure 7.8) indicate peaks at 12.5, 17.8, 21.5, 28 and 33.3 Θ, similar with the original NaP1.This experiment confirms claims of Chunfeng et al. (2009) of structural instability of NaP1 in an acid medium, making pH 5 the most preferred option for both metal removal and recovery process.

7.5 Determining optimum regeneration time

Following this observation, potassium chloride (KCl), sodium chloride (NaCl) and hydrochloric acid (HCl) were used in determining the optimum time for copper recovery in the second phase of regeneration tests at pH 5. The adsorption experiment ensued with a 1 l stock solution of 50 mg/l copper

concentration being prepared in a volumetric flask using copper nitrate. Zeolite sample (0.5 g) was mixed with 100 ml of 50 ppm copper solution in a 200 ml beaker for metal removal. The mixture was stirred at 300 rpm for 3 h while maintaining a pH 5 with 68% HNO_3 and 1 M NaOH solution. After 3 h, the mixture was centrifuged at 4000 rpm for 6 min to separate the liquid from the solid. The liquid was filtered with Minisart 0.45 µm syringe filters for ICP analyses while the filtrate was used for regeneration tests. Regeneration experiments were performed with acid (HCl: 10^{-5} M), and salts (NaCl and KCl) of 3 M concentration at pH 5 for 24 hours at temperature 20 ± 2 °C in a batch system. Results from the metal removal process are displayed in Tables 7.4 and 7.5.

The regeneration experiment was performed shortly after, when 0.5 g dried zeolite samples obtained after the adsorption was mixed in a 100 ml of fixed regeneration solution at pH 5 over a period of 24 h at 20 ± 2 °C. Samples (1 ml) were taken at time interval (e.g. 15 min, 30 min, 1 h, 3 h, 6 h, 24 h), filtered through a 0.45 µm syringe filter and diluted with distilled water by 10ml for ICP analyses. The regeneration process was then repeated 3x for the selected regeneration solutions (KCl, NaCl and HCl). Results from this experiment are displayed in Table 7.6.

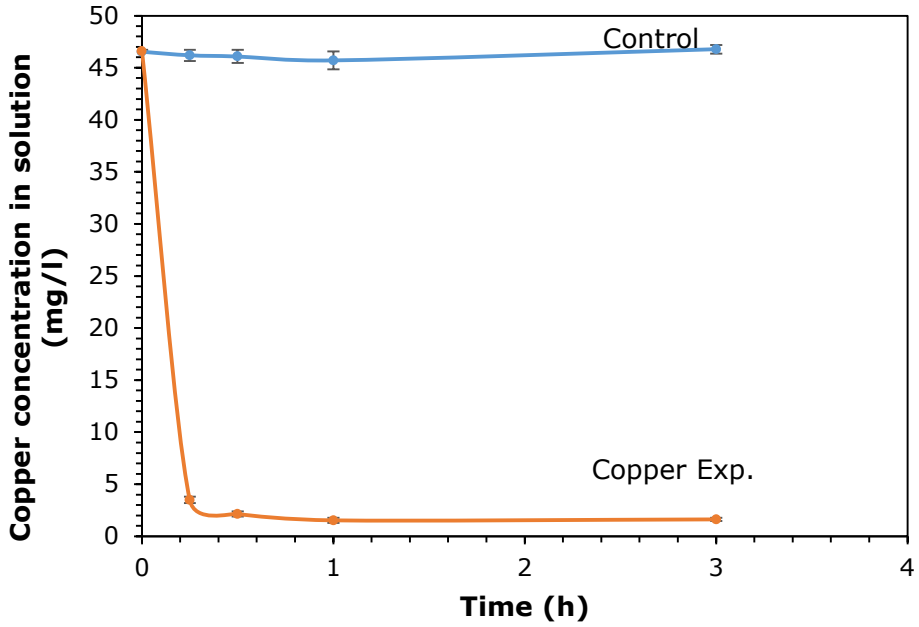


Figure 7.9: Results from copper removal experiment, mixing 100 ml copper solution of (50 mg/l) with 0.5 g NaP1 at pH 5, temperature 20 ± 2 °C. Samples were taken at time 15, 30 mins, 1 and 3 h.

Figure 7.9 shows the result of control and copper removal experiments at pH 5. From the Figure 7.9, distilled water is noted not to have copper before the preparation of the stock solution. The initial concentration of the stock copper solution was measured as 46.59 ± 0.15 mg/l and observed to reduce over 3 hrs to an average of 1.63 ± 0.15 mg/l across all three repeats. At the end of the adsorption experiment, 96.51 ± 0.1% copper was calculated to have been removed from solution by NaP1. On the other hand, the concentration of copper in the control experiment was observed not to have changed during the experiment period using the same conditions. It can be

concluded that copper removal was only by the presence of NaP1 and not precipitation. Following this observation, repeated adsorption experiments were performed under the same conditions for 3 hours without sample extraction and tested.

Table 7.4 shows results from repeated copper adsorption experiment for 3 hours without sample extraction under the following conditions: 0.5 g of NaP1 used for copper removal of concentration 50 mg/l of 100 ml volume at temperature 20 ± 2 °C and pH 5.

Table 7.4: Results from repeated copper removal experiment for 3 h without sample extraction under the following conditions: 0.5 g of NaP1 used for copper removal of concentration 50 mg/l of 100 ml volume at 20 ± 2 °C and pH 5.

Sample	**Mean Cu concentration in solution (mg/l)**
Initial	46.36 ± 0.43
3 h	2.88 ± 0.97
Cu removed	43.48 ± 0.97

Similar quantity of copper removal was noticed for all repeated experiments from Table 7.4, indicating an average of 43.5 ±

0.979 mg/l, when compared to results from previous Figure 7.9. A confirmation of the method was necessary to confirm the expected copper removed as the spent NaP1 was used for subsequent regeneration tests.

Following the copper removal experiments, copper regeneration was attempted with 10^{-5} M hydrochloric acid (HCl), 3 M potassium chloride (KCl) and 3 M sodium chloride (NaCl) at pH 5. This was done to determine the best regeneration solution and conditions suitable for metal recovery from spent NaP1. Table 7.5, shows the mean and standard deviation of triplicate results obtained from the regeneration experiments for 24 hours, performed with 0.5 g spent NaP1 laden with ~ 4.5 mg copper and mixed with 100 ml of selected regeneration solutions (HCl, KCl, NaCl) at pH 5 and temperature 20 ± 2 °C.

The results indicate a quick metal recovery process for 3 M NaCl compared to HCl and 3 M KCl, however both NaCl and KCl produced the same quantity of copper (~ 13 mg/l) in solution within 3 hours, equivalent to 30% copper. On the other hand, HCl managed about ~ 15% copper recovery (from spent NaP1 over the same 3 h period, which is half the amount of copper recovered using NaCl and KCl. Potassium chloride (KCl) solution recorded the highest copper recovery in 24 hours (37%)

compared to sodium chloride NaCl, (32%). It is noteworthy that the selected regeneration time according to all the experiments is 3 hours since the increase in metal recovery over the remaining 21 hours yielded little results or made no significant change.

The pH of all regeneration solutions was set at 5 meaning that the hydrogen ion concentration was a common condition across all regeneration solutions. This condition can be described as the exact concentration of HCl (10^{-5} M HCl). Strong acids dissociate completely in water to produce hydrogen ions of the same concentration as the acid. Thus, preparing a 10^{-5} M HCl means, the solution would have the concentration of H^+ ions as 10^{-5} M which is equivalent to pH 5. This demonstrates that all the regeneration solutions had 10^{-5} M H^+ ions at pH 5 as a common denominator (e.g. 3 M NaCl at pH 5 = 3 M Na/Cl + 10^{-5} M H^+). Hence, conditioning the regeneration solution at pH 5 already influences metal recovery and this effect can be quantified as ~ 15% copper recovered (demonstrated in Table 7.5).

Table 7.5: Mean and standard deviation of triplicate results obtained from the regeneration experiments for 24 h, performed with 0.5 g spent NaP1 with ~ 4.5 mg copper and mixed with 100 ml of selected regeneration solutions (HCl, KCl, NaCl) at pH 5 at 20 ± 2 °C.

3 M NaCl	**Time (h)**	**Control**	**Exp. 1**	**Exp. 2**	**Exp. 3**	**Mean Cu Conc. /0.5g NaP1**	**Cu (mg/g)**	**Mmol/g**
	0	0.02	0.00	0.00	0.00	0.00 ± 0.00	0.0	0.0000
	0.25	0.03	9.29	9.12	8.80	9.07 ± 0.25	1.8	0.0285
	0.5	0.02	10.61	10.02	10.10	10.24 ± 0.32	2.0	0.0322
	1	0.00	11.72	10.79	11.17	11.23 ± 0.46	2.2	0.0353
	3	0.00	13.13	13.02	12.33	12.82 ± 0.43	2.6	0.0404
	24	0.00	15.32	14.63	13.43	14.46 ± 0.95	2.9	0.0455

10^{-5} M HCl	**Time (h)**	**Control**	**Exp. 1**	**Exp. 2**	**Exp. 3**	**Mean Cu Conc. /0.5g NaP1**	**Cu (mg/g)**	**Mmol**
	0	0.07	0.14	0.09	0.00	0.08 ± 0.07	0.0	0.0003
	0.25	0.11	3.70	3.58	3.49	3.59 ± 0.10	0.7	0.0113
	0.5	0.17	4.21	4.11	4.18	4.17 ± 0.05	0.8	0.0131
	1	0.17	5.36	5.02	5.28	5.22 ± 0.18	1.0	0.0164
	3	0.15	6.56	6.45	6.64	6.55 ± 0.09	1.3	0.0206
	24	0.19	5.83	5.95	5.62	5.80 ± 0.17	1.2	0.0182

Table 7.5: ……*continued.*

3 M KCl	**Time (h)**	**Control**	**Exp. 1**	**Exp. 2**	**Exp. 3**	**Mean Cu Conc. /0.5g NaP1**	**Cu (mg/g)**	**Mmol**
	0	0.02	0.00	0.00	0.00	0.00 ± 0.00	0.0	0.0000
	0.25	0.01	7.27	7.41	7.07	7.25 ± 0.17	1.5	0.0228
	0.5	0.01	8.43	8.24	8.88	8.52 ± 0.33	1.7	0.0268
	1	-0.03	9.94	10.01	9.66	9.87 ± 0.19	2.0	0.0311
	3	-0.04	12.79	12.99	13.51	13.10 ± 0.37	2.6	0.0412
	24	-0.04	15.81	16.91	17.38	16.70 ± 0.80	3.3	0.0526

In view of this, the actual effect of each regeneration solution without the influence of H^+ can be identified as ~ 15% copper recovery for both potassium chloride and sodium chloride in 3 hours. However, it should be noted that without pH conditioning, metal recovery is almost impossible thus making hydrogen ions a necessary element and can be classified as a catalyst in the regeneration process. In industrial application of the regeneration process, 3 - 4 successive regeneration stages would be required to obtain above 95% metal recovery. Unlike pH 5, pH 3.5 was not a suitable condition as identified from previous regeneration experiments. As mentioned before, the strong acidity at pH 3.5 possibly washed off the elements (Al, Na and Si) responsible in forming the NaP1 structure.

It is noteworthy that both salts obtained the same amount of copper recovery in 3 h (29% copper recovered), representative of 2.6 mg/g zeolite. 10^{-5} M HCl produced ~15% of copper recovery in 3 h. The effective regeneration time according to the kinetics of the copper recovery process was identified as 3 h for all the regeneration agents (NaCl, KCl and HCl) since the remaining 4 - 5% increase in copper recovery was observed in the final 21 hours. This was a positive result as 3 successive regeneration processes could be used to achieve a 100% copper recovery in less than 8 h (1 working day). Again, the process

will not require much acid dosing to maintain pH 5 and would also use cheap or readily accessible salts (NaCl and KCl) as regeneration agents, which are environmentally friendly. The downside is the concentration of the salts, which can be explored further as the final concentration of salt needed to achieve this recovery may be far lesser than what was used in this experiment.

To the best of knowledge, there is no current work on the regeneration of NaP1 to date in literature. Fly-ash derived NaP1 has demonstrated a similar preference for potassium to sodium ions such as other natural zeolites such as Clinoptilolite, Philipsite, Chabazite and Mordenite as shown by Ouki et al. (1994). Katsou et al. (2011) investigated the potential of regeneration agents (HNO_3, KCl, NaCl and NH_4Cl) for lead and zinc removal from Clinoptilolite and their findings identified KCl to possess superior regeneration efficiency compared to its counterparts. Erwe et al. (2003) treated zinc-loaded synthetic zeolite P (57 mg/l) with 20 wt% NaCl at pH 5 and obtained 95% desorption. Chunfeng et al. (2009) also used 5% NaCl to achieve 93% Cu^{2+} and 86% Zn^{2+} recovery from spent synthetic zeolite A (50 mg/l) at pH 3. This study obtained 30 – 35% copper recovery (2.6 mg/g NaP1) with 3 M KCl and NaCl in 3 h at pH 5 in one cycle and could be used in successive cycles.

The scope of regeneration studies was limited to a few substances namely potassium chloride, sodium chloride and hydrochloric acid with pH and duration/period of experiment as two parameters of many to be assessed. This is mainly due to the limited amount of synthesized NaP1. Other parameters that could be studied further are the minimum concentration of regeneration solution required to obtain optimum percentage metal recovery, effect of temperature on regeneration and the influence of anions present in regeneration solutions.

7.6 Chapter summary

Suitable pH for metal removal and regeneration is pH 5 while the optimum time for efficient metal removal and recovery is 1 h and 3 h respectively. Successive regeneration would be required as a maximum of 30 – 35% regeneration is obtained with both KCl and NaCl salts. XRF and XRD scans were used to validate dealumination at pH below 5 within a contact time of 24 h while pH 5 was identified as the most suitable for NaP1 performance.

8 Pelleting study

8.1 Introduction

In line with health and safety and handling of adsorbents, pellets are preferred to powder adsorbents. Hence, this section aims at converting NaP1 powder into pellets and testing it for lead and multi-element adsorption. An NaP1 pellet was characterized by nitrogen adsorption to identify surface area, pore volume and nature of pores. Comparisons were drawn with commercial 3A pellet while mole-based adsorption values were used to identify trends and competition in multi-element adsorption.

8.2 Adsorption using NaP1 pellets

Fine powder NaP1 of particle size from 2.99 - 91.64 µm were used in the hydraulic press. The hydraulic press is used in preparing disc shaped tablets with the aid of applied pressure to a die assembly. The pelleting tests started with identifying the amount of NaP1 powder required to produce durable pellets of similar sizes to current industrial liquid phase granular activated carbon (e.g. 2.38 x 0.59 mm, 1.68 x 0.84 mm, 1.68 x 0.42 mm and 0.84 x 0.30 mm).

Hence, 0.20 – 0.05 grams of zeolite powder was used for the experiments while the loading was optimized between 3 – 5 tons

as specified by the manufacturers for a 10 mm die assembly. Duration of the loading was optimized between 1- 10 mins as a longer duration implied a longer pellet preparation time, making the process industrially unattractive. Table 8.1 gives a summarized outlook of the tests performed through optimizing the above-mentioned parameters to achieve the desired results.

Table 8.1: Summary of pelleting parameter optimization tests.

Exp. No.	Zeolite amount (g)	Time (mins)	Load (tons)	Water used	Binder used	Drying	Conditions
1	0.20	5	5	No	No	No	Breaks
2	0.10	5	5	No	No	No	Most suitable
3	0.05	5	5	No	No	No	Very thin
Identify the most appropriate mass							
4	0.10	1	5	No	No	No	cracked
5	0.10	5	5	No	No	No	5 was maintained
6	0.10	10	5	No	No	No	cracked
Identify the most appropriate time							
7	0.10	5	5	No	No	No	Max used
8	0.10	5	4	No	No	No	cracked
9	0.10	5	3	No	No	No	cracked
Identify the most appropriate loading							

Pelleting parameters were discarded on observation, when the final product formed (pellets) had cracks or did not maintain a disc shape after removal from the die assembly. Perfectly formed pellets were then taken for further characterization tests.

8.2.1 Amount of zeolite required

The first parameter to be tested was amount of zeolite required for pelleting. When 0.05 grams was pressed with 5 tons (maximum loading for a 10 mm die) loading for 5 min, the product obtained was a thin wafer disc-shaped pellet, which was cracked after removal from die. Following this experiment, 0.20 g zeolite was pressed under 5 tons loading for 5 min and the results proved negative as the pellet formed had cracks. When 0.10 g was used under the same conditions, a well-formed disc shaped pellet without cracks was obtained, as shown in Figure 8.1. Table 8.1 shows a matrix of the experiments described.

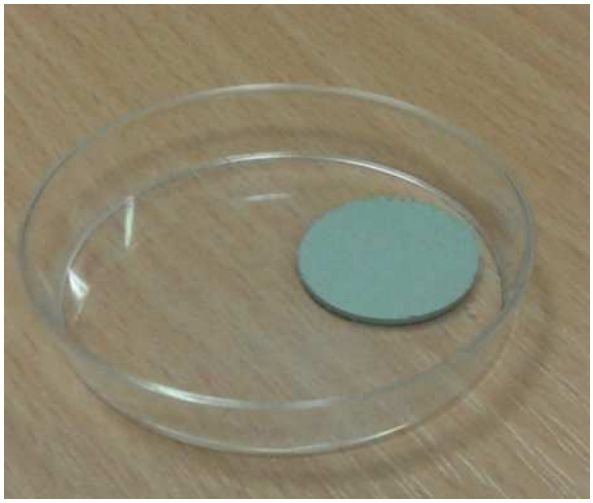


Figure 8.1: Pellet pressed from 0.10 grams NaP1 powder using 5 tons loading for 5 min.

Hence, 0.10 g of zeolite was maintained throughout the rest of the pelleting experiments as the amount to produce the desired disc-shaped pellets.

8.2.2 Loading pressure

The loading pressure was selected from the user manual of the hydraulic press and is presented in Table 8.2. Hence, for a 10 mm die pressing assembly, the appropriate loading pressure was assessed between 3 – 5 tons, where, 3 tons is the typical loading and 5 tons was the maximum loading. A precaution was taken not to exceed the maximum loading for the die assembly to prevent damaging the equipment.

Table 8.2: Manufacturer's typical loads to producing quality pellets.

Die Size (mm)	Typical load (tons)	Maximum load (tons)
5	1.25	2.0*
10	3.0	5.0*
13	7.0	10.0*
20	18.0	25.0*
32	25.0	50.0*
40	25.0	85.0*

* Warning: Do not exceed the maximum load.

Using the maximum, mid and minimum loading pressure (5, 4 and 3 tons, respectively), experiments were performed by pressing 0.10 grams zeolite powder for 5 minutes (Table 8.1). Compared to 5 tons, both 3 and 4 tons did not produce the required pellets in 5 min as their compressive force was not enough to put the particles together. However, when 5 tons loading pressure was used, the resulting pellet was compact without loose particles (Figure 8.1). Hence, 5 tons loading pressure was maintained as the optimal loading pressure.

8.2.3 Loading pressure time

The period of compression was assessed with the aim of obtaining the appropriate time to maintain loading pressure. Determining the most appropriate time was important to identify the cost-effectiveness of the hydraulic press. A longer time would render the process unattractive although pellets are achieved while a shorter time without achieving pellets would not meet the aim of this study. This section of pelleting study was conducted with pressing of 0.10 g zeolite with 5 tons of loading pressure for 10-15 seconds as instructed by the manual. However, there was no pellet obtained during this timeframe.

Table 8.1 indicates the time periods tested to obtain a pellet of zeolite NaP1. When 1 min loading time was used, particles of

zeolite NaP1 powder were loose and unable to form pellets. Conversely, when 10 min loading time was used in experiment 6, the pellet formed were cracked into pieces. This might be the over-compression of particles beyond the point of tablet formation, where, the tablet begins to break into pieces. Again, over-compression is likely to close the possible formation of macro pores. Finally, when 5 min loading time was assessed, it proved to produce the best pellet without cracks and this time was kept constant throughout this study. The pelleting study was concluded on the following parameters: 0.10 g of NaP1 zeolite powder compressed with 5 tons loading pressure for 5 min produced the best quality pellets. These pellets were obtained without the aid of a binder or water as this has been the norm in the past to obtain pellets from powder.

8.3 Characterization of pellets

Characterization was performed to identify the quality and properties of pellets obtained. Pellets were dried in the oven at 150 °C for 2 hours to draw out all forms of moisture and trapped gases before storage. The pellets were tested for pore size, pore distribution, pore volume, cation exchange capacity and adsorptive capacity.

8.3.1 Nitrogen adsorption isotherms

Surface area and pore size characterization of both NaP1 powder and pellet were performed with nitrogen adsorption isotherms. Figure 8.2 shows the N_2 isotherms. The adsorption and desorption isotherms observed for both powder and NaP1 pellet are as Type II IUPAC classification with an H3 hysteresis loop. This is characteristic of a mesoporous material of pore size between 2 and 50 nm. The Type II isotherm (adsorption) is indicative of an unrestricted monolayer – multilayer adsorption while the H3 hysteresis loop (desorption) represents a non-rigid aggregate of plate-like particles forming slit-shaped pores.

Sections of nitrogen adsorption and desorption isotherms below the region ($P/P^o < 0.05$) shows the presence of micropores whereas sections in the region ($P/P^o > 0.06$) demonstrates larger pores filled at higher pressure. Section A ($0.01 > P/P^o < 0.06$) of the plot also known as the knee, shows the region ending monolayer adsorption coverage of adsorbent surface. Section A is observed to be dense with several points along the plot, which spreads out with increasing relative pressure (P/P^o). This is evidence of low-pressure uptake of nitrogen gas over NaP1 surface without the need of excessive force indicating accessible micro-pores, which can take a limited quantity of nitrogen gas.

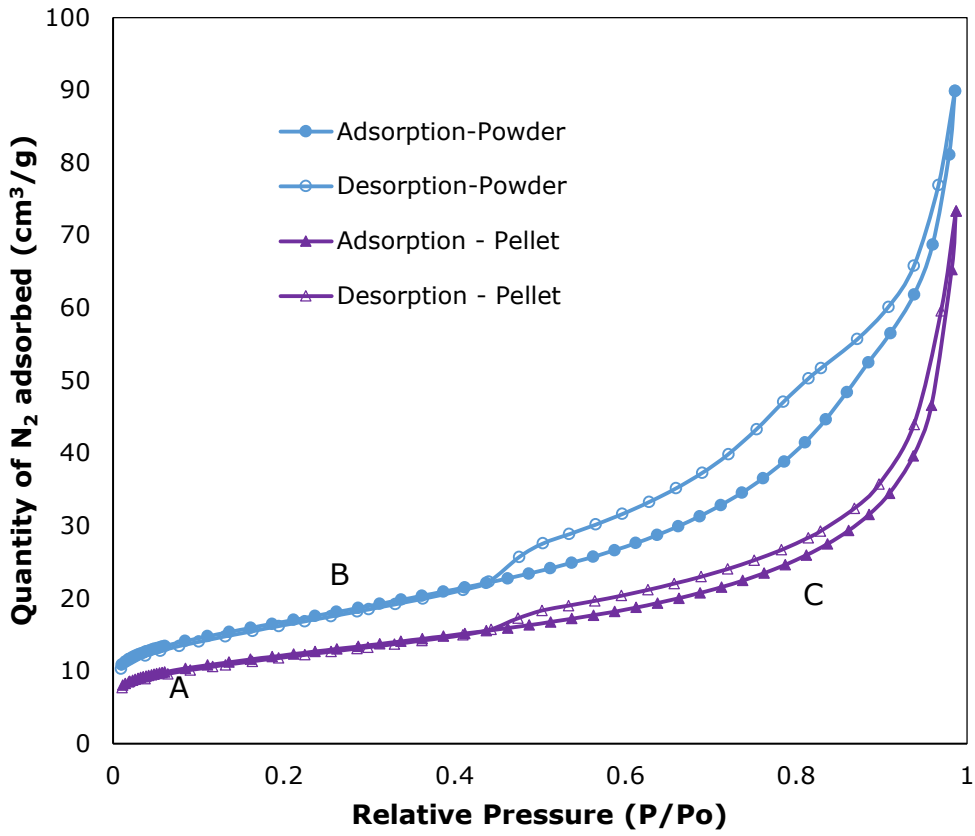


Figure 8.2: Nitrogen adsorption/desorption isotherms for NaP1 powder and pellets at 77 K.

Section B shows the region of multilayer adsorption and this begins from relative pressure $0.06 > P/P^o < 0.45$, where, larger pores are accessed. Thus, the volume of nitrogen adsorbed is seen to increase gradually with an increase in relative pressure. At section C, where, the curve is observed ($P/P^o > 0.50$), a high-pressure behaviour is noticed of the isotherm indicating capillary condensation. This is caused by the clogging of available pores generated by the increasing film thickness of multi-layered adsorbates along the sides of the pores. Comparing the adsorption isotherm of NaP1 powder to pellet in

Figure 8.2, the volume of nitrogen gas adsorbed across the entire plot of NaP1 pellet is lower than NaP1 powder. This suggests that the reduction in pore volume of NaP1 pellet caused by pelleting/compression of NaP1 powder.

However, sections along the isotherm follow a similar pattern. Desorption isotherm is also seen to follow the same pattern, where, the hysteresis loop generated by the NaP1 powder is wider than that of the NaP1 pellet. The wider hysteresis loop present in the NaP1 powder is the result of low volume of nitrogen retrieved during desorption from narrow pores (generating capillary condensation). Unlike NaP1 pellets, the width of NaP1 powder hysteresis loop is not constant across the curve ($P/P^o > 0.50$). This is an indication of varying pore sizes along the curve at that section, contrary to what was observed from NaP1 pellet.

However, desorption isotherm of NaP1 pellet appears uniform compared to NaP1 powder. As mentioned earlier, H3 hysteresis loop (desorption) represents a non-rigid aggregate of plate-like particles forming slit-shaped pores. Hence, the uniformity displayed by NaP1 pellet desorption isotherm may be due to the creation of a more uniform meso-pore structure generated through fine packing/compression to make the non-rigid plate-like particles rigid by means of the pelleting process.

Pore size distribution of both NaP1 powder and pellet are seen to be within a broad spectrum from the micro – macro pore range (2 nm > pore diameter > 50 nm) from Figure 8.3. It appears that the pelleting process may have increased the porosity of NaP1 pellet by creating larger pores over 115 nm compared to its powder counterpart. These larger pores meso to macro pores (> 30 nm) in the designed pellets are seen to poses more volume than their counterparts in the NaP1 powder. However, they may be harder to reach since a higher pressure was required to fill these larger volumes while the smaller pore were occupied at very low pressure from Figure 8.2. Majority of the pore size distribution is within the micro to mesoporous range (2 nm > pore diameter ≤ 50 nm) for both NaP1 powder and pellet.

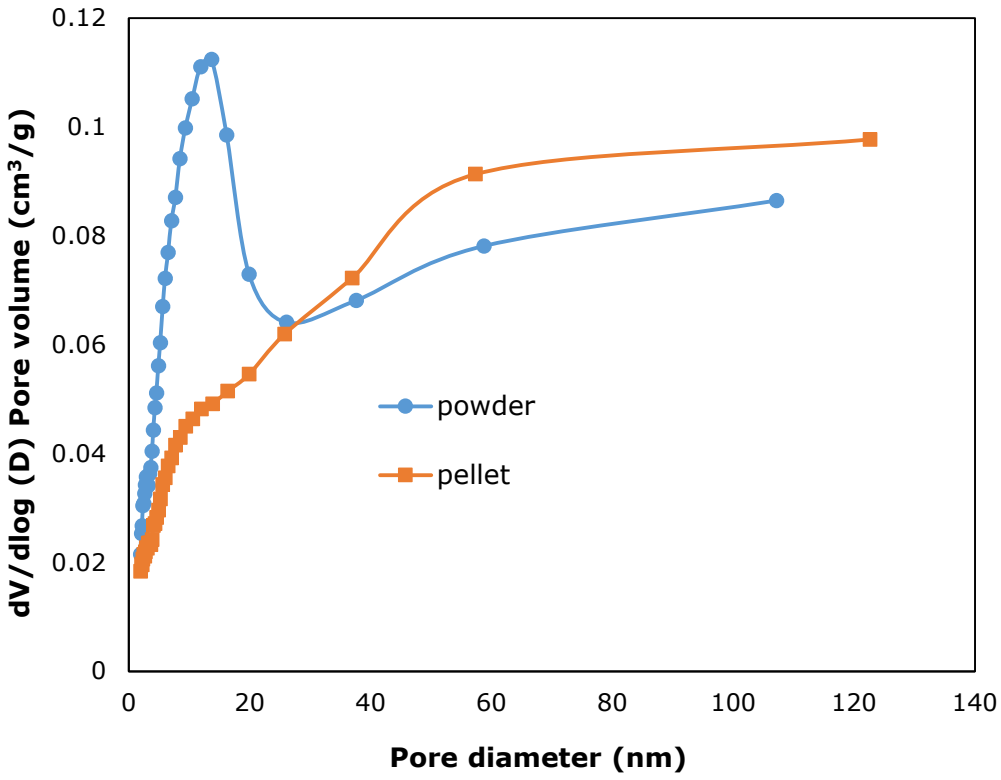


Figure 8.3: Pore size distribution of NaP1 powder and pellet obtained from the nitrogen isotherm experiment.

Despite this, the pore volumes of NaP1 pellet within (1 – 20 nm) are seen to be 200% more than NaP1 powder. This may be as a result of the pelleting process, where,larger pore diameters with volumes that may be inaccessible without high pressure are created at the expense of reducing the pore volume of previously accessible small pore diameters at low pressure.

The mean pore diameter obtained from the distribution for NaP1 pellet was 14.3 ± 0.275 nm compared to 10.95 ± 0.069 nm from Table 8.3. Although NaP1 pellet has the advantage of a

higher pore diameter than NaP1 powder, it will be disadvantaged with a low uptake volume of adsorbates than that of NaP1 powder. On the other hand, NaP1 powder will also be disadvantaged since it will not be able to accommodate elemental take-up of larger pore diameters. However, NaP1 powder and pellet could be used for selective elemental uptake based on their pore diameter.

Table 8.3 presents relevant parameters obtained automatically from the nitrogen adsorption experiment. The total surface area of NaP1 powder (60 m^2/g) is noticed to be 28% lower in NaP1 pellet (43 m^2/g). This is largely contributed by the external surface area derived from the small particulate nature of the NaP1 powder. Hence, the external surface area of the NaP1 powder was obtained as ~ 52 m^2/g as seen from Table 8.3.

Table 8.3: Surface area, pore volume, pore size obtained from the nitrogen adsorption of NaP1 powder and pellet at 77 K.

Parameters	Powder	Pellet
C (BET parameter)	179 ± 1.21	205 ± 5.73
Q_m (cm^3/g) (monolayer amount)	13.8 ± 0.0975	9.98 ± 0.0212
Surface Area (m^2/g)	**Mean**	**Mean**
Total Surface Area	60.1 ± 0.0599	43.4 ± 0.0901
Micropore Area	8.18 ± 0.151	9.13 ± 0.176
External surface area	52.0 ± 0.576	34.3 ± 0.261
Pore Volume (cm^3/g)	**Mean**	**Mean**
Total pore volume	0.139 ± 0.000151	0.114 ± 0.00161
Micropore volume	0.0034 ± 0.0000701	0.00385 ± 0.0000712
Pore Size (4V/A) (nm)	**Mean**	**Mean**
Adsorption average pore diameter	11.0 ± 0.0696	14.3 ± 0.275
Desorption average pore diameter	9.28 ± 0.0442	12.5 ± 0.0712

However, it is noteworthy that the micropore area of NaP1 pellet is more than NaP1 powder due to a higher micropore volume/low pore diameter ratio. Other studies from Rongsayamanont & Sopajaree (2007), Izidoro et al. (2012) and Chansiriwat et al. (2016) reported the total surface area of fly-ash derived NaP1 as 56.2, 65.8 and 69.3 m^2/g, respectively. NaP1 powder from this study has a higher total surface area (60.1 ± 0.0599 m^2/g) than that of Rongsayamanont &

Sopajaree 2007 but lower than Izidoro et al. (2012) and Chansiriwat et al. (2016). Franus et al. (2015) reported a surface area of 70 m^2/g for NaP1, Alvarez-Ayuso et al. (2003) reported 27.7 m^2/g from fly-ash derived NaP1 and 20.1 m^2/g for clinoptilolite while Aldahri et al. (2016) reported 68.8 m^2/g for fly-ash derived NaP1 and Zhang et al. (2020) obtained 80.4 m^2/g area for NaP1 modified with cyclohexanol. Except for Alvarez-Ayuso et al. (2003), all the studies presented on zeolite NaP1 have reported a surface area within the range (56 – 80 m^2/g). This may be closely linked to the particle sizes, composition of the zeolite with regards Si/Al ratio and purity of the zeolite NaP1 synthesized.

With the exception of Rongsayamanont & Sopajaree (2007), none of the other works reported the particle size of the NaP1 samples analysed nor the sample purity of the zeolites, making it difficult to identify particle size/percentage purity as possible causes to the different total surface area measured. However, the average particle size of NaP1 from this study (17 microns) was lower than that reported by Rongsayamanont & Sopajaree (2007) (63.6 microns) and as mentioned could be responsible for the higher surface area obtained from this study.

Table 8.4: Comparison of zeolite parameters from literature.

Zeolite	Surface area (m^2/g)	Pore volume (cm^3/g)	Pore diameter (nm)	C parameter from BET	Particle size (um)	References
NaP1	65.8	-	-	-	-	Izidoro et al., 2012
NaP1	69.3	-	-	-	-	Chansiriwat et al., 2016
FA NaP1 modified by cyclohexanol	80.4	0.0348	2.78	-	-	Zhang et al., 2020
NaP1	26.8	0.00880	3.856	-	2.78	Zhang et al., 2020
NaP1	27.7	0.0015	3.3	-	< 100	Alvarez-Ayuso et al., 2003
Clinoptilolite	20.3	0.0018	3.5	-	< 100	Alvarez-Ayuso et al., 2003
NaP1	68.8	0.132	1.09	-	< 35	Aldahri et al., 2016
Zeolite 4A	497	0.16		-	-	Ismail et al., 2010
ZSM-5	450	0.133	<4.0	-	-	Iliopoulou et al., 2012
Commercial Mordenite (NaA)	332	0.162	-	71.2	-	Kim and Ahn, 2012
Commercial Y	663	0.284	-	73.2	-	Kim and Ahn, 2012
Commercial X	582	0.215	-	70.1	-	Kim and Ahn, 2012
NaP1	60.1	0.139	11.0	179	< 100	This study

The pore volume demonstrated in Table 8.3 showed total pore volume of NaP1 powder (0.1391 cm^3/g) was more than NaP1 pellet (0.1137 cm^3/g) while NaP1 pellet (0.0039 cm^3/g) possessed a higher micropore volume than NaP1 powder (0.0034 cm^3/g). Other relevant parameters generated from the experiment were the Langmuir adsorptive capacity (Q_m) for monolayer adsorption and the BET parameter (C).

The monolayer adsorptive capacity for NaP1 powder (13.82 cm^3/g) was also more than NaP1 pellet (9.98 cm^3/g), however, the BET (C) parameter of NaP1 pellet (204) was more than that of the NaP1 powder (178). The BET (C) parameter is described as exponentially related to the energy of monolayer adsorption or magnitude of adsorbate/adsorbent interaction. Thus, NaP1 pellet has a higher adsorbate/adsorbent interaction compared to NaP1 powder and furthermore, significant porosity as the C value (204) is more than 200. This claim is further emphasized by the visual plot presented in Figure 8.3 where, NaP1 pellet is seen to have a wide range of pores compared to NaP1 powder.

In comparison to other works from literature (Table 8.4), NaP1 from this study displayed a pore volume 0.139 cm^3/g, higher than its fly-ash derived counterparts including ZSM-5 (Iliopoulou et al., 2012). The only zeolites with a higher pore

volume came from zeolite 4A (0.16 cm^3/g) and commercial zeolites (NaA: 0.162 cm^3/g, Y: 0.284 cm^3/g, X: 0.215 cm^3/g) tested from works of Ismail et al. (2010) and Kim and Ahn (2012), respectively. Secondly, the pore diameter of NaP1 from this study was observed to be higher than all its counterparts as well as the C_{BET} constant obtained from the BET analysis. This is a good indication of a higher energy of monolayer adsorption for NaP1 as well as a higher magnitude of adsorbate/adsorbent interaction.

8.3.2 Leaching from pellet vs powder

Leaching test was performed at pH 5 to identify leachable elements from the zeolites during operation conditions. The test was conducted on NaP1 powder, NaP1 pellet and commercial grade 3A zeolite pellets, for comparison. One gram (1 g) of each material was stirred in 1 litre of distilled water at 300 rpm, room temperature of 25 ± 2 °C and pH 5. The pH was kept constant by means of acid dosing with 1 M nitric acid for 3 hours while 10 ml samples were drawn within the following time intervals (0, 15, 30 min, 1 h and 3 h) for ICP testing and analysis.

Table 8.5 shows leached metals from the samples observed and it can be concluded that NaP1 powder produced the maximum quantity of metals in 180 min compared to pellets. A total of

32.2 mg leachates per gram of NaP1 powder was obtained in 3 hours compared to 19 mg and 9.6 mg leachates per gram of NaP1 pellets and 3A pellets, respectively. Commercial zeolite 3A produced the lowest quantity of leachates among the 3 samples. Alkali metals namely sodium and potassium (Na and K), formed majority of the leachates comprising 93% in NaP1 powder, 97% in NaP1 pellet and 91.8% in 3A pellet while other elements constituted the remaining percentage.

Table 8.5: Comparison of mean leaching results from NaP1 powder, NaP1 pellet and 3A pellet. Experimental conditions: 1-gram zeolite in 1 l distilled water, stirred at 300 rpm at pH 5 and room temperature 25 ± 2 °C.

NaP1 Powder	Na	Mg	P	K	Ca	Al	Fe	Total
Time (min)	(mg/l)	(mg/l)	(mg/l)	(mg/l)	(mg/l)	(µg/l)	(µg/l)	(mg/l)
0	0.01	0.002	0.034	0.02	0.01	3.79	19.4	0.10
15	18.6	0.042	0.145	1.07	0.134	25.1	56.4	20.1
30	22.3	0.127	0.202	1.28	0.260	40.0	106.7	24.4
60	24.9	0.336	0.243	1.53	0.530	56.4	134.1	27.8
180	27.8	0.947	0.229	1.95	0.874	115.9	232.3	32.2

NaP1 Pellet	Na	Mg	P	K	Ca	Al	Fe	Total
Time (min)	(mg/l)	(mg/l)	(mg/l)	(mg/l)	(mg/l)	(µg/l)	(µg/l)	(mg/l)
0	0.061	0.004	0.013	0.007	0.015	3.4	27.3	0.13
15	5.11	0.016	0.038	0.299	0.102	23.2	26.6	5.61
30	6.91	0.019	0.051	0.391	0.111	19.3	30.5	7.53
60	9.85	0.024	0.087	0.512	0.108	18.2	29.3	10.6
180	17.5	0.110	0.177	0.921	0.202	45.2	35.0	19.0

Table 8.5: ……*continued.*

3A - Pellet	Na	Mg	S	K	Ca	Al	Fe	Total
Time (min)	(mg/l)	(mg/l)	(mg/l)	(mg/l)	(mg/l)	(µg/l)	(µg/l)	(mg/l)
0	0.02	0.00	0.60	0.02	0.02	1.30	18.08	0.68
15	0.41	0.01	0.63	0.86	0.05	5.63	22.30	2.01
30	0.66	0.02	0.57	1.33	0.04	5.58	20.84	2.66
60	1.68	0.07	0.61	3.06	0.03	4.90	20.40	5.49
180	3.21	0.18	0.55	5.60	0.02	11.16	21.04	9.60
AWL	**200**	**50**	**1.0**[c]	**8.0**[b]	**100**[a]	**200**	**300**	

AWL: Acceptable Water Standards obtained from W.H.O

b: Health Canada (2008).
a: W.H.O, 2011

Unlike in zeolite 3A pellets where, potassium accounts for 58.4% while sodium accounts for the remaining 33% in the 91.8% majority of leachates, sodium dominated the majority in both NaP1 powder and pellet by 86 and 92% respectively. This is possibly due to potassium (K) being a precursor in the formation of zeolite 3A, as sodium (Na) was a precursor in the formation of NaP1. Aluminium and iron contributed the least to the leachates in micrograms and together formed 0.3% in 3A pellet and 0.4% in NaP1 pellet except in NaP1 powder where, they contributed to 1% of the total leachates.

However, the concentration of all leachates from the adsorbents were below their allowable concentrations in water. Making them safe for use. Comparing NaP1 powder to NaP1 pellet, the percentage composition of leachates was observed to have decreased for all metals except sodium (Na) although the quantities of all metals had decreased from NaP1 powder to pellet. This is a good indication to note that pelleting of powder adsorbents helps to reduce the quantity of leachates produced during treatment as this process tends to trap possible leachates within the pellet. This is because, loose powder particles which could release leachates have now been bound together into a mesoporous structure and preventing the release of leachates.

Alkaline earth metals such as calcium (Ca) and magnesium (Mg), which contributed ~ 3% leachates individually to the total leachates in the NaP1 powder, were observed to now reduce to 1% each in the NaP1 pellet. In contrast, calcium contributed 0.2% leachates while magnesium contributed 2% leachates in solution when 3A pellet was observed. Sulphur (S) was the only unexpected leachate produced from 3A zeolite and contributed 6% to the total leachates monitored and this should be coming from the original source of parent material used in creating the 3A zeolite. Phosphorus on the other hand, was also obtained in the case of NaP1 but contributed approximately 1% to the total leachates from both NaP1 powder and pellet. As mentioned in the case of 3A pellet, this should also be originating from its parent material.

This section concludes that leachates produced from NaP1 pellets were reduced by 40% of the original quantity produced from NaP1 powder. Zeolite 3A pellets leached the lowest concentration compared to both powdered and pelletized NaP1. It is also note-worthy that concentration of leachates are below acceptable standards for all the adsorbents and NaP1 pellets would not pose challenges when used for water treatment purposes as demonstrated in Table 8.5. The concentration of leachates is within 10 – 25% of the allowable leachate

concentration in wastewater effluents (Acceptable Water Standards obtained from Health Canada (2008) and W.H.O (2011).

As mentioned by Querol et al. (2002), a major drawback in the application of fly-ash derived zeolites was the prospect of leaching potentially hazardous elements in processed wastewaters. However, this concern was eliminated with the advent of pelleting powdered zeolites and the observations from Table 8.5 are evident where, both pelletized zeolites NaP1 and 3A produced the least concentration of leachates compared to NaP1 powder. This was possible through caging of leachable elements within the new pelletized structure as compression brought together loose particles under pressure and had the leachates bound in a new mesoporous structure.

8.3.3 Cation exchange capacity (CEC) determination

The Cation exchange capacity (CEC) of NaP1 and 3A were determined by means of ammonium acetate with results displayed in Table 8.6. 1 M ammonium acetate solution was prepared by dissolution made up in 1 litre volumetric flask. A 100 ml of this solution was poured into a 200 ml beaker and stirred with 0.25 g of zeolite NaP1/3A for 24 h. The solution was filtered with a 0.45-micron Minisart filter and analysed by the

ICP-MS. A sample of the ammonium acetate solution was measured as a blank and compared to results from NaP1 powder and pellet and 3A pellet.

Table 8.6 shows the result from 3 repetitions at 25 ± 2 °C with the mean and standard deviations calculated. The initial concentration of ammonium acetate recorded low concentrations of metals and non-metals of 1.1 mg/l. The final concentration of metals exchanged from NaP1 powder and pellet were determined to be 2.1 mg/g zeolite, representing 3% difference. This is an indication of no loss in the cation exchange capacity after pelleting NaP1.

Table 8.6: Cation exchange capacity (CEC) of NaP1 and 3A determined by stirring 100 ml of 1 M ammonium acetate solution with 0.25 g of zeolite NaP1/3A for 24 h at 25 ± 2 °C.

	1 M NH_4Oac	**1 M NH_4Oac**	**Zeolite**		
Elements (mg/l)	**Initial (NaP1)**	**Initial (3A)**	**NaP1 powder**	**NaP1 pellet**	**3A pellet**
Na (mg/l)	0.706	0.517	8.93 ± 0.124	8.93 ± 0.103	7.52 ± 0.023
Mg (mg/l)	0.004	0.002	0.956 ± 0.038	0.865 ± 0.015	0.623 ± 0.014
S (mg/l)	0.221	0.258	0.191 ± 0.071	0.304 ± 0.044	0.314 ± 0.027
K (mg/l)	0.174	0.138	1.25 ± 0.023	1.23 ± 0.01	16.3 ± 0.113
Ca (mg/l)	0.024	0.018	5.43 ± 0.047	5.13 ± 0.073	0.151 ± 0.004
Al (µg/l)	1.76	0.842	51.3 ± 49.7	2.08 ± 0.213	319 ± 41.9
Fe (µg/l)	11.1	15.1	68.3 ± 51.2	1.11 ± 0.64	14.6 ± 1.73
Sr (µg/l)	0.134	0.085	144 ± 1.14	124 ± 2.45	0.393 ± 0.028
Ba (µg/l)	0.056	0.056	191 ± 2.39	71.1 ± 2.83	0.856 ± 0.464
CEC (mg/g)			**68.8 ± 1.39**	**66 .7 ± 0.986**	**101 ± 0.547**

The difference in CEC (mg/g) between the NaP1 and 3A is ~ 33%, indicating that 3A (101 mg/g) has a higher capacity for exchanging metals and would perform better in an ion-exchange system of metal removal than NaP1 (66.7 mg/g). Calcium (Ca), Sodium (Na) and potassium (K) were identified as the major exchange elements in NaP1 while potassium (K) and sodium (Na) were the major elements in 3A pellet. Again, potassium is identified as the most abundant exchange ion from 3A pellet whereas sodium is the most abundant in NaP1.

The CEC (mg/g) presented in Table 8.6 of each major contributing element was used in calculating the CEC in (meq/g) and compared to other results found in literature. Hence, Table 8.7 compares the cation exchange capacity of other NaP1 powder from literature. As observed with the mass cation exchange capacity (mg/g) from Table 8.7, there is no significant difference (3%) between NaP1 powder and pellet CEC in (meq/g). This is a positive result and indicates that the pelleting process did not have a huge adverse effect on the cation exchange capacity. However, a 7% difference in cation exchange capacity (meq/g) is observed between NaP1 pellet and commercial zeolite 3A pellet. This is also a positive result encouraging the benefit of replacing commercial 3A zeolite with fly-ash derived zeolite NaP1.

Table 8.7: A Cation exchange capacity (CEC) comparison between this study and in literature.

Sample	Na (meq/g)	Mg (meq/g)	K (meq/g)	Ca (meq/g)	Total (CEC) (meq/g)	Reference
NaP1 powder	1.55	0.319	0.128	1.09	3.08	This study
NaP1 pellet	1.55	0.288	0.127	1.03	2.99	
3A pellet	1.31	0.208	1.67	0.030	3.22	
NaP1 powder	-	-	-	-	1.9	Izidoro et al., 2012
	-	-	-	-	1.6	
	-	-	-	-	2.2	Cardoso et al., 2015a
	-	-	-	-	2.7	Querol et al., 2002
	-	-	-	-	2.6 - 2.8	Cardoso et al., 2015b
	-	-	-	-	2.3	Prasad and Mortimer, 2011

It is evident from Table 8.7, that the cation exchange capacity of powdered fly-ash derived zeolites from this study is more than results obtained from other sources. Izidoro et al. (2012) has so far reported the lowest CEC value of 1.6 – 1.9 meq/g, followed by Cardoso et al. (2015a) and Prasad and Mortimer, 2011. The cation exchange of Querol et al. (2002) and Cardoso et al. (2015b) were within the same range. The difference in cation exchange capacity may be due to the elements present in the parent/source material used in synthesizing the zeolite and the synthesis process. Regardless, pelletized zeolite NaP1 can be a suitable replacement for current commercial synthetic zeolites as demonstrated in this section with strong ion exchange property demonstrated through its cation exchange capacity.

8.4 Lead removal with NaP1 and 3A

Lead was used to compare metal removal capabilities of NaP1 and 3A zeolite, since, it was best adsorbed among the other metals against NaP1 powder from previous experiments. Hence, 5 g of each zeolite was introduced into a litre of 90 mg/l concentration lead solution, stirred at 300 rpm for 3 h at a constant pH 5 and temperature 25 ± 2 °C. Samples drawn from the experiments at 15, 30, 60 and 180 min were analysed by ICP-MS. The experiment was repeated 3 times with the mean

and standard deviation calculated. A control experiment was also performed under the same conditions without any zeolite to check precipitation. Figure 8.4 shows results obtained from these experiments.

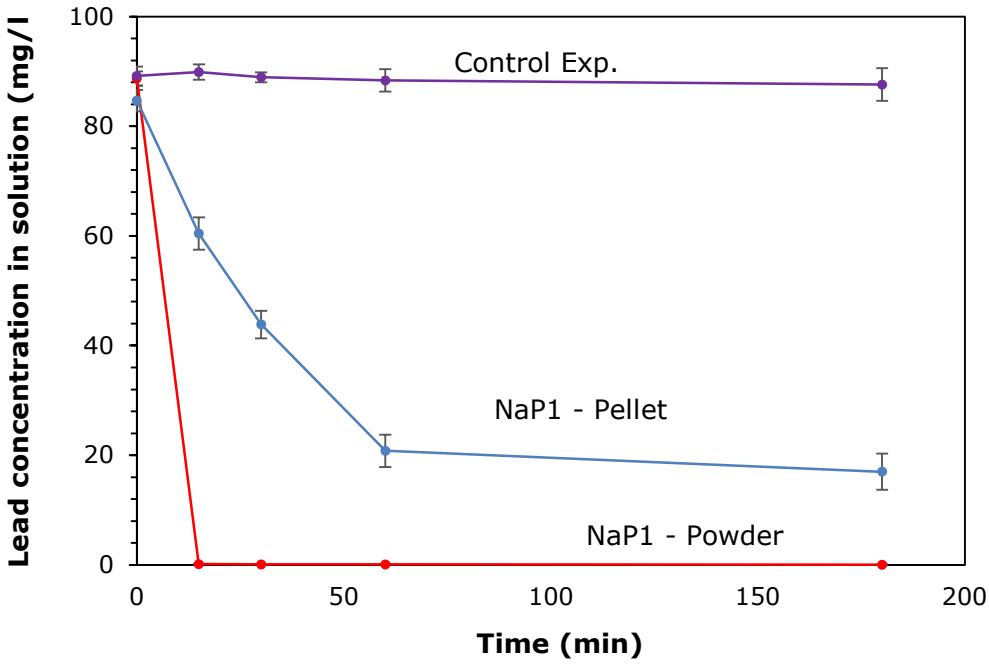


Figure 8.4: Decrease in lead concentration in solution over time without an adsorbent (control), with NaP1 powder and pellet using the following conditions: 5 g of zeolite, 1 litre of 90, 89 and 85 mg/l concentration lead solution respectively, stirring at 300 rpm for 3 h at pH 5 and at 25 ± 2 °C.

Figure 8.4 demonstrates the absence of precipitation at pH 5 by lead as there was no concentration change over 180 min from the control experiment. However, NaP1 powder reduced lead concentration within 15 min from 89 mg/l to 0.14 ± 0.025 mg/l. This concentration finally drops to zero by the end of the experimental period. On the other hand, NaP1 pellets is

observed to also gradually reduce lead concentration in solution over the experimental period (180 min) without achieving a 100% lead removal. An average lead removal of 20 mg/l was removed in 15, 30 and 60 min respectively, with the least amount of 3 mg/l lead removed in the last 2 h (from 60 – 180 min). Thus, NaP1 pellet achieved 80% lead removal compared to 100% by NaP1 powder. This was expected as the initially loose particulate NaP1 had been compressed into pellets reducing the surface area of the adsorbents.

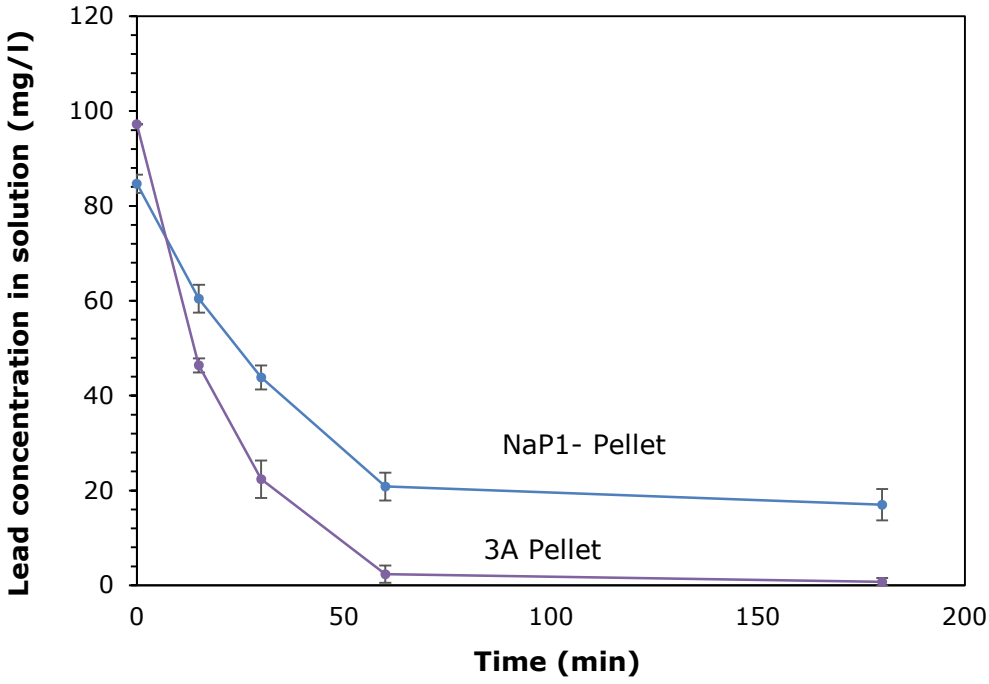


Figure 8.5: A graph comparing lead concentration decrease in solution over time with NaP1 pellet and 3A pellet using the following conditions: 5 g zeolite, 1 litre of 98 and 85 mg/l concentration lead solution respectively, stirred at 300 rpm for 3 h at pH 5 and at 25 ± 2 °C.

Hence, we can account for a 20% reduction in adsorbent efficiency after pelleting. Lead removal using NaP1 pellets was also compared using 3A pellets (Figure 8.5). Zeolite 3A showed 3 times more lead removal with NaP1 pellet within 15 min. This was followed by ~ 20 mg/l lead removal in 30 and 60 min respectively. A final 99% lead removal was achieved in 180 min (3 h). Lead uptake by 3A pellet was ~ 33 mg/l more than NaP1 pellet demonstrating superiority over NaP1 pellet on this occasion. This may be due to zeolite 3A having regular pore size 3 Å compared to NaP1 ~ 2.7 – 2.9 Å with irregular pores making lead removal relatively quicker with zeolite 3A. Lead removal experiments conducted with all three adsorbents reveal 3A pellets possesses a quicker kinetics for lead compared to its NaP1 pellet counterpart. Hence, the kinetics will be explored by attempting to describe the underlining principles using kinetic models.

8.4.1 Kinetics of lead removal by NaP1 versus 3A

The kinetics of NaP1 powder, NaP1 pellet and 3A pellets were examined using kinetic models, which describes the lead uptake mechanism of these adsorbents. NaP1 powder displayed the quickest uptake in 15 mins compared to both NaP1 pellet and 3A pellet. This was mainly due its small size and porous nature presenting a larger surface area than its counterpart pellets.

However, comparing both pellets, 3A pellet also demonstrated a quicker lead uptake than NaP1 pellet owing to its pore size. The kinetic models explored were pseudo-first and second order model, diffusion kinetic model, Elovich model and intra-particle diffusion model. These models were obtained by plotting the modified lead uptake quantity against time in different ways. Table 8.8 presents the R^2 values obtained from the plots of each kinetic model to assist is the decision-making system.

Table 8.8: Kinetic models tested with lead uptake experimental data by NaP1 powder, NaP1 pellet and 3A pellet.

Kinetic Model	**NaP1 Powder**	**NaP1 Pellet**	**3A Pellet**
		R^2	
Pseudo-first order	0.014	0.580	0.404
Pseudo-second order	1.00	0.973	0.994
Diffusion Kinetic	0.509	0.828	0.746
Elovich	0.779	0.928	0.959
Intra-particle diffusion	0.472	0.861	0.779

The R^2 value also known as the coefficient of determination indicates the proportion of data set, which supports the dependency between the two variables compared for each model and would be suitable in describing the kinetics of that

model. Therefore, an R^2 value of 75 – 95% is always preferred during this decision-making process as this indicates a strong correlation between the experimental data and the model. Beginning with NaP1 powder, the least preferred kinetic model is the pseudo-first order because it produced an R-squared value of 0.014 indicating that only 1.4% of the data set obtained from the lead removal experiment affirms that time influences the uptake mechanism.

Consequently, 98% of the data set is due to other factors. Figure 8.6 gives a visual representation of the plot with a line of best fit, which does not fit well to the data set. Thus, eliminating the pseudo-first order kinetic model. The diffusion kinetic model and intra-particle diffusion were also not suitable as they did not meet the preferred R-squared requirement and were eliminated. The Elovich model for NaP1 powder showed a strong correlation as it produced 77% conformity to the data set signalling surface heterogeneity of NaP1 powder.

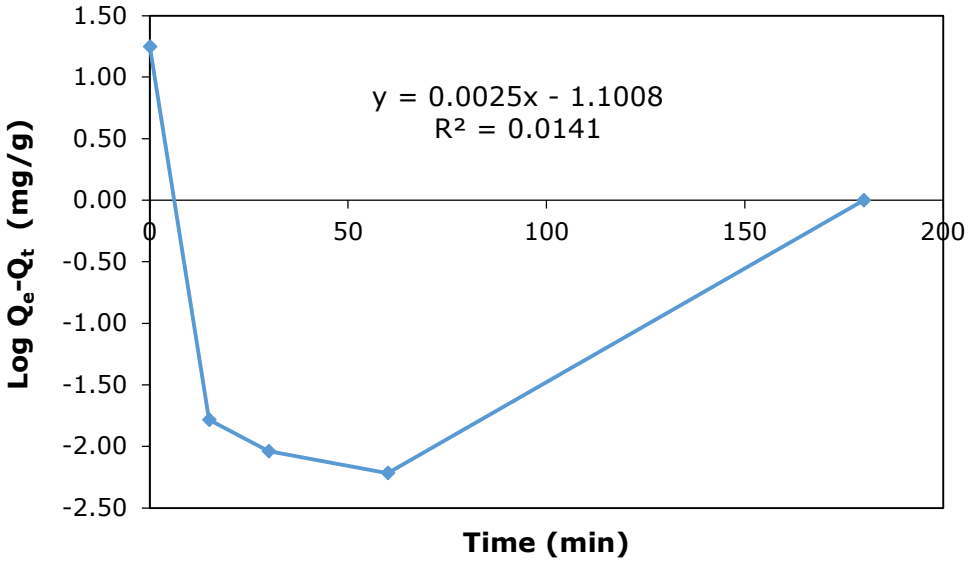


Figure 8.6: A graph demonstrating pseudo-first order kinetic model of lead uptake by NaP1 powder at 25 ± 2 °C.

The pseudo-first order reaction model, which depicts single-site occupancy of adsorbed ions did not fit with this model, suggesting the presence of double-site adsorption theory proven by a good fit to pseudo-second order reaction model. This is in line with kinetic characteristics of zeolites identified by the research of Blanchard et al. (1984). Pseudo-second order kinetic model displayed in Figure 8.7, produced a good fit to the regression line and an R-squared value of 1.0.

This indicates, 100% of the dataset purports the relationship between the rates of removal to the up-taken lead amount as a function of time. A corresponding rate of removal to lead amount removed (t/q_t) versus time (t) was observed over the

time period from Figure 8.7. The pseudo-second order reaction model fits well with experiments of samples possessing a heterogeneous surface and suggests the surface heterogeneity of NaP1 powder in this case.

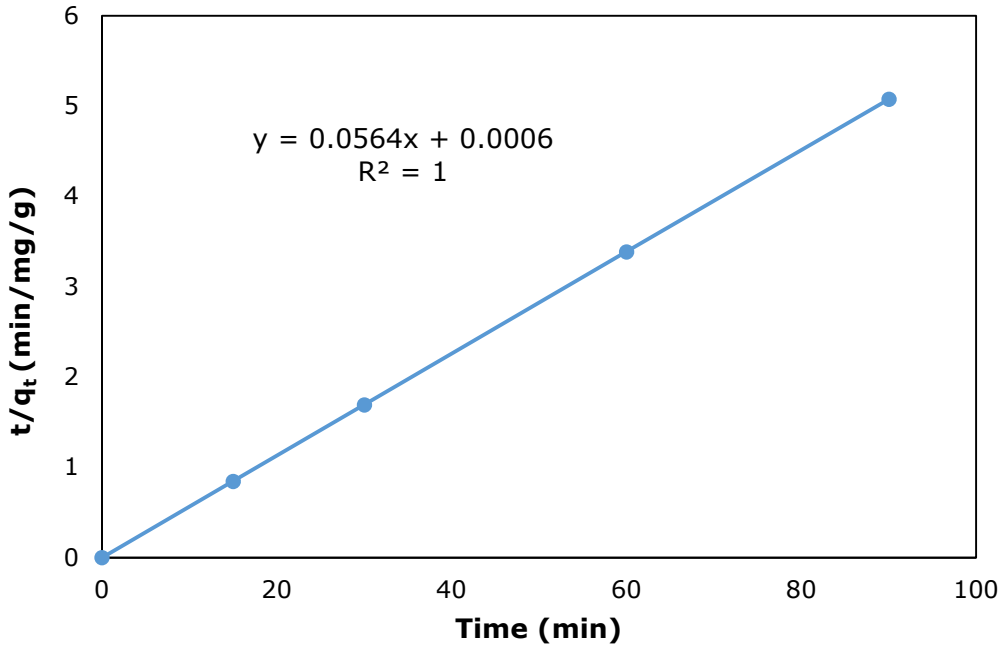


Figure 8.7: Pseudo-second order kinetic model of lead uptake by NaP1 powder at 25 ± 2 °C.

Among all five kinetic models employed in this section, pseudo-second order, diffusion kinetic, intra-particle diffusion and Elovich proved to be more appropriate in describing the lead uptake mechanism for NaP1 pellet. Only pseudo-first order kinetic model did not produce the acceptable fit to the regression line as well as the required R-squared value from Table 8.8. Hence, it can be observed from Table 8.8 that four models produced R-squared values between 0.83 – 0.97

indicating 83 – 97% conformity of the kinetic models to the experimental data set. In this scenario, there is no dominance of one mechanism. It can be suggested that there is the existence of all four mechanisms at different periods of the experimental phase, where, a single occupancy is experienced during lead uptake before the augmentation of a double-site occupancy and this is initiated by a diffusion process followed by the intraparticle diffusion through the porous NaP1 pellet.

None the less, pseudo-second order model produced the highest R-squared value (0.97) presented in Table 8.8 as the best model to describe the lead up-take mechanism for NaP1 pellet. However, the intraparticle diffusion model producing the 3rd highest R-squared value was highlighted in Figure 8.8 for NaP1 pellet.

Figure 8.8 shows the plot of lead removed per gram of NaP1 pellet versus the square-root of the time taken for metal removal. The amount of lead removed from solution per gram of NaP1 pellet was gradual over time till $t^{0.5}$ value of 4.0, where, more lead uptake occurred till $t^{0.5}$ value of 8.0, when no further uptake was recorded. This indicates the presence of intraparticle diffusion from the start of the lead uptake process till $t^{0.5}$ value of 8.0 corresponding to ~ 90 min, where, the process must have stopped.

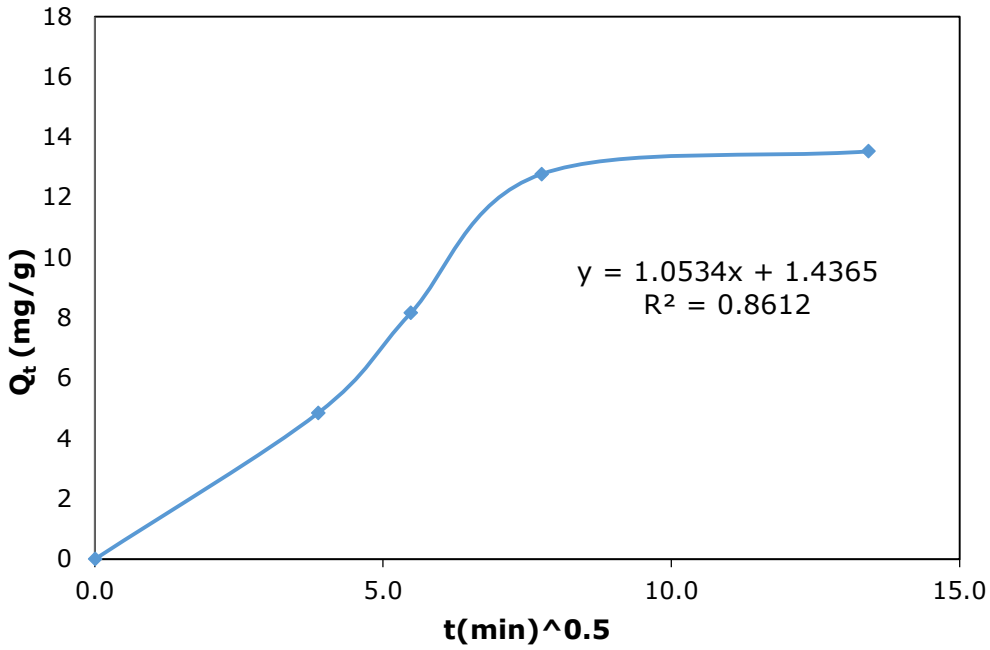


Figure 8.8: A graph demonstrating intraparticle diffusion kinetic model of lead uptake by NaP1 pellet at 25 ± 2 °C.

Unlike both NaP1 powder and pellet, lead uptake mechanism by zeolite 3A pellet from Table 8.8 had all the kinetic models producing a good fit for the experimental dataset except pseudo-first order model. Hence, all the models produced the desired R-squared value with the Elovich model demonstrating the second highest R-squared value. Again, pseudo-second order demonstrated the highest R-squared value for the experimental data with 3A pellets. However, the Elovich model is highlighted in Figure 8.9, which shows the plot of lead removed per gram versus the natural logarithm of time with 3A pellets.

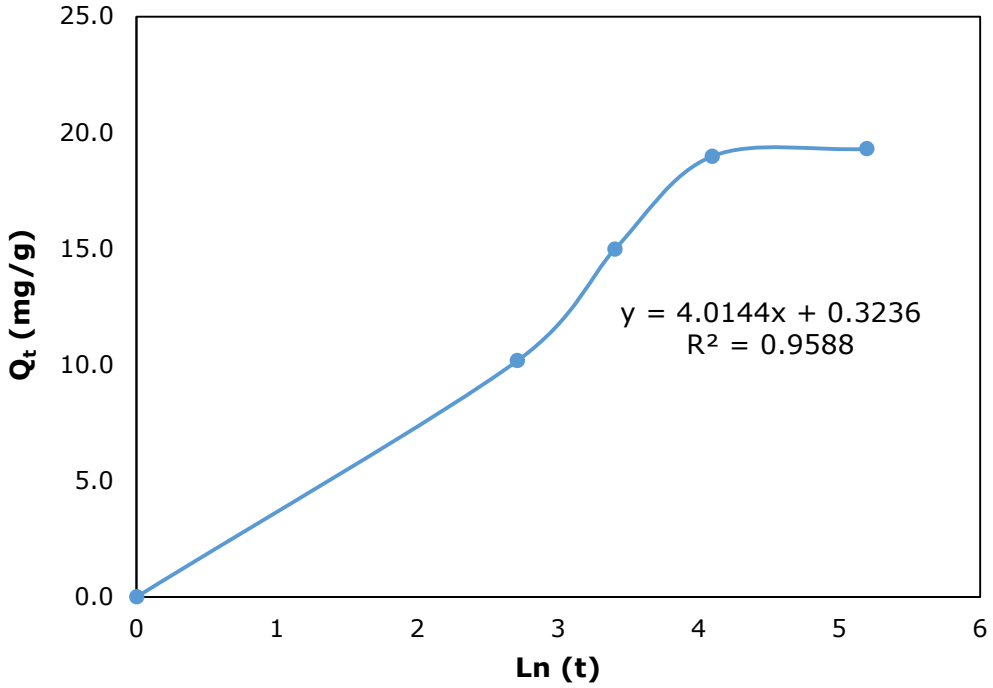


Figure 8.9: Elovich kinetic model of lead uptake by 3A pellet at 25 ± 2 °C.

From Figure 8.9, lead uptake per gram of 3A zeolite was observed to correspond to the natural logarithm of the time taken till Ln 2.8, where, there was more lead uptake over the remaining time taken until Ln 4. The Elovich model is known to demonstrate a second order kinetics for heterogeneous surface adsorbents but does not propose any definite mechanism for adsorbate-adsorbent interaction and thus will not be enough in describing the lead uptake mechanism completely. To complement this finding, Table 8.8 earlier indicates the pseudo-second order model produced a good fit to the experimental

data signifying the correspondence of the lead uptake mechanism to a second order kinetics model.

It was useful to note that both 3A and NaP1 pellets' lead uptake mechanisms could be described by 4 common models (i.e. pseudo-second order, Elovich, diffusion and intra-particle diffusion models) out of which, NaP1 powder could not be described by diffusion and intra-particle diffusion models. Both diffusion and intra-particle diffusion were applicable to NaP1 pellet due to the creation of pellets from particles, generating a much larger porous (micropores and mesopores) structure with interconnections and semi-connections but not NaP1 powder. The designed pellets tend to change the original kinetic dynamics of the powdered zeolite material, hence, introducing a heterogeneous surface (satisfied by Elovich model) and a larger porous structure with connections (satisfied by diffusion model and intra-particle diffusion models).

To conclude on this section, the kinetic models were a good complement to each other in the lead-uptake mechanism of describing pellets. NaP1 powder possessed heterogeneous surfaces which removed lead from solution incorporating a double occupancy packing system. However, when NaP1 pellets were formed from the powdered particles, it produced another

large heterogeneously porous structure requiring both initial diffusion of lead into the large structure and further intra-particle diffusion into the smaller NaP1 particles. In this case, there is the possibility of an initial single site occupancy by the NaP1 pellet for the lead metal followed by a secondary double-site occupancy.

This phenomenon is reinforced by the BET results showing the presence of monolayer – multilayer uptake for both NaP1 powder and pellet. However, zeolite 3A pellet is identified to possess a heterogeneous surface with double-site occupancy while going through both diffusion and intra-particle diffusion. Hence, it can be concluded that both pellets have diffusion as their main lead uptake mechanism.

Unfortunately, not much work has been done in identifying the uptake mechanism of metals with NaP1. This has been because other zeolites such as A and X have been preferred to zeolite NaP1 (Querol et al., 2002) as mentioned earlier in the literature review section (Chapter 2). Therefore, results regarding the adsorbent kinetics from this section are compared to other adsorbents. It is also worth mentioning that over the past 15 - 20 years, many researchers have been fixated on new adsorbent development, adsorbent modification and pollutant

removal (CEC, equilibrium and isotherm information) while neglecting the pollutant removal mechanism described by adsorption kinetic models.

Table 8.9: Kinetic models of metal uptake mechanism of NaP1 compared to other adsorbents

Kinetic Models (R^2)								
Zeolite	**Metals**	**Pseudo-first order**	**Pseudo-second order**	**Diffusion Kinetic**	**Elovich**	**Intra-particle diffusion**	**Form**	**Reference**
Fly-ash NaP1	Pb	0.014	1.00	0.509	0.779	0.472	Powder	This study
Fly-ash NaP1	Pb	0.581	0.973	0.828	0.928	0.861	Pellet	
Commercial 3A	Pb	0.404	0.994	0.746	0.959	0.779	Pellet	
Fly-ash Zeolite P	Pb	0.302	0.975	-	-	-	powder	Kobayashi, 2020
Clinoptilolite	Pb	0.989	0.994	-	0.993	-	-	Gunay et al., 2007
Synthetic Faujasite	Cu	0.964	1.00	-	-	0.992	powder	Chen et al., 2020
Commercial NaX	Pb	0.972	0.999	-	-	0.873	Pellet	Ezzeddine et al., 2018

Table 8.9: ……*continued.*

Zeolites	Metals	Pseudo-first order	Pseudo-second order	Diffusion Kinetic	Elovich	Intra-particle diffusion	Form	Reference
LTA	Fe^{3+}	0.697	0.976	-	-	-	-	Hashemian et al., 2013
NaY	Zn	0.980	0.973	-	-	-	-	Ostroki et al., 2009
	Fe^{3+}	0.934	0.974	-	-	-	-	
Synthetic NaA	U^{6+}	0.998	0.997	-	-	0.698	powder	Nibou et al., 2011
Synthetic NaA	Zn	0.942	0.991	-	-	0.986	powder	Nibou et al., 2010
Synthetic NaX	Zn	0.951	0.992	-	-	0.999	powder	
Commercial X	Ni	0.989	0.574	-	-	0.504	pellet	Singh et al., 2008
Commercial 4A	Cd	-	0.999	-	-	-	pellet	Kulkarni et al., 2012
Synthetic NaA	Cu	0.891	0.994	-	0.945	0.773	Granules	Georgiev et al., 2012

Table 8.9 compares results from the kinetic models employed in this study to other adsorbents from literature. Kobayashi (2020), depicted a similar correlation coefficient for pseudo-second order kinetic with lead using fly-ash zeolite P just as this research, attesting to the pseudo-second order kinetic model being the best to describe the uptake of lead with fly-ash derived NaP1. Pseudo-second order kinetic model has demonstrated dominance in describing the adsorption mechanism for all zeolites except for commercial X used by Singh et al. (2008) for nickel removal (Table 8.9). Lead uptake with all adsorbents was described by pseudo-second order with an R^2 value greater than 0.97. Diffusion kinetic model was only reported in this study while Gunay et al. (2007) and Georgiev et al. (2012) were the researches to have used the Elovich model.

Intraparticle diffusion was the 3rd most popular kinetic model after the pseudo-first order kinetic model. Intraparticle diffusion mechanism with lead for fly-ash derived NaP1 pellet from this study closely relates to that of Ezzeddine et al. (2018) with commercial NaX. Again, the R^2 value of the intraparticle diffusion of NaP1 pellet from this study was more than all the other commercial pellets in Table 8.9; demonstrating a stronger intraparticle diffusion mechanism of lead through NaP1 pellets

as a result of better porosity developed through the pelleting process. However, large porous particles of synthetic composition NaX (0.74 nm), NaA (0.42 nm) and Faujasite (0.74 nm) (Koshy and Singh, 2016) with zinc and copper uptake is also observed to follow an intraparticle diffusion mechanism reported by Nibou et al. (2010) and Chen et al. (2020) with high R^2 values greater than 0.986. This is contrary to NaP1 powder (R^2 = 0.47) and could be due to inconsistent pore dimensions of NaP1 powder.

8.4.2 Multi–element removal with NaP1 pellets compared to 3A pellets

Multi-element removal test with NaP1 powder, NaP1 pellet and 3A were required to understand the performance of NaP1 pellet in an industrial setting. This is because industrial wastewater usually contains other elements, increasing the complexity of metal removal processes. Multi-elements used were zinc, copper and lead as the metals of concern in this research.

The experiments were performed by mixing 5 g of zeolite at 300 rpm with a litre of 460 - 500 mg/l concentration of multi-elements (composition: Zn - 250 mg/l, Cu – 150 mg/l and Pb – 100 mg/l) at pH 5 for 3 h at 25 ± 2 °C. 10 ml samples were taken from the solutions at 0, 15, 30, 60, 180 min and analysed

with the ICP-MS. Figure 8.10 exhibits the results of multi-element removal using NaP1 powder.

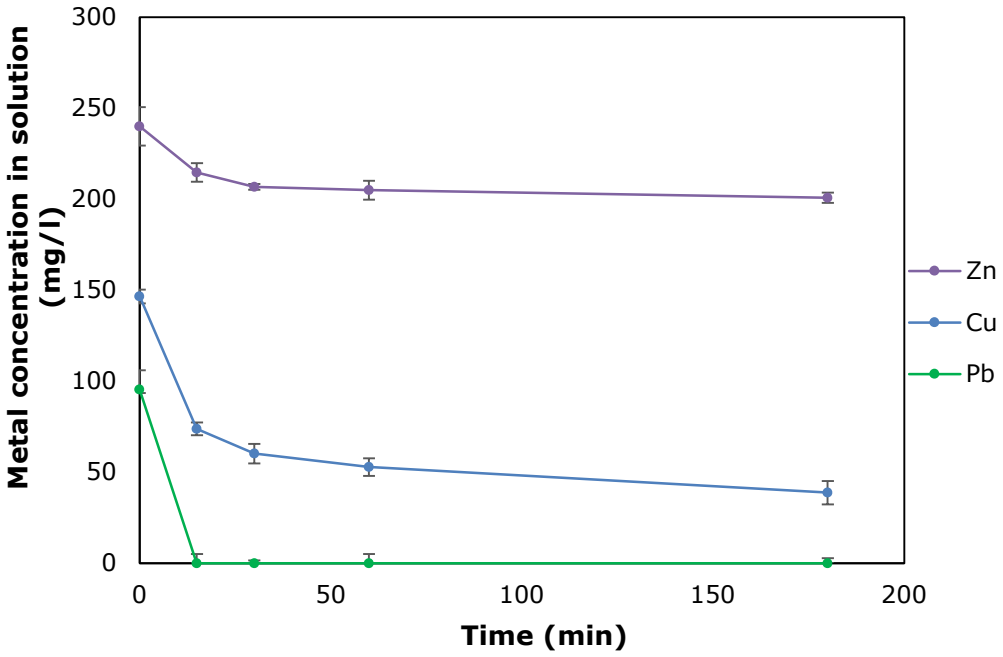


Figure 8.10: Decrease of metal concentration in solution over time with NaP1 powder using the following conditions; 5 grams of each zeolite, 1 litre of 486 mg/l total metal concentration (98 mg/l lead, 240 mg/l zinc, 148 mg/l copper), stirred at 300 rpm for 3 h at pH 5 and 25 ± 2 °C.

Lead was completely removed when compared to the other metals in the solution, achieving a 100% removal within the first 15 min. This was followed by 73% and 16% copper and zinc removals, respectively over the 3 h period. The total quantity of all multi-elements removed by NaP1 powder was calculated as 241 ± 6.79 mg/l, which is 39% of the starting concentration. As established in section 6.5, metal affinity

towards NaP1 powder were in the order Pb > Zn> Cu due to the size of hydrated ions and hydration energy. However, the selectivity is noticed to conform to the order Pb > Cu > Zn from the multi-element removal proposed by Zamzow et al. (1990), Steenbruggen and Hollman (1998), Lee et al. (2000), Erdem et al. (2004) and Hui et al. (2005), in accordance with sorption quantity. Arguably, this order of selectivity takes precedence over the selectivity achieved from the single element adsorption capacity as this represents the appropriate system to check selectivity. Figure 8.11 shows concentration decrease in solution over time with NaP1 pellets.

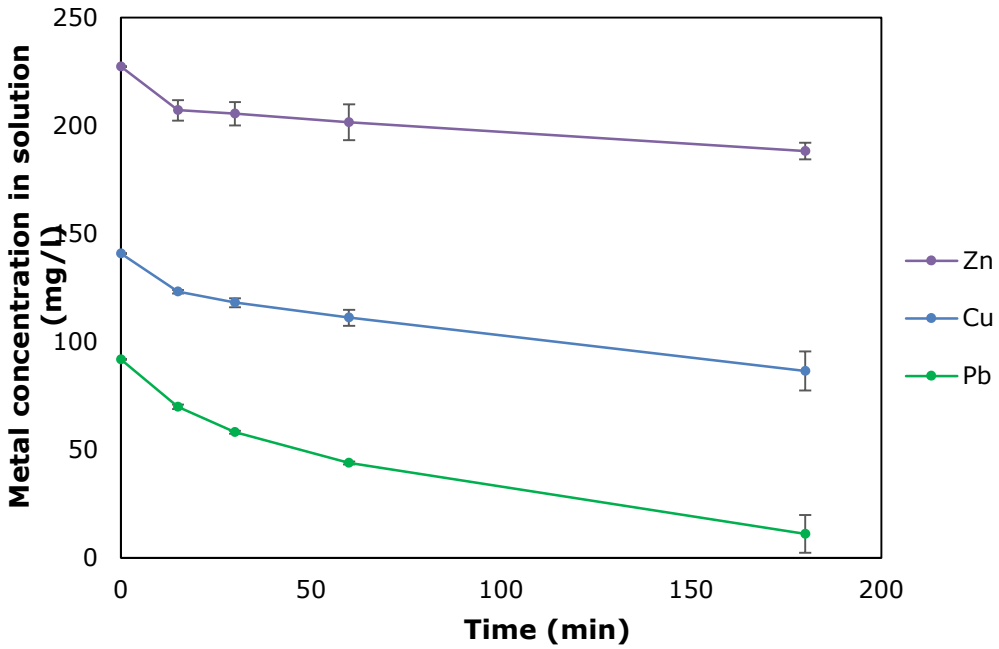


Figure 8.11: Decrease of metal concentration in solution over time with NaP1 pellet. Conditions; 5 g of each zeolite, 1 l of 462 mg/l total metal concentration (92 mg/l lead, 230 mg/l zinc, 140 mg/l copper), stirred at 300 rpm for 3 h (180 min) at constant pH 5 and temperature 25 ± 2 °C.

Comparing Figure 8.11 to 8.10, the trends showing the progress of individual metal removal processes appeared different. Figure 8.10 shows a plateau region for all metal removal from 30 min to 180 min, indicating the end of the metal removal process while the same elements did not come to that point even at 180 min using pellets (Figure 8.11). Hence, Figure 8.11, gives further hint of the removal process requiring more time and this may be due to slower kinetics displayed by NaP1 pellet compared to NaP1 powder. Figure 8.11 shows the progress of individual element removal process by pelletized NaP1. The uptake of all the elements followed a gradual removal process over the 3-hour period.

Lead is observed to reduce in solution by 23% in the first 15 min, following a gradual removal process till 88% removal is obtained at 180 min. Lead removal by NaP1 powder was 12% more than the one obtained from NaP1 pellets. Copper removal was the second highest with a 38.6% removal outcome at the end of 180 min. Zinc removal by NaP1 pellet followed with the 3rd highest percentage removal at 17%. Copper removal by NaP1 pellets was reduced by ~ 50% when compared to NaP1 powders while that of zinc remained constant for both NaP1 pellets and powders.

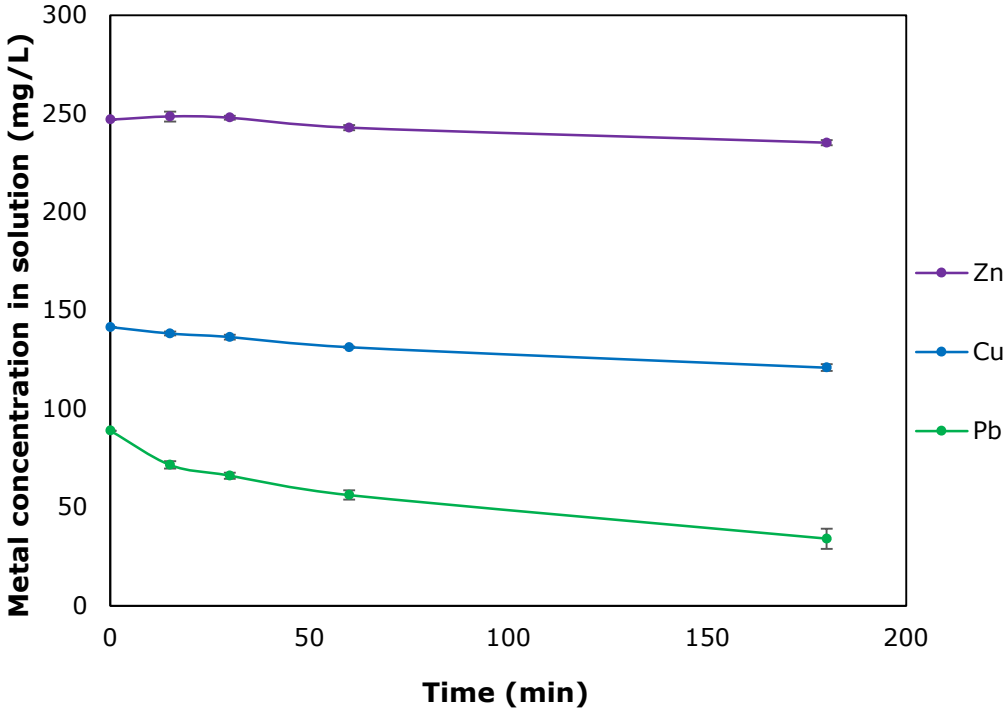


Figure 8.12: Decrease of metal concentration in solution over time with 3A pellet. Conditions; 5 grams of each zeolite, 1 litre of 477 mg/ total metal concentration (92 mg/l lead, 245 mg/l zinc, 140 mg/l copper), stirred at 300 rpm for 3 h (180 min) at a constant pH 5 and temperature 25 ± 2 °C.

Multi-element removal using zeolite 3A pellets (Figure 8.12) was investigated and compared with NaP1 pellets (Figure 8.11). The affinity of metals towards 3A was determined as Pb > Cu > Zn as the pattern achieved for NaP1 powder and pellets. Just as NaP1, lead (19.5%) and copper (2.3%) removal with 3A pellet started within the first 15 min. However, zinc removal took longer (slow kinetics) with concentrations slightly reduced by 1.7% even after 3 h. Zeolite 3A removed 19.5% lead within

the first 15 min, followed by a gradual removal till 61% lead in 3 h. Just like NaP1 pellet, 3A pellet removal of multi-elements is likely to continue for all metals beyond the 180 min/ 3 h period, since the uptake progress of all the elements from Figure 8.12 is seen not to have come to a plateau region. This may be reflective of a very slow kinetic/metal uptake process for zeolite 3A, which was not the case with single-element removal with lead. Hence, it can be suggested that 3A would require even more removal time with multi-elements than NaP1 pellets.

Overall, the total percentage of multi-elements removed in 3 hours with 3A pellets was 14.5% (72.5 mg/l) compared to 31.4% (157 mg/l) for NaP1 pellet and 39% (195 mg/l) for NaP1 powder. NaP1 pellet has demonstrated 54% more efficiency in multi-element removal compared to its commercial counterpart zeolite 3A pellets. Although single–element lead removal with 3A pellet produced 33 mg/l more lead removed from solution than NaP1 pellet, the multi-element results prove NaP1 pellet to be superior with a total 76 mg more multi-element removed than 3A pellet.

This value is 54% more than the total multi-element removal obtained. Putting this into perspective, 3A pellet was only able

to remove 15% of the total multi-elements even though it had performed better in the singe-element adsorption setting. Multi-element removal efficiency was identified in the order NaP1 powder > NaP1 pellet > 3A pellet.

Table 8.10 presents a molar uptake perspective of the multi-element removal process with all three adsorbents, showing the mean and standard deviation values in mmol. The total number of copper elements removed across all adsorbents was the highest compared to all other metals (NaP1 powder: 0.34 mmol/g, NaP1 pellet: 0.172 mmol/g and 3A pellet: 0.066 mmol).

From Table 8.10, the total amount of zinc removed (2nd highest) remained the same (0.12 mmol/g) regardless of which NaP1 form was used (powdered or pellet). However, the number of zinc elements for both NaP1 was 3 times more than that removed by zeolite 3A (0.036 mmol/g). Lead removal was the 3rd highest uptake with both NaP1 forms. The uptake process (removal kinetics) of lead by NaP1 pellet compared to NaP1 powder was identified to be very slow. 3A pellet uptake of metals was both lowest in quantity among the three and slowest in uptake time.

Table 8.10: Multi-element concentration decrease in solution over time with NaP1 powder/pellet and 3A pellet using the following conditions; 1 gram of each zeolite, 1 litre of 1.7 mmol/l total metal concentration stirred at 300 rpm for 3 h (180 min) at a constant pH= 5 and temperature 25 ± 2 °C.

Zeolite	Time (min)	Cu (mmol/g)	Pb (mmol/g)	Zn (mmol/g)
NaP1 powder	0	0.462 ± 0.012	0.092 ± 0.002	0.734 ± 0.032
	180	0.122 ± 0.02	0.0002 ± 0.00004	0.614 ± 0.008

	Time (min)	Cu (mmol/g)	Pb (mmol/g)	Zn (mmol/g)
NaP1 pellet	0	0.444 ± 0.012	0.088 ± 0.002	0.696 ± 0.032
	180	0.272 ± 0.028	0.01 ± 0.008	0.576 ± 0.012

Table 8.10: *……continued.*

Zeolite	Time (min)	Cu (mmol/g)	Pb (mmol/g)	Zn (mmol/g)
3 A pellet	0	0.446 ± 0.012	0.086 ± 0.002	0.756 ± 0.032
	180	0.38 ± 0.004	0.032 ± 0.002	0.72 ± 0.016

Using the number of moles, it can be stated that copper metals are preferred to zinc regardless of whether powdered or pellet NaP1 is used for the adsorption process. However, this conclusion cannot be made with lead since the starting concentration of lead compared to either zinc or copper is so low (non-equal molar quantities). Also, the number of moles of zinc uptake from Table 8.10 shows that zinc uptake was not influenced by the nature of the adsorbent (powder or pellet NaP1) or the starting concentration since the same number of moles of zinc was recorded (0.12 mol/g) with both powder and pellet NaP1.

On the other hand, copper uptake was affected the most with a 45% reduction in mole uptake when NaP1 pellet was used compared to its powder counterpart.

Hence, multi-element removal efficiency with regards total moles of elements removed within 3 hours is in the order Cu > Zn > Pb for NaP1 powder and pellet and Cu > Pb > Zn for zeolite 3A. The order of removal efficiency is different from metal selectivity, where, selectivity relating to affinity refers to maximum number of elements removed in the shortest possible time. In this case, metal removal within the first 15 min was considered, thus showing metal selectivity of the multi-

elements of interest in the order Cu > Pb > Zn for NaP1 powder, Zn > Cu > Pb for NaP1 pellet and Pb > Cu > Zn for zeolite 3A pellet. This claim is not conclusive as the number of particles for all elements were not equal in the initial concentration and can be improved by starting with an equi-molar number of elements. However, the variation in selectivity at different times of these metals demonstrated by the molar quantities of adsorption is evidence of multi-element competition between elements.

8.4.3 Multi-element interaction

Further investigation of the multi-element competition was performed using the kinetic models (pseudo-first and second order) in comparing metal removal of single/multi-element with NaP1 powder/pellet and 3A pellet. The results shown in Table 8.11 were modelled from pseudo-first/second order kinetic models using the same data obtained from single element/Multi-element removal with NaP1 powder/pellet and 3A pellet experiments.

Table 8.11: Adsorptive capacity of powder and pellet NaP1 obtained from single/multi-element systems using pseudo-first*/second order kinetic models.

Metal	Removal with NaP1 Powder (mg/g)		Removal with NaP1 Pellet (mg/g)		Removal with 3A Pellet (mg/g)	
	Single	Multi	Single	Multi	Single	Multi
Zn	6.84	8.02	-	8.27	-	1.51*
Pb	17.7	19.1	14.7	18.6	20.1	12.4
Cu	7.20	22.1	-	12.2	-	5.64

All the metal-uptake capacity/adsorptive capacity displayed in Table 8.11, were obtained through the pseudo-second order kinetic model as best fitted model to the experimental data with R-squared values above 0.90 except zinc removal with 3A pellet. This exception could only be determined by the pseudo-first order kinetic models since the experimental data was best fitted to this model and produced r-squared values above 0.90.

Comparing the metal-uptake per gram of NaP1 powder for single and multi-element results, an increase is observed with zinc (17%), copper (300%) and lead reduced (8%) during multi-element metal uptake. Copper recorded the highest removal uptake from the multi-element uptake, which was three times (3x) more than the uptake obtained from the single-

element uptake. This could be the result of increased kinetic drive caused by the increased metal concentration from the multi-element solution (500 mg/l) compared to the individual metal concentration from the single-element solutions (100 mg/l lead, 250 mg/l zinc, 150 mg/l copper).

An increase in concentration of solute in solution reflects an increase in the number of particles, leading to more collision and interaction between particles and with adsorbent. Thus, an increased collision with adsorbent consequently will produce more metal uptake while an increased collision between multi-elements will lead to competitive uptake. However, copper uptake from the multi-element system with NaP1 powder was not hindered by the presence of other competitive metals such as lead and zinc as it recorded the highest uptake (22 mg/g) in comparison to the others in a multi-element system compared to single-element system.

As mentioned earlier, lead is preferred to the other elements due to its small hydrated radius allowing it to pass through narrow porous channels presented by NaP1 powder with ease compared to its counterparts. In contrast, lead uptake capacity from single-element experiment with NaP1 pellet had reduced by 17% compared to its multi-element experiment. Zinc uptake

by NaP1 pellet in a multi-element removal compared to NaP1 powder increased by 3% while lead and copper had reduced by 3% and 45% respectively. This occurrence was also reported by Sánchez-Hernández et al. (2018), when cadmium and mercury amounts were observed to have increased in proportion to the Al-waste zeolite NaP1 in a multi-element system. This could be attributed to the new porous structure created through pelleting as stated earlier. Whereas, a new mesoporous structure was developed through pelleting, increasing the channels for zinc, some previously existing micropores would have been closed due to compression of the pellet and reducing copper/lead uptake (causing low pore volume). This phenomenon is supported with the aid of nitrogen adsorption experiment performed in section 8.2.1.

Even though zinc uptake capacity was improved with NaP1 pellets, the total uptake capacity of metals with NaP1 pellets was still lower than that of NaP1 powder with multi-element removal as expected. This again is due to the closure of already existing micropores (low pore volume generated) after pelleting due to compaction. It is observed from Table 8.11, that the same sorption capacity values obtained for multi-element removal using 3A pellets was the least for all elements.

In conclusion, copper uptake was the most affected component as it was influenced by the absence of already existing micropores within the zeolite powder due to pelleting whereas zinc uptake was slightly improved through pellets. Lead uptake was only affected in its uptake when low concentration (He et al., 2015) was used during its uptake with NaP1 pellet. He et al. (2015) suggested competitive adsorption to be stronger at lower concentrations in multi-element systems. Compared to NaP1 pellet, zeolite 3A pellet performed very poorly with metal uptake in a multi-element system as observed from Table 8.11.

Table 8.12: Multi-element results from literature using 2nd Order uptake capacity.

Adsorbent	Metals	Surface area (m^2/g)	Conc (mg/l)	2nd order (single) (mg/g)	2nd order (Multi) (mg/g)	pH	Temp	S/L ratio (g/l)	Si/Al ratio	Time	Ref
Fly-ash X	Ni Cd Cu Pb	67	500 500 500 1000	-	65.73 121.4 106.1 254.9	6.8	25	2	2	24 h	Jha et al., 2008 Jha et al., 2009
Fly-ash zeolite	Pb Zn Cd	37.97	1350 350 700	-	2500 18.87 30.21	6.6	25	5	2.4	1.5 h	Visa et al., 2012
Bentonite	Cu Zn Ni		127 130.8 117.4	-	33.33 6.060 1.338	5	20	3	4.8	24 h	Hamdache et al., 2019
Fly-ash 4A	Co Cr Cu Ni Zn	54.82	100	-	5.50 56.47 72.73 4.95 20.10	4	25	5	1.32	4 h	Hui et al., 2005

Table 8.12: ……*continued.*

Adsorbent	Metals	Surface area (m^2/g)	Conc (mg/l)	2nd order (single) (mg/g)	2nd order (Multi) (mg/g)	pH	Temp	S/L ratio (g/l)	Si/Al ratio	Time	Ref
Fly-ash Linde F	Ni Cd Cu Pb	-	100	-	8.757 21.59 18.31 46.51	6	25	2	-	8 h	Cheng et al., 2018
NaCl modified Clinoptilolite	Zn Cd Cu Pb	-	400	-	28.98 38.80 29.96 177.6	5	25	10	5.36	4 h	Li et al., 2019
Fly-ash NaP1 Powder	Zn Pb Cu	60.1	245 92 140	6.84 17.7 7.20	8.02 19.1 22.1	5	25	5	1.51	3 h	This Study
Fly-ash NaP1 Pellet				- 14.7 -	8.27 18.6 12.2						
Commercial 3A Pellet				- 20.1 -	1.51* 12.4 5.64						

Compared to multi-element adsorption with other adsorbents from literature in Table 8.12, lead uptake showed superiority above all other metals in a multi-element system regardless of the adsorbent and concentration used. This was followed by copper and zinc in order of the magnitude with uptake demonstrated by the pseudo-second order kinetic model (Pb > Cu > Zn). Other similarities observed from literature (Table 8.12) were the pH range between 4 and 6, temperature of 25 degrees, solid/liquid ratio of 2 – 5 g/l and contact time between 1.5 – 24 h for fly-ash zeolites.

The metal uptake values for all metals obtained from this study were the lowest compared to others from literature. This could be resulting from the combined effect of the low concentration used, pore size and pore dimensions in comparison to others. NaP1 does not only have the lowest pore diameter of 0.29 nm but has an inconsistent pore dimension (0.31 nm x 0.45 nm) and (0.28 nm x 0.48 nm) compared to its counterparts. Having a silicon/aluminium ratio of 1.51, which is the second lowest amongst its counterpart, it boasts the second fastest uptake time of 3 hours. Fly-ash derived NaP1 has overall demonstrated the ability to be effective in single and multi-element systems and will be a viable preference for industrial wastewater and water treatment.

8.4.4 Chapter summary

Pelleting did not have a negative impact on the cation exchange capacity as the difference between NaP1 powder and pellet was (3%). i.e. NaP1 powder possessed 68.8 mg/g and NaP1 pellet demonstrated 66.7 mg/g. However, zeolite 3A demonstrated the largest cation exchange capacity of 101 mg/g. In contrast, pelleting had reduced leachates produced from NaP1 pellets by 40% the original quantity produced from NaP1 powder.

With regards single-element (lead) removal, NaP1 powder showed the fastest kinetic time for lead removal followed by zeolite 3A and lastly pellet zeolite. All adsorbents (NaP1 powder/pellet and zeolite 3A) could be described by the pseudo-second order and Elovich models. Thus, indicating the adsorbents have a heterogeneous surface and follow the double-site occupancy principle. Both intraparticle diffusion and diffusion models could only be used to describe kinetics of NaP1 pellet and zeolite 3A pellet but not NaP1 powder.

Nitrogen adsorption isotherm identified NaP1 powder and pellet with a type II isotherm (adsorption), indicative of an unrestricted monolayer – multilayer adsorption with an H3 hysteresis loop (desorption) representing a non-rigid aggregate of plate-like particles forming slit-shaped pores. Pore size

distribution of NaP1 powder and pellet were within a broad spectrum from the micro – macro pore range (2 nm > pore diameter > 50 nm). The total surface area of NaP1 powder (60 m^2/g) was noticed to be 28% lower in NaP1 pellet (43 m^2/g).

Results from multi-element adsorption showed lead to be the most adsorbed element from solution compared to its counterparts achieving a 100% removal within the first 15 min. This was followed by 73% copper removal and 16% zinc removal over the 3 h period (180 min). Multi-element removal efficiency was identified in the order NaP1 powder > NaP1 pellet > 3A pellet. Metal affinity towards NaP1 powder/pellet and zeolite 3A pellet was in the order Pb > Cu > Zn while varying metal affinity at different times is evidence of competition between elements in a multi-element adsorption system.

9 Conclusions and future work

9.1 Advancement of results to this field

This research has demonstrated the potential of using fly-ash derived NaP1 as a suitable adsorbent for heavy metal removal from wastewater. NaP1 achieved > 80% of its adsorption within the first 15 mins in comparison to other zeolites from literature using a minimum of 2 hours contact time. This would be a profitable adsorbent in industry as the minimum contact time utilized in industry is 1 hour.

Secondly, the working pH 5 of NaP1 implies that limited acid dosing would be required for pH adjustment during operations and this is a cost-effective feature. In selective adsorption of multi-elements, this study demonstrated pH 3.5 as suitable for zinc adsorption, pH 6.1 for lead adsorption and pH 5.2 for copper adsorption, whiles, pH 4.2 for equal removal of metals. This knowledge will be vital in industrial systems, where, pH adjustment will help in selective adsorption of metals from multi-element effluents.

A major concern of leachates during the use of fly-ash derived zeolites has been dismissed through this research. Some researchers have proposed washing off leachates before using them for adsorption, but this is not sustainable, as leachates in

the wash-water would also require treatment. Hence, it is great news to identify that this problem is curbed with the advent of pelleting powdered zeolites. Zeolite NaP1 pellet was created without the presence of a binder as a result of the pozzolanic nature of NaP1 powder. This presents a huge advantage over other adsorbents, since pellets are traditionally created with the addition of clay binders. As mentioned earlier in this research, clay binders either change the adsorbent surface attraction or clog micropores of their adsorbents. Although, pelleting had slowed down the kinetics of NaP1 pellets compared to NaP1 powder and reduced metal uptake by 20%. Furthermore, pelleting was noticed to have created mesopores, which could be utilized for separation of molecules, gases and liquids but would require the use of pressure to access those pores.

Finally, fly-ash derived zeolite NaP1 will be a sustainable replacement for current adsorbents, since it can be regenerated with cheap eluents like NaCl and KCl. These have managed to produce 30 % regeneration of copper in 3 hours and can achieve 100 % with successive regeneration at pH 5.

9.2 Limitations of this research

- The inability of producing more fly-ash derived NaP1 with the same purity from different batches is a limitation to this research. This limited the amount of NaP1 for the entire project and the number of repeats for experiments. This can be improved by the design and construction of a continuous process for producing NaP1 from coal fly-ash.
- Although, there was no notable influence of performing adsorption experiments at variable room temperatures, this could be improved by standardizing experimental temperatures with a cold/warm water bath.
- Another limitation was the labour-intensive way of creating pellets with the hydraulic press and this can be improved with a mechanized system or different means of pelleting.
- Time was the greatest limitation to this project as I could not test the performance of pellets in a continuous flow system with real-world industrial effluents.

9.3 Future work

Further work in the following areas is recommended to establish the benefits of NaP1 as the future of low-cost adsorbents:

- Experiments using pellets should be conducted in a continuous flow system, which is more relevant to industrials processes.
- Continuous tests using pellets should be conducted using real wastewater samples from relevant industries in order to determine the performance of the pellets and scale-up.
- Regeneration of pellet using multi-elements using KCl/NaCl solutions should be explored further. The influence of temperature and concentration of regeneration solutions on the efficiency should be investigated.

9.4 Conclusion

Fly-ash derived zeolites could be the possible solution to replacing expensive adsorbents for water and waste-water treatment in industry. It is also another solution to utilizing coal fly-ash; waste from the coal power plants being dumped into landfills causing pollution of soil and water bodies.

- NaP1 displayed fast kinetics with all metals, removing > 80% of the total capacity in 15 minutes.
- All the metals could be described by the Langmuir isotherm and fitted well to the pseudo-second order kinetic models.
- pH 5 was the best working condition for NaP1
- NaP1 demonstrated multi-layer adsorption with heterogenous surfaces.
- NaP1 powder can be converted into binder-less pellets of dimensions 10 mm diameter and 0.10 mm height.
- Pore size distribution of both powdered (2 nm – 115 nm) and NaP1 pellet (2 nm - 125 nm) are seen to be within a broad spectrum from the micro – macro pore range (2 nm > pore diameter > 50 nm).
- NaP1 pellet has the advantage of a higher pore diameter than NaP1 powder but disadvantaged with a low pore volume for adsorbates than that of NaP1 powder.
- The mean pore diameter obtained from the distribution for NaP1 pellet was 14.3 ± 0.275 nm compared to 10.95 ± 0.069 nm for NaP1 powder.
- The total surface area of NaP1 powder (60 m^2/g) is noticed to be 28% lower in NaP1 pellet (43 m^2/g). Pelleting had resulted in the reduction of adsorbent surface area.

- The monolayer adsorptive capacity for NaP1 powder (13.82 cm^3/g) was also more than the NaP1 pellet (9.98 cm^3/g).
- Pelleting process may have increased the porosity of NaP1 pellet by creating larger pores over 115 nm compared to its powdered counterpart.
- NaP1 powder has the advantage of higher pore volume than NaP1 pellet but smaller size pore diameters than NaP1 pellet. However, both NaP1 powder and pellet could be used for selective elemental uptake based on their pore diameter.
- The pelleting process had reduced leachates produced from NaP1 pellets by 40% the original quantity produced from NaP1 powder.
- Metal affinity towards NaP1 powder/pellet and zeolite 3A pellet was in the order Pb > Cu > Zn
- Multi-element removal efficiency was identified in the order NaP1 powder > NaP1 pellet > 3A pellet.
- Uptake of metals in moles was understudied to present a different perspective of metal removal and to indicate number of metals removed instead of their total mass.
- Multi-element removal efficiency in moles of elements removed within 3 h is in the order Cu > Zn > Pb for both NaP1 powder and pellet and Cu > Pb > Zn for zeolite 3A.

- NaP1 has fast kinetics (15 min) and a short equilibrium time (1 h) while having a good regeneration capability (30% recovery in 1h) with common salts (NaCl and KCl).
- Overall, NaP1 has outperformed commercial 3A zeolite in the multi-element system by 54% removal efficiency with selective ability and would be suitable replacement in industry.

10 References

ABAS, S. N. A., ISMAIL, M. H. S., KAMAL, M. L. & IZHAR, S. 2013. Adsorption Process of Heavy Metals by Low-Cost Adsorbent: A Review. *World Applied Sciences Journal* 28**,** 1518-1530.

ABDEL SALAM, O. E., REIAD, N. A. & ELSHAFEI, M. M. 2011. A study of the removal characteristics of heavy metals from wastewater by low-cost adsorbents. *Journal of Advanced Research,* 2**,** 297-303.

ADHOUM, N., MONSER, L., BELLAKHAL, N. & BELGAIED, J.-E. 2004. Treatment of electroplating wastewater containing Cu2+, Zn2+ and Cr(VI) by electrocoagulation. *Journal of Hazardous Materials,* 112**,** 207-213.

AEISYAH, A., ISMAIL, M. H. S., LIAS, K. & IZHAR, S. 2014. Adsorption process of heavy metals by low-cost adsorbent: A review. *Research Journal of Chemistry and Environment,* 18**,** 91-102.

AGARWAL, S. K. 2009. *Heavy Metal Pollution*, APH Publishing Corporation.

AHMARUZZAMAN, M. 2009. Role of Fly Ash in the Removal of Organic Pollutants from Wastewater. *Energy & Fuels,* 23**,** 1494-1511.

AHMARUZZAMAN, M. 2010. A review on the utilization of fly ash. *Progress in Energy and Combustion Science,* 36**,** 327-363.

AHUJA, S. 2018. *Advances in Water Purification Techniques: Meeting the Needs of Developed and Developing Countries*, Elsevier Science.

AINSCOUGH, A. N., DOLLIMORE, D. & SPOONER, P. 1982. Analysis of nitrogen adsorption isotherms obtained on activated fibre carbons. *In:* ROUQUEROL, J. & SING, K. S. W. (eds.) *Studies in Surface Science and Catalysis.* Elsevier.

AKHTAR, F., ANDERSSON, L., OGUNWUMI, S., HEDIN, N. & BERGSTRÖM, L. 2014. Structuring adsorbents and catalysts by processing of porous powders. *Journal of the European Ceramic Society,* 34**,** 1643-1666.

AKSU, Z. & İŞOĞLU, İ. A. 2005. Removal of copper(II) ions from aqueous solution by biosorption onto agricultural waste sugar beet pulp. *Process Biochemistry,* 40**,** 3031-3044.

ALDAHRI, T., BEHIN, J., KAZEMIAN, H. & ROHANI, S. 2016. Synthesis of zeolite Na-P from coal fly ash by thermo-sonochemical treatment. *Fuel,* 182**,** 494-501.

ALI, I. 2010. The Quest for Active Carbon Adsorbent Substitutes: Inexpensive Adsorbents for Toxic Metal Ions Removal from Wastewater. *Separation & Purification Reviews,* 39**,** 95-171.

ALI, I., ASIM, M. & KHAN, T. A. 2012. Low cost adsorbents for the removal of organic pollutants from wastewater. *Journal of Environmental Management,* 113**,** 170-183.

ALLEN, S. J. & BROWN, P. A. 1995. Isotherm analyses for single component and multi-component metal sorption onto lignite. *Journal of Chemical Technology & Biotechnology,* 62**,** 17-24.

ALVAREZ-AYUSO, E., GARCÍA-SÁNCHEZ, A. & QUEROL, X. 2003. Purification of metal electroplating waste waters using zeolites. *Water Res,* 37**,** 4855-62.

AMARASINGHE, B. M. W. P. K. & WILLIAMS, R. A. 2007. Tea waste as a low cost adsorbent for the removal of Cu and Pb from wastewater. *Chemical Engineering Journal,* 132**,** 299-309.

AMYOTTE, P. & KHAN, F. 2020. *Methods in Chemical Process Safety*, Elsevier Science & Technology.

ANYANWU, B. O., EZEJIOFOR, A. N., IGWEZE, Z. N. & ORISAKWE, O. E. 2018. Heavy Metal Mixture Exposure and Effects in Developing Nations: An Update. *Toxics,* 6**,** 65.

APIRATIKUL, R. & PAVASANT, P. 2008. Sorption of Cu2+, Cd2+, and Pb2+ using modified zeolite from coal fly ash. *Chemical Engineering Journal,* 144**,** 245-258.

APPENROTH, K.-J. 2010. What are "heavy metals" in Plant Sciences? *Acta Physiologiae Plantarum,* 32**,** 615-619.

ARMBRUSTER, D. A. & PRY, T. 2008. Limit of blank, limit of detection and limit of quantitation. *The Clinical biochemist. Reviews,* 29 Suppl 1**,** S49-S52.

ARSHADI, M., AMIRI, M. J. & MOUSAVI, S. 2014. Kinetic, equilibrium and thermodynamic investigations of Ni(II), Cd(II), Cu(II) and Co(II) adsorption on barley straw ash. *Water Resources and Industry,* 6**,** 1-17.

ASSOCIATION, A. W. W. & EDZWALD, J. K. 2010. *Water Quality & Treatment: A Handbook on Drinking Water*, McGraw-Hill Education.

ATWOOD, D. A. 2016. *Sustainable Inorganic Chemistry*, Wiley.

AWASTHI, A. K., ZENG, X. & LI, J. 2016. Environmental pollution of electronic waste recycling in India: A critical review. *Environmental Pollution,* 211**,** 259-270.

AZIZ, H. A., ADLAN, M. N. & ARIFFIN, K. S. 2008. Heavy metals (Cd, Pb, Zn, Ni, Cu and Cr(III)) removal from water in Malaysia: Post treatment by high quality limestone. *Bioresource Technology,* 99**,** 1578-1583.

BABEL, S. & KURNIAWAN, T. A. 2003. Low-cost adsorbents for heavy metals uptake from contaminated water: a review. *Journal of Hazardous Materials,* 97**,** 219-243.

BANKOLE, M. T., ABDULKAREEM, A. S., MOHAMMED, I. A., OCHIGBO, S. S., TIJANI, J. O., ABUBAKRE, O. K. & ROOS, W. D. 2019. Selected Heavy Metals Removal From Electroplating Wastewater by Purified and Polyhydroxylbutyrate Functionalized Carbon Nanotubes Adsorbents. *Scientific Reports,* 9**,** 4475.

BARAKAT, M. A. 2011. New trends in removing heavy metals from industrial wastewater. *Arabian Journal of Chemistry,* 4**,** 361-377.

BARDESTANI, R., PATIENCE, G. S. & KALIAGUINE, S. 2019. Experimental methods in chemical engineering: specific surface area and pore size distribution measurements—BET, BJH, and DFT. *The Canadian Journal of Chemical Engineering,* 97**,** 2781-2791.

BARRETT, E. P., JOYNER, L. G. & HALENDA, P. P. 1951. The Determination of Pore Volume and Area Distributions in Porous Substances. I. Computations from Nitrogen Isotherms. *Journal of the American Chemical Society,* 73**,** 373-380.

BARTRAM, J. 2009. *Calcium and Magnesium in Drinking-water: Public Health Significance*.

BAZRAFSHAN, E., MOHAMMADI, L., ANSARI-MOGHADDAM, A. & MAHVI, A. H. 2015. Heavy metals removal from aqueous environments by electrocoagulation process- a systematic review. *Journal of environmental health science & engineering,* 13**,** 74-74.

BERGMAN, R. 2007. *Reverse Osmosis and Nanofiltration*, American Water Works Association.

BERNARD, A. 2008. Cadmium & its adverse effects on human health. *India Journal of Medical Research,* 128**,** 557-564.

BERNARD, E., JIMOH, A. & ODIGURE, J. 2013. Heavy metals removal from industrial wastewater by activated carbon prepared from coconut shell. 3**,** 3-9.

BHARDWAJ, S., SHARMA, R. & AGGARWAL, R. 2019. Impact Appraisal of Industrialization on Heavy Metal Contamination of Sirsa River Located

in the Shivalik Foothills of North Western Himalayas. *Current World Environment,* 14**,** 245-259.
BHATERIA, R. & SINGH, R. 2019. A review on nanotechnological application of magnetic iron oxides for heavy metal removal. *Journal of Water Process Engineering,* 31**,** 100845.
BHATNAGAR, A. 2012. *Application of Adsorbents for Water Pollution Control*, Bentham Science Publishers.
BHATNAGAR, A. & MINOCHA, A. 2006. Conventional and non-conventional adsorbents for removal of pollutants from water – A review. *Indian Journal of Chemical Technology,* 13.
BHATNAGAR, A. & SILLANPÄÄ, M. 2010. Utilization of agro-industrial and municipal waste materials as potential adsorbents for water treatment—A review. *Chemical Engineering Journal,* 157**,** 277-296.
BHUSHAN, B. 2013. *Introduction to Tribology*, Wiley.
BINGRE, R., LOUIS, B. & NGUYEN, P. 2018. An Overview on Zeolite Shaping Technology and Solutions to Overcome Diffusion Limitations. *Catalysts,* 8.
BISEN, P. S. & SHARMA, A. 2012. *Introduction to Instrumentation in Life Sciences*, Taylor & Francis.
BISHT, R., AGARWAL, M. & SINGH, K. 2017. Methodologies for removal of heavy metal ions from wastewater: an overview. *interdisciplinary enviornmental review,* 18**,** 124-142.
BLANCHARD, G., MAUNAYE, M. & MARTIN, G. 1984. Removal of heavy metals from waters by means of natural zeolites. *Water Research,* 18**,** 1501-1507.
BOECHAT, C. L., PISTÓIA, V. C., LUDTKE, A. C., GIANELLO, C. & CAMARGO, F. A. D. O. 2016. Solubility of Heavy Metals/Metalloid on Multi-Metal Contaminated Soil Samples from a Gold Ore Processing Area: Effects of Humic Substances. *Revista Brasileira de Ciência do Solo,* 40.
BOUHAMED, F., ELOUAER, Z., BOUZID, J. & OUDDANE, B. 2015. Multi-component adsorption of copper, nickel and zinc from aqueous solutions onto activated carbon prepared from date stones. *Environmental science and pollution research international,* 23.
BRADL, H. 2005. *Heavy Metals in the Environment: Origin, Interaction and Remediation*, Elsevier Science.
BRÄNNVALL, E. & KUMPIENE, J. 2016. Fly ash in landfill top covers – a review. *Environmental Science: Processes & Impacts,* 18**,** 11-21.
BRECK, D. W. 1973. *Zeolite Molecular Sieves: Structure, Chemistry*, Wiley.
BRECK, D. W. 1984. *Zeolite molecular sieves: structure, chemistry, and use*, R.E. Krieger.
BRUNAUER, S., DEMING, L. S., DEMING, W. E. & TELLER, E. 1940. On a Theory of the van der Waals Adsorption of Gases. *Journal of the American Chemical Society,* 62**,** 1723-1732.
BUISSON, R. S. K., KIRK, P. W. W. & LESTER, J. N. 1984. Determination of Chlorinated Phenols in Water, Wastewater, and Wastewater Sludge by Capillary GC/ECD. *Journal of Chromatographic Science,* 22**,** 339-342.
BUISSON, R. S. K., KIRK, P. W. W. & LESTERA, J. N. 1988. The behavior of selected chlorinated organic micropollutants in the activated sludge process: A pilot plant study. *Water, Air, and Soil Pollution,* 37**,** 419-432.
CAMPBELL, L. S., CHIMEDTSOGZOL, A. & DYER, A. 2018. Species sensitivity of zeolite minerals for uptake of mercury solutes. *Mineralogical Magazine,* 70**,** 361-371.
CANADA, H. 2008. Guidance on Potassium from Water Softeners. Canada: Ministry of Health Canada.

CARDOSO, A. M., HORN, M. B., FERRET, L. S., AZEVEDO, C. M. N. & PIRES, M. 2015. Integrated synthesis of zeolites 4A and Na–P1 using coal fly ash for application in the formulation of detergents and swine wastewater treatment. *Journal of Hazardous Materials,* 287**,** 69-77.

CARPENTER, K. E. 1925. ON THE BIOLOGICAL FACTORS INVOLVED IN THE DESTRUCTION OF RIVER-FISHERIES BY POLLUTION DUE TO LEAD-MINING. *Annals of Applied Biology,* 12**,** 1-13.

CEJKA, J., VAN BEKKUM, H., CORMA, A. & SCHUETH, F. 2007. *Introduction to Zeolite Molecular Sieves*, Elsevier Science.

CHANSIRIWAT, W., TANANGTEERAPONG, D. & WANTALA, K. 2016. Synthesis of zeolite from coal fly ash by hydrothermal method without adding alumina and silica sources: Effect of aging temperature and time. 45**,** 1723-1731.

CHAUDHURI, M. & SAMINAL, S. 2011. *Coconut coir activated carbon: An adsorbent for removal of lead from aqueous solution*.

CHEN, Q., TIAN, Y., LI, P., YAN, C., PANG, Y., ZHENG, L., DENG, H., ZHOU, W. & MENG, X. 2017. Study on Shale Adsorption Equation Based on Monolayer Adsorption, Multilayer Adsorption, and Capillary Condensation. *Journal of Chemistry,* 2017**,** 1496463.

CHEN, Y., ARMUTLULU, A., SUN, W., JIANG, W., JIANG, X., LAI, B. & XIE, R. 2020. Ultrafast removal of Cu(II) by a novel hierarchically structured faujasite-type zeolite fabricated from lithium silica fume. *Science of The Total Environment,* 714**,** 136724.

CHENG, T., CHEN, C., TANG, R., HAN, C. H. & TIAN, Y. 2018. Competitive adsorption of Cu, Ni, Pb, and Cd from aqueous solution onto fly ash-based linde F(K) Zeolite. *Iranian Journal of Chemistry and Chemical Engineering,* 37**,** 61-72.

CHEREMISINOFF, N. P. 2017. *Groundwater Remediation: A Practical Guide for Environmental Engineers and Scientists*, Wiley.

CHEREMISINOFF, N. P. & KNOVEL 2002. *Handbook of Water and Wastewater Treatment Technologies*, Elsevier Science.

CHIBUIKE, G. U. & OBIORA, S. C. 2014. Heavy Metal Polluted Soils: Effect on Plants and Bioremediation Methods. *Applied and Environmental Soil Science,* 2014**,** 752708.

CHIEN, S. H. & CLAYTON, W. R. 1980. Application of Elovich Equation to the Kinetics of Phosphate Release and Sorption in Soils. *Soil Science Society of America Journal,* 44**,** 265-268.

CHUNG, H.-K., KIM, W.-H., PARK, J., CHO, J., JEONG, T.-Y. & PARK, P.-K. 2015. Application of Langmuir and Freundlich isotherms to predict adsorbate removal efficiency or required amount of adsorbent. *Journal of Industrial and Engineering Chemistry,* 28**,** 241-246.

CHUTIA, P., KATO, S., KOJIMA, T. & SATOKAWA, S. 2009. Arsenic adsorption from aqueous solution on synthetic zeolites. *Journal of Hazardous Materials,* 162**,** 440-447.

CLONEY, C. & SNOEYS, J. 2019. Chapter Three - Dust explosions: A serious concern. *In:* AMYOTTE, P. R. & KHAN, F. I. (eds.) *Methods in Chemical Process Safety.* Elsevier.

COHEN, J. M., KAMPHAKE, L. J., HARRIS, E. K. & WOODWARD, R. L. 1960. Taste Threshold Concentrations of Metals in Drinking Water. *Journal - AWWA,* 52**,** 660-670.

COMNINELLIS, C. 1994. Electrocatalysis in the electrochemical conversion/combustion of organic pollutants for waste water treatment. *Electrochimica Acta,* 39**,** 1857-1862.

CRINI, G. & LICHTFOUSE, E. 2019. Advantages and disadvantages of techniques used for wastewater treatment. *Environmental Chemistry Letters,* 17**,** 145-155.

CRITTENDEN, J. C., TRUSSELL, R. R., HAND, D. W., HOWE, K. J. & TCHOBANOGLOUS, G. 2012. *MWH's Water Treatment: Principles and Design*, Wiley.

CRUCIANI, G. 2006. Zeolites upon heating: Factors governing their thermal stability and structural changes. *Journal of Physics and Chemistry of Solids,* 67**,** 1973-1994.

CUI, H., LI, L. & GRACE, J. 2006. Exploration of remediation of acid rock drainage with clinoptilolite as sorbent in a slurry bubble column for both heavy metal capture and regeneration. *Water research,* 40**,** 3359-66.

CUNHA, L. S. T., SOUZA, J. S., KASPER, D., CAVALCANTE, R. M. & TORRES, J. P. M. 2018. VI International Workshop on Pollutants in the Environment. *Orbital: The Electronic Journal of Chemistry,* 10**,** i+.

CUPPETT, J. D., DUNCAN, S. E. & DIETRICH, A. M. 2006. Evaluation of copper speciation and water quality factors that affect aqueous copper tasting response. *Chem Senses,* 31**,** 689-97.

CUSHNIE, G. C. 1985. *Electroplating Wastewater Pollution Control Technology*, Noyes Publications.

CZIKKELY, M., NEUBAUER, É., FEKETE, I., YMERI, P. & FOGARASSY, C. 2018. Review of Heavy Metal Adsorption Processes by Several Organic Matters from Wastewaters. *Water,* 10.

DA'NA, E. & SAYARI, A. 2012. Adsorption of heavy metals on amine-functionalized SBA-15 prepared by co-condensation: Applications to real water samples. *Desalination,* 285**,** 62-67.

DA SILVA, F. A. & RODRIGUES, A. E. 1999. Adsorption Equilibria and Kinetics for Propylene and Propane over 13X and 4A Zeolite Pellets. *Industrial & Engineering Chemistry Research,* 38**,** 2051-2057.

DĄBROWSKI, A., HUBICKI, Z., PODKOŚCIELNY, P. & ROBENS, E. 2004. Selective Removal of the Heavy Metal Ions from Waters and Wastewaters by Ion-exchange Method. *Chemosphere,* 56**,** 91-106.

DAHMAN, Y. 2017. Chapter 6 - Nanopolymers**By Yaser Dahman, Kevin Deonanan, Timothy Dontsos, and Andrew Iammatteo. *In:* DAHMAN, Y. (ed.) *Nanotechnology and Functional Materials for Engineers.* Elsevier.

DAL BOSCO, S. M., JIMENEZ, R. S. & CARVALHO, W. A. 2005. Removal of toxic metals from wastewater by Brazilian natural scolecite. *Journal of Colloid and Interface Science,* 281**,** 424-431.

DAS, K. K., DAS, S. N. & DHUNDASI, S. A. 2008. Nickel, its adverse health effects & oxidative stress. *Indian J Med Res,* 128**,** 412-25.

DAS, N. 2010. Recovery of precious metals through biosorption — A review. *Hydrometallurgy,* 103**,** 180-189.

DAVIES, N. T. & NIGHTINGALE, R. 1975. The effects of phytate on intestinal absorption and secretion of zinc, and whole-body retention of Zn, copper, iron and manganese in rats. *Br J Nutr,* 34**,** 243-58.

DAVIS, T. A., VOLESKY, B. & MUCCI, A. 2003. A review of the biochemistry of heavy metal biosorption by brown algae. *Water Research,* 37**,** 4311-4330.

DE GISI, S., LOFRANO, G., GRASSI, M. & NOTARNICOLA, M. 2016. Characteristics and adsorption capacities of low-cost sorbents for wastewater treatment: A review. *Sustainable Materials and Technologies,* 9**,** 10-40.

DE OLIVEIRA DA MOTA, I., DE CASTRO, J. A., DE GÓES CASQUEIRA, R. & DE OLIVEIRA JUNIOR, A. G. 2015. Study of electroflotation method for treatment of wastewater from washing soil contaminated by heavy metals. *Journal of Materials Research and Technology,* 4**,** 109-113.

DEAN, J. G., BOSQUI, F. L. & LANOUETTE, K. H. 1972. Removing heavy metals from waste water. *Environmental Science & Technology,* 6**,** 518-522.

DEHARIYA, N. K. & LAL, N. 2018. Removal of Zinc from waste water by using Low Cost Adsorbent: A

comprehensive Review. *International Research Journal of Engineering and Technology,* 5**,** 1021-1032.

DENG, H. & GE, Y. 2015. Formation of NaP zeolite from fused fly ash for the removal of Cu(ii) by an improved hydrothermal method. *RSC Advances,* 5**,** 9180-9188.

DENKHAUS, E. & SALNIKOW, K. 2002. Nickel essentiality, toxicity, and carcinogenicity. *Crit Rev Oncol Hematol,* 42**,** 35-56.

DESTA, M. B. 2013. Batch Sorption Experiments: Langmuir and Freundlich Isotherm Studies for the Adsorption of Textile Metal Ions onto Teff Straw (Eragrostis tef) Agricultural Waste. *Journal of Thermodynamics,* 2013**,** 375830.

DIXIT, A., DIXIT, S. & CS, G. 2015. Eco-friendly Alternatives for the Removal of Heavy Metal Using Dry Biomass of Weeds and Study the Mechanism Involved. *Journal of Bioremediation & Biodegradation,* 6.

DO, D. D. 1998. *Adsorption Analysis: Equilibria and Kinetics*, PUBLISHED BY IMPERIAL COLLEGE PRESS AND DISTRIBUTED BY WORLD SCIENTIFIC PUBLISHING CO.

DUBEY, A., GOYAL, D. & MISHRA, A. 2013. Zeolites in wastewater treatment. *RSC Green Chemistry***,** 82-104.

DUFFUS, J. H. 2002. "Heavy metals" a meaningless term? (IUPAC Technical Report). 74**,** 793.

DUTTA, S. & SHARMA, R. K. 2019. Chapter 15 - Sustainable Magnetically Retrievable Nanoadsorbents for Selective Removal of Heavy Metal Ions From Different Charged Wastewaters. *In:* AHUJA, S. (ed.) *Separation Science and Technology.* Academic Press.

DYER, A., HRILJAC, J., EVANS, N., STOKES, I., RAND, P., KELLET, S., HARJULA, R., MOLLER, T., MAHER, Z., HEATLIE-BRANSON, R., AUSTIN, J., WILLIAMSON-OWENS, S., HIGGINS-BOS, M., SMITH, K., O'BRIEN, L., SMITH, N. & BRYAN, N. 2018. The use of columns of the zeolite clinoptilolite in the remediation of aqueous nuclear waste streams. *Journal of Radioanalytical and Nuclear Chemistry,* 318**,** 2473-2491.

EKENGREN, Ö. 2002. *Environmentally Acceptable Metalworking Processes*, Nordic Council of Ministers.

EMAMJOMEH, M. M. & SIVAKUMAR, M. 2009. Review of pollutants removed by electrocoagulation and electrocoagulation/flotation processes. *J Environ Manage,* 90**,** 1663-79.

ERDEM, E., KARAPINAR, N. & DONAT, R. 2004. The removal of heavy metal cations by natural zeolites. *Journal of Colloid and Interface Science,* 280**,** 309-314.

ERWE, T., MAVROV, V. & CHMIEL, H. 2003. Characterization of a synthetic zeolite P as a heavy metal bonding agent. *Chemical Papers,* 57**,** 45-49.

ESCUDERO, G., ESPINOZA ESTRADA, E. & RAO, F. 2017. Chemical Precipitation of Nickel Species from Waste Water. *International Research Journal of Pure and Applied Chemistry,* 15**,** 1-7.

ESMAEILI, H. & FOROUTAN, R. 2015. INVESTIGATION INTO ION EXCHANGE AND ADSORPTION METHODS FOR REMOVING HEAVY METALS FROM AQUEOUS SOLUTIONS. *International Journal of Biology, Pharmacy and Allied Sciences,* 4**,** 620-629.

EZZEDDINE, Z., BATONNEAU-GENER, I., POUILLOUX, Y., HAMAD, H. & SAAD, Z. 2018. Synthetic Nax Zeolite as a Very Efficient Heavy Metals

Sorbent in Batch and Dynamic Conditions. *Colloids and Interfaces,* 2**,** 22.

FALLAH, A., MOHAMMAD-HASANI, A. & COLAGAR, A. 2018. Zinc is an Essential Element for Male Fertility: A Review of Zn Roles in Men's Health, Germination, Sperm Quality, and Fertilization. *Journal of Reproduction and Infertility,* 19**,** 69-81.

FAUR-BRASQUET, C., KADIRVELU, K. & LE CLOIREC, P. 2002. Removal of metal ions from aqueous solution by adsorption onto activated carbon cloths: adsorption competition with organic matter. *Carbon,* 40**,** 2387-2392.

FAWAZ, E., SALAM, D., NOUALI, H., DÉROCHE, I., RIGOLET, S., LEBEAU, B. & DAOU, T. J. 2018. *Synthesis of Binderless ZK-4 Zeolite Microspheres at High Temperature*.

FERGUSSON, J. E. 1990. *The heavy elements: chemistry, environmental impact, and health effects*, Pergamon Press.

FERNANDES, A., PACHECO, M. J., CIRÍACO, L. & LOPES, A. 2015. Review on the electrochemical processes for the treatment of sanitary landfill leachates: Present and future. *Applied Catalysis B: Environmental,* 176-177**,** 183-200.

FERRARINI, S. F., CARDOSO, A. M., PAPROCKI, A. & PIRES, M. 2016. Integrated Synthesis of Zeolites Using Coal Fly Ash: Element Distribution in the Products, Washing Waters and Effluent. *Journal of the Brazilian Chemical Society,* 27**,** 2034-2045.

FLORA, G., GUPTA, D. & TIWARI, A. 2012. Toxicity of lead: A review with recent updates. *Interdisciplinary toxicology,* 5**,** 47-58.

FOOD, NATIONS, A. O. F. T. U., FOOD & NATIONS, A. O. O. T. U. 1998. *World Reference Base for Soil Resources*, Food and Agriculture Organization of the United Nations.

FRANUS, W., WDOWIN, M. & FRANUS, M. 2014. Synthesis and characterization of zeolites prepared from industrial fly ash. *Environmental Monitoring and Assessment,* 186**,** 5721-5729.

FRIBERG, L., NORDBERG, G. & VOUK, V. B. 1986. *Handbook on the Toxicology of Metals: General aspects*, Elsevier.

FU, F. & WANG, Q. 2011. Removal of heavy metal ions from wastewaters: A review. *Journal of Environmental Management,* 92**,** 407-418.

FURNESS, R. W. 2018. *Heavy Metals in the Marine Environment*, CRC Press.

GALAL-GORCHEV, H. 1991. Dietary intake of pesticide residues: cadmium, mercury, and lead. *Food Addit Contam,* 8**,** 793-806.

GAO, Z., BANDOSZ, T. J., ZHAO, Z., HAN, M. & QIU, J. 2009. Investigation of factors affecting adsorption of transition metals on oxidized carbon nanotubes. *Journal of Hazardous Materials,* 167**,** 357-365.

GARDNER, M., COMBER, S., SCRIMSHAW, M. D., CARTMELL, E., LESTER, J. & ELLOR, B. 2012. The significance of hazardous chemicals in wastewater treatment works effluents. *Science of The Total Environment,* 437**,** 363-372.

GARDNER, M., JONES, V., COMBER, S., SCRIMSHAW, M. D., COELLO-GARCIA, T., CARTMELL, E., LESTER, J. & ELLOR, B. 2013. Performance of UK wastewater treatment works with respect to trace contaminants. *Sci Total Environ,* 456-457**,** 359-69.

GASAWAY, W. C. & BUSS, I. O. 1972. Zinc Toxicity in the Mallard Duck. *The Journal of Wildlife Management,* 36**,** 1107-1117.

GEANKOPLIS, C. J. 2003. *Transport Processes and Separation Process Principles: (includes Unit Operations)*, Prentice Hall Professional Technical Reference.

GEORGIEV, D. & MARKOVSKA, I. 2020. The Removal of Cu (II) Ions from Aqueous Solutions on Synthetic Zeolite NaA.

GHOBARKAR, H., SCHÄF, O. & GUTH, U. 1999. Zeolites—from kitchen to space. *Progress in Solid State Chemistry,* 27**,** 29-73.

GHORPADE, A. & AHAMMED, M. 2017. Water treatment sludge for removal of heavy metals from electroplating wastewater. *Environmental Engineering Research,* 23.

GIARDINA, A., LARSON, S. F., WISNER, B., WHEELER, J. & CHAO, M. 2009. Long-term and acute effects of zinc contamination of a stream on fish mortality and physiology. *Environmental Toxicology and Chemistry,* 28**,** 287-295.

GILES, C. H., D'SILVA, A. P. & EASTON, I. A. 1974a. A general treatment and classification of the solute adsorption isotherm part. II. Experimental interpretation. *Journal of Colloid and Interface Science,* 47**,** 766-778.

GILES, C. H., SMITH, D. & HUITSON, A. 1974b. A general treatment and classification of the solute adsorption isotherm. I. Theoretical. *Journal of Colloid and Interface Science,* 47**,** 755-765.

GLEICHMANN, K., UNGER, B. & BRANDT, A. 2016. Industrial Zeolite Molecular Sieves.

GLEICK, P. H., GLEICK, D. G. E. P. P. H., PACIFIC INSTITUTE FOR STUDIES IN DEVELOPMENT, E., SECURITY & INSTITUTE, S. E. 1993. *Water in Crisis: A Guide to the World's Fresh Water Resources*, Oxford University Press.

GODE, F. & PEHLIVAN, E. 2005. Removal of Cr(VI) from aqueous solution by two Lewatit-anion exchange resins. *Journal of hazardous materials,* 119**,** 175-82.

GOLLAKOTA, A. R. K., VOLLI, V. & SHU, C.-M. 2019. Progressive utilisation prospects of coal fly ash: A review. *Science of The Total Environment,* 672**,** 951-989.

GOUGAZEH, M. & BUHL, J. C. 2014. Synthesis and characterization of zeolite A by hydrothermal transformation of natural Jordanian kaolin. *Journal of the Association of Arab Universities for Basic and Applied Sciences,* 15**,** 35-42.

GOVERNMENT, U. S. 2011. *Membrane Filtration Guidance Manual*, General Books.

GRÉGORIO, C. & LICHTFOUSE, E. 2018. Advantages and disadvantages of techniques used for wastewater treatment. *Environmental Chemistry Letters***,** 1-11.

GRÉGORIO, C., LICHTFOUSE, E., WILSON, L. & CRINI, N. 2018. Adsorption-Oriented Processes Using Conventional and Non-conventional Adsorbents for Wastewater Treatment.

GUNATILAKE, S. 2015. Methods of Removing Heavy Metals from Industrial Wastewater. *Journal of Multidiciplinary Engineering Science Studies,* 1.

GÜNAY, A., ARSLANKAYA, E. & TOSUN, İ. 2007. Lead removal from aqueous solution by natural and pretreated clinoptilolite: Adsorption equilibrium and kinetics. *Journal of Hazardous Materials,* 146**,** 362-371.

GUPTA, V. K. & ALI, I. 2013. *Environmental Water: Advances in Treatment, Remediation and Recycling*, Elsevier Science.

HAMDACHE, F., CHERGUI, A., HALET, F., YEDDOU, A. R. & NADJEMI, B. 2079. Copper, Zinc and Nickel's removal by bentonite clay: Case

study in mono and multicomponent systems. *Algerian Journal of Environmental Science and Technology,* 5.

HARRISON, R. M. *Pollution 5th Edition: Causes, Effects and Control*, Royal Society of Chemistry.

HASAN, M. R., KHAN, M. Z. H., KHAN, M., AKTAR, S., RAHMAN, M., HOSSAIN, F. & HASAN, A. S. M. M. 2016. Heavy metals distribution

and contamination in surface water of the Bay of Bengal coast. *Cogent Environmental Science,* 2.

HASHEMIAN, S., HOSSEINI, S., SALEHIFAR, H. & SALARI, K. 2013. Adsorption of Fe(III) from Aqueous Solution by Linde Type-A Zeolite. *American Journal of Analytical Chemistry,* 04**,** 123-126.

HE, K., CHEN, Y., TANG, Z. & HU, Y. 2015. Removal of heavy metal ions from aqueous solution by zeolite synthesized from fly ash. *Environmental science and pollution research international,* 23.

HE, Z. L., YANG, X. E. & STOFFELLA, P. J. 2005. Trace elements in agroecosystems and impacts on the environment. *J Trace Elem Med Biol,* 19**,** 125-40.

HEGAZI, H. A. 2013. Removal of heavy metals from wastewater using agricultural and industrial wastes as adsorbents. *HBRC Journal,* 9**,** 276-282.

HELFFERICH, F. 1962. Theories of Ion-Exchange Column Performance: A Critical Study. *Angewandte Chemie International Edition in English,* 1**,** 440-453.

HENDRICKS, D. 2016. *Fundamentals of Water Treatment Unit Processes: Physical, Chemical, and Biological*, CRC Press.

HENDRICKS, D. W. 2006. *Water Treatment Unit Processes: Physical and Chemical*, Taylor & Francis.

HERNANDEZ-RAMIREZ, O. & HOLMES, S. M. 2008. Novel and modified materials for wastewater treatment applications. *Journal of Materials Chemistry,* 18**,** 2751-2761.

HERNANDO, H., OCHOA-HERNÁNDEZ, C., SHAMZHY, M., MORENO, I., FERMOSO, J., PIZARRO, P., CORONADO, J. M., ČEJKA, J. & SERRANO, D. P. 2019. The crucial role of clay binders in the performance of ZSM-5 based materials for biomass catalytic pyrolysis. *Catalysis Science & Technology,* 9**,** 789-802.

HINZ, C. 2001. Description of sorption data with isotherm equations. *Geoderma,* 99**,** 225-243.

HO, Y. S. & MCKAY, G. 1999. Pseudo-second order model for sorption processes. *Process Biochemistry,* 34**,** 451-465.

HOGSTRAND, C. 2011. 3 - Zinc. *In:* WOOD, C. M., FARRELL, A. P. & BRAUNER, C. J. (eds.) *Fish Physiology.* Academic Press.

HOLLMAN, G. 1999. *Synthesis of zeolites from coal fly ash*, Faculteit Aardwetenschappen, Universiteit Utrecht.

HOLLMAN, G. G., STEENBRUGGEN, G. & JANSSEN-JURKOVIČOVÁ, M. 1999. A two-step process for the synthesis of zeolites from coal fly ash. *Fuel,* 78**,** 1225-1230.

HOLMGREN, G. G. S., MEYER, M. W., CHANEY, R. L. & DANIELS, R. B. 1993. Cadmium, Lead, Zinc, Copper, and Nickel in Agricultural Soils of the United States of America. *Journal of Environmental Quality,* 22**,** 335-348.

HOSSEINI, T., DE GIROLAMO, A. & ZHANG, L. 2018. Energy Evaluation and Techno-economic Analysis of Low-Rank Coal (Victorian Brown Coal) Utilization for the Production of Multi-Products in a Drying - Pyrolysis Process. *Energy & Fuels,* 32.

HOU, S., ZHENG, N., TANG, L., JI, X., LI, Y. & HUA, X. 2019. Pollution characteristics, sources, and health risk assessment of human exposure to Cu, Zn, Cd and Pb pollution in urban street dust across China between 2009 and 2018. *Environment International,* 128**,** 430-437.

HOWE, K. J., HAND, D. W., CRITTENDEN, J. C., TRUSSELL, R. R. & TCHOBANOGLOUS, G. 2012. *Principles of Water Treatment*, Wiley.

HUBER, M., WELKER, A. & HELMREICH, B. 2016. Critical review of heavy metal pollution of traffic area runoff: Occurrence, influencing factors, and partitioning. *Science of The Total Environment,* 541**,** 895-919.

HUI, K. S., CHAO, C. Y. H. & KOT, S. C. 2005. Removal of mixed heavy metal ions in wastewater by zeolite 4A and residual products from recycled coal fly ash. *Journal of Hazardous Materials,* 127**,** 89-101.

HUSAIN, A. & KHAN, N. 2014. Characterization and treatment of electroplating industry wastewater using Fenton's reagent. *Journal of Chemical and Pharmaceutical Research,* 6**,** 622-627.

IBRAHIM, K., ED-DEEN, N. T. & KHOURY, H. 2002. Use of natural chabazite–phillipsite tuff in wastewater treatment from electroplating factories in Jordan. *Environmental Geology,* 41**,** 547-551.

ILIOPOULOU, E. F., STEFANIDIS, S. D., KALOGIANNIS, K. G., DELIMITIS, A., LAPPAS, A. A. & TRIANTAFYLLIDIS, K. S. 2012. Catalytic upgrading of biomass pyrolysis vapors using transition metal-modified ZSM-5 zeolite. *Applied Catalysis B: Environmental,* 127**,** 281-290.

INGLEZAKIS, V. J., LOIZIDOU, M. D. & GRIGOROPOULOU, H. P. 2003. Ion exchange of Pb2+, Cu2+, Fe3+, and Cr3+ on natural clinoptilolite: selectivity determination and influence of acidity on metal uptake. *Journal of Colloid and Interface Science,* 261**,** 49-54.

INYANG, M. I., GAO, B., YAO, Y., XUE, Y., ZIMMERMAN, A., MOSA, A., PULLAMMANAPPALLIL, P., OK, Y. S. & CAO, X. 2016. A review of biochar as a low-cost adsorbent for aqueous heavy metal removal. *Critical Reviews in Environmental Science and Technology,* 46**,** 406-433.

IQBAL, A., SATTAR, H., HAIDER, R. & MUNIR, S. 2019. Synthesis and characterization of pure phase zeolite 4A from coal fly ash. *Journal of Cleaner Production,* 219**,** 258-267.

ISMADJI, S., EDI-SOETAREDJO, F. & AYUCITRA, A. 2015. *Clay Materials for Environmental Remediation*.

ISMAIL, A. I. M., EL-SHAFEY, O. I., AMR, M. H. A. & EL-MAGHRABY, M. S. 2014. Pumice Characteristics and Their Utilization on the Synthesis of Mesoporous Minerals and on the Removal of Heavy Metals. *International Scholarly Research Notices,* 2014**,** 259379.

IZAH, S. C., INYANG, I. R., ANGAYE, T. C. N. & OKOWA, I. P. 2016. A Review of Heavy Metal Concentration and Potential Health Implications of Beverages Consumed in Nigeria. *Toxics,* 5**,** 1.

IZIDORO, J. D. C., FUNGARO, D. A., DOS SANTOS, F. S. & WANG, S. 2012. Characteristics of Brazilian coal fly ashes and their synthesized zeolites. *Fuel Processing Technology,* 97**,** 38-44.

JAIN, M., GARG, V. K., KADIRVELU, K. & SILLANPÄÄ, M. 2016. Adsorption of heavy metals from multi-metal aqueous solution by sunflower plant biomass-based carbons. *International Journal of Environmental Science and Technology,* 13**,** 493-500.

JAMIL, T. S., IBRAHIM, H. S., ABD EL-MAKSOUD, I. H. & EL-WAKEEL, S. T. 2010. Application of zeolite prepared from Egyptian kaolin for removal of heavy metals: I. Optimum conditions. *Desalination,* 258**,** 34-40.

JÄNCHEN, J., SCHUMANN, K., THRUN, E., BRANDT, A., UNGER, B. & HELLWIG, U. 2012. Preparation, hydrothermal stability and thermal adsorption storage properties of binderless zeolite beads. *International Journal of Low-Carbon Technologies,* 7**,** 275-279.

JARUP, L. 2003. Hazards of heavy metal contamination. *British Medical Bulletin,* 68**,** 167-182.

JASRA, R. V., TYAGI, B., BADHEKA, Y., NETTEM, V. & BHAT, T. 2003. Effect of Clay Binder on Sorption and Catalytic Properties of Zeolite Pellets.

Industrial & Engineering Chemistry Research - IND ENG CHEM RES, 42.

JEEJEEBHOY, K. 2009. Zinc: An Essential Trace Element for Parenteral Nutrition. *Gastroenterology,* 137**,** S7-S12.

JEEVANANTHAM, S., SARAVANAN, A., HEMAVATHY, R. V., KUMAR, P. S., YAASHIKAA, P. R. & YUVARAJ, D. 2019. Removal of toxic pollutants from water environment by phytoremediation: A survey on application and future prospects. *Environmental Technology & Innovation,* 13**,** 264-276.

JHA, B. & SINGH, D. N. 2016. Basics of Zeolites. *Fly Ash Zeolites: Innovations, Applications, and Directions.* Singapore: Springer Singapore.

JHA, V. K., MATSUDA, M. & MIYAKE, M. 2008. Sorption properties of the activated carbon-zeolite composite prepared from coal fly ash for Ni2+, Cu2+, Cd2+ and Pb2+. *Journal of Hazardous Materials,* 160**,** 148-153.

JHA, V. K., NAGAE, M., MATSUDA, M. & MIYAKE, M. 2009. Zeolite formation from coal fly ash and heavy metal ion removal characteristics of thus-obtained Zeolite X in multi-metal systems. *Journal of Environmental Management,* 90**,** 2507-2514.

JIAO, X., TENG, Y., ZHAN, Y., WU, J. & LIN, X. 2015. Soil Heavy Metal Pollution and Risk Assessment in Shenyang Industrial District, Northeast China. *PLOS ONE,* 10**,** e0127736.

JUAN, R., HERNÁNDEZ, S., QUEROL, X., ANDRÉS, J. M. & MORENO, N. 2002. Zeolitic material synthesised from fly ash: use as cationic exchanger. *Journal of Chemical Technology & Biotechnology,* 77**,** 299-304.

JUDD, S. & STEPHENSON, T. 2002. *Process Science and Engineering for Water and Wastewater Treatment*, IWA Publishing.

JÜTTNER, K., GALLA, U. & SCHMIEDER, H. 2000. Electrochemical Approaches to Environmental Problems in the Process Industry. *Electrochimica Acta,* 45**,** 2575-2594.

KABIR, E., RAY, S., KIM, K.-H., YOON, H.-O., JEON, E.-C., KIM, Y., CHO, Y.-S., YUN, S.-T. & BROWN, R. 2012. Current Status of Trace Metal Pollution in Soils Affected by Industrial Activities. *TheScientificWorldJournal,* 2012**,** 916705.

KABWADZA-CORNER, P., JOHAN, E. & MATSUE, N. 2015. pH Dependence of Lead Adsorption on Zeolites. *Journal of Environmental Protection,* 06**,** 45-53.

KADIRVELU, K., THAMARAISELVI, K. & NAMASIVAYAM, C. 2001. Removal of heavy metals from industrial wastewaters by adsorption onto activated carbon prepared from an agricultural solid waste. *Bioresource technology,* 76**,** 63-5.

KATSOU, E., MALAMIS, S., TZANOUDAKI, M., HARALAMBOUS, K. J. & LOIZIDOU, M. 2011. Regeneration of natural zeolite polluted by lead and zinc in wastewater treatment systems. *J Hazard Mater,* 189**,** 773-86.

KERMAN, H., BAGHE, A., HIGHWAY, MALAKOOTIAN, M., TOOLABI, A., GH, S., MOUSSAVI & AHMADIAN, M. 2011. Equilibrium and Kinetic Modeling of Heavy Metals Biosorption from Three Different Real Industrial Wastewaters Onto Ulothrix Zonata Algae. *Australian Journal of Basic and Applied Sciences,* 5**,** 1030-1037.

KERR, G. T. 1979. Natural Zeolites: Occurrence, Properties, Use. *Clays and Clay Minerals,* 27**,** 309-309.

KESRAOUI-OUKI, S., CHEESEMAN, C. R. & PERRY, R. 1994. Natural zeolite utilisation in pollution control: A review of applications to metals' effluents. *Journal of Chemical Technology & Biotechnology,* 59**,** 121-126.

KHAN RAO, R. A. & KHATOON, A. 2017. Aluminate treated Casuarina equisetifolia leaves as potential adsorbent for sequestering Cu(II), Pb(II) and Ni(II) from aqueous solution. *Journal of Cleaner Production,* 165**,** 1280-1295.

KHATTAB, I. A., SHAFFEI, M. F., SHAABAN, N. A., HUSSEIN, H. S. & ABD EL-REHIM, S. S. 2013. Electrochemical removal of copper ions from dilute solutions using packed bed electrode. Part II. *Egyptian Journal of Petroleum,* 22**,** 205-210.

KIM, K.-J. & AHN, H.-G. 2012. The effect of pore structure of zeolite on the adsorption of VOCs and their desorption properties by microwave heating. *Microporous and Mesoporous Materials,* 152**,** 78–83.

KLEYNHANS, E. L. J., BEUKES, J. P., VAN ZYL, P. G., KESTENS, P. H. I. & LANGA, J. M. 2012. Unique challenges of clay binders in a pelletised chromite pre-reduction process. *Minerals Engineering,* 34**,** 55-62.

KLUČÁKOVÁ, M. & PAVLÍKOVÁ, M. 2017. Lignitic Humic Acids as Environmentally-Friendly Adsorbent for Heavy Metals. *Journal of Chemistry,* 2017**,** 7169019.

KOBAYASHI, Y., OGATA, F., NAKAMURA, T. & KAWASAKI, N. 2020. Synthesis of novel zeolites produced from fly ash by hydrothermal treatment in alkaline solution and its evaluation as an adsorbent for heavy metal removal. *Journal of Environmental Chemical Engineering,* 8**,** 103687.

KOCAOBA, S., ORHAN, Y. & AKYÜZ, T. 2007. Kinetics and equilibrium studies of heavy metal ions removalby use of natural zeolite. *Desalination,* 214**,** 1-10.

KOSHY, N. & SINGH, D. N. 2016. Fly ash zeolites for water treatment applications. *Journal of Environmental Chemical Engineering,* 4**,** 1460-1472.

KRAGOVIĆ, M., DAKOVIĆ, A., MARKOVIĆ, M., KRSTIĆ, J., GATTA, G. D. & ROTIROTI, N. 2013. Characterization of lead sorption by the natural and Fe(III)-modified zeolite. *Applied Surface Science,* 283**,** 764-774.

KRĘŻEL, A. & MARET, W. 2016. The biological inorganic chemistry of zinc ions. *Archives of Biochemistry and Biophysics,* 611**,** 3-19.

KROBBA, A., NIBOU, D., AMOKRANE, S. & MEKATEL, H. 2012. Adsorption of copper (II) onto molecular sieves NaY. *Desalination and Water Treatment,* 37**,** 31-37.

KU, Y. & JUNG, I. L. 2001. Photocatalytic reduction of Cr(VI) in aqueous solutions by UV irradiation with the presence of titanium dioxide. *Water Res,* 35**,** 135-42.

KUILA, U. & PRASAD, M. 2013. Specific surface area and pore-size distribution in clays and shales. *Geophysical Prospecting,* 61**,** 341-362.

KUL, M. & OSKAY, K. O. 2015. Separation and recovery of valuable metals from real mix electroplating wastewater by solvent extraction. *Hydrometallurgy,* 155**,** 153-160.

KULKARNI, R. 2013. Equilibrium and kinetic studies for the adsorption of cadmium ion on Zeolite 4A. *Journal of Biochemical Technology,* 3**,** 158-160.

KUMAR, K. V. 2007. Pseudo-second order models for the adsorption of safranin onto activated carbon: Comparison of linear and non-linear regression methods. *Journal of Hazardous Materials,* 142**,** 564-567.

KUMARA, D. Removal of Nickel ions from Aqueous Solutions on Packed bed of Zeolite NaX. 2007.

KURNIAWAN, T. A., CHAN, G. Y. S., LO, W.-H. & BABEL, S. 2006. Physico–chemical treatment techniques for wastewater laden with heavy metals. *Chemical Engineering Journal,* 118**,** 83-98.

LABORATORY, I. E. R., SOCIETY, A. E. & AGENCY, U. S. E. P. 1979. *Second Conference on Advanced Pollution Control for the Metal Finishing*

Industry, presented at Orlando Hyatt House, Kissimmee, Fl., February 5-7, 1979, Environmental Protection Agency, Office of Research and Development, Industrial Environmental Research Laboratory.

LAGERGREN, S. K. 1898. About the Theory of So-called Adsorption of Soluble Substances. *Sven. Vetenskapsakad. Handingarl,* 24**,** 1-39.

LAKHERWAL, D. 2014. Adsorption of Heavy Metals: A Review. *International Journal of Environmental Research and Development,* 4**,** 41-48.

LANGMUIR, I. 1918. THE ADSORPTION OF GASES ON PLANE SURFACES OF GLASS, MICA AND PLATINUM. *Journal of the American Chemical Society,* 40**,** 1361-1403.

LATA, S., SINGH, P. K. & SAMADDER, S. R. 2015. Regeneration of adsorbents and recovery of heavy metals: a review. *International Journal of Environmental Science and Technology,* 12**,** 1461-1478.

LEE, C.-R., KIM, H.-S., JANG, I.-H., IM, J.-H. & PARK, N.-G. 2011. Pseudo First-Order Adsorption Kinetics of N719 Dye on TiO2 Surface. *ACS Applied Materials & Interfaces,* 3**,** 1953-1957.

LEE, J.-W., CHOI, H., HWANG, U.-K., KANG, J.-C., KANG, Y. J., KIM, K. I. & KIM, J.-H. 2019. Toxic effects of lead exposure on bioaccumulation, oxidative stress, neurotoxicity, and immune responses in fish: A review. *Environmental Toxicology and Pharmacology,* 68**,** 101-108.

LEE, M.-G., YI, G., AHN, B.-J. & RODDICK, F. 2000. Conversion of coal fly ash into zeolite and heavy metal removal characteristics of the products. *Korean Journal of Chemical Engineering,* 17**,** 325-331.

LEWINSKY, A. A. 2007. *Hazardous Materials and Wastewater: Treatment, Removal and Analysis*, Nova Science Publishers.

LI, P.-S. & TAO, H.-C. 2015. Cell surface engineering of microorganisms towards adsorption of heavy metals. *Critical Reviews in Microbiology,* 41**,** 140-149.

LI, Y., BAI, P., YAN, Y., YAN, W., SHI, W. & XU, R. 2019. Removal of Zn2+, Pb2+, Cd2+, and Cu2+ from aqueous solution by synthetic clinoptilolite. *Microporous and Mesoporous Materials,* 273**,** 203-211.

LI, Y., LI, L. & YU, J. 2017. Applications of Zeolites in Sustainable Chemistry. *Chem,* 3**,** 928-949.

LICHTFOUSE, E., SCHWARZBAUER, J. & ROBERT, D. 2013. *Green Materials for Energy, Products and Depollution*, Springer Netherlands.

LIM, A. P. & ARIS, A. Z. 2014. A review on economically adsorbents on heavy metals removal in water and wastewater. *Reviews in Environmental Science and Bio/Technology,* 13**,** 163-181.

LIN, S.-H. & JUANG, R.-S. 2009. Adsorption of phenol and its derivatives from water using synthetic resins and low-cost natural adsorbents: A review. *Journal of Environmental Management,* 90**,** 1336-1349.

LIU, C., WU, T., HSU, P.-C., XIE, J., ZHAO, J., LIU, K., SUN, J., XU, J., TANG, J., YE, Z., LIN, D. & CUI, Y. 2019. Direct/Alternating Current Electrochemical Method for Removing and Recovering Heavy Metal from Water Using Graphene Oxide Electrode. *ACS Nano,* 13**,** 6431-6437.

LIU, Z.-R., ZHOU, L.-M., WEI, P., ZENG, K., WEN, C.-X. & LAN, H.-H. 2008. Competitive adsorption of heavy metal ions on peat. *Journal of China University of Mining and Technology,* 18**,** 255-260.

LOKHANDE, R. S., SINGARE, P. U. & PIMPLE, D. S. 2011. Toxicity Study of Heavy Metals Pollutants in Waste Water Effluent Samples Collected from Taloja Industrial Estate of Mumbai, India. *Resources and Environment,* 1**,** 13-19.

LUQMAN, M. 2012. *Ion Exchange Technology II: Applications*, Springer Netherlands.

MADDEN, D. & CURTIN, T. 2016. Carbon dioxide capture with amino-functionalised zeolite-β: A temperature programmed desorption study under dry and humid conditions. *Microporous and Mesoporous Materials,* 228**,** 310-317.

MAHMOUD, T., IBRAHIM, H., HAMDY, I. & EL-WAKEEL, S. 2010. Application of Zeolite Prepared from Egyptian Kaolin for Removal of Heavy Metals: I. Optimum Conditions. *Desalination,* 258**,** 34-40.

MAJCHRZAK-KUCĘBA, I., WAWRZYŃCZAK, D., ŚCIUBIDŁO, A., ZDEB, J., SMÓŁKA, W. & ZAJCHOWSKI, A. 2019. Stability and regenerability of acivated carbon used for CO2 removal in pilot DR-VPSA unit in real power plant conditions. *Journal of CO2 Utilization,* 29**,** 1-11.

MALIK, A. & THAPLIYAL, A. 2009. Eco-friendly Fly Ash Utilization: Potential for Land Application. *Critical Reviews in Environmental Science and Technology,* 39**,** 333-366.

MALIK, D. S., JAIN, C. K. & YADAV, A. K. 2017. Removal of heavy metals from emerging cellulosic low-cost adsorbents: a review. *Applied Water Science,* 7**,** 2113-2136.

MAMTANI, R., STERN, P., DAWOOD, I. & CHEEMA, S. 2011. Metals and Disease: A Global Primary Health Care Perspective. *Journal of Toxicology,* 2011**,** 319136.

MAPP, C. E., BOSCHETTO, P., MAESTRELLI, P. & FABBRI, L. M. 2005. Occupational Asthma. *American Journal of Respiratory and Critical Care Medicine,* 172**,** 280-305.

MARETTO, M., BLANCHI, F., VIGNOLA, R., CANEPARI, S., BARIC, M., IAZZONI, R., TAGLIABUE, M. & PAPINI, M. 2014. Microporous and mesoporous materials for the treatment of wastewater produced by petrochemical activities. *Journal of Cleaner Production,* 77**,** 22-34.

MARGETA, K., ZABUKOVEC LOGAR, N., ŠILJEG, M. & FARKAS, A. 2013. Natural Zeolites in Water Treatment – How Effective is Their Use.

MARTÍNEZ-HUITLE, C. A. & BRILLAS, E. 2009. Decontamination of wastewaters containing synthetic organic dyes by electrochemical methods: A general review. *Applied Catalysis B: Environmental,* 87**,** 105-145.

MICKOVA, I. L. 2015. Advanced Electrochemical Technologies in Wastewater Treatment. Part II: Electro-Flocculation and Electro-Flotation. *American Scientific Research Journal for Engineering, Technology and Sciences* 14**,** 273-294.

MINCEVA, M., MARKOVSKA, L. & MESHKO, V. 2007. Removal of Zn2+, Cd2+ and Pb2+ from binary aqueous solution by natural zeolite and granulated activated carbon. *Maced. J. Chem. Chem. Eng.,* 26**,** 125-134.

MISHRA, S. P. 2014. Adsorption–desorption of heavy metal ions. *Current Science,* 107**,** 601-612.

MOHAN, D. & PITTMAN, C. U. 2007. Arsenic removal from water/wastewater using adsorbents—A critical review. *Journal of Hazardous Materials,* 142**,** 1-53.

MOHAN, D. & SINGH, K. P. 2002. Single- and multi-component adsorption of cadmium and zinc using activated carbon derived from bagasse—an agricultural waste. *Water Research,* 36**,** 2304-2318.

MOHAN, S. & GANDHIMATHI, R. 2009. Removal of heavy metal ions from municipal solid waste leachate using coal fly ash as an adsorbent. *Journal of Hazardous Materials,* 169**,** 351-359.

MOLLAH, M. Y. A., SCHENNACH, R., PARGA, J. R. & COCKE, D. L. 2001. Electrocoagulation (EC) — science and applications. *Journal of Hazardous Materials,* 84**,** 29-41.

MONTANHER, S. F., OLIVEIRA, E. A., ROLLEMBERG, M. D. C. & LEWINSKY, A. A. 2007. Utilization of Agro-residues in the metal ions removal from

aqueous solutions. *Hazardous materials and wastewater: Treatment, removal and analysis***,** 51-78.

MOO-YOUNG, M. 2019. *Comprehensive Biotechnology*, Elsevier Science.

MORADI, S., MOOSAVI, E. & KARIMZADEH, R. 2019. Stability Determination of the Modified Activated Carbon to Adsorb Thiophenic Compounds from Model Diesel Fuel. *Iranian Journal of Chemistry and Chemical Engineering (IJCCE),* 38**,** 149-165.

MORENO, N., QUEROL, X., AYORA, C., ALASTUEY, A., FERNÁNDEZ-PEREIRA, C. & JANSSEN-JURKOVICOVÁ, M. 2001a. Potential Environmental Applications of Pure Zeolitic Material Synthesized from Fly Ash. *Journal of Environmental Engineering,* 127**,** 994-1002.

MORENO, N., QUEROL, X., AYORA, C., PEREIRA, C. F. & JANSSEN-JURKOVICOVÁ, M. 2001b. Utilization of Zeolites Synthesized from Coal Fly Ash for the Purification of Acid Mine Waters. *Environmental Science & Technology,* 35**,** 3526-3534.

MOTSI, T., ROWSON, N. A. & SIMMONS, M. J. H. 2009. Adsorption of heavy metals from acid mine drainage by natural zeolite. *International Journal of Mineral Processing,* 92**,** 42-48.

MURALEEDHARAN, T. R., IYENGAR, L. & VENKOBACHAR, C. 1991. Biosorption: An attractive alternative for metal removal and recovery. *Current Science,* 61**,** 379-385.

MUSYOKA, N. M., PETRIK, L. F., HUMS, E., KUHNT, A. & SCHWIEGER, W. 2015. Thermal stability studies of zeolites A and X synthesized from South African coal fly ash. *Research on Chemical Intermediates,* 41**,** 575-582.

NASCIMENTO, M., SOARES, P. S. M. & SOUZA, V. P. D. 2009. Adsorption of heavy metal cations using coal fly ash modified by hydrothermal method. *Fuel,* 88**,** 1714-1719.

NAWAR, S. S. & DOMA, H. S. 1989. Removal of dyes from effluents using low-cost agricultural by-products. *Science of The Total Environment,* 79**,** 271-279.

NDI NSAMI, J. & KETCHA MBADCAM, J. 2013. The Adsorption Efficiency of Chemically Prepared Activated Carbon from Cola Nut Shells *Journal of Chemistry,* 2013**,** 469170.

NERIS, J. B., LUZARDO, F. H. M., DA SILVA, E. G. P. & VELASCO, F. G. 2019. Evaluation of adsorption processes of metal ions in multi-element aqueous systems by lignocellulosic adsorbents applying different isotherms: A critical review. *Chemical Engineering Journal,* 357**,** 404-420.

NGUYEN, T. C., LOGANATHAN, P., NGUYEN, T. V., VIGNESWARAN, S., KANDASAMY, J. & NAIDU, R. 2015. Simultaneous adsorption of Cd, Cr, Cu, Pb, and Zn by an iron-coated Australian zeolite in batch and fixed-bed column studies. *Chemical Engineering Journal,* 270**,** 393-404.

NIBOU, D., KHEMAISSIA, S., AMOKRANE, S., BARKAT, M., CHEGROUCHE, S. & MELLAH, A. 2011. Removal of UO22+ onto synthetic NaA zeolite. Characterization, equilibrium and kinetic studies. *Chemical Engineering Journal,* 172**,** 296-305.

NIBOU, D., MEKATEL, H., AMOKRANE, S., BARKAT, M. & TRARI, M. 2010. Adsorption of Zn2+ ions onto NaA and NaX zeolites: Kinetic, equilibrium and thermodynamic studies. *Journal of Hazardous Materials,* 173**,** 637-646.

NOLL, K. E. 1991. *Adsorption Technology for Air and Water Pollution Control*, Taylor & Francis.

NRIAGU, J. O. 1980. *Zinc in the Environment: Ecological cycling*, Wiley.

O'CONNELL, D., BIRKINSHAW, C. & O'DWYER, T. 2008. Heavy metal adsorbents prepared from the modification of cellulose: A review. *Bioresource technology,* 99**,** 6709-24.

O'CONNELL, D. W., BIRKINSHAW, C. & O'DWYER, T. F. 2008. Heavy metal adsorbents prepared from the modification of cellulose: A review. *Bioresource Technology,* 99**,** 6709-6724.

OHGAKI, S., FUKUSHI, K., KATAYAMA, H., TAKIZAWA, S. & POLPRASERT, C. 2005. *Southeast Asian Water Environment 1*, IWA Publishing.

OJOVAN, M. I. & LEE, W. E. 2014. 14 - Treatment of Radioactive Wastes. *In:* OJOVAN, M. I. & LEE, W. E. (eds.) *An Introduction to Nuclear Waste Immobilisation (Second Edition).* Oxford: Elsevier.

OLIVEIRA DE MAGALHÃES, G. 2018. *Granulation and mechanic strength evaluation of nanomaterials with*
high potential as adsorbents and desiccants. Masters Masters Dissertation, UNIVERSIDADE FEDERAL DE MINAS GERAIS.

ONGEN, A., DOKMECI, H., CELIK, S., SABUDAK, T., KAYKıOĞLU, G. & DÖKMECI, A. 2008. Copper and Cadmium and Ground and Surface Water in Corlu. *Journal of environmental protection and ecology,* 9**,** 753-762.

ONYESTYÁK, G., SHEN, D. & REES, L. V. C. 1995. Frequency-response study of micro- and macro-pore diffusion in manufactured zeolite pellets. *Journal of the Chemical Society, Faraday Transactions,* 91**,** 1399-1405.

ORGANIZATION, W. H. 2008. *Guidelines for Drinking-water Quality* [Online]. Geneva. 1].

OSTROSKI, I., BARROS, M. A., DA SILVA, E., DANTAS, J., ARROYO, P. & MOTTA LIMA, O. 2008. A comparative study for the ion exchange of Fe(III) and Zn(II) on zeolite NaY. *Journal of hazardous materials,* 161**,** 1404-12.

OTER, O. & AKCAY, H. 2007. Use of Natural Clinoptilolite to Improve Water Quality: Sorption and Selectivity Studies of Lead(II), Copper(II), Zinc(II), and Nickel(II). *Water Environment Research,* 79**,** 329-335.

OTIENO, S. O., KENGARA, F. O., KEMMEGNE-MBOUGUEN, J. C., LANGMI, H. W., KOWENJE, C. B. O. & MOKAYA, R. 2019. The effects of metakaolinization and fused-metakaolinization on zeolites synthesized from quartz rich natural clays. *Microporous and Mesoporous Materials,* 290**,** 109668.

OUKI, S. K. & KAVANNAGH, M. 1997. PERFORMANCE OF NATURAL ZEOLITES FOR THE TREATMENT OF MIXED METAL-CONTAMINATED EFFLUENTS. *Waste Management & Research,* 15**,** 383-394.

OUYANG, D., ZHUO, HU, W., ZENG, X. & HE 2019. Research on the Adsorption Behavior of HeavyMetal Ions by Porous Material Prepared with Silicate Tailings. *Minerals,* 9**,** 291.

PANDAY, K. K., PRASAD, G. & SINGH, V. N. 1985. Copper(II) removal from aqueous solutions by fly ash. *Water Research,* 19**,** 869-873.

PAP, S., RADONIĆ, J., TRIFUNOVIĆ, S., ADAMOVIĆ, D., MIHAJLOVIĆ, I., VOJINOVIĆ MILORADOV, M. & TURK SEKULIĆ, M. 2016. Evaluation of the adsorption potential of eco-friendly activated carbon prepared from cherry kernels for the removal of Pb(2+), Cd(2+) and Ni(2+) from aqueous wastes. *J Environ Manage,* 184**,** 297-306.

PATEL, H. 2019. Fixed-bed column adsorption study: a comprehensive review. *Applied Water Science,* 9**,** 45.

PAVLOV, M. L., TRAVKINA, O. S., BASIMOVA, R. A., PAVLOVA, I. N. & KUTEPOV, B. I. 2009. Binder-free syntheses of high-performance zeolites A and X from kaolin. *Petroleum Chemistry,* 49**,** 36-41.

PEREGO, C. & MILLINI, R. 2013. Porous materials in catalysis: challenges for mesoporous materials. *Chemical Society Reviews,* 42**,** 3956-3976.

PERIĆ, J., TRGO, M. & VUKOJEVIĆ MEDVIDOVIĆ, N. 2004. Removal of zinc, copper and lead by natural zeolite—a comparison of adsorption isotherms. *Water Research,* 38**,** 1893-1899.

PETRUZZELLI, D., PAGANO, M., TIRAVANTI, G. & PASSINO, R. 1999. LEAD REMOVAL AND RECOVERY FROM BATTERY WASTEWATERS BY NATURAL ZEOLITE CLINOPTILOLITE. *Solvent Extraction and Ion Exchange,* 17**,** 677-694.

PICKERING, Q. H. & HENDERSON, C. 1966. The acute toxicity of some heavy metals to different species of warmwater fishes. *Air Water Pollut,* 10**,** 453-63.

PITCHER, S. K., SLADE, R. C. T. & WARD, N. I. 2004. Heavy metal removal from motorway stormwater using zeolites. *Science of The Total Environment,* 334-335**,** 161-166.

PITOT, H. C. & CHAPMAN, D. V. 1996. *Water Quality Assessments: A guide to the use of biota, sediments and water in environmental monitoring, Second Edition*, CRC Press.

PIZZI, N. G. & ASSOCIATION, A. W. W. 2010. *Water Treatment*, American Water Works Association.

PLAZINSKI, W., DZIUBA, J. & RUDZINSKI, W. 2013. Modeling of sorption kinetics: the pseudo-second order equation and the sorbate intraparticle diffusivity. *Adsorption,* 19**,** 1055-1064.

PLUM, L. M., RINK, L. & HAASE, H. 2010. The essential toxin: impact of zinc on human health. *International journal of environmental research and public health,* 7**,** 1342-1365.

POLLARD, S. J. T., FOWLER, G. D., SOLLARS, C. J. & PERRY, R. 1992. Low-cost adsorbents for waste and wastewater treatment: a review. *Science of The Total Environment,* 116**,** 31-52.

POURRUT, B., SHAHID, M., DUMAT, C., WINTERTON, P. & PINELLI, E. 2011. Lead uptake, toxicity, and detoxification in plants. *Rev Environ Contam Toxicol,* 213**,** 113-36.

POWELL, M. R. 2014. *Science at EPA: Information in the Regulatory Process*, Taylor & Francis.

POWELL, M. R. & FUTURE, R. F. T. 1997. *The 1991 Lead/copper Drinking Water Rule and the 1995 Decision Not to Revise the Arsenic Drinking Water Rule: Two Case Studies in EPA's Use of Science*, Resources for the Future.

PRAHARAJ, T., POWELL, M. A., HART, B. R. & TRIPATHY, S. 2002. Leachability of elements from sub-bituminous coal fly ash from India. *Environment International,* 27**,** 609-615.

PRASAD, B., MAHATO, A., MONDAL, H. & TEWARY, B. 2013. Removal of Ions and Acidity from Acid Mine Water Using Transformed Fly Ash. *Mine Water and the Environment,* 32.

PRASAD, B. & MORTIMER, R. 2011. Treatment of Acid Mine Drainage Using Fly Ash Zeolite. *Water Air and Soil Pollution,* 218**,** 667-679.

PROCTOR, A. & TORO-VAZQUEZ, J. F. 1996. The Freundlich isotherm in studying adsorption in oil processing. *Journal of the American Oil Chemists' Society,* 73**,** 1627-1633.

PROGRAMME, U. N. E., ASPECTS, W. T. G. O. E. H. C. F. L.-.-E., ORGANISATION, I. L., ORGANIZATION, W. H. & SAFETY, I. P. O. C. 1989. *Lead: Environmental Aspects*, World Health Organization.

PURNA CHANDRA RAO, G., SATYAVENI, S., RAMESH, A., SESHAIAH, K., MURTHY, K. S. N. & CHOUDARY, N. V. 2006. Sorption of cadmium and zinc from aqueous solutions by zeolite 4A, zeolite 13X and bentonite. *Journal of Environmental Management,* 81**,** 265-272.

QIU, W. & ZHENG, Y. 2009. Removal of lead, copper, nickel, cobalt, and zinc from water by a cancrinite-type zeolite synthesized from fly ash. *Chemical Engineering Journal,* 145**,** 483-488.

QUEROL, X., MORENO, N., ALASTUEY, A., MAINAR, R., ANDRÉS, J., SOLER, Á., AYORA, C., MEDINACELI, A. & VALERO, A. 2007. Synthesis of high ion exchange zeolites from coal fly ash. *Geologica Acta,* 5**,** 47.

QUEROL, X., MORENO, N., UMAÑA, J. C., JUAN, R., HERNÁNDEZ, S., FERNANDEZ-PEREIRA, C., AYORA, C., JANSSEN, M., GARCÍA-MARTÍNEZ, J., LINARES-SOLANO, A. & CAZORLA-AMOROS, D. 2002. Application of zeolitic material synthesised from fly ash to the decontamination of waste water and flue gas. *Journal of Chemical Technology & Biotechnology,* 77**,** 292-298.

QUEROL, X., UMAÑA, J. C., PLANA, F., ALASTUEY, A., LOPEZ-SOLER, A., MEDINACELI, A., VALERO, A., DOMINGO, M. J. & GARCIA-ROJO, E. 2001. Synthesis of zeolites from fly ash at pilot plant scale. Examples of potential applications. *Fuel,* 80**,** 857-865.

QUINN, M. J. & SHERLOCK, J. C. 1990. The correspondence between U.K. 'action levels' for lead in blood and in water. *Food Additives & Contaminants,* 7**,** 387-424.

RAHMAN, M. L., SARKAR, S. M. & YUSOFF, M. M. 2016. Efficient removal of heavy metals from electroplating wastewater using polymer ligands. *Frontiers of Environmental Science & Engineering,* 10**,** 352-361.

RAJAKOVIĆ, L. V., MARKOVIĆ, D. D., RAJAKOVIĆ-OGNJANOVIĆ, V. N. & ANTANASIJEVIĆ, D. Z. 2012. Review: The approaches for estimation of limit of detection for ICP-MS trace analysis of arsenic. *Talanta,* 102**,** 79-87.

RAO, M. N., SULTANA, R., KOTA, H., SHAH, A. & DAVERGAVE, N. 2016. *Solid and Hazardous Waste Management: Science and Engineering*, Elsevier Science.

RAO, M. N., SULTANA, R. & KOTA, S. H. 2017. Chapter 5 - Hazardous Waste. *In:* RAO, M. N., SULTANA, R. & KOTA, S. H. (eds.) *Solid and Hazardous Waste Management.* Butterworth-Heinemann.

RASHED, M. N. 2013. Adsorption technique for the removal of organic pollutants from water and wastewater. *Organic Pollutants-Monitoring, Risk and Treatment***,** 167-194.

RATTANACHAIWONG, S. & SINGER, P. 2019. Diets and Diet Therapy: Trace Elements. *In:* FERRANTI, P., BERRY, E. M. & ANDERSON, J. R. (eds.) *Encyclopedia of Food Security and Sustainability.* Oxford: Elsevier.

REDDY, K. J., WANG, L. & GLOSS, S. P. 1995. Solubility and mobility of copper, zinc and lead in acidic environments. *Plant and Soil,* 171**,** 53-58.

RENGARAJ, S., JOO, C. K., KIM, Y. & YI, J. 2003. Kinetics of removal of chromium from water and electronic process wastewater by ion exchange resins: 1200H, 1500H and IRN97H. *Journal of Hazardous Materials,* 102**,** 257-275.

RINAUDO, M. & GOYCOOLEA, F. M. 2019. *Advances in Chitin/Chitosan Characterization and Applications*, MDPI AG.

ROBERTS, B. F. 1967. A procedure for estimating pore volume and area distributions from sorption isotherms. *Journal of Colloid and Interface Science,* 23**,** 266-273.

RONEY, N., OSIER, M., PAIKOFF, S. J., SMITH, C. V., WILLIAMS, M. & DE ROSA, C. T. 2006. ATSDR evaluation of the health effects of zinc and relevance to public health. *Toxicology and Industrial Health,* 22**,** 423-493.

RONGSAYAMANONT, C. & SOPAJAREE, K. 2007. Modification of Synthetic Zeolite Pellets from Lignite Fly Ash A : The Pelletization.

ROUQUEROL, J., LLEWELLYN, P. & ROUQUEROL, F. 2007. Is the bet equation applicable to microporous adsorbents. *Studies in Surface Science and Catalysis,* 160**,** 49-56.

ROVIRA, J. & DOMINGO, J. L. 2019. Human health risks due to exposure to inorganic and organic chemicals from textiles: A review. *Environmental Research,* 168**,** 62-69.

RUDZINSKI, W. & PANCZYK, T. 2002. The Langmuirian Adsorption Kinetics Revised: A Farewell to the XXth Century Theories? *Adsorption,* 8**,** 23-34.

RUDZINSKI, W. & PLAZINSKI, W. 2006. Kinetics of Solute Adsorption at Solid/Solution Interfaces: A Theoretical Development of the Empirical Pseudo-First and Pseudo-Second Order Kinetic Rate Equations, Based on Applying the Statistical Rate Theory of Interfacial Transport. *The Journal of Physical Chemistry B,* 110**,** 16514-16525.

RULE, K. L., COMBER, S. D. W., ROSS, D., THORNTON, A., MAKROPOULOS, C. K. & RAUTIU, R. 2006. Diffuse sources of heavy metals entering an urban wastewater catchment. *Chemosphere,* 63**,** 64-72.

RUTHVEN, D. M. 1984. *Principles of Adsorption and Adsorption Processes*, Wiley.

SANCHEZ HERNANDEZ, R., PADILLA, I., LÓPEZ-ANDRÉS, S. & LÓPEZ-DELGADO, A. 2018. Single and competitive adsorptive removal of lead, cadmium, and mercury using zeolite adsorbent prepared from industrial aluminum waste. *Desalination and water treatment,* 126**,** 181-195.

SANTÉ, O. M. D. L., ORGANIZATION, W. H., PROGRAMME, W.-.-W., STAFF, W. H. O., ZDROWIA, Ś. O. & WHO 2004. *Guidelines for Drinking-water Quality*, WHO.

SAPARI, N., IDRIS, A. & HAMID, N. 1996. Total removal of heavy metal from mixed plating rinse wastewater. *Desalination,* 106**,** 419-422.

SÄRKKÄ, H., BHATNAGAR, A. & SILLANPÄÄ, M. 2015. Recent developments of electro-oxidation in water treatment — A review. *Journal of Electroanalytical Chemistry,* 754**,** 46-56.

SCHOCK, M. R. 1990. Causes of temporal variability of lead in domestic plumbing systems. *Environmental Monitoring and Assessment,* 15**,** 59-82.

SCHULZ-BALDES, M. 1972. Toxizität und anreicherung von blei bei der miesmuschel Mytilus edulis im laborexperiment. *Marine Biology,* 16**,** 226-229.

SCHUMANN, K., UNGER, B., BRANDT, A. & SCHEFFLER, F. 2012. Investigation on the pore structure of binderless zeolite 13× shapes. *Microporous and Mesoporous Materials,* 154**,** 119-123.

ŠĆIBAN, M., RADETIĆ, B., KEVREŠAN, Ž. & KLAŠNJA, M. 2007. Adsorption of heavy metals from electroplating wastewater by wood sawdust. *Bioresource Technology,* 98**,** 402-409.

SHARMA, P. & DUBEY, R. S. 2005. Lead toxicity in plants. *Brazilian Journal of Plant Physiology,* 17**,** 35-52.

SHARMA, P., SONG, J.-S., HAN, M. H. & CHO, C.-H. 2016. GIS-NaP1 zeolite microspheres as potential water adsorption material: Influence of initial silica concentration on adsorptive and physical/topological properties. *Scientific Reports,* 6**,** 22734.

SHEN, C., SHEN, Y., WEN, Y., WANG, H. & LIU, W. 2011. Fast and highly efficient removal of dyes under alkaline conditions using magnetic chitosan-Fe(III) hydrogel. *Water Research,* 45**,** 5200-5210.

SHERMAN, J. D. 1999. Synthetic zeolites and other microporous oxide molecular sieves. *Proceedings of the National Academy of Sciences,* 96**,** 3471-3478.

SHEVADE, S. & FORD, R. G. 2004. Use of synthetic zeolites for arsenate removal from pollutant water. *Water Res,* 38**,** 3197-204.

SHUKLA, P., DONG, K., RUDOLPH, V., BHATIA, S. K., BAJAJ, H. C. & JASRA, R. V. 2019. Adsorptive dehydration of ethanol using 3A zeolite: an

evaluation of transport behaviour in a two-phase zeolite pellet. *Adsorption,* 25**,** 1611-1623.

SHUMBA, M., CHIGONDO, M., GUYO, U., CHIGONDO, F., MOYO, M., NHARINGO, T. & DUBE, E. 2011. Synthesis of Zeolites and Their Applications in Heavy Metals Removal: A Review. *IRACST – Engineering Science and Technology: An International Journal*.

SINGH, S., VERMA, L., SAMBI, S. & SHARMA, S. 2008. Adsorption Behaviour of Ni (II) from Water onto Zeolite X: Kinetics and Equilibrium Studies. *Lecture Notes in Engineering and Computer Science,* 2173.

SIRCAR, S. 2000. Publications on Adsorption Science and Technology. *Adsorption,* 6**,** 359-365.

SONI, S. 2014. *Handbook of Research on Diverse Applications of Nanotechnology in Biomedicine, Chemistry, and Engineering*, IGI Global.

SOTOMAYOR, F. J., CYCHOSZ, K. A. & THOMMES, M. Characterization of Micro / Mesoporous Materials by Physisorption : Concepts and Case Studies. 2018.

SOUSA, F., OLIVEIRA, A., RIBEIRO, J., ROSA, M., DE KEUKELEIRE, D. & NASCIMENTO, R. 2010. Green coconut shells applied as adsorbent for removal of toxic metal ions using fixed-bed column technology. *Journal of environmental management,* 91**,** 1634-40.

SPEARS, J. W. & ENGLE, T. E. 2016. Feed Ingredients: Feed Supplements: Microminerals. *Reference Module in Food Science.* Elsevier.

SPRYNSKYY, M., BUSZEWSKI, B., TERZYK, A. P. & NAMIEŚNIK, J. 2006. Study of the selection mechanism of heavy metal (Pb2+, Cu2+, Ni2+, and Cd2+) adsorption on clinoptilolite. *Journal of Colloid and Interface Science,* 304**,** 21-28.

SRIVASTAVA, S. K., PANT, N. & PAL, N. 1987. Studies on the efficiency of a local fertilizer waste as a low cost adsorbent. *Water Research,* 21**,** 1389-1394.

STEENBRUGGEN, G. & HOLLMAN, G. G. 1998. The synthesis of zeolites from fly ash and the properties of the zeolite products. *Journal of Geochemical Exploration,* 62**,** 305-309.

STEVENS, L., WILLIAMS, K., HAN, W. Y., DRAGE, T., SNAPE, C., WOOD, J. & WANG, J. 2013. Preparation and CO2 adsorption of diamine modified montmorillonite via exfoliation grafting route. *Chemical Engineering Journal,* 215-216**,** 699-708.

STRAIN, H. H. & SHERMA, J. 1967. M. Tswett: "Adsorption analysis and chromatographic methods: Application to the chemistry of chlorophylls". *Journal of Chemical Education,* 44**,** 238.

SUD, D., MAHAJAN, G. & KAUR, M. P. 2008. Agricultural waste material as potential adsorbent for sequestering heavy metal ions from aqueous solutions – A review. *Bioresource Technology,* 99**,** 6017-6027.

SUGIARTI, S. 2019. Synthesis of NaP1 and faujasite zeolite from natural zeolite of ende-ntt as lead (Pb(II))adsorbent. *Rasayan Journal of Chemistry,* 12.

SUN, H., SUN, Z., SHEN, B., LIU, J., LI, G., WU, D. & ZHANG, Y. 2018. One-pot synthesis of binderless zeolite A spheres via in situ hydrothermal conversion of silica gel precursors. *AIChE Journal,* 64**,** 4027-4038.

SURISETTY, V. R., KOZINSKI, J. & RAO NAGESWARA, L. 2013. Biosorption of Lead Ions from Aqueous Solution Using Ficus benghalensis L. *Journal of Engineering,* 2013**,** 167518.

SURVEY, G. & SURVEY, G. 2015. *Mineral Commodity Summaries, 2015*, U.S. Government Printing Office.

TARACHAND, N., SHARMA, D. & DUBEY, A. 2016. Utilization of Natural Adsorbents in the Elimination of Toxic Metal Ions in Industrial Effluents: A Review. *Asian Journal of Research in Chemistry,* 9**,** 70.

TCHOUNWOU, P. B., YEDJOU, C. G., PATLOLLA, A. K. & SUTTON, D. J. 2012. Heavy metal toxicity and the environment. *Exp Suppl,* 101**,** 133-64.

TEODOR, V., GHERGHE, L., PREDICA, V. & KREBS, R. 2008. Heavy metal contamination in the vicinity of an industrial area near Bucharest. *Environmental science and pollution research international,* 16 Suppl 1**,** S27-32.

TESTING, A. S. F., CONCRETE, M. C. C.-O., AGGREGATES, C. & MATERIALS, A. S. C. S. C. 2005. *Standard Specification for Coal Fly Ash and Raw Or Calcined Natural Pozzolan for Use in Concrete*, ASTM International.

THOMAS, M. 2007. Optimizing the use of fly ash in concrete.

THOMAS, M. P. 2010. Calcium and Magnesium in Drinking-water: Public Health Significance. *International Journal of Environmental Studies,* 67**,** 612-613.

TING, Y. P. & TEO, W. K. 1994. Uptake of cadmium and zinc by yeast: Effects of co-metal ion and physical/chemical treatments. *Bioresource Technology,* 50**,** 113-117.

TIWARI, M. K., BAJPAI, S., DEWANGAN, U. K. & TAMRAKAR, R. K. 2015. Suitability of leaching test methods for fly ash and slag: A review. *Journal of Radiation Research and Applied Sciences,* 8**,** 523-537.

TRAN, T.-K., LEU, H.-J., CHIU, K.-F. & LIN, C.-Y. 2017. Electrochemical Treatment of Heavy Metal-containing Wastewater with the Removal of COD and Heavy Metal Ions. *Journal of the Chinese Chemical Society,* 64**,** 493-502.

TRIPATHI, A. & RANJAN, M. R. 2015. Heavy Metal Removal from Wastewater Using Low Cost Adsorbents. *Journal of Bioremediation & Biodegradation,* 6.

UAF, M., HINA, A., SAEED, A., SABAHAT, S., JANNAT, F. & ASLAM, M. 2017. Impact of Heavy Metals on Plants and Animals in Relation to Sewage Water – A Review. *Science, Technology and Development,* 36**,** 215-226.

U.N. (UNITED NATIONS), 2020. *Water and Sanitation – United Nations Sustainable Development, United Nations*. Viewed by 21 September 2020. https://www.un.org/sustainabledevelopment/water-and-sanitation/

VEGLIÒ, F. & BIRLOAGA, I. 2018. Waste Electrical and Electronic Equipment Recycling: Aqueous Recovery Methods, Elsevier Science.

VELEA, T., GHERGHE, L., PREDICA, V. & KREBS, R. 2009. Heavy metal contamination in the vicinity of an industrial area near Bucharest. *Environmental Science and Pollution Research,* 16**,** 27-32.

VENABLES, J. 2000. *Introduction to Surface and Thin Film Processes*, Cambridge University Press.

VERBINNEN, B., BLOCK, C., VAN CANEGHEM, J. & VANDECASTEELE, C. 2015. Recycling of spent adsorbents for oxyanions and heavy metal ions in the production of ceramics. *Waste Management,* 45**,** 407-411.

VERMA, N. & KAUR, G. 2016. Trends on Biosensing Systems for Heavy Metal Detection.

VISA, M. & CHELARU, A.-M. 2014. Hydrothermally modified fly ash for heavy metals and dyes removal in advanced wastewater treatment. *Applied Surface Science,* 303**,** 14-22.

VON-KITI, E. 2012. *Synthesis of Zeolites and their Application to the Desalination of Seawater.* Masters' degree Dissertation, Kwame Nkrumah University of Science and Technology.

VÖRÖSMARTY, C. J., MCINTYRE, P. B., GESSNER, M. O., DUDGEON, D., PRUSEVICH, A., GREEN, P., GLIDDEN, S., BUNN, S. E., SULLIVAN, C. A., LIERMANN, C. R. & DAVIES, P. M. 2010. Global threats to human water security and river biodiversity. *Nature,* 467**,** 555-561.

W JOHN THOMAS, F. E. & CRITTENDEN, B. 1998. *Adsorption Technology and Design*, Elsevier Science.

WAN NGAH, W. S. & HANAFIAH, M. A. K. M. 2008. Removal of heavy metal ions from wastewater by chemically modified plant wastes as adsorbents: A review. *Bioresource Technology,* 99**,** 3935-3948.

WANG, C., LI, J., SUN, X., WANG, L. & SUN, X. 2009a. Evaluation of zeolites synthesized from fly ash as potential adsorbents for wastewater containing heavy metals. *Journal of Environmental Sciences,* 21**,** 127-136.

WANG, L. K., HUNG, Y. T. & SHAMMAS, N. K. 2009b. *Handbook of Advanced Industrial and Hazardous Wastes Treatment*, CRC Press.

WANG, S. & PENG, Y. 2010. Natural zeolites as effective adsorbents in water and wastewater treatment. *Chemical Engineering Journal,* 156**,** 11-24.

WANG, S., SOUDI, M., LI, L. & ZHU, Z. H. 2006. Coal ash conversion into effective adsorbents for removal of heavy metals and dyes from wastewater. *J Hazard Mater,* 133**,** 243-51.

WATER, N. R. C. U. C. O. C. I. D. 2000. *Copper in Drinking Water*, National Academies Press.

WDOWIN, M., FRANUS, M., PANEK, R., BADURA, L. & FRANUS, W. 2014. The conversion technology of fly ash into zeolites. *Clean Technologies and Environmental Policy,* 16**,** 1217-1223.

WEI, X., KONG, X., WANG, S., XIANG, H., WANG, J. & CHEN, J. 2013. Removal of Heavy Metals from Electroplating Wastewater by Thin-Film Composite Nanofiltration Hollow-Fiber Membranes. *Industrial & Engineering Chemistry Research,* 52**,** 17583-17590.

WELTJE, L., DEN HOLLANDER, W. & WOLTERBEEK, H. T. 2003. Adsorption of metals to membrane filters in view of their speciation in nutrient solution. *Environmental Toxicology and Chemistry,* 22**,** 265-271.

WHITING, G. T., CHOWDHURY, A. D., OORD, R., PAALANEN, P. & WECKHUYSEN, B. M. 2016. The curious case of zeolite–clay/binder interactions and their consequences for catalyst preparation. *Faraday Discussions,* 188**,** 369-386.

WINGENFELDER, U., HANSEN, C., FURRER, G. & SCHULIN, R. 2005. Removal of Heavy Metals from Mine Waters by Natural Zeolites. *Environmental Science & Technology,* 39**,** 4606-4613.

WORCH, E. 2012. *Adsorption Technology in Water Treatment: Fundamentals, Processes, and Modeling*, De Gruyter.

WORLD HEALTH, O. 2009. Potassium in drinking-water : background document for development of WHO guidelines for drinking-water quality. Geneva: World Health Organization.

WORLD HEALTH, O. 2010. Hardness in drinking-water : background document for development of WHO guidelines for drinking-water quality. Geneva: World Health Organization.

WORLD HEALTH ORGANIZATION. REGIONAL OFFICE FOR, E. 2000. Air quality guidelines for Europe. 2nd ed ed.: Copenhagen : WHO Regional Office for Europe.

WU, Y. 2017. Chapter 11 - Photobioreactor–Wetland System Removes Organic Pollutants and Nutrients. *In:* WU, Y. (ed.) *Periphyton.* Boston: Elsevier.

WUANA, R. A. & OKIEIMEN, F. E. 2011. Heavy Metals in Contaminated Soils: A Review of Sources, Chemistry, Risks and Best Available Strategies for Remediation. *ISRN Ecology,* 2011**,** 402647.

XIAO, F. S. & MENG, X. 2015. *Zeolites in Sustainable Chemistry: Synthesis, Characterization and Catalytic Applications*, Springer Berlin Heidelberg.

XU, R., PANG, W., YU, J., HUO, Q. & CHEN, J. 2009a. *Chemistry of Zeolites and Related Porous Materials: Synthesis and Structure*, Wiley.

XU, R., PANG, W., YU, J., HUO, Q. & CHEN, J. 2009b. Preparation, Secondary Synthesis, and Modification of Zeolites. *Chemistry of Zeolites and Related Porous Materials: Synthesis and Structure.*

XU, W., LI, L. Y. & GRACE, J. R. 2012. Regeneration of natural Bear River clinoptilolite sorbents used to remove Zn from acid mine drainage in a slurry bubble column. *Applied Clay Science,* 55**,** 83-87.

XU, Y., ZHANG, J., LIANG, Y., ZHOU, J., ZHAO, J., RUAN, X., XU, Z. P. & QIAN, G. 2015. Synchronous cyanide purification with metals removal in the co-treatment of Zn–CN and Ni electroplating wastewaters via the Ni2+-assisted precipitation of LDH. *Separation and Purification Technology,* 145**,** 92-97.

YADAV, M., GUPTA, R. & SHARMA, R. K. 2019. Chapter 14 - Green and Sustainable Pathways for Wastewater Purification. *In:* AHUJA, S. (ed.) *Advances in Water Purification Techniques.* Elsevier.

YAMASAKI, H., PILON, M. & SHIKANAI, T. 2008. How do plants respond to copper deficiency? *Plant Signaling & Behavior,* 3**,** 231-232.

YAN, K., GUO, Y., MA, Z., ZHAO, Z. & CHENG, F. 2018. Quantitative analysis of crystalline and amorphous phases in pulverized coal fly ash based on the Rietveld method. *Journal of Non-Crystalline Solids,* 483**,** 37-42.

YANG, Q., ZHONG, Y., LI, X., LI, X., LUO, K., WU, X., CHEN, H., LIU, Y. & ZENG, G. 2015. Adsorption-coupled reduction of bromate by Fe(II)–Al(III) layered double hydroxide in fixed-bed column: Experimental and breakthrough curves analysis. *Journal of Industrial and Engineering Chemistry,* 28**,** 54-59.

YAO, Z. T., JI, X. S., SARKER, P. K., TANG, J. H., GE, L. Q., XIA, M. S. & XI, Y. Q. 2015. A comprehensive review on the applications of coal fly ash. *Earth-Science Reviews,* 141**,** 105-121.

YASEEN, D. A. & SCHOLZ, M. 2019. Textile dye wastewater characteristics and constituents of synthetic effluents: a critical review. *International Journal of Environmental Science and Technology,* 16**,** 1193-1226.

YRUELA, I. 2005. Copper in plants. *Brazilian Journal of Plant Physiology,* 17**,** 145-156.

YU, C. & HAN, X. Adsorbent Material Used In Water Treatment-A Review. 2015 2nd International Workshop on Materials Engineering and Computer Sciences, 2015/10 2015. Atlantis Press, 286-289.

YUE, M. B., YANG, N., JIAO, W. Q., WANG, Y. M. & HE, M.-Y. 2013. Dry-gel synthesis of shaped binderless zeolites composed of nanosized ZSM-5. *Solid State Sciences,* 20**,** 1-7.

ZAMZOW, M. J., EICHBAUM, B. R., SANDGREN, K. R. & SHANKS, D. E. 1990. Removal of Heavy Metals and Other Cations from Wastewater Using Zeolites. *Separation Science and Technology,* 25**,** 1555-1569.

ZANIN, E., SCAPINELLO, J., DE OLIVEIRA, M., RAMBO, C. L., FRANSCESCON, F., FREITAS, L., DE MELLO, J. M. M., FIORI, M. A., OLIVEIRA, J. V. & DAL MAGRO, J. 2017. Adsorption of heavy metals from wastewater graphic industry using clinoptilolite zeolite as adsorbent. *Process Safety and Environmental Protection,* 105**,** 194-200.

ZHANG, L. & WANG, M. 2011. Biosorption of C. I. Reactive Red 2 by Immobilized Fungal Biomass. *Advanced Materials Research,* 213**,** 432-436.

ZHANG, M. 2011. Adsorption study of Pb(II), Cu(II) and Zn(II) from simulated acid mine drainage using dairy manure compost. *Chemical Engineering Journal,* 172**,** 361-368.

ZHANG, M., ZHANG, H., XU, D., HAN, L., NIU, D., TIAN, B., ZHANG, J., ZHANG, L. & WU, W. 2011a. Removal of ammonium from aqueous

solutions using zeolite synthesized from fly ash by a fusion method. *Desalination,* 271**,** 111-121.

ZHANG, X., YANG, L., LI, Y., LI, H., WANG, W. & YE, B. 2011b. Impacts of lead/zinc mining and smelting on the environment and human health in China. *Environmental monitoring and assessment,* 184**,** 2261-73.

ZHU, S., YANG, N. & ZHANG, D. 2009. Poly(N,N-dimethylaminoethyl methacrylate) modification of activated carbon for copper ions removal. *Materials Chemistry and Physics,* 113**,** 784-789.

ZUEVA, S. B. 2018. 9 - Current legislation and methods of treatment of wastewater coming from waste electrical and electronic equipment processing. *In:* VEGLIÒ, F. & BIRLOAGA, I. (eds.) *Waste Electrical and Electronic Equipment Recycling.* Woodhead Publishing.

ZWAIN, H. M., VAKILI, M. & DAHLAN, I. 2014. Waste Material Adsorbents for Zinc Removal from Wastewater: A Comprehensive Review. *International Journal of Chemical Engineering,* 2014**,** 347912.